THE UNIVERSITY OF HULL

Some Problems in the Analysis of Spatial Pattern

being a Thesis submitted for the Degree of

Doctor of Philosophy

in the University of Hull

by

Trevor Frederick Cox, B.Sc.(Bristol), M.Sc.(Sheffield)

August, 1976

Summary of Thesis submitted for Ph.D. degree

by Trevor Frederick Cox

on

Some Problems in the Analysis of Spatial Pattern

Measurement of spatial pattern is of interest in many fields of study including forestry, ecology, archaeology, geography, astronomy, etc. Some new methods for measuring various aspects of spatial patterns formed by point events in the plane, are proposed.

Sampling a population in the plane is usually carried out using either quadrat counts or distance measurements. Only the latter are used in this Thesis, as the methods introduced are aimed at the plant biologist or forester studying patterns formed by trees in a forest stand, where distance sampling is the easiest.

The first method introduced is a new conditioned distance ratio method for analysing spatial pattern, which attempts to place patterns on an envisaged regular/random/aggregation scale. Instead of using an index as with most previous methods, a histogram of certain distances is formed, and analysis is based on viewing and hypothesis testing of this histogram.

Two new robust estimators of the density of a forest stand are described, which are unbiased for a wide range of spatial patterns. The first estimator has a coefficient which varies according to some quantitative feature of the spatial pattern. This is a new idea for obtaining robust estimators.

What constitutes a clumped or sparse area within a spatial pattern is very subjective. A method for the defining and marking of such areas is described. A computer package is used for the actual drawing of the clumped and sparse areas.

The final topic to be discussed is that of two species in the plane. The spectral theory of two-dimensional, bivariate point processes is given, and then used to study the relationship between two species cohabiting in the plane.

All the methods described are used on data, some of which are simulated, the rest being the coordinates of real trees in a forest stand.

Acknowledgments

I am extremely grateful to Professor T. Lewis for his profound guidance and encouragement as supervisor of this work. I also wish to thank Mr. P. J. Diggle and Dr. E. D. Ford for helpful discussions, and am grateful to Mr. P. J. Diggle, Dr. E. D. Ford and Professor D. J. Gerrard for providing data. Thanks also go to Mrs. J. Williams for typing this difficult manuscript. To the S.R.C., I am grateful for a research studentship, and finally my thanks go to my wife Patricia for her understanding and encouragement over the two years of preparation of this Thesis.

Parts of Chapter 2 have been published as

"A Conditioned Distance Ratio Method for Analysing Spatial Patterns"

by TREVOR F. COX and TOBY LEWIS.

Biometrika 63, (1976).

Parts of Chapter 3 have been published as

"The Robust Estimation of the Density of a Forest Stand Using a New Conditioned Distance Method"

by TREVOR F. COX.

Biometrika 63, (1976).

CONTENTS

CHAPTER 1

ANALYSIS OF SPATIAL PATTERN

1.1 Introduction

The term spatial pattern is used to refer to the pattern formed by a population of individuals in n-dimensional Euclidean space. It is usual however to consider only n = 2, or sometimes 3, higher dimensions rarely lending themselves to practical purposes. The special case of n = 1 is often referred to as the theory of point processes or series of events, there being a natural ordering of individuals in one dimension, which does not easily or necessarily generalize to higher dimensions.

The analysis of spatial pattern is of great importance in the fields of astronomy, geography, ecology, forestry, oceanography, archaeology and many others. For example, the astronomer may be interested in the pattern taken up by a group of stars, the geographer in the pattern formed by villages in a county, the ecologist by the patterns formed by herds of elephants, etc.

As with most authors, only patterns in the Euclidean plane formed by point events, which are usually the positions of individuals in a population, will be considered. Attention is also restricted to the spatial variation of the pattern. Thus the temporal variation is assumed to be non-existent or negligible, as for example when dealing with the pattern formed by pyramids in Egypt, or trees in a

forest. However in the cases where there is appreciable temporal variation, instantaneous spatial variation can be studied, e.g. when dealing with the spatial pattern at a particular instant of a flock of birds in the air. Also, populations occupying discrete habitable units, e.g. aphids on leaves, will not be studied here, but only populations occupying a continuum, or more specifically the two-dimensional Euclidean space, although the results can easily be generalized to n-dimensions.

All examples given of analysis of data will be from the area of forestry, and theory is developed with a view to aid the ecologist concerned with forest or plant communities, Warren (1972) having reviewed the role of point processes in forestry. However all the theory and methods proposed for analysing spatial patterns can be used by any investigator of spatial pattern following his own bent. Usually the individuals within a population will be referred to as trees, rather than points in the plane. This is so that random "sampling points" will not be confused with the individuals in the population, thus making for clarity of exposition. It is suggested that the investigator mentally alter "trees" to his own liking throughout the text.

1.2 Poisson Forests

The first question one usually asks when analysing a spatial pattern is whether the individuals, considered as points, are placed randomly, i.e. whether they form a 2-dimensional Poisson process, or what is often referred to as a Poisson forest. For this to be so, the individuals are positioned so that

i) in any area of size A, the probability of finding i individuals depends on A and not on the shape of the area;

ii) if A is small, the probability of finding more than one individual within the area is small compared to A;

iii) occurrences of individuals in non overlapping areas are independent.

It has been noted by many authors, for example, Evans (1953), Greig-Smith (1964), Pielou (1969, 1974), Whitford (1949), that random patterns in forestry or plant communities are seldom found. If a population is not random, then the individuals either tend to occur together to form an aggregated or clumped pattern, or tend to "repel" each other to form a pattern with regularity. There is an envisaged scale on which patterns can be placed. At one end is extreme regularity where individuals are situated at the vertices of an equilateral triangular lattice, this being the pattern symmetric about each individual with the highest density for a given minimum distance between any two individuals. At the other end of the scale, individuals cluster together, and the

extreme case can be considered as a pattern formed by clumps of coincident points. In between these extremes lies the Poisson forest which can be thought of as the frontier between regular and aggregated patterns. Fig. 1(1) shows examples of a regular pattern, a Poisson forest, and an aggregated pattern. In the sequel, the term "regular" will usually refer to patterns which are neither random nor aggregated. It is not restricted to the special cases of the regular lattices which will be referred to as regular triangular lattice, regular square lattice, and regular hexagonal lattice, (sometimes with "regular" omitted).

The above described scale of pattern is obviously not adequate to characterize <u>all</u> spatial patterns. For example, difficulty arises when one tries to place a pattern formed by pairs of coincident points situated at the vertices of a triangular lattice, upon the described pattern scale.

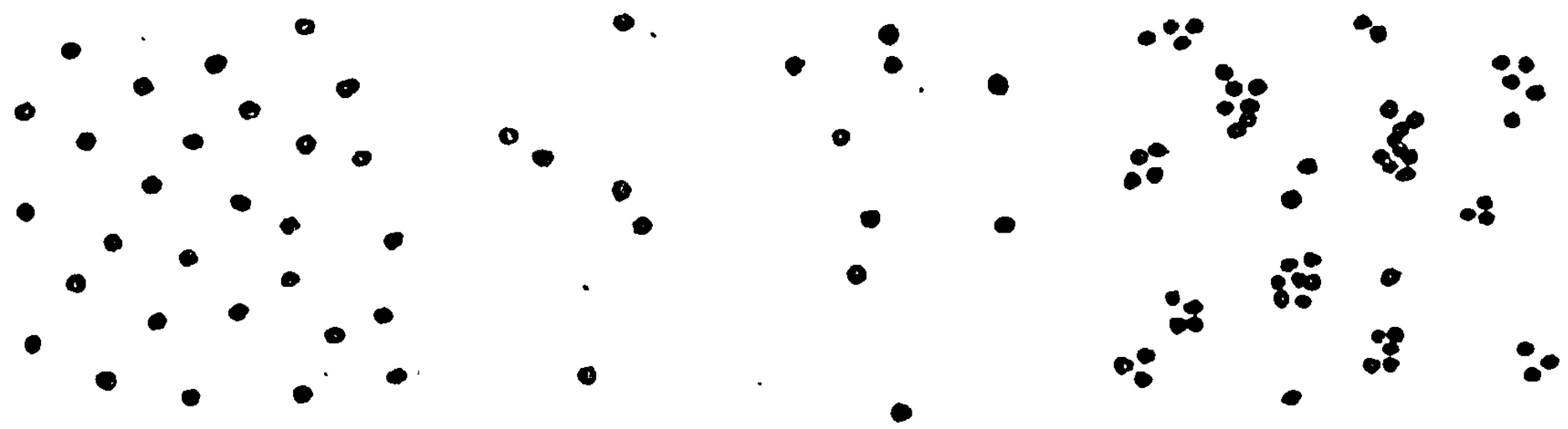

regular random aggregated

Fig. 1(1) Examples of a regular pattern, a Poisson forest and an aggregated pattern

It may be possible to find some physical reason why individuals in a population take up a particular pattern. For example, a particular kind of plant may reproduce vegetatively, and thus one would expect the stems to form an aggregated pattern. Again the instantaneous pattern formed by the positions of individuals in a particular solitary species of animal may be regular due to repulsion between individuals.

1.3 Sampling within a spatial pattern

Sampling a population in the plane provides many problems. In general there are two methods of sampling the individuals in order to measure some aspect of the spatial pattern. The first is quadrat sampling where sample plots of specified area and shape are located within the population. The second method is distance sampling, where distances between individuals, and other such distances are used for measuring the pattern. These two methods are analogous to those used for point processes in one dimension where either counts of events in certain intervals are made (quadrat sampling), or the intervals between events are measured (distance sampling).

The first sampling method is probably most useful for sampling small plants or insects, and the second method for sampling trees within a forest. In this thesis, the only methods used are distance methods, which can be easily implemented by the forester who will only need to pace out the distances.

1.4 Testing for randomness

Many authors have proposed methods for testing a population for randomness (see e.g. Besag and Gleaves (1973), Clark and Evans (1954), David and Moore (1954), Diggle, Besag and Gleaves (1974), Eberhart (1967), Greig-Smith (1952), Holgate (1965a, 1965b), Hopkins and Skellam (1954), Mountford (1961), Pielou (1959), Stiteler and Patil (1971). Some use quadrat methods and some use distance methods. Also many indices of non-randomness have been proposed, e.g. the variance to mean ratio, (Clapham (1936)), the index of clumping, (David and Moore (1954)), Lloyd's index of mean crowding, (Lloyd (1967)), Hopkins and Skellam's index, (Hopkins and Skellam (1954)), Pielou's index, (Pielou (1959)) etc., to measure the extent to which patterns are removed from randomness. These indices form a useful guide to the type of pattern under investigation. In chapter two a new diagnostic distance method for analysing spatial patterns is described which attempts to supply more information about the pattern, rather than one value of an index as most previous methods do. The method allows various tests of hypotheses to be made including tests of randomness against various alternatives.

The idea behind the method is to sample the population using randomly placed sampling origins, and then to form a histogram which hopefully sheds light onto the type of pattern. Also defined in chapter two is a random variable formed from two distance measurements, which has the remarkable property of being distributed uniformly for a wide range of spatial patterns ranging from regular, through random, to aggregated patterns.

1.5 Robust estimation of density

A problem of great interest is that of the estimation of the density of individuals within a large area in the plane. This may be of special interest in forestry, as an estimate may be needed of the number of trees per unit area within a forest, maybe to aid with yield estimates, etc. Rather than counting every tree, an estimate needs to be made using a sample of observations.

In forestry quadrat methods suffer from the disadvantage of being impractical and thus distance methods are preferred. Holgate (1972) has reviewed distance methods for estimating the density. Most estimators used so far are designed for a particular spatial pattern, usually the Poisson forest, such that they are unbiased for this particular pattern, and are then used on other spatial patterns where bias may be appreciable, Persson (1971) quantifying the matter. If an estimator of the density is unbiased or approximately unbiased for a wide range of spatial patterns, then it is robust. To this end, Diggle (1975) uses two distance measurements, biased in opposite directions, combined to reduce bias. S. M. Lewis (1975) also linearly combines two distance measurements to form an estimator which is unbiased for two different types of pattern and reduces bias for others.

In chapter three, two new estimators are proposed which are approximately unbiased for a very wide range of spatial patterns.

1.6 The mapping of clumped and sparse areas within a spatial pattern of points

There exist now many computer packages for the drawing of various maps, e.g. contour (or isopleth) maps, conformant (or chloropleth) maps. These packages are very useful to geographers as they save time and effort in the construction of such maps, only a set of data needing to be supplied.

Given a set of point events in the plane, e.g. weeds in a cornfield, it may be of interest to know where any clumps may be situated, and in the other extreme, where there are sparse areas, i.e. where the point events "tend not to occur". A simple method to determine this may be to view a dot map consisting of a dot for each event (cf. page 34). However, as noted by Stiteler (1970), and others, unless one is dealing with extreme cases, it is often difficult to distinguish visually between regular and random populations, and between random and aggregated populations. Hence it may be difficult to determine the clumped and sparse areas within a population with this method.

In chapter four, a method is described which, with the aid of a computer package named SYMAP, defines clumped and sparse areas within a spatial pattern, the computer package drawing contours of the various areas. Obviously the idea of a clumped or sparse area is very subjective and depends on the case in hand. Nevertheless, these ideas are expanded in chapter four, with a view to mapping the clumped and sparse areas within a forest.

Pielou (1974) discusses various types of maps for use with spatial pattern, and in particular how an isopleth map of the density of a spatial pattern can be constructed by counting the number of points within small sampling quadrats. However this method suffers from the use of arbitrary sized quadrats.

1.7 Two-dimensional, bivariate spectral theory for analysing spatial pattern

An area in the theory of statistical ecology or spatial point processes which has not as yet received much attention, is the analysis of two types of species, or point events, in the plane. The ecologist may be interested in the relationship between two species of plants cohabiting in the same area, and from this point of view, Pielou (1961, 1969, 1974) discusses two relationships between species, namely association and segregation, on which further details can be found in chapter five. However useful probabilistic or statistical results connected with 2-dimensional, bivariate point processes will be welcomed by the ecologist, and at present there seem to be only a few.

From a probabilistic view, Bartlett (1964) discusses the spectral theory of two-dimensional, univariate point processes, generalised from his paper on the spectral theory of point processes in one-dimension, Bartlett (1963). Results using the spectral theory on various data, and also a summary of the theory are reported in Bartlett (1974, 1975). D. R. Cox and P. A. W. Lewis (1972) discuss the theory of bivariate point processes in one-dimension.

In chapter five the spectral theory of two-dimensional bivariate point processes is discussed. The theory is applied to some tree position data, with the auto spectra being used for the study of individual species, while the cross spectra are used to shed light on the relationship between the species.

1.8 Data

All methods and theory described for analysing spatial patterns are used on data, both actual and simulated. One type of data, kindly made available by Dr. E. D. Ford of the Institute of Terrestrial Ecology, Penicuik, and described in Ford (1975), is in the form of the coordinates of trees planted on rectangular lattices with death of some of the individuals. A second type consists of the coordinates of the six species of trees in Lansing Woods, Michigan, U.S.A., kindly supplied by Professor D. J. Gerrard. The trees are within a square area of 19.6 acres, but is scaled to be represented by a 15in x 15in area (i.e. 1 in. represents 61.6 ft.). The types and numbers of trees are as follows

Type of tree	No. of trees
Black oaks	136
Red oaks	363
White oaks	460
Hickories	716
Maples	530
Miscellaneous	107.

Diagrams showing subsets of the positions of the trees are on pages 91-106.

Data for the third type are simulated. The models used include modified Thomas processes, Thomas processes, Poisson forests, a regular type pattern, and an aggregated type pattern. All the models will be described fully in the appropriate part of the text.

CHAPTER 2

ANALYSING SPATIAL PATTERNS

2.1 Introduction

In this chapter a method is proposed for investigating the spatial pattern formed by point events in the plane, which will be referred to as trees for convenience, even though they may be representing stars, pyramids, villages etc. The aim is to analyse spatial pattern with regard to an envisaged regular/random/aggregation scale, by considering a histogram of certain distance measurements, rather than the usual methods of using pattern indices and testing for randomness.

The method requires that N random points be selected within the spatial pattern, ensuring that the area sampled is well within the boundaries of the population. This enables edge effects to be neglected. The random points will be referred to as the sampling origins. From each of these sampling origins, the distance, X, to the nearest tree, and the distance, Y, from this tree to its nearest neighbour are measured. The N pairs of measurements $(X_1, Y_1), \ldots, (X_N, Y_N)$ are then split into two sets, A and B, where

$$A = \{(X_i, Y_i) : Y_i \leq 2X_i, \qquad (i = 1, \ldots, n)\}$$

$$B = \{(X_j, Y_j) : Y_j > 2X_j, \qquad (j = 1, \ldots, m)\} \quad (m + n = N).$$

For convenience the members of A and B are relabelled as (X_{1i}, Y_{1i}) and (X_{2j}, Y_{2j}) respectively. Fig 2(1) illustrates the geometrical configuration for these random variables, where O is the random sampling origin, P is the nearest tree to O, Q is P's nearest neighbour.

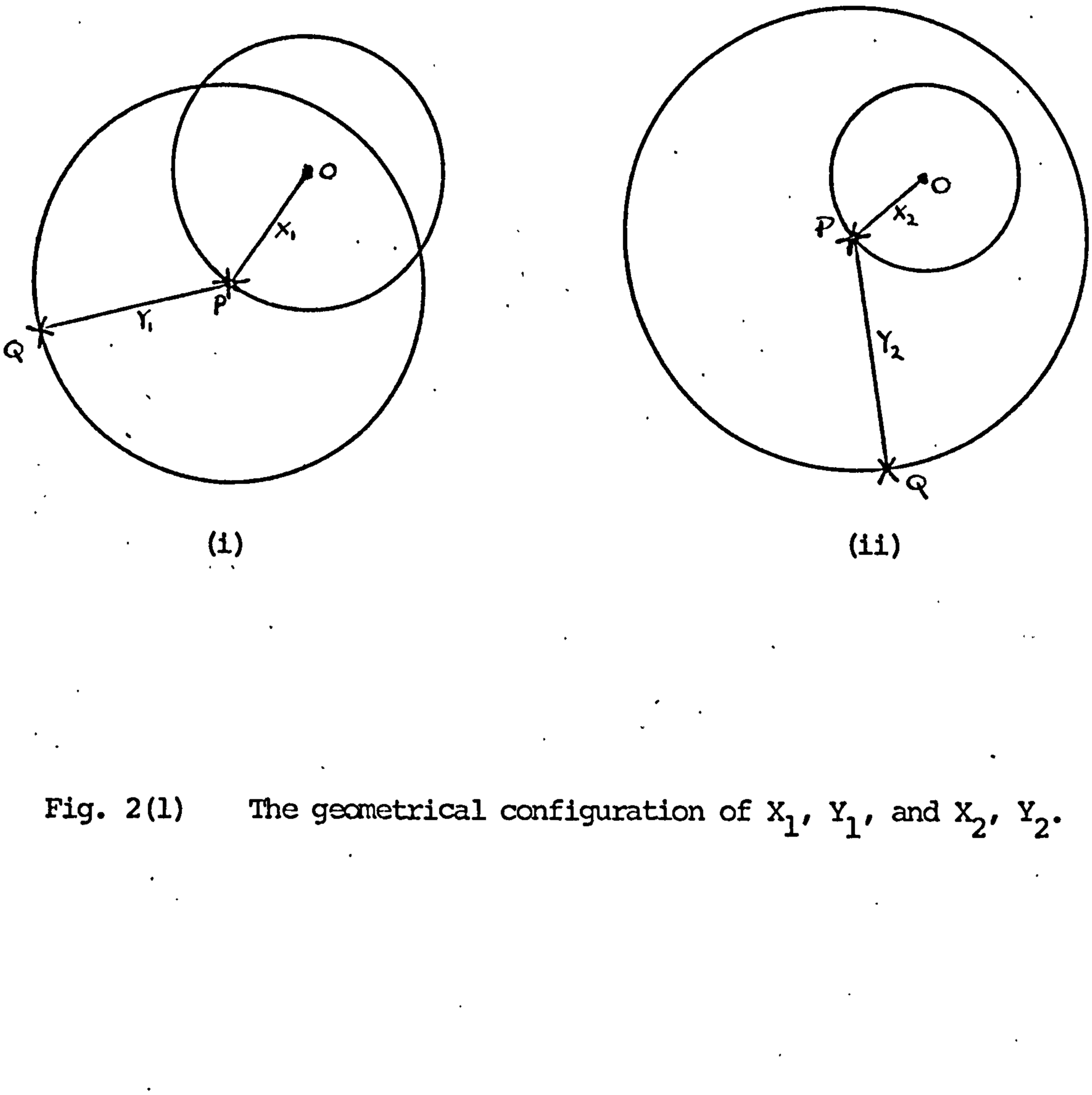

Fig. 2(1) The geometrical configuration of X_1, Y_1, and X_2, Y_2.

Define the random variables W_{1i} and W_{2j} as

$$W_{1i} = 1/\{2\pi + \sin\Phi_i - (\pi + \Phi_i)\cos\Phi_i\} \qquad (i = 1, \ldots, n)$$

where $\sin(\frac{1}{2}\Phi_i) = \frac{1}{2}Y_{1i}/X_{1i}$, and

$$W_{2j} = 4X_{2j}^2/Y_{2j}^2 \qquad (j = 1, \ldots, m).$$

The reasons for defining W_{1i} and W_{2j} in this manner will become clear later. The W_{1i}'s will be used for the analysis of spatial pattern, and the W_{2j}'s will be shown to have the same distribution for a wide range of patterns. That is, the information about the spatial pattern resides essentially in the W_{1i}'s.

2.2 The Poisson forest

The Poisson forest is the most widely used model in the analysis of spatial pattern. It occurs when any small area of size δa contains one "tree" with probability $\lambda\delta a + o(\delta a)$, contains no trees with probability $1 - \lambda\delta a + o(\delta a)$, where λ is a constant known as the rate or density. Also the events that the area δa contains or does not contain trees are independent of those for any other area $\delta a'$ which does not intersect δa. Thus the Poisson forest is only another name for the two dimensional Poisson process or random process.

Fig. 2(2) illustrates the geometrical configuaration of the random variable X, the distance from a random sampling origin, O, to the nearest tree P.

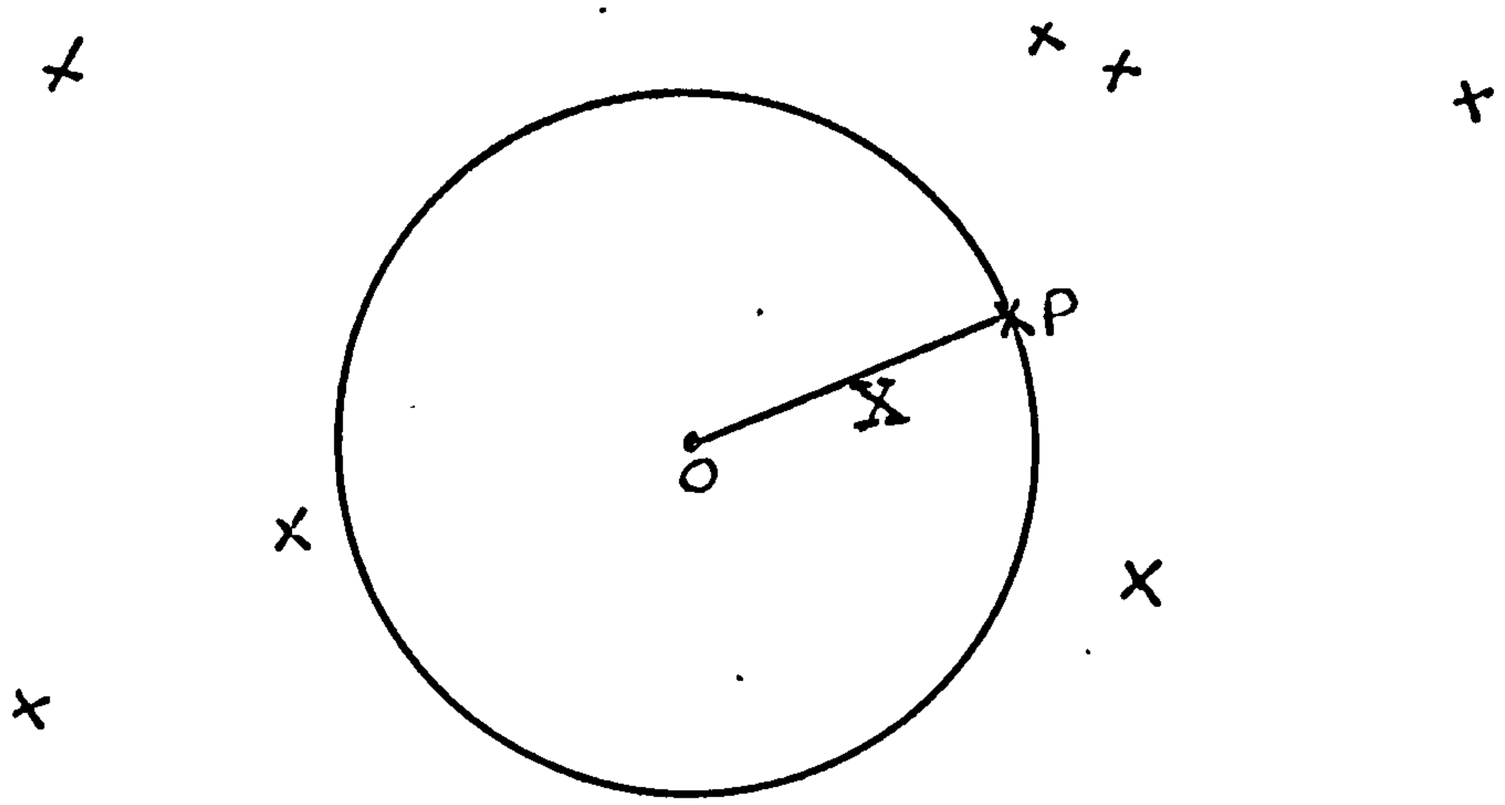

Fig. 2(2) To find the p.d.f. of X for the Poisson forest.

Let $F(x)$ be the distribution function of X for the Poisson forest. From Fig. 2(2), the probability that there are no trees in the circle through P, centre O, is $\exp(-\lambda\pi x^2)$, where λ is the density of the process. Thus

$$1 - F(x) = \exp(-\lambda\pi x^2),$$

and on differentiating, we have the probability density function (p.d.f.) of X to be

$$2\lambda\pi x \exp(-\lambda\pi x^2) \qquad (0 \leqslant x < \infty). \qquad (1)$$

This is a well known result (see e.g. Skellam (1952), Pollard (1971) etc.).

For $Y \leqslant 2X$, in order to obtain the p.d.f. of W_1, it is easier to work in terms of angle Φ and X_1 as shown in Fig. 2(3), rather than Y_1 and X_1. For $0 \leqslant \Phi \leqslant \pi$ denote

$$\text{pr}\{\, x < X \leqslant x + dx, \quad Y > 2x \sin(\tfrac{1}{2}\phi)\} \text{ by } H_1(x, \phi)dx.$$

For $Y > 2X$ denote

$$\text{pr}\{\, x < X \leqslant x + dx, \quad Y > y\} \quad \text{by } H_2(x,y)dx.$$

Now $H_1(x,0) = \text{pr}\{\, x < X \leqslant x + dx, \; Y > 0\}$, which is the unconditioned p.d.f. of X. Thus

$$H_1(x,0) = 2\lambda\pi x \exp(-\lambda\pi x^2). \tag{2}$$

$$\text{Also } H_1(x,\pi) = \text{pr}\{\, x < X \leqslant x + dx, \; Y > 2x\,\}$$

$$= H_2(x, 2x), \tag{3}$$

and it is easily seen that

$$\text{pr}(Y > 2X) = \int_0^\infty H_1(x,\pi)dx. \tag{4}$$

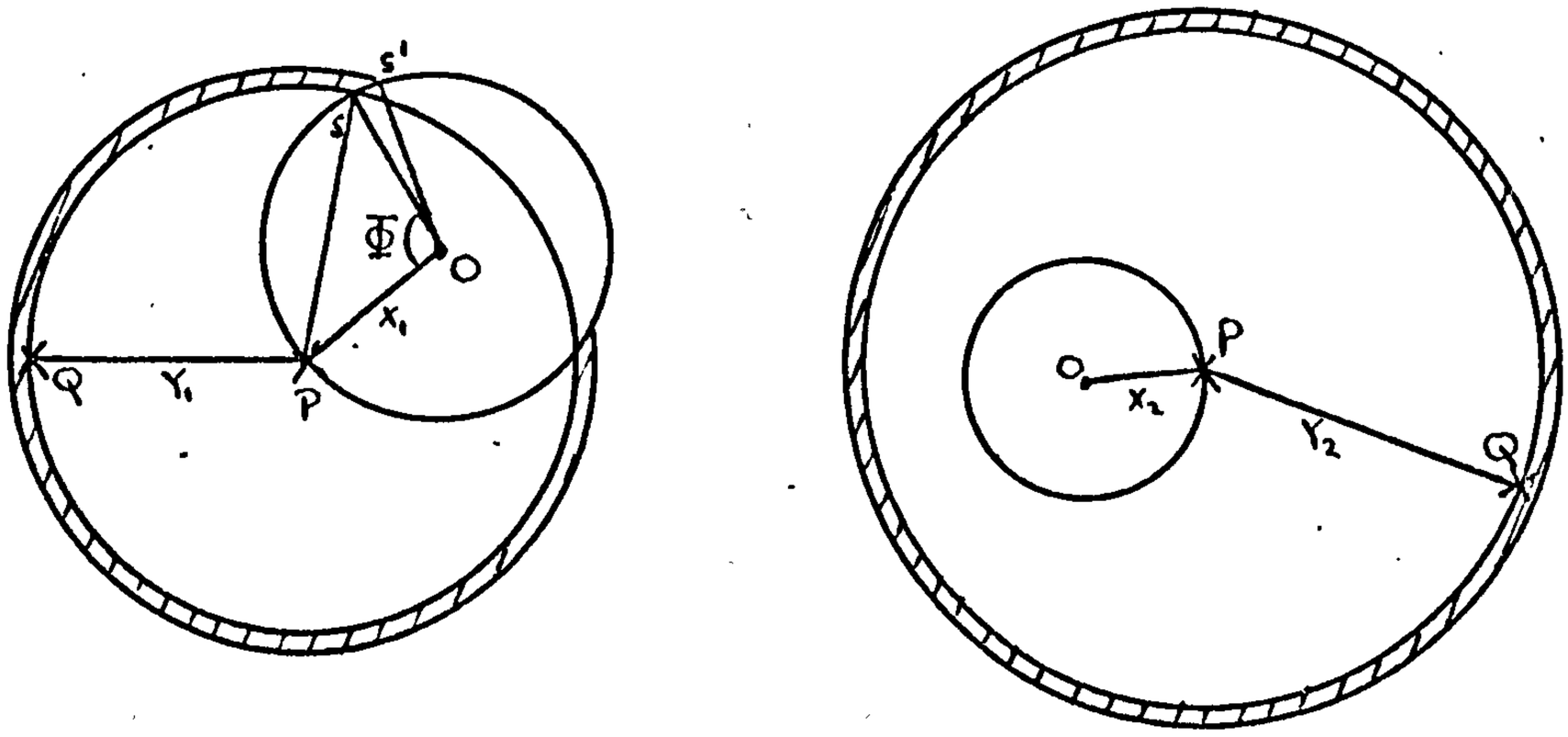

Fig. 2(3) To find $H_1(x, \phi)$ and $H_2(x, y)$

From Fig. 2(3)(i),

$$H_1(x, \phi + d\phi) = H_1(x,\phi) \times \text{pr}\{\text{no trees in shaded region}\}.$$

For the Poisson forest,

$$\text{pr}\{\text{no tree in shaded region}\} = 1 - (2\pi - 2\hat{SPO})\lambda y dy.$$

Now $y = 2x \sin(\frac{1}{2}\phi)$, and thus for fixed x,

$$dy = x \cos(\tfrac{1}{2}\phi)d\phi ,$$

and thus

$$H_1(x, \phi + d\phi) = H_1(x,\phi)\{1 - \lambda(\pi+\phi)2x \sin(\tfrac{1}{2}\phi)\ x \cos(\tfrac{1}{2}\phi)\}\ d\phi. \quad (5)$$

From Fig. 2(3)(ii)

$$H_2(x,y + dy) = H_2(x,y) \times \text{pr}\{\text{no trees in shaded region}\},$$

$$= H_2(x,y)(1 - 2\lambda\pi y dy). \quad (6)$$

Thus from equations (5) and (6)

$$\frac{\partial H_1(x,\phi)}{\partial \phi} = -2H_1(x,\phi)\lambda(\pi+\phi)x \sin(\tfrac{1}{2}\phi)\ \cos(\tfrac{1}{2}\phi), \quad (7)$$

$$\frac{\partial H_2(x,y)}{\partial y} = -2\ H_2(x,y)\lambda\pi y dy. \quad (8)$$

Integrating equations (7) and (8) with respect to y

$$H_1(x,\phi) = C_1(x)\ \exp[-\lambda x^2\{\sin\phi - (\pi+\phi)\cos\phi\}] \qquad (0 \leqslant x < \infty,\ 0 \leqslant \phi \leqslant \pi), \quad (9)$$

$$H_2(x,y) = C_2(x)\ \exp(-\lambda\pi y^2) \qquad (0 \leqslant x < \infty,\ 2x < y < \infty), \quad (10)$$

where $C_1(x)$ and $C_2(x)$ are functions of x.

The boundary conditions (2) and (3) give

$$2\lambda\pi x \exp(-\lambda\pi x^2) = C_1(x) \exp(\lambda\pi x^2)$$

and $$C_1(x) \exp(-2\lambda\pi x^2) = C_2(x) \exp(-4\lambda\pi x^2),$$

whence $$C_1(x) = 2\lambda\pi x \exp(-2\lambda\pi x^2) \text{ and } C_2(x) = 2\lambda\pi x.$$

Substituting these values in equations (9) and (10)

$$H_1(x,\phi) = 2\lambda\pi x \exp\left[-\lambda x^2\{2\pi + \sin\phi - (\pi+\phi)\cos\phi\}\right] \quad (0 < x < \infty,\ 0 \leq \phi \leq \pi), \tag{11}$$

and $$H_2(x,y) = 2\lambda\pi x \exp(-\lambda\pi y^2) \quad (0 < x < \infty,\ 2x < y < \infty). \tag{12}$$

From equation (4)

$$\text{pr}\{Y > 2X\} = \int_0^\infty 2\lambda\pi x \exp(-4\lambda\pi x^2)dx ,$$

$$= 1/4.$$

The joint p.d.f. of X_1 and Φ is thus from equation (11)

$$-\frac{\partial H_1(x,\phi)}{\partial\phi} \Big/ \frac{3}{4} = \frac{8}{3}\lambda^2\pi(\pi+\phi)x^3 \sin\phi \exp\left[-\lambda x^2\{2\pi + \sin\phi - (\pi+\phi)\cos\phi\}\right]$$

$$(0 \leq x < \infty,\ 0 \leq \phi \leq \pi), \tag{13}$$

and the joint p.d.f. of X_2 and Y_2 is from equation (12)

$$-\frac{\partial H_2(x,y)}{\partial y} \Big/ \frac{1}{4} = 16\lambda^2\pi^2 xy \exp(-\lambda\pi y^2) \quad (0 \leq x < \infty,\ 2x < y < \infty). \tag{14}$$

Putting $W_1 = 1/\{2\pi + \sin\Phi - (\pi+\Phi)\cos\Phi\}$, it is easily seen that $-w_1^{-2}dw_1 = (\pi+\phi)\sin\phi\, d\phi$, and thus from equation (13), the marginal p.d.f. of W_1 is

$$\frac{8}{3}\lambda\pi\int_0^\infty x^3 w^{-2}\exp(-\lambda\pi x^2/w)\,dx \qquad (\tfrac{1}{4}\pi^{-1} \leq w \leq \pi^{-1}),$$

which reduces to $\frac{4}{3}\pi$. Hence if we define $R_1 = \frac{4}{3}(1 - \pi W_1)$, then R_1 is distributed uniformly over $[0,1]$.

Putting $W_2 = 4X_2^2/Y_2^2$, the marginal p.d.f. of W_2 is from equation (14)

$$32\pi^2\lambda^2 \int_0^\infty x^3 w^{-2}\exp(-4\lambda\pi x^2/w^2)\,dx \qquad (0 \leq w \leq 1),$$

which reduces to unity. Thus W_2 is distributed uniformly over $[0,1]$.

The argument of the exponential function in equation (13) indicates why W_1 was so defined. Instead of dealing with the random variables X_1 and Y_1, or X_1 and Φ, which have complicated distribution it is now possible to use W_1 which has a simple distribution for the Poisson forest. Essentially W_1 is a function of the ratio Y_1/X_1 and is thus independent of the density of the Poisson process.

2.3 The triangular, square and hexagonal lattices

If points are packed symmetrically into a plane so that each point is a distance d from n other points, then the only values n can take are 3, 4 and 6. The patterns are shown in Fig. 2(4), and are referred to as the regular triangular lattice for n = 6, the regular square lattice for n = 4, and the regular hexagonal lattice for n = 3.

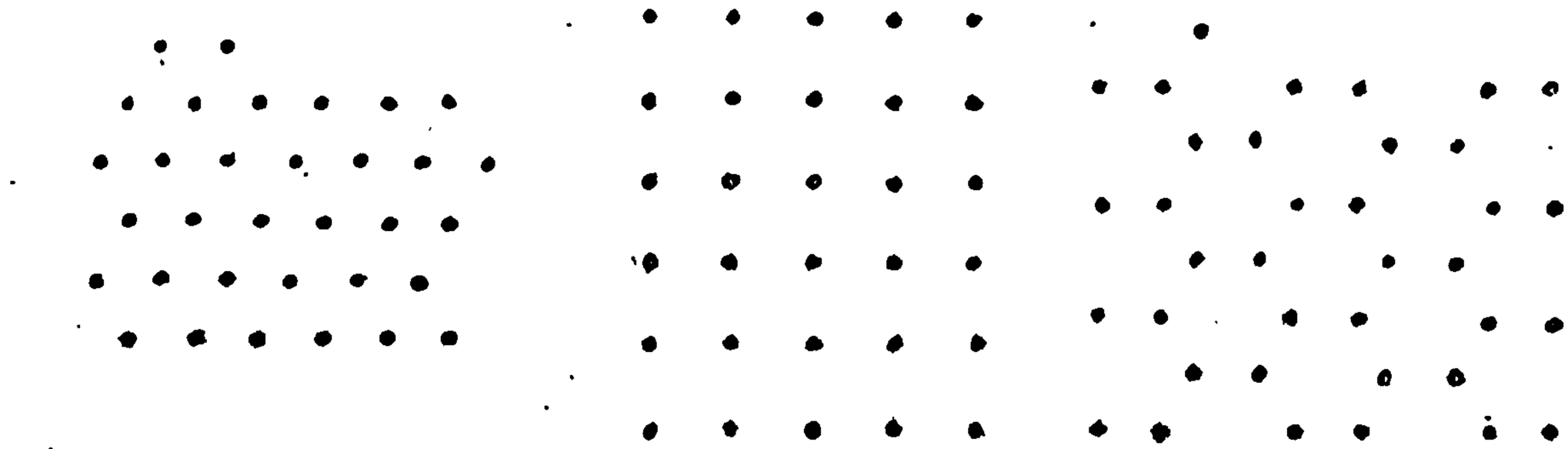

triangular square hexagonal

Fig. 2(4) Three types of regular lattices

It is easily seen that the densities of the three lattices are $(2/\sqrt{3})d^{-2}$, d^{-2}, and $(4/3\sqrt{3})d^{-2}$ respectively for the triangular, square and hexagonal lattices. Thus the triangular lattice can be considered as the most regular pattern obtainable.

For each lattice $Y = d$ with probability one. The p.d.f. of X is given by

$$\begin{cases} \pi x \Big/ \left(\frac{\sqrt{3}}{4}d^2\right) & (0 \leq x \leq \tfrac{1}{2}d), \\ x\left\{\pi - 6\cos^{-1}(\tfrac{1}{2}d/x)\right\} \Big/ \left(\frac{\sqrt{3}}{4}d^2\right) & (\tfrac{1}{2}d < x \leq d/\sqrt{3}), \end{cases} \quad (15)$$

for the triangular lattice,

$$\begin{cases} 2\pi x/d^2 & (0 \leq x \leq \tfrac{1}{2}d), \\ x\left\{2\pi - 8\cos^{-1}(\tfrac{1}{2}d/x)\right\}/d^2 & (\tfrac{1}{2}d < x \leq d/\sqrt{2}), \end{cases} \quad (16)$$

for the square lattice,

$$\begin{cases} \frac{2}{3}\pi x \Big/ \left(\frac{\sqrt{3}}{4}d^2\right) & (0 \leq x \leq \tfrac{1}{2}d), \\ x\left\{\frac{2}{3}\pi - 2\cos^{-1}(\tfrac{1}{2}d/x)\right\} \Big/ \left(\frac{\sqrt{3}}{4}d^2\right) & (\tfrac{1}{2}d < x \leq d), \end{cases} \qquad (17)$$

for the hexagonal lattice.

The p.d.f. of X_2 is thus

$$\frac{4\pi x}{\sqrt{3}d^2} \Big/ \frac{\pi}{2\sqrt{3}} = 8x/d^2 \quad (0 \leq x \leq \tfrac{1}{2}d) \quad \text{for the triangular lattice,}$$

$$\frac{2\pi x}{d^2} \Big/ \frac{\pi}{4} = 8x/d^2 \quad (0 \leq x \leq \tfrac{1}{2}d) \quad \text{for the square lattice,}$$

$$\frac{8\pi x}{3\sqrt{3}} \Big/ \frac{\pi}{3\sqrt{3}} = 8x/d^2 \quad (0 \leq x \leq \tfrac{1}{2}d) \quad \text{for the hexagonal lattice.}$$

Thus the p.d.f. of X_2 is the same for all three lattices. Now $W_2 = 4X_2^2/Y_2^2$, and hence it follows that W_2 is again distributed uniformly over $[0,1]$ for all three of the lattices.

For the distance ratios in set A,

$$\sin(\tfrac{1}{2}\phi) = \tfrac{1}{2}d/x,$$

and thus

$$\frac{dx}{d\phi} = -d\cos(\tfrac{1}{2}\phi)/\{4\sin^2(\tfrac{1}{2}\phi)\}.$$

As $W_1 = 1/\{2\pi + \sin\Phi - (\pi+\Phi)\cos\Phi\}$, it is easily seen that

$$\frac{dW_1}{d\Phi} = -\{2\pi + \sin\Phi - (\pi+\Phi)\cos\Phi\}^{-2} \quad (\pi+\Phi)\sin\Phi,$$

or

$$\frac{d\Phi}{dW_1} = -\left\{2\pi + \sin\Phi - (\pi+\Phi)\cos\Phi\right\}^2 \Big/ \left\{(\pi+\Phi)\sin\Phi\right\}.$$

Hence from equation (15) the p.d.f. of $R_1 = \frac{4}{3}(1 - \pi W_1)$ for the triangular lattice is

$$\frac{4}{3}\left[1 - \frac{\pi\{\pi - 6(\frac{1}{2}\pi - \frac{1}{2}\phi)\}}{2\sin(\frac{1}{2}\phi)(1 - \pi/(2\sqrt{3}))\frac{1}{4}\sqrt{3}} \quad \frac{\{2\pi + \sin\phi - (\pi+\phi)\cos\phi\}^2}{(\pi+\phi)\sin\phi} \quad \frac{\cos(\frac{1}{2}\phi)}{4\sin^4(\frac{1}{2}\phi)}\right] \quad (18)$$

where $\frac{4}{3}\left[1 - \pi/\{2\pi + \sin\phi - (\pi+\phi)\cos\phi\}\right] = r$, $\frac{4}{3}\left(\frac{11\pi + 3\sqrt{3}}{17\pi + 3\sqrt{3}}\right) \leq r \leq 1$.

(i.e. $.904 \leq r \leq 1$).

Expression (18) does not simplify much and is thus calculated by computer program. Similar expressions can be obtained for the p.d.f. of R_1 for the square and hexagonal lattices, viz.

$$\frac{4}{3}\left[1 - \frac{\pi(2\phi - \pi)}{8(1 - \frac{1}{4}\pi)} \quad \frac{\{2\pi + \sin\phi - (\pi+\phi)\cos\phi\}^2}{(\pi+\phi)\sin^4(\frac{1}{2}\phi)}\right] \quad \text{(square lattice)},$$

$\frac{4}{3}\left(\frac{\pi+1}{2\pi+1}\right) \leq r \leq 1$ (i.e. $.758 \leq r \leq 1$), and

$$\frac{4}{3}\left[1 - \frac{\pi(\phi - \frac{1}{3}\pi)}{8(1 - \frac{1}{3}\pi/\sqrt{3})\frac{1}{4}\sqrt{3}} \quad \frac{\{2\pi + \sin\phi - (\pi+\phi)\cos\phi\}^2}{(\pi+\phi)\sin^4(\frac{1}{2}\phi)}\right] \quad \text{(hexagonal lattice)}$$

$\frac{4}{3}\left(\frac{2\pi + 3\sqrt{3}}{8\pi + 3\sqrt{3}}\right) \leq r \leq 1$ (i.e. $.505 \leq r \leq 1$).

Fig. 2(5) shows the p.d.f. of R_1 for the three lattice patterns and also for the Poisson forest.

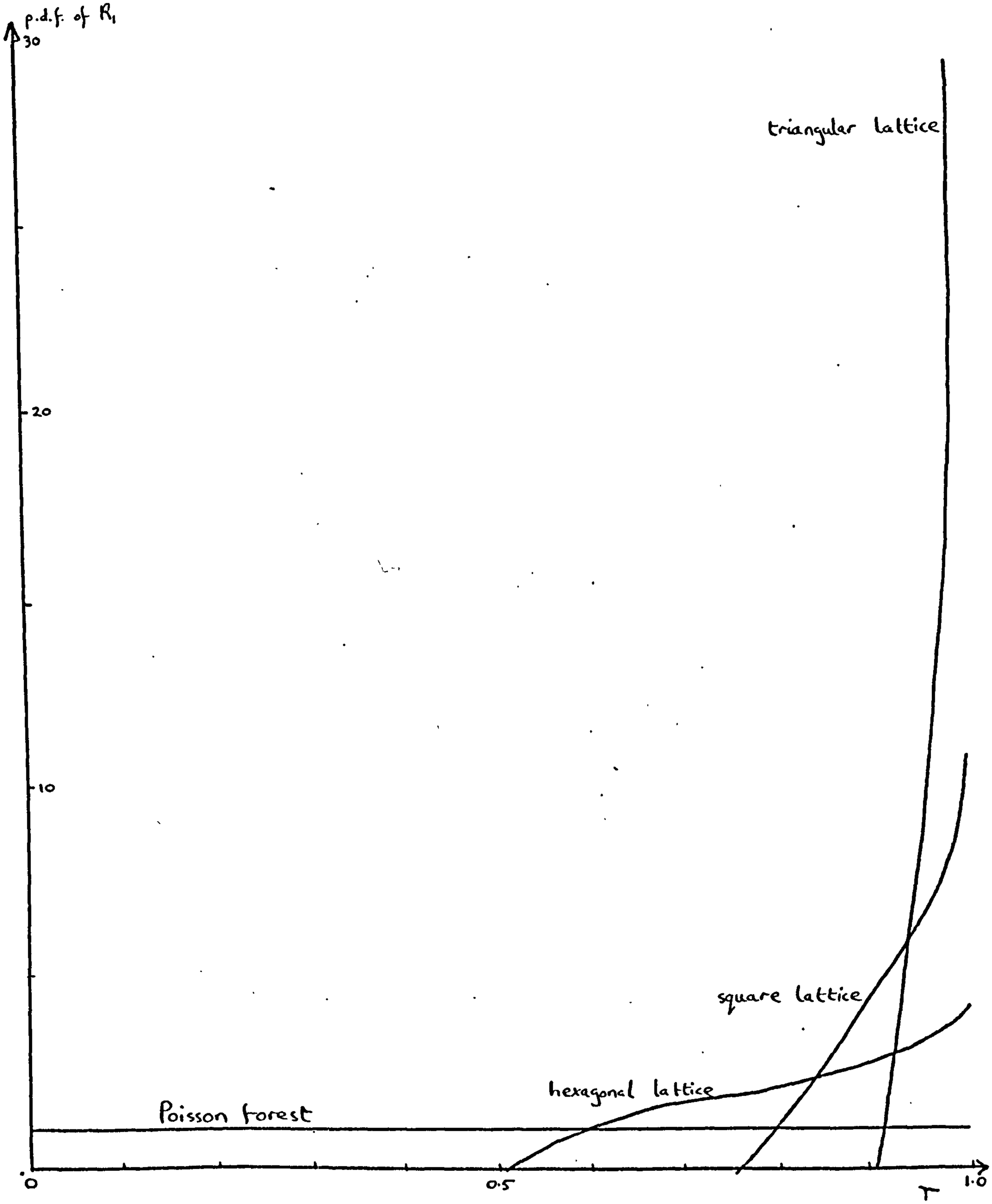

Fig. 2(5) The p.d.f. of R_1 for the triangular, square and hexagonal lattices, and also for the Poisson forest.

2.4 An aggregation model

Now consider an idealised extreme aggregation pattern. This occurs when the trees are in clumps of at least two individuals occupying the same point. In this case R_1 is zero with probability one. One should note that the proposed sampling procedure cannot differentiate in this case between different distributions of clump sizes; for example R_1 is zero for pairs of coincident trees situated at the vertices of a square lattice and also zero for 100 trees situated at each of the vertices of a square lattice. However when the pattern is formed by dense clumps of small area, it is more natural to work in terms of the spatial pattern of the clump centres, together with the distribution of the number of trees within a clump.

In the idealised extreme aggregation case the mass of the R_1-distribution is concentrated entirely at zero. The mass is uniformly spread between zero and one in the random case, and concentrated more and more towards one for the cases of increasing regularity (hexagonal, square and triangular lattices). This suggests that aggregation patterns can be regarded as characterised by R_1-distributions concentrated toward zero.

Suppose "clump centres" form a Poisson forest in the plane with density λ_1, and suppose a proportion of these clumps are single trees while the remainder are small local Poisson forests with local density μ, where $\mu >> \lambda_1$. Fig. 2(6) shows a realisation of this process.

Fig. 2(6) A realisation of the clumped model

There are three situations arising in the sampling procedure: (i) if the random sampling origin, O, falls within one of the local Poisson forest clumps, then so do P and Q, where P is the nearest tree to O and Q is P's nearest neighbour. Thus in effect we are taking observations in a Poisson forest of density μ, and the R_1 value will belong to the uniform distribution on $[0, 1]$. (ii) If O falls outside one of the clumps, and P is a single tree clump, we are in effect taking observations in a Poisson forest of density λ_1, and the R_1 value will again belong to the uniform distribution on $[0,1]$. (iii) If O falls outside one of the clumps and P is a tree on the periphery of a multi-tree clump, then the same argument which led to the uniform distribution for R_1 in section 2.2 applies, except that the density for Y is μ instead of λ_1. Hence the random variable

$$Z = 1/\{ (1 + \lambda_1\mu^{-1})\pi + \sin\Phi - (\pi+\Phi)\cos\Phi \}$$

is uniformly distributed over the range $[\mu(3\mu\pi + \lambda_1\pi)^{-1}, \mu(\lambda_1\pi)^{-1}]$, noting that $pr(Y \leq 2X) = 3\mu/(3\mu+\lambda_1)$, (which $\to 1$ as $\mu/\lambda_1 \to \infty$, and $= \frac{3}{4}$ when $\mu/\lambda_1 = 1$).

The distribution of W_1 conditioned on case (iii) is therefore given by

$$\begin{aligned} pr\{W_1 \leq w\} &= pr\{ 2\pi + \sin\Phi - (\pi+\Phi)\cos\Phi \geq 1/w \} \\ &= pr\{ 1/Z + (1 - \lambda_1/\mu)\pi \geq 1/w \} \\ &= pr\{ Z \leq 1/[1/w - (1 - \lambda_1/\mu)\pi] \} \\ &= \frac{[1/w - (1-\sigma)\pi]^{-1} - [(3+\sigma)\pi]^{-1}}{(\sigma\pi)^{-1} - [(3+\sigma)\pi]^{-1}}, \end{aligned}$$

Where $\lambda_1/\mu = \sigma$.

Again putting $R_1 = \frac{4}{3}(1 - \pi W_1)$, the p.d.f. of R_1 in case (iii) is

$$f(r) = \frac{4\sigma(\sigma+3)}{9(1-\sigma)^2} \left[\frac{4\sigma}{3(1-\sigma)} + r \right]^{-2} \qquad (0 \leq r \leq 1),$$

$$= (1 + k)(1 + kr)^2,$$

where $k = \frac{3}{4}(1-\sigma)/\sigma$. i.e. a censored Pareto distribution.

It is assumed that case (i) or case (ii) happens with probability ν, and that case (iii) happens with probability $1 - \nu$; the unconditioned p.d.f. of R_1 is then

$$g(r; \nu, k) = \nu + (1 - \nu)(1 + k)(1 + kr)^{-2} \quad (0 \leq r \leq 1, k > 0). \quad (19)$$

Parameters ν and k can be considered as parameters of aggregation. Thus ν indicates to what extent the population tends towards clumping, and k measures the actual clumping, increasing as clumping increases. Thus for slight clumping one expects ν to be near one with k large or small depending on whether the clumps are dense or not. For intense clumping ν will be near zero and k will again be large or small depending on whether the clumps are dense or not. Fig. 2(7) shows the p.d.f. $g(r;\nu, k)$ for various values of ν and k.

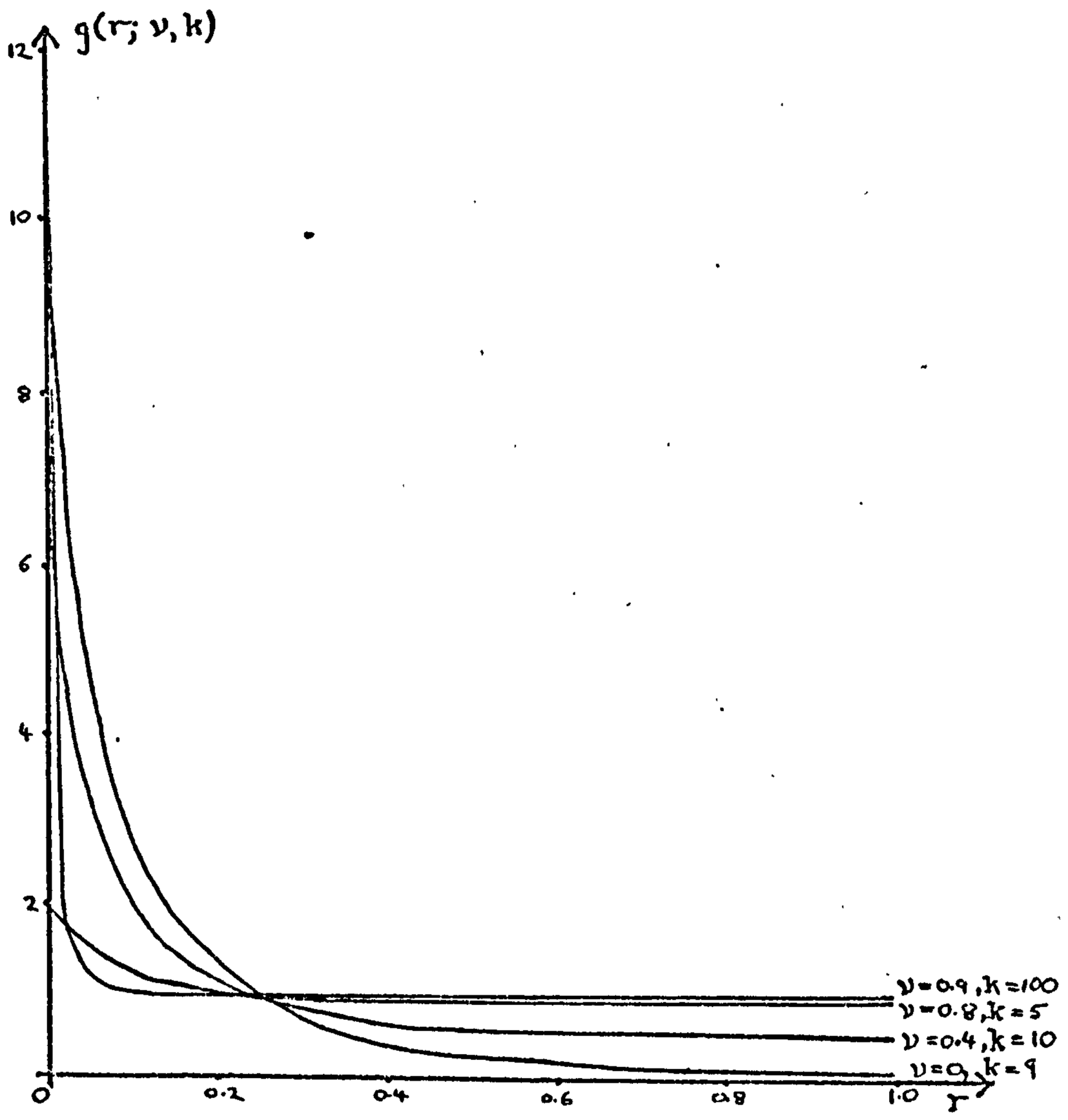

Fig. 2(7) The p.d.f. of R_1 for the clumped model

Now consider the distribution of W_2 in the three cases above. In case (i) W_2 will be defined in a local Poisson forest and is thus distributed uniformly over $[0,1]$. In case (ii) W_2 is defined in a Poisson forest of density λ_1 and is again distributed uniformly over $[0, 1]$. No values of W_2 arise in case (iii), since the probability that $Y > 2X$ may be assumed negligible. Overall therefore W_2 is distributed uniformly in the aggregation model.

2.5 Estimation of ν and k.

Given observations $r_1, \ldots, r_n$ in the aggregation case described above, rough estimates $\tilde{\nu}$ and $\tilde{k}$ of ν and k can be obtained by equating the sample mean, $\bar{r}$, and the proportion of r's greater than $\frac{1}{2}$, $\bar{s}$, to the theoretical values thus:

$$\bar{r} = \tfrac{1}{2}\tilde{\nu} + (1 - \tilde{\nu})\left\{(1 + \tilde{k})\log(1 + \tilde{k}) - \tilde{k}\right\}/\tilde{k}^2, \qquad (20)$$

and $$\bar{s} = \tfrac{1}{2}\tilde{\nu} + (1 - \tilde{\nu})/(2 + \tilde{k}). \qquad (21)$$

Substituting $\tilde{\nu} = 2\left\{(2 + \tilde{k})\bar{s} - 1\right\}/\tilde{k}$ from equation (21) into equation (20), $\tilde{k}$ is the solution of the equation

$$\frac{\bar{r} - \bar{s}}{(1 - 2\bar{s})} = \frac{(1 + \tilde{k})}{\tilde{k}^3}\left\{(2 + \tilde{k})\log(1 + \tilde{k}) - 2\tilde{k}\right\} = K(k) \qquad (22)$$

$$(0 \leqslant \bar{s} < \tfrac{1}{2}, \quad 0 \leqslant \bar{r} \leqslant 1, \quad \tilde{k} > 0).$$

Fig. 2(8) shows the graph of $K(k)$ plotted against $k > 0$. From equations (20) and (21) it is easily seen that $\bar{r} - \bar{s} \geqslant 0$ and $\bar{s} < \frac{1}{2}$ for this clumped case. Thus in practice $(\bar{r} - \bar{s})/(1 - 2\bar{s})$ should be greater than zero, and hence this value determines k from Fig. 2(8).

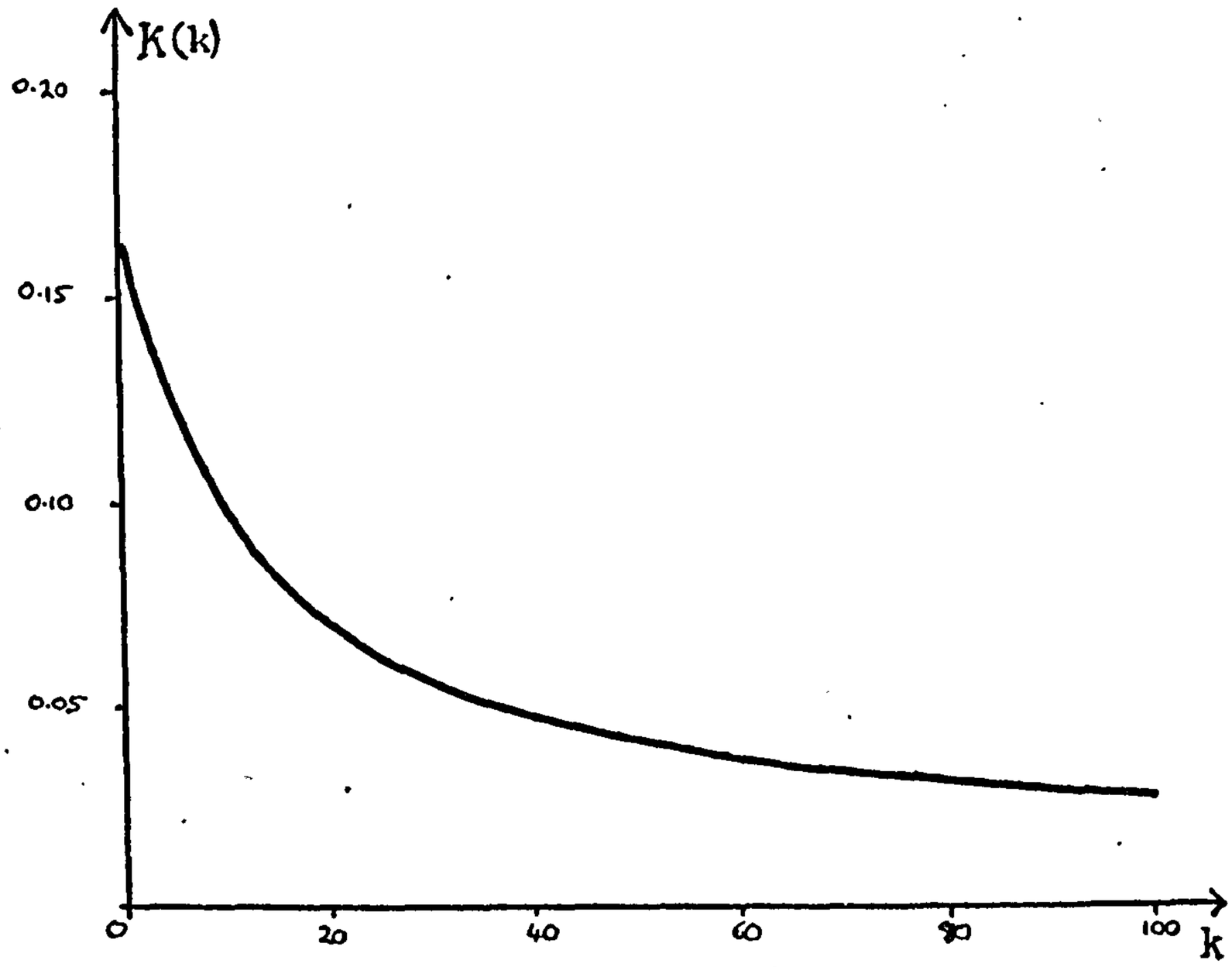

Fig. 2(8) The function K(k) to estimate $\tilde{k}$

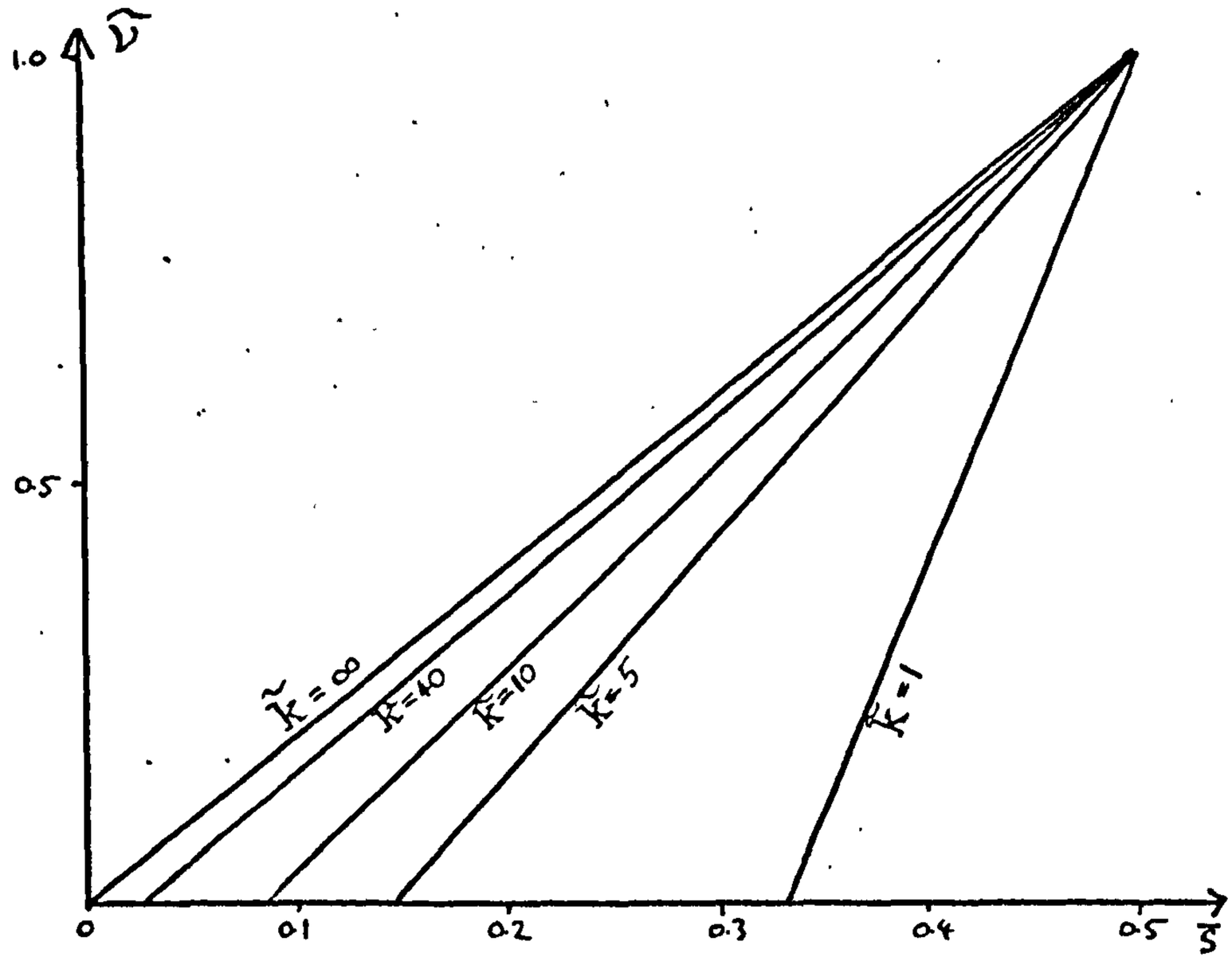

Fig. 2(9) $\tilde{\nu}$ for given $\bar{r}$ and $\bar{s}$ and $\tilde{k}$ determined from K(k).

After determining $\hat{k}$, $\hat{\nu}$ is obtained from equation (21) as

$$\hat{\nu} = 2\{(2 + \hat{k})\bar{s} - 1\}/\hat{k} .$$

Fig. 2(9) shows values of $\hat{\nu}$ for given $\bar{s}$ and $\tilde{k}$.

The log likelihood $L(\nu,k)$ of the observations $r_1, \ldots, r_n$ is given by

$$L(\nu,k) = \sum_{i=1}^{n} \log\{\nu + (1-\nu)(1+k)(1+kr_i)^{-2}\}$$, and hence the maximum likelihood estimates $\hat{\nu}$ and $\hat{k}$ of ν and k can be found by calculating values of $L(\nu,k)$ over a grid of values for ν and k surrounding the initial estimates $\tilde{\nu}$, $\tilde{k}$, and fitting a quadratic surface over the grid points in the neighbourhood of the observed maximum. The maximum point of this fitted surface gives the values of $\hat{\nu}$ and $\hat{k}$, and the coefficients of the second degree terms give the estimated terms of the information matrix, and hence by inversion the estimated variance-covariance matrix of $\hat{\nu}$ and $\hat{k}$.

Appendix A gives the details of the fitting of the quadratic surface described above.

Recapitulating, the proposed method for analysing spatial pattern is to select N sampling origins, measure the distances (x_i, y_i), $i = 1, \ldots, N$ and then form a histogram of the values r_i obtained from these distances. The histogram will then give insight into the type of pattern.

2.6 Testing hypotheses about the pattern

First consider the two simple hypotheses,

H_0 : the r_i's are from a Poisson forest, i.e. $R_1 \sim U(0,1)$.

H_1 : the r_i's are from a square lattice population.

As a test of H_0 against H_1, H_0 can be rejected if all the observed r_i's are greater than the smallest possible value of R_1 under H_1 i.e. if

$$M = \min\{r_1, \ldots, r_n\} \geqslant \tfrac{4}{3}(\pi+1)/(2\pi+1) = 0.758.$$

Under H_0, $\text{pr}\{M \geqslant \tfrac{4}{3}(\pi+1)/(2\pi+1)\} = \{\tfrac{1}{3}(2\pi-1)/(2\pi+1)\}^n = (0.242)^n$.

Under H_1, $\text{pr}\{M \geqslant \tfrac{4}{3}(\pi+1)/(2\pi+1)\} = 1.0$.

Thus the power of this test is unity and the Type 1 error is $(0.242)^n$ which converges to zero very fast as n increases, e.g. for n = 8, its value is about 10^{-5}.

Similar considerations apply if the pattern under the alternative hypothesis is a triangular lattice or a hexagonal lattice, the critical values for M being 0.904 and 0.505 respectively.

Consider now the problem of testing for the presence of aggregation, taking as null hypothesis, H_0, that $R_1 \sim U(0,1)$, corresponding to the assumption of a Poisson forest, and as alternative, H_1, that R_1 has the p.d.f. $g(r;\nu,k)$ of equation (19), corresponding to the above described aggregation model with parameters ν and k. A conventional large sample test of $\hat{\nu}$, $\hat{k}$ against their hypothetical values under H_0, using their estimated variance-covariance matrix is not possible, since $\nu = 1$ and $k = 0$ separately imply H_0, and the

likelihood surface contains horizontal generators lying in the planes $\nu = 1$ and $k = 0$. However all that is required is to test the sample $(r_1, \ldots, r_n)$ for uniformity over $[0,1]$ against an alternative implying concentration of the R_1-distribution toward zero. A suitable procedure is a 1-tailed test of $(\frac{1}{2} - \bar{r})\sqrt{12n}$ as $N(0,1)$. (See Cox (1955)). If the test leads to the rejection of H_0, the estimates $\hat{\nu}$, $\hat{k}$ and their estimated variance-covariance matrix can be used for the estimation of $\nu(\neq 0)$ and $k(\neq 0)$, the log likelihood surface having the required paraboloidal form in the neighbourhood of the true parameter values.

One should note that inference based on the observed values of R_1 implies a loss of information inasmuch as only n out of the N observations of X and Y are used. However it has been shown that the expectation of n ranges from 0.093N for the triangular lattice, to $\frac{3}{4}$N for the Poisson forest, and then increases to N as aggregation increases. In light of the fact that lattice patterns are self evident and the test of randomness against the hypothesis of a lattice population is very powerful, the information loss is greatest where it can most be spared, and smallest where it is most needed.

In section 2.7 data will be tested for randomness against an alternative of aggregation using Cox's test described above. The results will be compared to those obtained by testing for randomness using Holgate's (1965) test statistic, $T = \sum x_i^2/v_i^2$, where x_i is the distance to the nearest tree from the sampling origin, and v_i is the distance of the second nearest tree to the sampling origin. For a large sample, T is distributed as $N(\frac{1}{2}, 1/(12N))$ for the Poisson forest.

In practical terms both tests require the same amount of work in collecting data.

2.7 Results

The method of analysis was used on data of three types. The first type is in the form of the co-ordinates of trees planted on rectangular lattices with death of some of the individuals. This was kindly made available by Dr. E. D. Ford of the Institute of Terrestrial Ecology, Penicuik, and described in Ford (1975). The second type consists of the co-ordinates of the six species of trees in Lansing Woods, Michigan, U.S.A., kindly supplied by Professor D. J. Gerrard. Data of the third type were simulated by a modified Thomas process (M.T.P.) as described in Diggle, Besag and Gleaves (1975), where clump centres, considered as trees, are distributed randomly, and a Poisson number of "offspring", with mean μ, are allocated to the clumps. The offspring are placed at distances distributed radially normally, with radial dispersion σ, from the clump centre, i.e. the joint p.d.f. of the radial co-ordinates of an offspring from the clump centre is

$$f(r,\theta) = r \exp(-\tfrac{1}{2}r^2/\sigma^2)/(2\pi\sigma^2) \qquad (r > 0, \quad 0 \leq \theta \leq 2\pi).$$

Fig. 2(10) shows sections of data from the rectangular lattices with death, and from the simulated data. Figures showing the data from Lansing Woods can be found in Chapter 4 on pages 91-107.

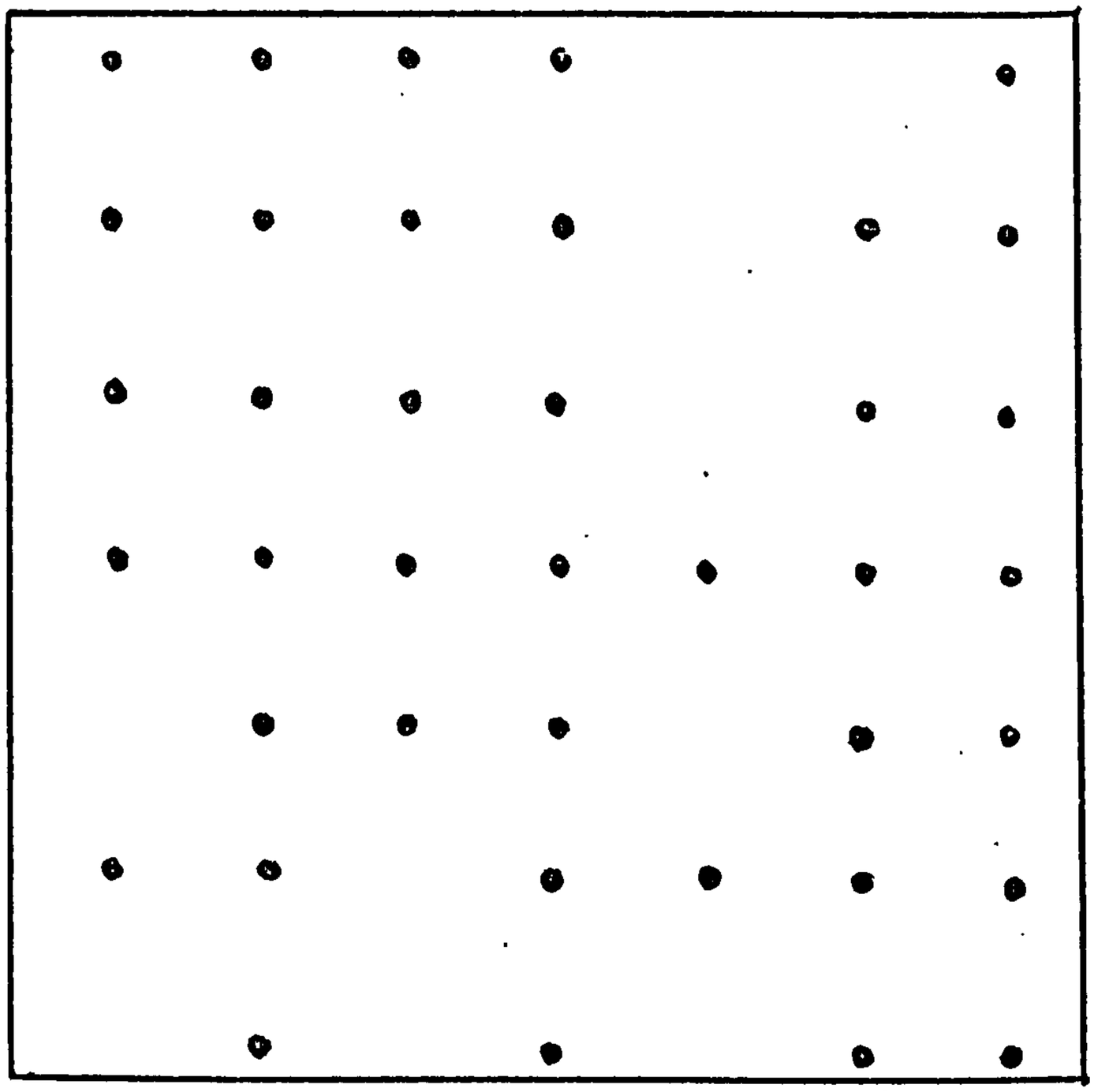

(i) Lattice popn. with death

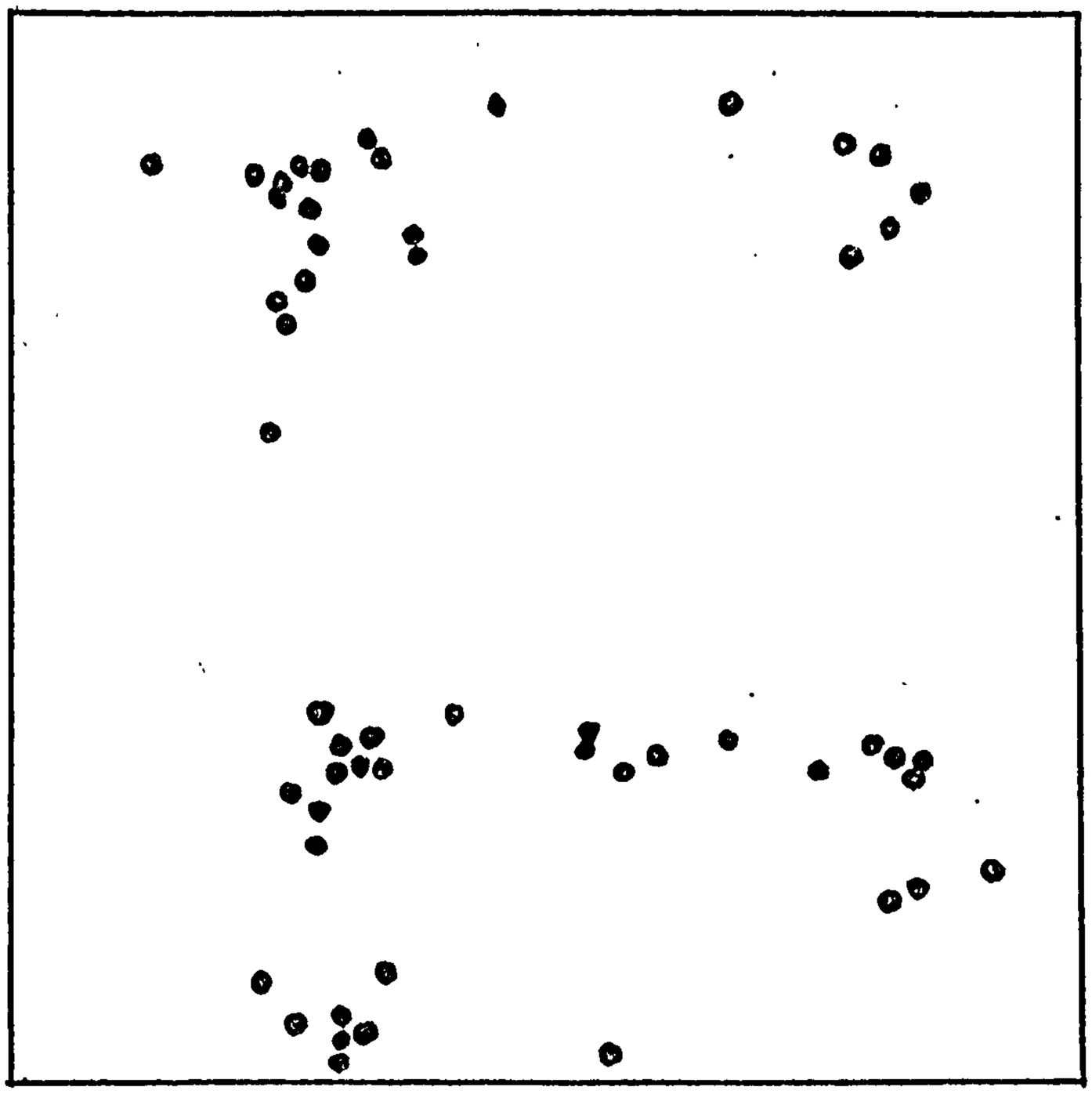

(ii) M.T.P. ($\mu = 5.0$, $\sigma = 0.2$)

Fig. 2(10) Examples of the data

For each set of data, 100 sample origins were selected at random, giving 100 pairs (X,Y) for analysis. Fig.2(11) shows histograms of the r_i's. Tables 1 and 2 summarise the results obtained.

The values of Cox's statistic for testing the r_i's in each data set for uniformity (and hence the spatial pattern for randomness) are shown in Table 1, together with the results of Holgate's randomness test for comparison. Table 1 also gives the results of a Kolmogorov-Smirnov test applied to each data set to test the hypothesis that the W_{2j}'s are from a uniform distribution.

Table 2 shows the estimated values, $\hat{p}$, $\hat{k}$ and their variance-covariance matrix for the sets of data for which Cox's test rejected randomness in favour of clumping. Also given in Table 2 are the results of a χ^2 test, to test the fit of the aggregation model. This is done by finding the expected number of the N points to be found in each of 20 disjoint intervals covering $[0,1]$ from the p.d.f. $g(r; \nu, k)$, ν and k having been estimated by $\hat{\nu}$ and $\hat{k}$. The χ^2 value is then found in the usual manner.

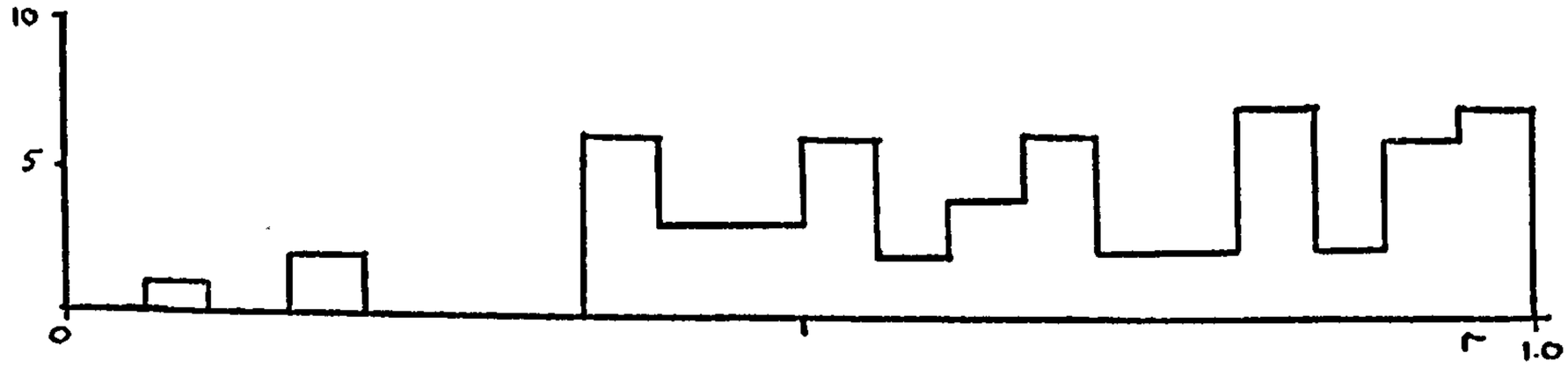

(i) Rect. lattice No. 1

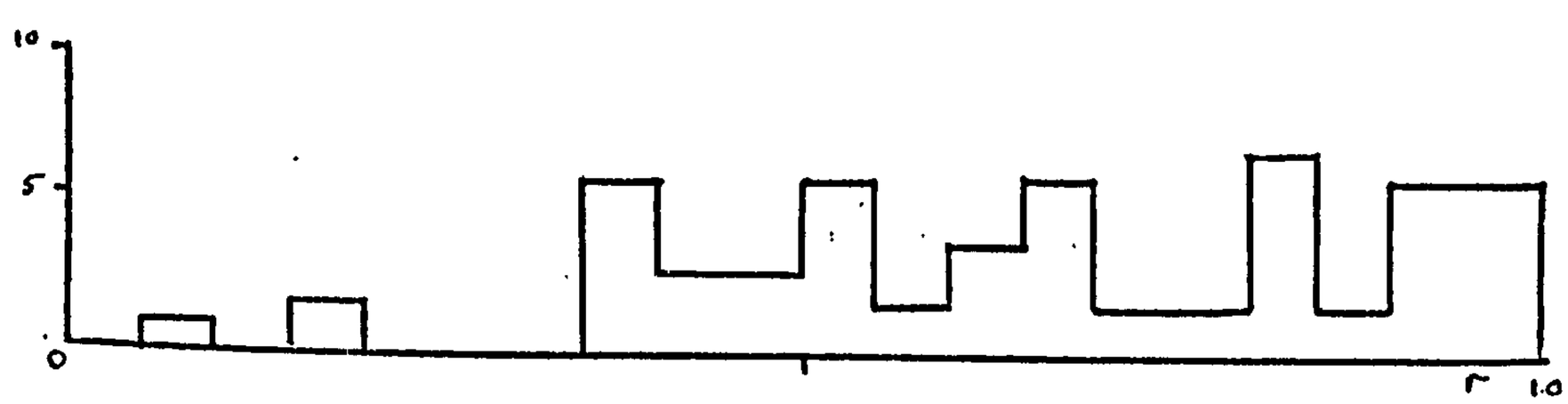

(ii) Rect. lattice No. 2

(iii) Rect. lattice No. 3

Fig. 2(11) Sample r_i's for the data sets.

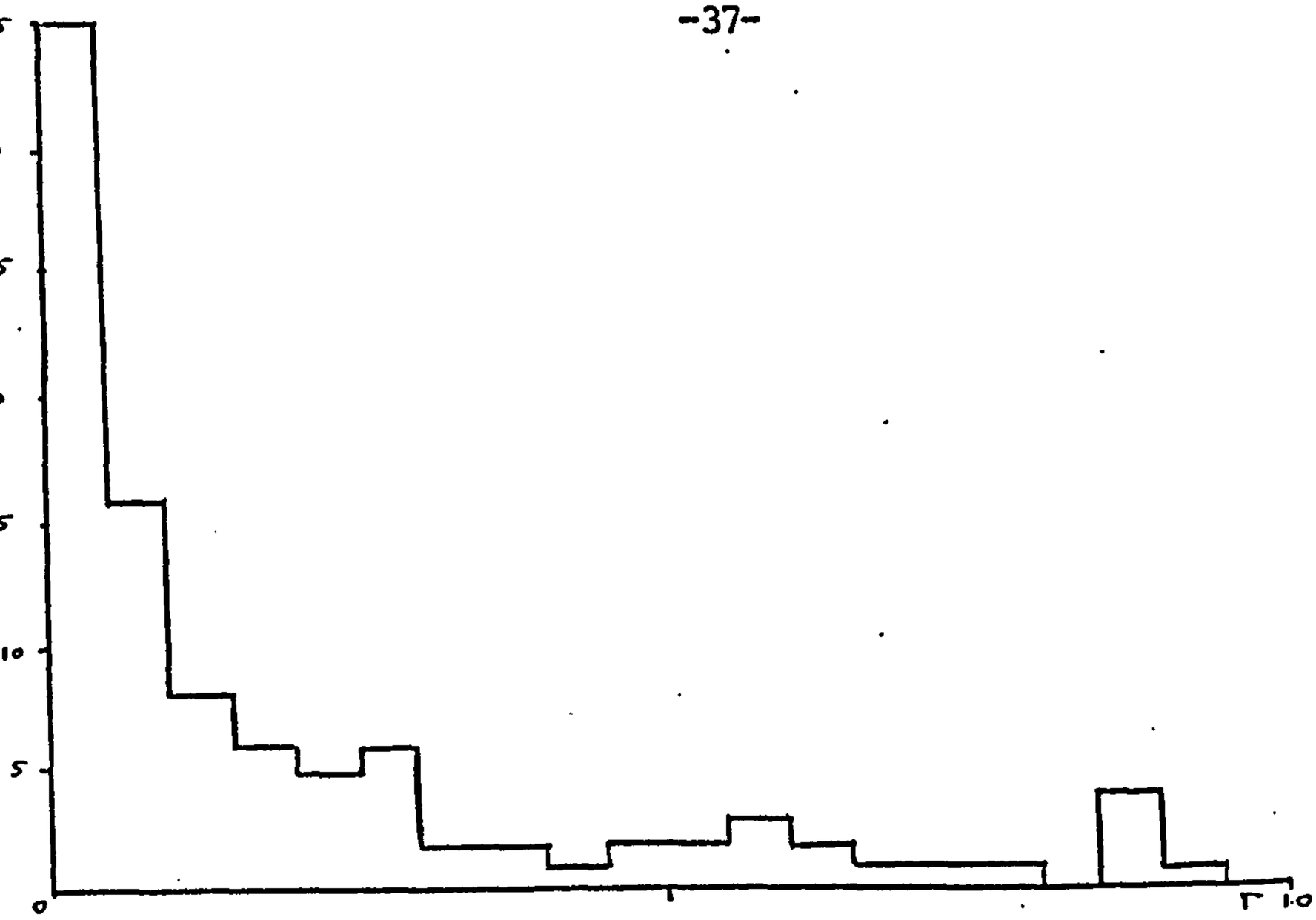

(iv) M.T.P. ($\mu = 5.0$, $\sigma = 0.2$)

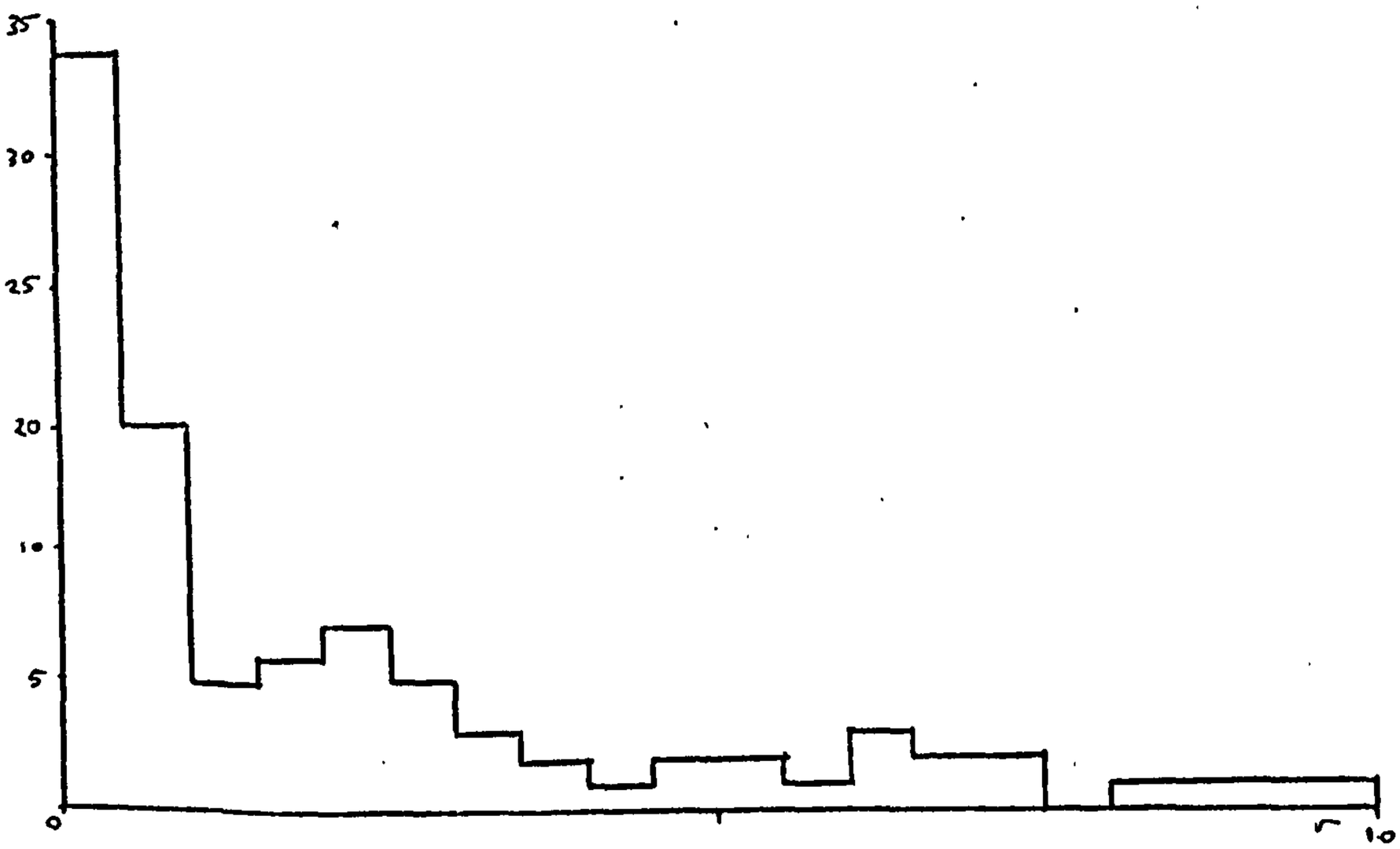

(v) M.T.P. ($\mu = 2.0$, $\sigma = 0.2$)

(vi) M.T.P. ($\mu = 5.0$, $\sigma = 1.0$)

Fig. 2(11) continued

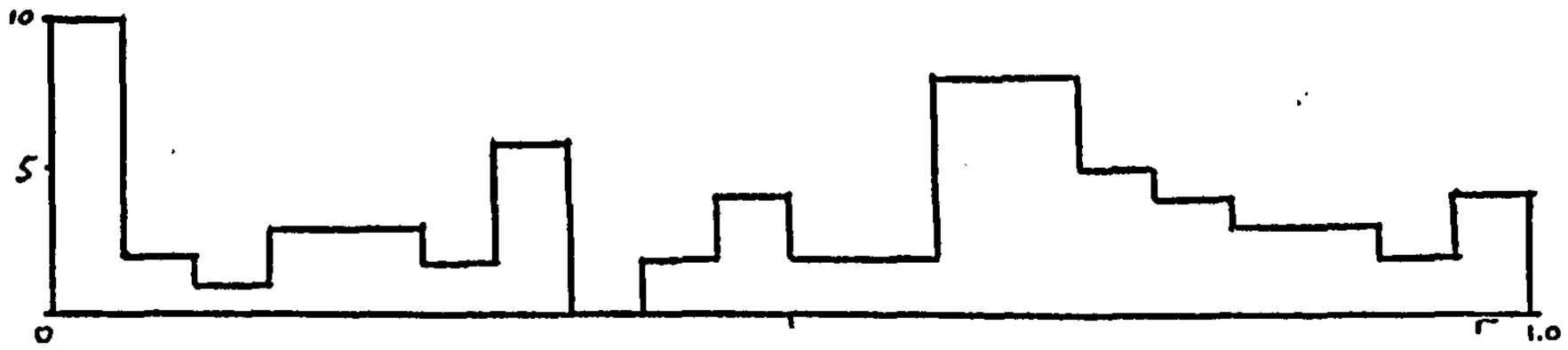

(vii) Hickories

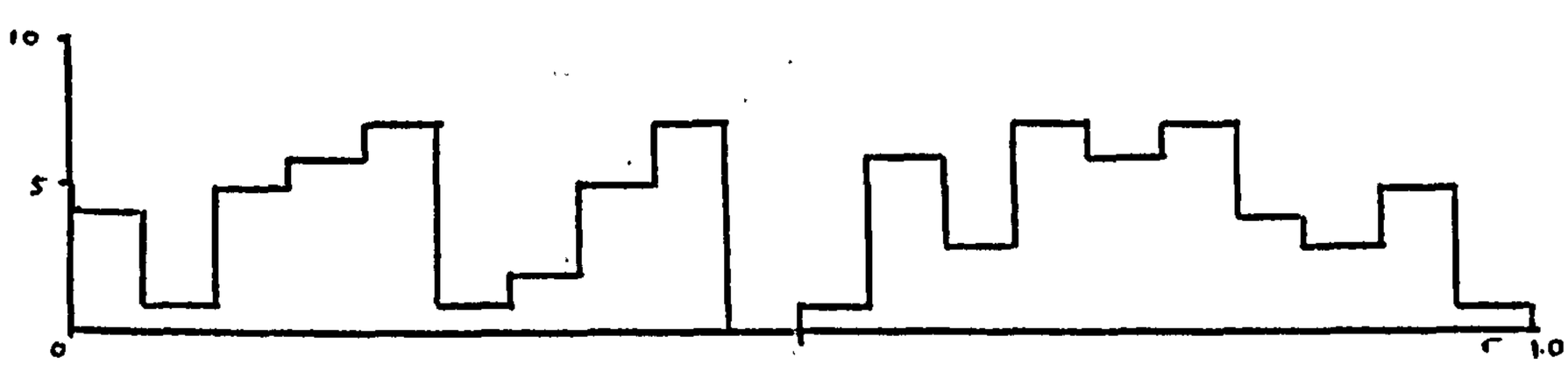

(viii) White oaks

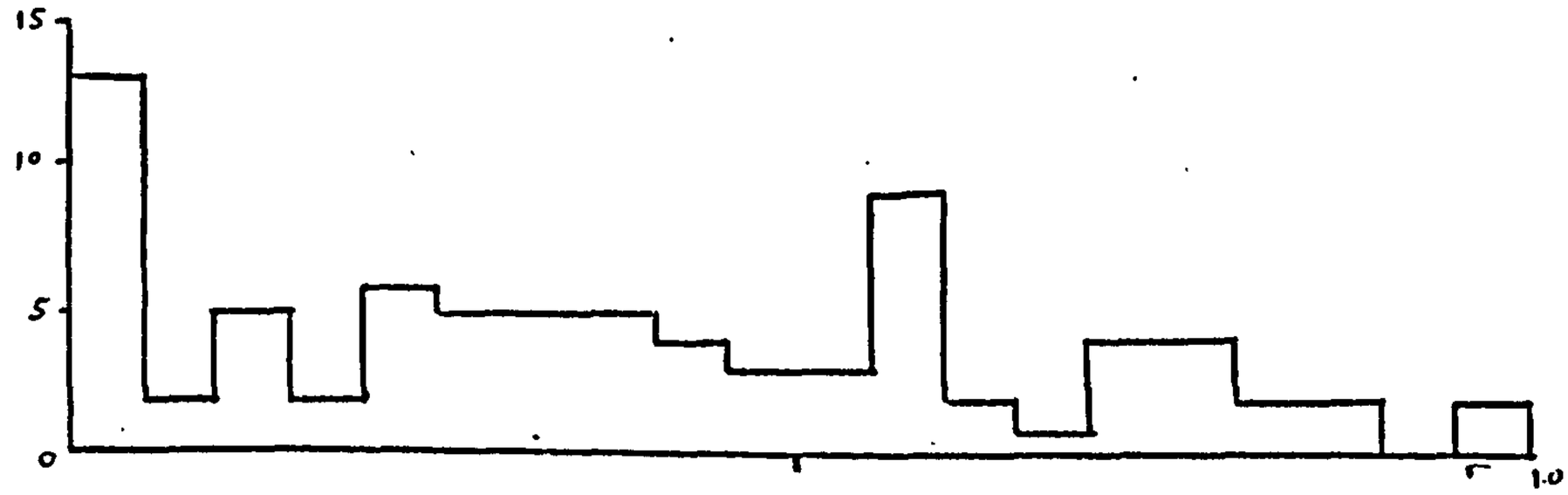

(ix) Red oaks

Fig. 2(11) continued

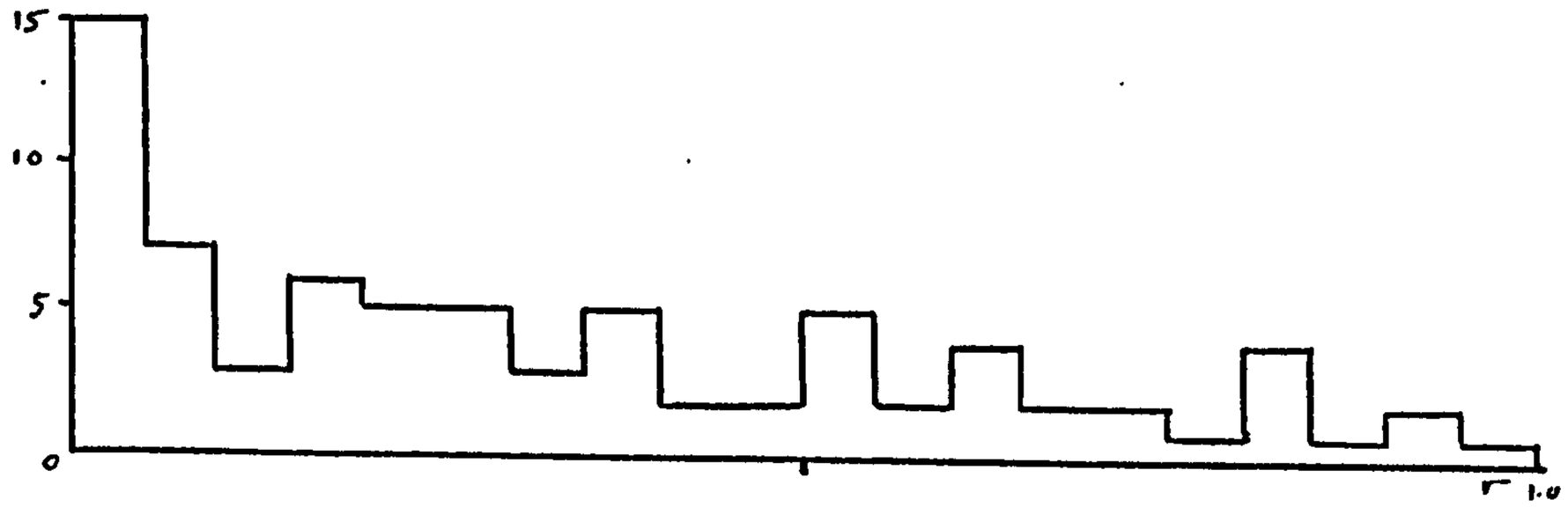

(x) Black oaks

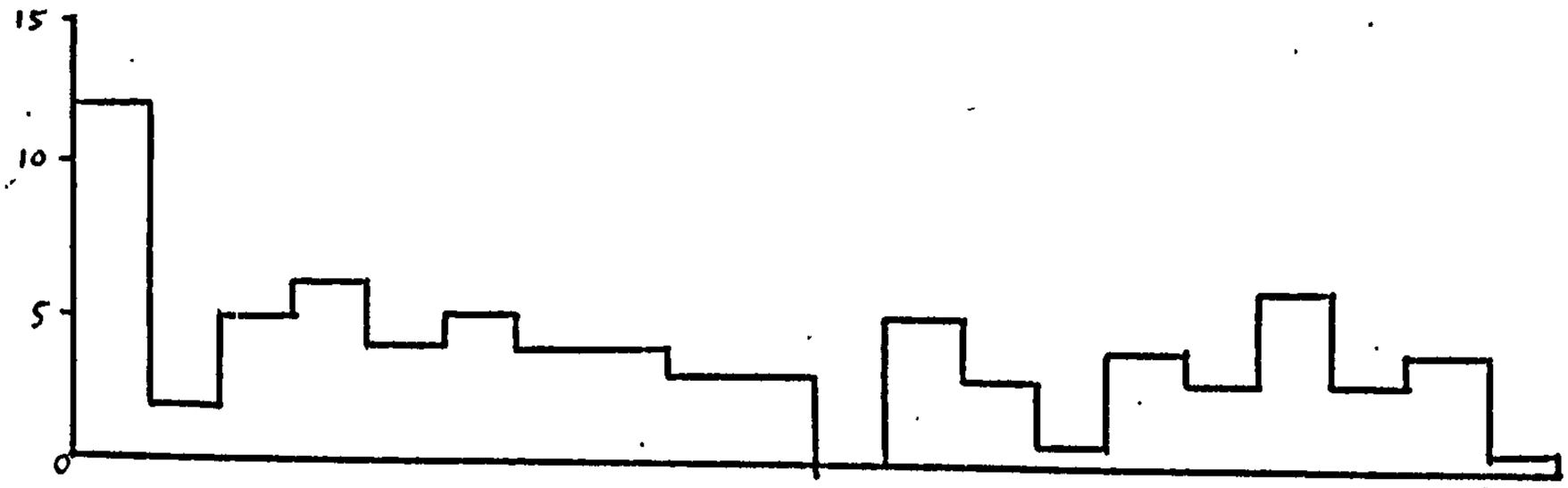

(xi) Maples

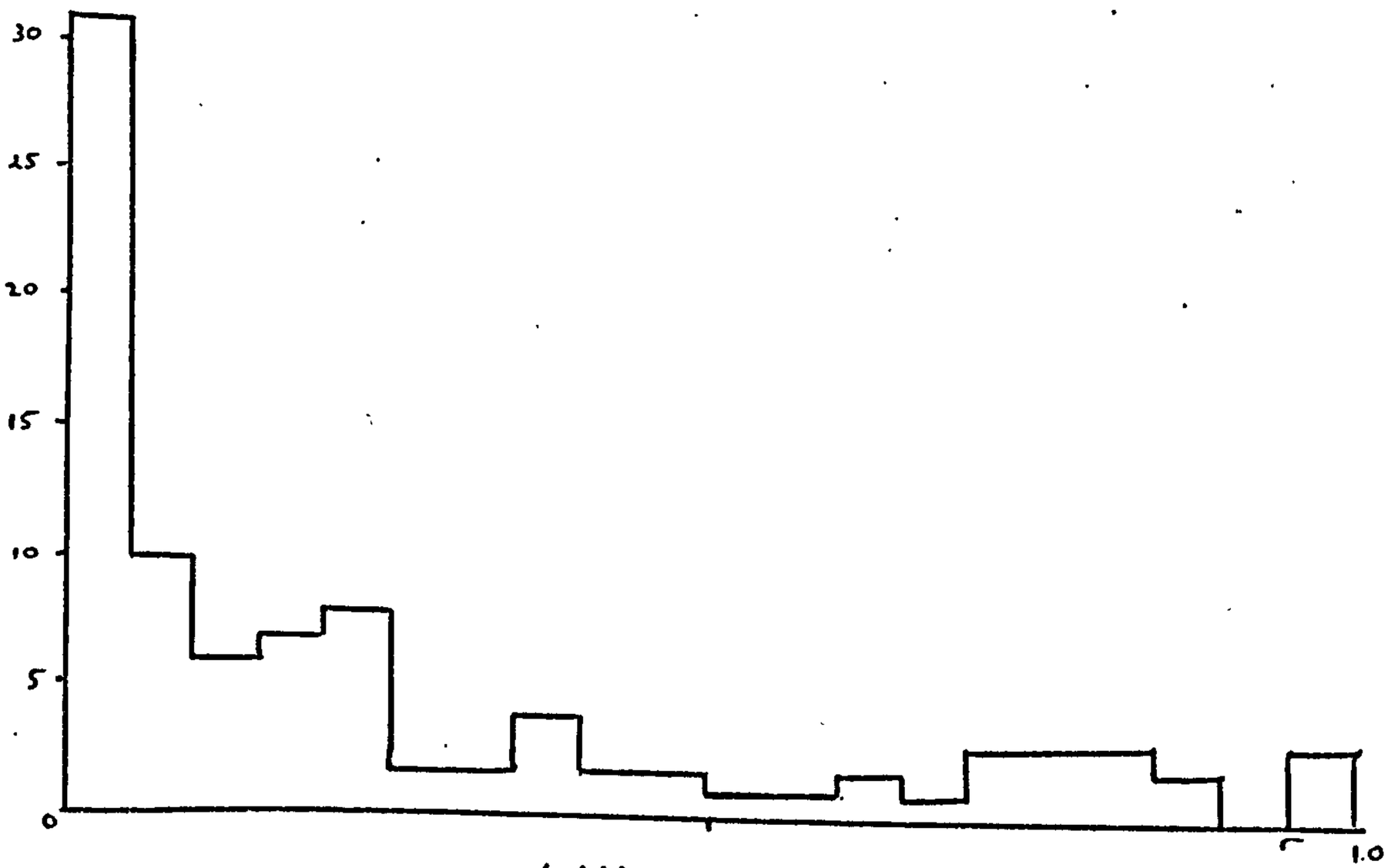

(xii) Miscellaneous trees

Fig. 2(11) continued

Table 1. Cox's test and Holgate's test for randomness, together with a Kolmogorov-Smirnov test for uniformity of the W_{2j}'s.

Type of forest	n	Cox's Test	Holgate's Test	K-S test for W_{2j}'s
Rect. lattice No. 1 with death	52	-	-	0.10
Rect. lattice No. 2 with death	59	-	-	0.07
Rect. lattice No. 3 with death	55	-	-	0.18
M.T.P. (μ= 5.0, σ = 0.2)	98	10.14**	0.71**	0.40
M.T.P. (μ= 2.0, σ = 0.2)	89	9.26**	0.64**	0.10
M.T.P. (μ= 5.0, σ = 1.0)	71	0.57	0.47	0.11
Hickories in Lansing Woods	74	0.06	0.45	0.11
White oaks in Lansing Woods	81	0.22	0.51	0.19
Red oaks in Lansing Woods	79	3.52**	0.89**	0.23
Black oaks in Lansing Woods	77	4.82**	0.57*	0.12
Maples in Lansing Woods	78	2.42**	0.56*	0.21
Miscellaneous in Lansing Woods	93	8.00**	0.69**	0.19

* significant at 5%, ** significant at 1%

Table 2: The values of $\hat{\nu}$, $\hat{k}$ and their estimated var-cov matrix, together with a χ^2 test for the fit of the aggregation model.

Type of forest	$\hat{\nu}$	$\hat{k}$	var-cov matrix	χ^2_7
M.T.P. (μ= 5.0, σ = 0.2)	0.17	12.58	$\begin{pmatrix} 0.02 & 0.21 \\ 0.21 & 5.13 \end{pmatrix}$	2.98
M.T.P. (μ= 2.0, σ= 0.2)	0.16	10.15	$\begin{pmatrix} 0.001 & 0.26 \\ 0.26 & 29.92 \end{pmatrix}$	4.63
Red oaks	0.92	16490	$\begin{pmatrix} 2.0 \times 10^{-3} & 62.6 \\ 62.6 & 64 \times 10^{7} \end{pmatrix}$	10.88
Black oaks	0.51	6.36	$\begin{pmatrix} 3.0 \times 10^{-3} & 0.93 \\ 0.93 & 428 \end{pmatrix}$	3.00
Maples	0.92	9706	$\begin{pmatrix} 1.0 \times 10^{-3} & 28.2 \\ 28.2 & 4.0 \times 10^{7} \end{pmatrix}$	4.69
Miscellaneous trees	0.34	14.31	$\begin{pmatrix} 0.04 & 0.32 \\ 0.32 & 6.25 \end{pmatrix}$	7.21

Inspection of the histograms of the r_i's for the rectangular lattices with death indicates that the patterns are obviously far from random. The effect of the missing individuals is shown up by values of the r_i's near to zero.

In the case of the simulated data, when the radial dispersion of the modified Thomas process becomes relatively large, the pattern becomes effectively indistinguishable from a Poisson forest. This is illustrated by the sample with $\lambda = 5.0$ and $\sigma = 1.0$, (the density of the clump centres being 0.44). The other two modified Thomas processes both fitted well to the aggregation model, as indeed they should do, the single trees occurring when there are no offspring in a clump, and the local Poisson forests occurring otherwise.

The data from Lansing Woods proves to be the most interesting. It appears that the Hickories and White oaks each form a Poisson forest, while the Red oaks, Black oaks, Maples and Miscellaneous trees tend towards clumping. In each case $\hat{\nu}$ measures the tendency towards clumping and $\hat{k}$ is a measure of the density of the clumps. Note that the Red oaks and Maples tend only to very slight clumping (i.e. $\hat{\nu}$ near 1), but with clumps which are very dense (i.e. $\hat{k}$ large). The Black oaks and Miscellaneous trees tend very much towards clumping.

It is pleasing to note that the test of randomness based on the r_i's has given the same results as Holgate's test of randomness. However when aggregation does occur, the new method may well give more insight into the pattern through $\hat{\nu}$ and $\hat{k}$.

In each of the twelve sets of data, which ranged from regular, to random, to aggregation, the Kolmogorov-Smirnov test gave

no evidence for rejecting the hypothesis that the W_{2j}'s were from a uniform distribution. It would be interesting to know what is the class of stationary spatial point processes, where multiple events do not dominate, for which W_2 is not distributed uniformly on $[0,1]$. This class would seem to be quite restricted.

Appendix A

A regression equation is fitted to the log likelihood, $L_{ij}(\nu, k)$ as described in Chapter 2. Thus let

$$L_{ij}(\nu, k) = a\nu_i^2 + b\nu_i k_j + ck_j^2 + d\nu_i + ek_j + f + \varepsilon_{ij}, \qquad (1)$$

where a, b, c, d, e, f are constants, and $\varepsilon_{ij} \sim N(0, \sigma^2)$. L_{ij} is the value of the log likelihood over a grid of points p_i, k_j which contains max(L). The constants are found in the usual way using least squares which is carried out by use of a statistical package, GLIM, developed by the Working Party on Statistical Computing of the Royal Statistical Society.

Fishers information matrix is given by $E\left[\left(\frac{\partial^2 L(x_i, x_j)}{\partial x_i \partial x_j}\right)\right]$, (see e.g. Silvey (1970)), i.e.

$$\begin{bmatrix} E\left(\frac{\partial^2 L(\nu,k)}{\partial \nu^2}\right) & E\left(\frac{\partial^2 L(\nu,k)}{\partial \nu \partial k}\right) \\ E\left(\frac{\partial^2 L(\nu,k)}{\partial \nu \partial k}\right) & E\left(\frac{\partial^2 L(\nu,k)}{\partial k^2}\right) \end{bmatrix}.$$

From equation (1), Fishers information matrix is thus

$$\begin{bmatrix} 2a & b \\ b & 2c \end{bmatrix}.$$

Hence by inversion, the variance-covariance matrix of ν and k is

$$\frac{1}{(4ac-b^2)} \begin{bmatrix} 2c & -b \\ -b & 2a \end{bmatrix}.$$

CHAPTER 3

THE ROBUST ESTIMATION OF DENSITY

3.1 Introduction

In chapter 2 a method for analysing spatial patterns was proposed which does not depend on the density of the spatial process. In fact only pairs of distances need to be measured each based on N sampling origins placed at random within the population.

As the density of the process may be of interest especially to the forester, two new robust density estimators are proposed which use the same distance measurements as for the method of analysing the spatial pattern, viz (X_i,Y_i) $i = 1, \ldots, N$, where X_i is the distance from the ith randomly placed sampling origin to the nearest tree (say), and Y_i is the distance from this tree to its nearest neighbour.

As in chapter 2, the N pairs of measurements (X_1,Y_1) ..., (X_N,Y_N) are split into two sets A and B, where

$$A = \{(X_i,Y_i) : Y_i \leq 2X_i \qquad (i = 1, \ldots, n)\},$$

$$B = \{(X_j,Y_j) : Y_j > 2X_j \qquad (j = 1, \ldots, m)\}, \quad (m + n = N).$$

For convenience we relabel the members of A and B as (X_{1i},Y_{1i}) and (X_{2j},Y_{2j}) respectively.

Define the random variables,

$$Z_{1i}^2 = X_{1i}^2 \{2\pi + \sin\Phi_{1i} - (\pi + \Phi_{1i})\cos\Phi_{1i}\} / \pi$$

$$(i = 1, \ldots, n),$$

where $\sin(\frac{1}{2}\Phi_{1i}) = \frac{1}{2}Y_{1i}/X_{1i}$.

The aim is to find estimators of the density, λ trees per unit area, or equivalently the mean area per tree or inverse density, $\Theta = \lambda^{-1}$, based on the random variables just defined.

3.2 The Poisson forest

The joint p.d.f. of X_1 and Φ_1 is

$$\frac{8}{3}\pi(\pi+\phi)\Theta^{-2}\, x^3 \sin\phi \exp\left[-x^2\Theta^{-1}\{2\pi + \sin\phi - (\pi+\phi)\cos\phi\}\right] \quad (1)$$

$$(0 < x < \infty\ ,\ 0 < \phi < \pi\ )$$

(see Chapter 2 equation (13)).

The joint p.d.f. of X_2 and Y_2 is

$$16\pi^2\Theta^{-2}\, xy \exp(-\Theta^{-1}\pi y^2) \quad (0 < x < \infty\ ,\ 2x < y < \infty\ ) \quad (2)$$

(see Chapter 2 equation (14)).

The likelihood of the observations $\{(x_{1i}, y_{1i})\}$, $\{(x_{2j}, y_{2j})\}$ is

$$L(\Theta) = \binom{N}{m} \prod_{i=1}^{n} \frac{8}{3}\pi(\pi+\phi_{1i})\Theta^{-2}\, x_{1i}^3 \sin(\phi_{1i}) \exp\left[-x_{1i}^2\Theta^{-1}\{2\pi + \sin(\phi_{1i}) - (\pi+\phi_{1i})\cos(\phi_{1i})\}\right]$$

$$\times \prod_{j=1}^{m} 16\pi^2\Theta^{-2}\, x_{2j}y_{2j} \exp(-\pi y_{2j}^2\,\Theta^{-1}).$$

Hence

$$\frac{\partial \log L(\Theta)}{\partial \Theta} = -2(n+m)\Theta^{-1} + \sum_{i=1}^{n}\left[x_{1i}^2\,\Theta^{-2}\{2\pi + \sin(\phi_{1i}) - (\pi+\phi_{1i})\cos(\phi_{1i})\}\right] + \sum_{j=1}^{m}\pi y_{2j}^2\,\Theta^{-2}.$$

Thus the maximum likelihood estimator of Θ is

$$\hat{\Theta}_L = \tfrac{1}{2}\pi\Big(\sum_{i=1}^{n} z_{1i}^2 + \sum_{j=1}^{m} y_{2j}^2\Big)/N.$$

Because $\frac{\partial \log L}{\partial \Theta} = 2N(\hat{\Theta}_L - \Theta)/\Theta^2$, $\hat{\Theta}_L$ is unbiased, fully efficient, with variance $\tfrac{1}{2}\Theta^2/N$.

From equation (1), the joint p.d.f. of X_1 and Z_1 is

$$\tfrac{16}{3}\pi^2\Theta^{-2}\, z_1 x_1 \exp(-\pi\Theta^{-1}z_1^2) \qquad (x_1 \leq z_1 \leq 2x_1,\ 0 \leq x_1 < \infty).$$

Hence the marginal p.d.f. of Z_1 is

$$\int_{z_1/2}^{z_1} \tfrac{16}{3}\pi^{-2}\Theta^{-2}\, z_1 x_1 \exp(-\pi\Theta^{-1}z_1^2)\, dx_1 \qquad (0 \leq z_1 < \infty),$$

which integrates to

$$2\pi^2\Theta^{-2}z_1^3 \exp(-\pi\Theta^{-1}z_1^2) \qquad (0 \leq z_1 < \infty).$$

Similarly the marginal p.d.f. of Y_2 is

$$\int_{0}^{y_2/2} 16\pi^2\Theta^{-2}\, x_2 y_2 \exp(-\pi\Theta^{-1}y_2^2)\, dx_2 \qquad (0 \leq y_2 < \infty),$$

which is

$$2\pi^2\Theta^{-2}y_2^3 \exp(-\pi\Theta^{-1}y_2^2) \qquad (0 \leq y_2 < \infty). \tag{3}$$

Thus Z_1^2 and Y_2^2 are identically distributed with mean $2\Theta/\pi$ and variance $2\Theta^2/\pi^2$.

Now $\hat{\Theta}_L$ has of course been derived specifically for the Poisson forest. We now modify it so that it is approximately unbiased for a

wide range of spatial patterns.

3.3 The Estimator $\hat{\theta}$

If $\hat{\theta}_L$ from the previous section were used for patterns other than the Poisson forest, it would generally be biased. In order to overcome this we vary the coefficient of the estimator according to some quantitative feature of the spatial pattern, whose value varies with the type of pattern. The feature chosen is p, the probability that $Y > 2X$, which varies from 0.91 for trees at the vertices of a triangular lattice, through 0.25 for a Poisson forest, to zero for the case of extreme aggregation, in which the trees form clumps of coincident points. In the sample situation, p can be estimated from the N pairs of measurements (X,Y) by m/N, the relative frequency of the event $Y > 2X$. Accordingly, consider the estimator

$$T = (a + bm/N)\,\hat{\theta}_L$$

$$= \tfrac{1}{2}\pi(a + bm/N)\left(\sum_{i=1}^{n} z_{1i}^2 + \sum_{j=1}^{m} y_{2j}^2\right)/N,$$

where a and b are constants chosen to make T effectively unbiased for a wide range of spatial patterns.

The expectation of T, conditional on m, is

$$\tfrac{1}{2}\pi(a + bm/N)(n\mu_z + m\mu_y),$$

where $\mu_z = E(Z_1^2)$, $\mu_y = E(Y_2^2)$, and hence

$$E(T) = \tfrac{1}{2}\pi\left\{(a + bp)(q\mu_z + p\mu_y) + bpq(\mu_y - \mu_z)/N\right\},$$

where $q = 1-p$.

Thus T is asymptotically unbiased for any particular spatial pattern if

$$a + bp = 2\theta/\{\pi(q\mu_z + p\mu_y)\} \qquad (= V, \text{ say}) \qquad (4)$$

for that spatial pattern.

V is a parameter with a value for each spatial pattern. In particular, for a Poisson forest $V = 1$ and $E(T) = \theta$ exactly if $a + \frac{1}{4}b = 1$.

For a forest formed by the vertices of a triangular lattice of side d, the p.d.f. of X is

$$\begin{aligned} &4\pi x/(\sqrt{3}d^2) && (0 \leqslant x \leqslant \tfrac{1}{2}d) \\ &4x\{\pi - 6\cos^{-1}(\tfrac{1}{2}d/x)\}/(\sqrt{3}d^2) && (\tfrac{1}{2}d \leqslant x \leqslant d/\sqrt{3}), \end{aligned}$$

(see Chapter 2, equation (15)).

Obviously $pr(Y = d) = 1$, $\theta = \frac{1}{2}\sqrt{3}\, d^2$, and

$$pr(Y > 2X) = p = \int_0^{\frac{1}{2}d} 4\pi x/(\sqrt{3}d^2)\, dx,$$

$$= \tfrac{1}{2}\pi/\sqrt{3}.$$

Hence $E(Y_2^2) = 2\theta/\sqrt{3}$ and $var(Y_2^2) = 0$. The expressions for the mean and variance of Z_1^2 are rather complicated and are best calculated by means of a computer program. Similar results can be obtained for square and hexagonal lattices. The values of p, V, and the means and variances of Z_1^2 and Y_2^2 are given in Table 3 for the triangular lattice, the square lattice, the hexagonal lattice, and also for the Poisson forest.

For an aggregation pattern, a Thomas process, Thomas (1949), is used. Here clump centres, considered as trees occur as a Poisson forest and each clump has a Poisson number, with mean α, of "offspring" trees which are coincident with the clump centre. This model is not completely realistic, but it does provide a good aggregation model when the pattern is almost a Poisson forest, i.e. when α is small. For the Thomas process $p = \frac{1}{4}\exp(-\alpha)$ and $E(T) = \{a + \frac{1}{4}b \exp(-\alpha)\} (1 + \alpha)\Theta$. The means and variances of Z_1^2 and Y_2^2 for the Thomas process for various values of α are shown in Table 3.

Table 3. The values of $p, \mu_z, \sigma_z^2, \mu_y, \sigma_y^2$, and V for various patterns where $\mu_z = E(Z_1^2)$, $\sigma_z^2 = \text{var}(Z_1^2)$, $\mu_y = E(Y_2^2)$, $\sigma_y^2 = \text{var}(Y_2^2)$ and $V = 2\Theta/\{\pi (q\mu_z + p\mu_y)\}$.

Pattern	p	μ_z/Θ	σ_z^2/Θ^2	μ_y/Θ	σ_y^2/Θ^2	V
Triangular lattice	0.91	1.16	8.0×10^{-5}	1.15	0	0.55
Square lattice	0.79	1.03	1.1×10^{-3}	1.00	0	0.63
Hexagonal lattice	0.60	0.88	9.7×10^{-3}	0.77	0	0.78
Poisson forest	0.25	0.64	0.20	0.64	0.20	1.00
Thomas Process ($\alpha = 0.1$)	0.23	0.70	0.25	0.70	0.25	0.91
" " ($\alpha = 0.5$)	0.15	0.95	0.46	0.95	0.46	0.67
" " ($\alpha = 1.0$)	0.09	1.27	0.81	1.27	0.81	0.50
" " ($\alpha = 2.0$)	0.03	1.91	1.82	1.91	1.82	0.33
" " ($\alpha = 3.0$)	0.01	2.55	3.24	2.55	3.24	0.25
" " ($\alpha = 5.0$)	0.002	3.82	7.30	3.82	7.30	0.17

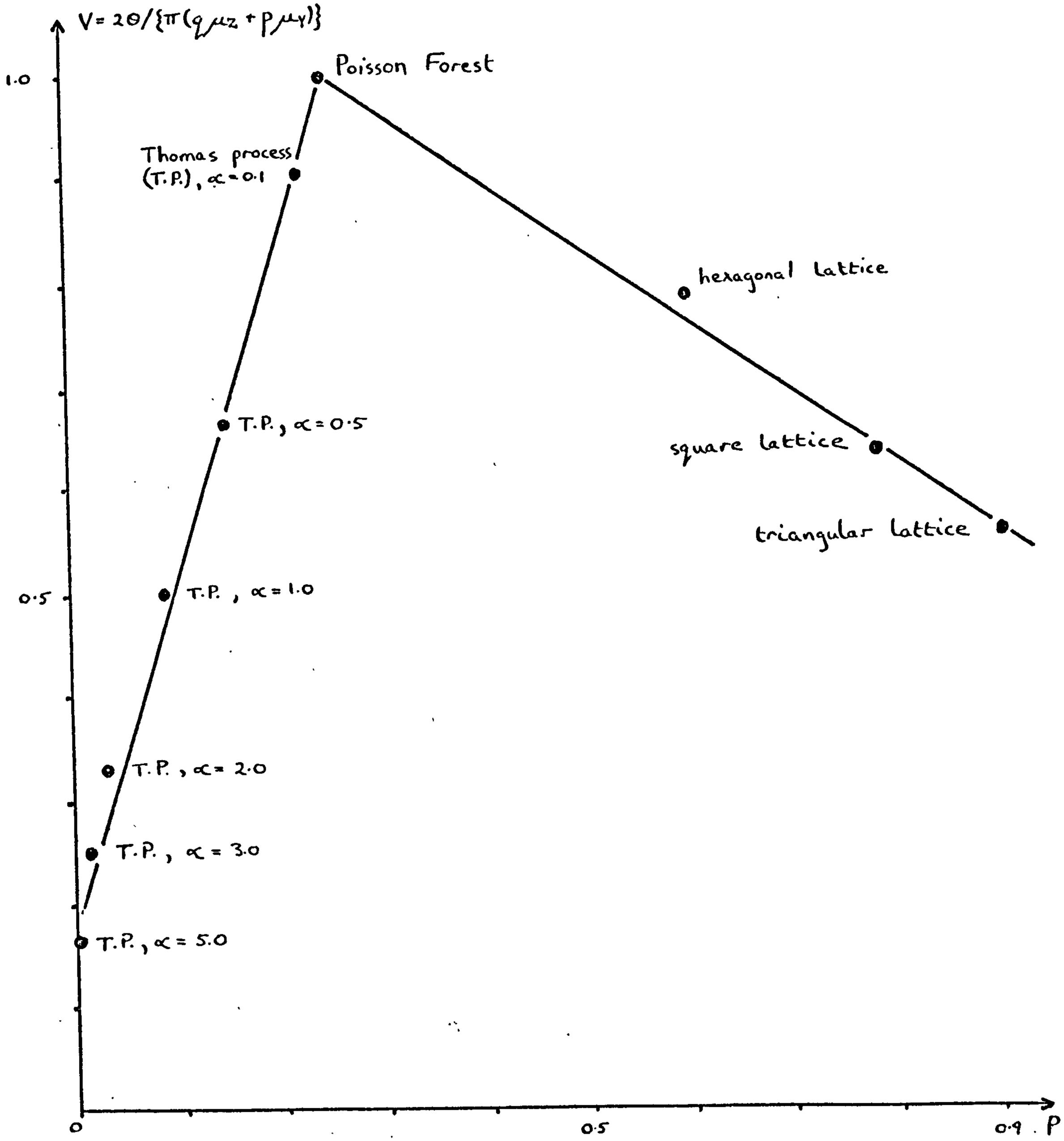

Fig. 3(1) Values of V plotted against p for various spatial patterns

Fig. 3(1) shows values of V plotted against the values of p for the various spatial patterns. It will be seen that the points happen to fall effectively on two straight lines, and thus the constants a and b from equation (4) can be calculated for each of these lines. The constant 'b' is given the value of the estimated slope of the line in each case, and the constant 'a' is given the value which makes the line pass through ($\frac{1}{4}$, 1) in each case. Hence consider the following two estimators based on T,

$$\hat{\Theta}_1 = \tfrac{1}{2}\pi(1.17 - 0.68m/N)\Big(\sum_{i=1}^{n} z_{1i}^2 + \sum_{j=1}^{m} Y_{2j}^2\Big)/N,$$

and

$$\hat{\Theta}_2 = \tfrac{1}{2}\pi(0.20 + 3.20m/N)\Big(\sum_{i=1}^{n} z_{1i}^2 + \sum_{j=1}^{m} Y_{2j}^2\Big)/N.$$

The appropriate estimator $\hat{\Theta}_1$ or $\hat{\Theta}_2$ is approximately unbiased for any spatial pattern whose value of V lies on or near one of the two straight lines in Fig.3(1). This is because V happens to be equal to the appropriate (a + bp).

The variance of $\hat{\Theta}_i$ (i = 1, 2) is after much algebra

$$\tfrac{1}{4}\pi^2\Big[(a_i + b_i p)(p\sigma_y^2 + q\sigma_z^2) + pq\{(a_i + b_i - 2b_i q)\mu_z - (a_i + 2b_i p)\mu_y\}^2\Big]/N$$

$$+ O(1/N^2) \qquad (i = 1, 2,),$$

where $a_1 = 1.17$, $b_1 = -0.68$, $a_2 = 0.20$ and $b_2 = 3.20$.

If we knew beforehand whether the spatial pattern underlying the data was on the regular or aggregated side of a random process, we would know which of $\hat{\Theta}_1$ or $\hat{\Theta}_2$ to use as an estimator of Θ. In practice this decision can be based on the value of m/N, and the following estimator $\hat{\Theta}$ is accordingly proposed,

$$\hat{\Theta} = \tfrac{1}{2}\pi(1.17 - 0.68m/N)\Big(\sum_{i=1}^{n} z_{1i}^2 + \sum_{j=1}^{m} y_{2j}^2\Big)/N \qquad (m \geqslant \tfrac{1}{4}N)$$

$$\tfrac{1}{2}\pi(0.20 - 3.20m/N)\Big(\sum_{i=1}^{n} z_{1i}^2 + \sum_{j=1}^{m} y_{2j}^2\Big)/N \qquad (m < \tfrac{1}{4}N).$$

The expectation and variance of Θ are not the same as those for $\hat{\Theta}_1$ ($\hat{\Theta}_2$) because of the risk of misclassification when $p > \frac{1}{4}$ and $m/N < \frac{1}{4}$ and vice versa. After much algebra

$$E(\hat{\Theta}) \doteq \tfrac{1}{2}\pi\Big[\{1.17-0.68p)-0.97(1-4p)\,\bar{\Phi}(L)-3.88(\tfrac{1}{2}pq/\pi)^{\frac{1}{2}}e^{-\frac{1}{2}L^2}/N^{\frac{1}{2}}\}\{q\mu_z+p\mu_y\}$$

$$+ pq(\mu_y-\mu_z)\{-0.68 + 3.88\,\bar{\Phi}(L)\}/N\Big],$$

where $L = N(\frac{1}{4}-p)/(Npq)^{\frac{1}{2}}$, and $\bar{\Phi}(\cdot)$ is the standard normal distribution function (see Appendix B for details).

$$\text{As } N\to\infty\ ,\ E(\hat{\Theta}) \to \begin{cases} \tfrac{1}{2}\pi(1.17-0.68p)(q\mu_z+p\mu_y) & (p > \tfrac{1}{4}) \\ \tfrac{1}{2}\pi(0.75\mu_z+0.25\mu_y) & (p = \tfrac{1}{4}) \\ \tfrac{1}{2}\pi(0.20+3.2p)(q\mu_z+p\mu_y) & (p < \tfrac{1}{4}). \end{cases}$$

Thus for patterns for which $2\Theta/\{\pi\ (q\mu_z + p\mu_y)\}$ lies on or near one of the straight lines in Fig.3(1), $\hat{\Theta}$ is approximately unbiased, except when p is near $\frac{1}{4}$ and for small N. However Table 4 shows that for the Poisson forest with N = 500, the bias is only 0.03Θ.

The variance of $\hat{\Theta}$ is extremely long and awkward. Details can be found in Appendix B. After much tedious algebra

$$\text{var}(\hat{\Theta}) \doteq \frac{\pi^2}{4N}\Big[\Big\{(1.17-0.68p)^2(1-\bar{\Phi})+(0.20+3.2p)^2\bar{\Phi}\Big\}\{q\sigma_z^2+p\sigma_y^2\}$$

$$+ 0.9409\,N\,\bar{\Phi}(1-\bar{\Phi})(q\mu_z+p\mu_y)^2+pq(\mu_z^2 d_z+2\mu_y\mu_z d_{zz}+\mu_z^2 d_z)$$

$$+ C\{\mu_z^2 g_z+\mu_y\mu_z g_{yz}+\mu_y^2 g_y\}$$

$$- 7.5272(1-4p)\,\bar{\Phi}(q\mu_z+p\mu_y)^2-15.0544\,C^2(q\mu_z+p\mu_y)^2/N\Big], \qquad (5)$$

where $\Phi = \Phi(L)$; $(L = N(\frac{1}{4}-p)/(Npq)^{\frac{1}{2}})$, $C = \sqrt{\frac{Npq}{2\pi}}\ e^{-\frac{1}{2}L^2}$,

$$d_z = (3.4225-5.0320p+1.8496p^2)+(4.0255-56.6480p+63.9424p^2)\Phi - 7.5272(1-p)(1-4p)\Phi^2,$$

$$d_{yz} = (-2.1645+4.1072p-1.8496p^2)+(3.5405+24.6768p-63.9424p^2)\Phi + 3.7636(1-2p)(1-4p)\Phi^2,$$

$$d_y = (1.3689-3.1824p+1.8496p^2)+(-1.3289+7.2944p+63.9424p^2)\Phi + 7.5272p(1-4p)\Phi^2,$$

$$g_z = 3.7636 - 33.2128p + 14.3172p^2 - 15.0544p^3$$

$$g_{yz} = (28.7896p+1.4744p^2+30.1088p^3),$$

$$g_y = -(10.6312p+15.7916p^2+15.0544p^3).$$

Table 4 shows $\mathrm{var}(\hat{\Theta})$ evaluated for the patterns considered in Table 3., for comparison with $\mathrm{var}(\hat{\Theta}_i)$, for the appropriate i. Also given in Table 4 are $E(\hat{\Theta})$ and $E(\hat{\Theta}_i)$ for the appropriate i. N is chosen as 50 and 500.

It can be shown from equation 5 that $\mathrm{var}(\hat{\Theta}) = 1.055\,\Theta^2/N$ for the Poisson forest, and so $\hat{\Theta}$ is 47% efficient compared to $\hat{\Theta}_L$ which is fully efficient. This is approximately midway between the efficiencies of $\hat{\Theta}_1$ and $\hat{\Theta}_2$ which are 85% and 21%. However if it is known that the spatial pattern is a Poisson forest, $\hat{\Theta}_L$ should of course be used as an estimator of Θ. From Table 4 it can be seen that $\mathrm{var}(\hat{\Theta}) \doteq \mathrm{var}(\hat{\Theta}_i)$ for p not near $\frac{1}{4}$ and for large N. Thus for this case $\mathrm{var}(\hat{\Theta})$ can be estimated using an estimate of $\mathrm{var}(\hat{\Theta}_i)$ based on equation (4), viz.

$$\tfrac{1}{4}\pi^2\left[(a_i+b_i\tilde{p})^2(\tilde{p}\,\tilde{\sigma}_y^2+\tilde{q}\,\tilde{\sigma}_z^2)+\tilde{p}\tilde{q}\left\{(a_i+b_i-2b_i\tilde{q})\tilde{\mu}_z - (a_i+2b_i\tilde{p})\tilde{\mu}_y\right\}^2\right]/N, \qquad (6)$$

Table 4. The values of $E(\hat{\theta})$ and $var(\hat{\theta})$ for comparison with $E(\hat{\theta}_i)$, $var(\hat{\theta}_i)$ (i = 1 or 2), for the lattice patterns, Poisson forest and Thomas processes.

Pattern	p	i	N = 50				N = 500			
			$\frac{E(\hat{\theta}_i)}{\theta}$	$\frac{E(\hat{\theta})}{\theta}$	$\frac{var(\hat{\theta}_i)}{\theta 2}$	$\frac{var(\hat{\theta})}{\theta 2}$	$\frac{E(\hat{\theta}_i)}{\theta}$	$\frac{E(\hat{\theta})}{\theta}$	$\frac{var(\hat{\theta}_i)}{\theta 2}$	$\frac{var(\hat{\theta})}{\theta 2}$
Triangular lattice	0.91	1	1.00	1.00	0.003	0.003	1.00	1.00	0.0003	0.0003
Square lattice	0.79	1	1.01	1.01	0.004	0.004	1.01	1.01	0.0004	0.0004
Hexagonal lattice	0.60	1	0.97	0.97	0.005	0.005	0.97	0.97	0.0005	0.0005
Poisson forest	0.25	1	1.0	0.91	0.01	0.02	1.0	0.97	0.001	0.002
Poisson forest	0.25	2	1.0	0.91	0.05	0.02	1.0	0.97	0.005	0.002
Thomas process $\alpha = 0.1$	0.23	2	1.02	0.96	0.05	0.03	1.02	1.01	0.005	0.005
Thomas process $\alpha = 0.5$	0.15	2	1.03	1.02	0.07	0.07	1.03	1.03	0.007	0.007
Thomas process $\alpha = 1.0$	0.09	2	0.99	0.99	0.08	0.08	0.99	0.99	0.008	0.008
Thomas process $\alpha = 2.0$	0.03	2	0.92	0.92	0.07	0.07	0.92	0.92	0.007	0.007
Thomas process $\alpha = 3.0$	0.01	2	0.96	0.96	0.05	0.05	0.96	0.96	0.005	0.005
Thomas process $\alpha = 5.0$	0.002	2	1.23	1.23	0.03	0.03	1.23	1.23	0.003	0.003

where $\tilde{p} = 1-\tilde{q} = m/N$, $\tilde{\mu}_z = n^{-1}\sum z_{1i}^2$, $\tilde{\mu}_y = m^{-1}\sum y_{2j}^2$,

$\tilde{\sigma}_z^2 = n^{-1}\sum z_{1i}^4 - \tilde{\mu}_z^2$ and $\tilde{\sigma}_y^2 = m^{-1}\sum y_{2j}^4 - \tilde{\mu}_y^2$.

In section 2.5 the estimator $\hat{\theta}$, together with another to be described next, will be used on the same data as in Chapter 2. Estimated standard errors will also be given, based on equation (5), and found in a similar manner to (6).

3.4 The second estimator

An approximately unbiased estimator, $\tilde{\lambda}$, of $\lambda = \theta^{-1}$, the density of the trees is now described. It is defined by

$$\tilde{\lambda} = 4(\pi N)^{-1} \sum_{j=1}^{m} (Y'_{2j})^{-2},$$

where $Y_{2j} = Y_{2j}$, given that Y_{2j} is greater than some small fixed value ε.

For the Poisson forest,

$$\text{pr}\{Y_{2j} > \varepsilon\} = \int_{\varepsilon}^{\infty} 2\pi^2\lambda^2 y_2^3 \exp(-\pi\lambda y_2^2)dy_2,$$

$$= (1 + \lambda\pi\varepsilon^2)\exp(-\lambda\pi\varepsilon^2).$$

Thus from equation (3), the p.d.f. of Y'_{2j} is

$$2\pi^2\lambda^2 y^3 \exp(-\lambda\pi y^2) / \{(1+ \lambda\pi\varepsilon^2)\exp(-\lambda\pi\varepsilon^2)\},$$

and hence

$$E\{(Y'_{2j})^{-2}\} = \lambda\pi/(1 + \lambda\pi\varepsilon^2),$$

$$\text{var}\{(Y'_{2j})^{-2}\} = \lambda^2\pi^2\{(1 + \lambda\pi\varepsilon^2)\text{Ei}(\lambda\pi\varepsilon^2) - 1\}/(1 + \lambda\pi\varepsilon^2)^2,$$

where Ei(·) is the exponential-integral.

Now $E(m/N)$ is no longer $\frac{1}{4}N$ for the Poisson forest, but is reduced by the factor, $pr(Y_2 > \xi)$. Hence for the Poisson forest

$$E(\tilde{\lambda}) = \lambda \exp(-\lambda \pi \xi^2),$$
$$= \lambda + O(\xi^2).$$

Thus $\tilde{\lambda}$ is unbiased for the Poisson forest as $\xi \to 0$. The reason for using Y_2' instead of Y_2 is to prevent very small values of Y_2 from inflating the estimate. Note that the variance of $(Y_2)^{-2}$ is infinite, while although that of $(Y_{2j}')^{-2}$ is not infinite, it is very large for small ξ.

Another criticism of this estimator is that m will be small for aggregated patterns, and thus much of the available information is lost. It is a high price to pay, but the estimator will be shown to be approximately unbiased for a wide range of spatial patterns.

For the triangular, square and hexagonal lattices, noting that Y_2' is always greater than ξ, we have the following

$$E(m/N) = \tfrac{1}{2}\pi/\sqrt{3}, \quad E\{(Y_2')^{-2}\} = \tfrac{1}{2}\sqrt{3}\lambda \quad \text{(triangular lattice)}$$
$$E(m/N) = \tfrac{1}{4}\pi, \quad E\{(Y_2')^{-2}\} = \lambda \quad \text{(square lattice)}$$
$$E(m/N) = \tfrac{1}{3}\pi/\sqrt{3}, \quad E\{(Y_2')^{-2}\} = \tfrac{3}{4}\sqrt{3}\lambda \quad \text{(hexagonal lattice)}.$$

Hence $E(\tilde{\lambda}) = \lambda$ for all three lattices and the variance is obviously zero for each. Now consider the following aggregation model.

Suppose the trees are aggregated in very small areas of average size δ, the areas being distributed with density γ. The sampling origin, O, will fall outside a clump with probability $1 - \gamma\delta$, and Y will almost certainly be much less than 2X. With probability $\gamma\delta$,

X and Y will both be measured within a clump, and then $\tilde{\lambda}$ will estimate the density, ρ say, of the trees within a clump. Hence overall, $E(\tilde{\lambda}) = \gamma\delta\rho$. However, in a large area K, there are γK clumps on average, and hence $\gamma K\rho\delta$ trees, and so the overall density, λ , equals $\gamma\rho\delta$. Thus $E(\tilde{\lambda}) = \lambda$.

It has been shown that $\tilde{\lambda}$ is unbiased for models from extreme regularity to extreme aggregation. Hence it may reasonably be conjectured that $\tilde{\lambda}$ is unbiased for a wide range of spatial patterns.

The variance of $\tilde{\lambda}$ is easily seen to be

$$16(\pi^2 N)^{-1} p\left[\operatorname{var}\left\{ (Y_2')^{-2} \right\} + q\left[E\left\{ (Y_2')^{-2} \right\}\right]^2 \right],$$

and can be estimated by

$$16(\pi^2 N)^{-1} \tilde{p}[\tilde{\sigma}^2 + \tilde{q}\,\tilde{\mu}^2] ,$$

where $\tilde{p} = 1 - \tilde{q} = m/N$, $\tilde{\mu} = \frac{1}{m}\sum (Y_{2j}')^{-2}$,

and $\tilde{\sigma}^2 = \frac{1}{m}\sum (Y_{2j}')^{-4} - \tilde{\mu}^2$.

3.5 Results

The same data were used as for the analysis of spatial pattern in Chapter 2. Table 5 summarizes the results obtained for $\tilde{\lambda}$ and $\hat{\theta}$ with N = 100, ε = 0.01. Estimated standard errors are also given.

In spite of the large loss of information when using $\tilde{\lambda}$ this estimator seems to work remarkably well for patterns of a more regular type. The estimator $\hat{\theta}$ did reasonably well although there were a few poor estimates, the worst being for the Black oaks and the last of the modified Thomas processes. Better results may be obtainable

Table 5. True values of λ, θ and their estimates $\tilde{\lambda}$, $\hat{\theta}$ for various sets of data, with sample size N = 100.

Type of forest	m	λ	$\tilde{\lambda}$	s.e. of $\tilde{\lambda}$	θ	$\hat{\theta}$	s.e. of $\hat{\theta}$
Lattice 1	25	1.54	1.08	0.21	0.65	0.58	0.05
Lattice 2	61	1.34	0.99	0.09	0.75	1.02	0.06
Lattice 3	50	1.34	1.35	0.14	0.75	0.70	0.04
Red oaks	27	1.61	1.81	0.47	0.62	0.75	0.06
Black oaks	24	0.60	0.47	0.12	1.65	2.98	0.40
White oaks	26	2.04	2.53	1.13	0.49	0.51	0.05
Hickories	21	3.18	2.66	1.15	0.31	0.46	0.07
Maples	20	2.36	3.61	1.19	0.42	0.56	0.08
Miscellaneous	11	0.48	0.45	0.22	2.10	3.00	0.53
M.T.P. ($\mu = 5.0, \sigma = 1.0$)	23	2.20	1.68	0.50	0.46	0.51	0.06
M.T.P. ($\mu = 2.0, \sigma = 1.0$)	16	1.18	0.65	0.20	0.85	0.63	0.11
M.T.P. ($\mu = 2.0, \sigma = 0.2$)	7	1.25	0.44	0.24	0.80	0.42	0.10

for a larger sample size, although one must bear in mind the practical aspects of collecting actual data. In view of the theoretical arguments discussed, it should be noted that $\hat{\theta}$ should be used in preference to $\tilde{\lambda}$.

Appendix B

To find the expectation and variance of $\hat{\Theta}$.

$$\hat{\Theta} = \tfrac{1}{2}\pi(1.17-0.68m/N)\Big\{\sum_{i=1}^{n} z_{1i}^2 + \sum_{j=1}^{m} y_{2j}^2\Big\}/N \qquad (m > \tfrac{1}{4}N)$$

$$= \tfrac{1}{2}\pi(0.20+3.20m/N)\Big\{\sum_{i=1}^{n} z_{1i}^2 + \sum_{j=1}^{m} y_{2j}^2\Big\}/N \qquad (m < \tfrac{1}{4}N)$$

Now $m \sim$ Binomial (N,p) and can thus be approximated by a Normal (Np, Npq) variate.

Let $L = N(\tfrac{1}{4}-p)/\sqrt{Npq}$, $C = \sqrt{\frac{Npq}{2\pi}}\exp(-\tfrac{1}{2}L^2)$, and $\Phi(\cdot)$ be the standard normal distribution function.

Lemma 1

$$\text{Let } I_r = (2\pi Npq)^{-\frac{1}{2}}\int_{-\infty}^{\frac{1}{4}N} m^r \exp\left\{-\tfrac{1}{2}(m-Np)^2/Npq\right\} dm \qquad (r \geq 2),$$

$$= (2\pi)^{-\frac{1}{2}}\int_{-\infty}^{L} (\sqrt{Npq}\,u + Np)^r e^{-\frac{1}{2}u^2}\, du,$$

$$= (Npq)^{\frac{1}{2}}(2\pi)^{-\frac{1}{2}}\int_{-\infty}^{L} (\sqrt{Npq}\,u + Np)^{r-1} ue^{-\frac{1}{2}u^2} + Np\, I_{r-1},$$

$$= -(\tfrac{1}{4}N)^{r-1}C + NpI_{r-1} + Npq(r-1)I_{r-2}.$$

Then

$$I_0 = \bar{\Phi}(L),$$

$$I_1 = -C + Np\,\bar{\Phi}(L),$$

$$I_2 = -C(\tfrac{1}{4}N + Np) + (N^2p^2 + Npq)\,\bar{\Phi}(L),$$

$$I_3 = -C(\tfrac{1}{16}N^2 + \tfrac{1}{4}N^2p + N^2p^2 + 2Npq) + (N^3p^3 + 3N^2p^2q)\,\bar{\Phi}(L),$$

$$I_4 = -C(\tfrac{1}{64}N^3 + \tfrac{1}{16}N^3p + \tfrac{1}{4}N^3p^2 + N^3p^3 + 5N^2p^2q + \tfrac{3}{4}N^2pq) +$$
$$+(N^4p^4 + 6N^3p^3q + 3N^2p^2q^2)\,\bar{\Phi}(L).$$

The expression for I_0, I_1 follow by elementary integration, and those for I_2, I_3, I_4 follow from the recurrence relation.

Lemma 2

$$\text{Let } H_r = (2\pi Npq)^{-\frac{1}{2}} \int_{\frac{1}{4}N}^{\infty} m^r \exp\left\{-\tfrac{1}{2}(m-Np)^2/Npq\right\} dm.$$

Then similarly to Lemma 1,

$$H_0 = 1 - \bar{\Phi}(L),$$

$$H_1 = C + Np(1 - \bar{\Phi}(L)),$$

$$H_2 = C(\tfrac{1}{4}N + Np) + (N^2p^2 + Npq)(1 - \bar{\Phi}(L)),$$

$$H_3 = C(\tfrac{1}{16}N^2 + \tfrac{1}{4}N^2p + N^2p^2 + 2Npq) + (N^3p^3 + 3N^2p^2q)(1 - \bar{\Phi}(L)),$$

$$H_4 = C(\tfrac{1}{64}N^3 + \tfrac{1}{16}N^3p + \tfrac{1}{4}N^3p^2 + N^3p^3 + 5N^2p^2q + \tfrac{3}{4}N^2pq)$$
$$+ (N^4p^4 + 6N^3p^3q + 6N^3p^3q + 3N^2p^2q^2)(1 - \bar{\Phi}(L)).$$

I_i, H_i $(i = 0, \ldots, 4)$ are now used to find $E(\hat{\theta})$, $\text{var}(\hat{\theta})$.

$$\text{Now } E(\hat{\theta}|m) = \tfrac{1}{2}\pi(1.17 - 0.68m/N)\left\{N\mu_z + m(\mu_y - \mu_z)\right\}/N \quad (M \geq \tfrac{1}{4}N)$$

$$\tfrac{1}{2}\pi(0.20 + 3.20m/N)\left\{N\mu_z + m(\mu_y - \mu_z)\right\}/N \quad (m < \tfrac{1}{4}N).$$

Hence

$$E(\hat{\theta}) \doteq \frac{\pi}{2N}\{1.17N\mu_z H_0 + (-1.85\mu_z + 1.17\mu_y)H_1 - 0.68(\mu_y - \mu_z)H_2$$

$$+ 0.20N\mu_z I_0 + (3.0\mu_z + 0.20\mu_y)I_1 + 3.20(\mu_y - \mu_z)I_2\} .$$

$$= \frac{\pi}{2N}\left[\{(1.17 - 0.68p) - 0.97(1-4p)\,\Phi(L)\}\{q\mu_z + p\mu_y\}\right.$$

$$\left. + pqN^{-1}(\mu_y - \mu_z)(-0.68 + 3.88\,\Phi(L)) - 3.88cN^{-1}\{q\mu_z + p\mu_y\}\right] ,$$

after some tedious algebra.

Finding the variance of $\hat{\theta}$ proves to be very complicated.

Firstly,

$$\mathrm{var}(\hat{\theta}) = E\{E(\hat{\theta}^2|m)\} - [E\{E(\hat{\theta}|m)\}]^2 .$$

Now

$$E(\hat{\theta}^2|m) = \frac{\pi^2}{4N^2}(1.17 - 0.68m/N)^2\{(N-m)\sigma_z^2 + m\sigma_y^2 + (N-m)^2\mu_z^2$$

$$+ 2(N-m)m\mu_y\mu_z + m^2\mu_y^2\} \qquad (m \geq \tfrac{1}{4}N),$$

$$\frac{\pi^2}{4N^2}(0.20 + 3.20m/N)^2\{(N-m)\sigma_z^2 + m\sigma_y^2 + (N-m)^2\mu_z^2$$

$$+ 2(N-m)m\mu_y\mu_z + m^2\mu_y^2\} \qquad (m < \tfrac{1}{4}N).$$

Thus

$$E(\hat{\theta}^2) = \frac{\pi^2}{4N^2}\left[\{1.3689N\alpha_z\}H_0 + \{-2.9601\alpha_z + 1.3689\alpha_y - 1.3689N(\mu_y - \mu_z)^2\}H_1\right.$$

$$+ \{2.0536\alpha_z N^{-1} - 1.5912\alpha_y N^{-1} + 2.9601(\mu_y - \mu_z)^2\}H_2$$

$$+ \{-.4624\alpha_z N^{-2} + .4624\alpha_y N^{-2} - 2.0536N^{-1}(\mu_y - \mu_z)^2\}H_3$$

$$+ \{.4624N^{-2}(\mu_y - \mu_z)^2\}H_4$$

$$\left. + \text{similar expression involving } I_i \quad (i = 0, \ldots, 4)\right] ,$$

where $\alpha_z = \sigma_z^2 + N\mu_z^2$, $\alpha_y = \sigma_y^2 + N\mu_y^2$.

On expanding this expression and subtracting $[E(\hat{\theta})]^2$, after much algebra one obtains the approximation to $\text{var}(\hat{\theta})$ given in section 3.3.

CHAPTER 4

THE LOCATION OF CLUMPED AND SPARSE AREAS WITHIN A SPATIAL PATTERN

4.1 Introduction

In this chapter a method is introduced which uses the idea of potential for the determination of clumped and sparse areas within a spatial pattern formed by point events in the plane. Once again the points will be referred to as trees as probably the most useful application is in the area of forestry.

Intuitively a particular small region within a spatial pattern contains a clump of trees or is within a clump of trees if the local density of trees there is somewhat grater than the overall density. Similarly, in vague terms, a sparse area occurs in a region where the local density is somewhat less than the overall density. Apart from these basic intuitive requirements of a definition for clumped and sparse areas within a spatial pattern, the definition is more or less arbitrary. For example one may define the most dense clump within a spatial pattern as those trees, say k (≥ 2) in number, which are contained in a circle D such that

$$\frac{k}{r_D^2} = \max_C \left(\frac{i}{r_c^2} \right), \quad \frac{k}{\pi r_D^2} > \lambda_o > \lambda ,$$

where the maximum is taken over all circles C; r_c is the radius of circle C, i is the number of tress contained in circle C, and λ_o is a constant greater than the overall density λ.

The same procedure is then carried out for finding the second most dense clump with the first clump removed from the measurements. Then the third, fourth, etc. clumps are found until no more circles can be found such that $i/(\pi r_c^2) > \lambda_o$.

This definition of the clumped areas is awkward to use in practice, but is one of many definitions that could be used for practical purposes, the value of λ_o adding to the subjective definition of a clump. Another method for defining clumps and sparse areas is now described, and is one which is easily implemented.

Consider a point P within the spatial pattern. Let $r_1, \ldots, r_n$ be the distances from P to the nearest tree, second nearest tree, etc., up to the nth nearest tree respectively. Define P as being within a clump of n trees, or within a sparse area of size n, according to whether

$$T_n = \left\{ b_1(n) \sum_{j=1}^{n} a(j)(\lambda \pi r_j^2) + b_2(n) \right\} < C_n \text{ or } > S_n$$

respectively, $(n = 2, 3, \ldots.)$

where $b_1(n)$, $b_2(n)$, C_n, S_n are constants dependent on n, the $a(j)$'s are weights given to each distance r_j, and λ is the overall density of the spatial pattern. If $C_n \leqslant T_n \leqslant S_n$, then P is not within a clump of n trees, nor within a sparse area of size n.

The choice of the $a(j)$'s, $b_1(n)$, $b_2(n)$, C_n and S_n reflects one's ideas or needs of what constitutes a clump or a sparse area. For example, if $a(j)$ is monotone decreasing with j, then the closer a tree is to the point P, the more the tree determines the state of P.

It should be noted that the point P could be within clumps of sizes n_1^c, n_2^c,...,n_i^c and at the same time within sparse areas of sizes n_1^s, n_2^s, ..., n_j^s from this definition. This is not a drawback but rather an advantage. For example Fig.4(1) shows a point P which by a certain defined T_n, may be within a clump of size 2, within a sparse area of size 3, within clumps of sizes 7 and 8, but not within clumped or sparse areas of sizes 4, 5 and 6.

As we shall see, the density, λ , is included in T_n in such a way as to make the definition independent of the density. Thus the results obtained for a particular pattern will be the same as those for the pattern scaled by some factor.

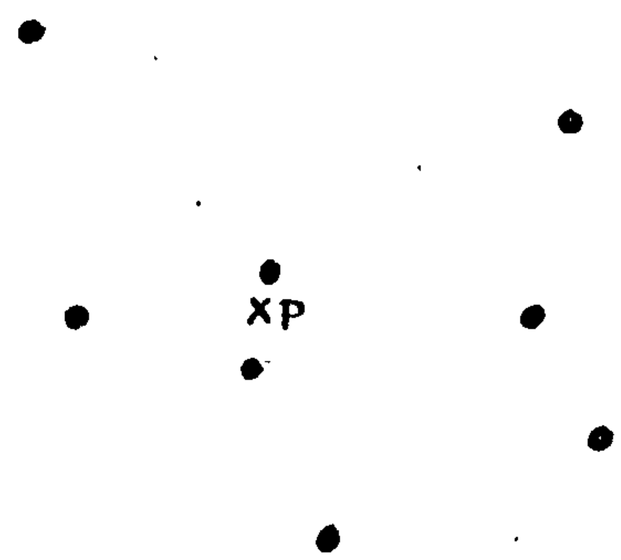

Fig. 4(1) The point P within various clumped and sparse areas.

One method for choosing C_n and S_n is given, and then the case $a(j) = 1$ $(j = 1, \ldots, n)$ is considered in detail with $b_1(n)$ and $b_2(n)$ suitably chosen. The method is then used on various sets of data including that from Lansing Woods.

Suppose the point P was a randomly placed point within a Poisson forest. Then define P as being within a clump of size n if

$$T_n < C_n(\alpha), \text{ where } \alpha = \Pr\{T_n < C_n(\alpha)\},$$

and within a sparse area of size n if

$$T_n > S_n(\alpha), \text{ where } 1-\alpha = \Pr\{T_n > S_n(\alpha)\};$$

i.e. $C_n(\alpha)$ and $S_n(\alpha)$ are the $100\alpha\%$ and $100(1-\alpha)\%$ points of the distribution of T_n. Once again the choice of α is arbitrary and reflects one's ideas of what constitutes a clump or sparse area. Intuitively for a Poisson forest, one expects roughly αM of every M points chosen at random within the Poisson forest, to fall within a clumped area, and αM to fall within a sparse area for every n. Note that the weights, a(j), still have not been defined.

It must be pointed out that λ must be known for use with T_n. However if the clumps and sparse areas of a spatial pattern are to be mapped, one would probably know the coordinates of all the trees and thus λ is known.

4.2 The distribution of T_n for the Poisson forest

Let $Y_i = \lambda\pi R_i^2$ $(i = 1, \ldots, n)$, where R_i is the distance from a randomly placed point P to the ith nearest tree.

Define $X_1 = Y_1$, $X_i = Y_i - Y_{i-1}$, $(i = 2, \ldots, n)$.

The joint p.d.f. of $R_1, \ldots, R_n$ is

$$\prod_{i=1}^{n} \exp\left\{-\lambda\pi(r_i^2 - r_{i-1}^2)\right\} 2\lambda\pi r_i dr_i \qquad (r_0 = 0 \leq r_1 \leq r_2 \leq \ldots < r_n < \infty),$$

whence the joint p.d.f. of $X_1, \ldots, X_n$ is

$$\exp\left\{-\sum_{i=1}^{n} x_i\right\} dx_1 \ldots dx_n \qquad (0 \leq x_1 < \infty, \ldots, 0 \leq x_n < \infty).$$

Thus $X_1, \ldots, X_n$ are independently distributed as exponential variates with mean unity.

$$\text{Let } T_n' = \sum_{j=1}^{n} a(j)\, Y_j,$$

$$= \sum_{j=1}^{n} a(j) \sum_{k=1}^{j} X_k.$$

Reversing the order of summation,

$$T_n' = \sum_{k=1}^{n} X_k \sum_{j=k}^{n} a(j),$$

$$= \sum_{k=1}^{n} A(k)X_k, \qquad (1)$$

where $A(k) = \sum_{j=k}^{n} a(j)$.

Now the p.d.f. of X_k is $\exp(-x)$, $(0 \leq x < \infty)$, and thus the p.d.f. of $A(k)X_k$ is

$$\frac{1}{A(k)} \exp\left\{-x/A(k)\right\} .$$

Hence it is easily seen that the characteristic function of $A(k)X(k)$ is $1/\{1 - iA(k)s\}$, giving the characteristic function of T_n' as

$$\prod_{k=1}^{n} \frac{1}{1-iA(k)s} = \sum_{k=1}^{n} \frac{D(k)}{1-iA(k)s} ,$$

where $D(k) = \prod_{\substack{j=1 \\ j\neq k}}^{n} \frac{1}{1-A(j)/A(k)}$.

Inverting the characteristic function, the p.d.f. of T_n' is

$$f_n'(t) = \sum_{k=1}^{n} \frac{D(k)}{A(k)} \exp\left\{-t/A(k)\right\} , \qquad (0 \leqslant t < \infty)$$

and hence the distribution function of T_n' is

$$F_n'(t) = 1 - \sum_{k=1}^{n} D(K) \exp\left\{-t/A(k)\right\} .$$

Now $T_n = b_1(n)T_n' + b_2(n)$, where $b_1(n)$ and $b_2(n)$ are constants. Therefore the p.d.f. of T_n is

$$f_n(t) = \frac{1}{b_1(n)} \sum_{k=1}^{n} \frac{D(k)}{A(k)} \exp\left\{-\left(\frac{t-b_2(n)}{b_1(n)}\right) \Big/ A(k)\right\} \quad (b_2(n) \leqslant t < \infty),$$

and the distribution function of T_n is

$$F_n(t) = 1 - \sum_{k=1}^{n} D(k) \exp\left\{-\left(\frac{t-b_2(n)}{b_1(n)}\right) \Big/ A(k)\right\} \qquad (b_2(n) \leqslant t < \infty).$$

4.3 The case of uniform weights

For the rest of the chapter only the case $a(j) \equiv 1$ (all j) will be considered. This implies in some sense that all the nearest n trees to a point P are equally important when determining whether P is within a clump or sparse area of size n or not.

For convenience choose

$$b_1(n) = \sqrt{\frac{6}{n(n+1)(2n+1)}}, \quad b_2(n) = -\sqrt{\frac{3n(n+1)}{2(2n+1)}} .$$

It is easily seen that

$$A(k) = n + 1 - k, \quad D(k) = \frac{(n+1-k)^{n-1}\ (-1)^{k-1}}{(n-k)!\ (k-1)!}$$

After some algebra, the p.d.f. of T_n is

$$g_n(t) = \sqrt{\frac{n(n+1)(2n+1)}{6}}\ \frac{1}{n!}\ \sum_{k=1}^{n} \binom{n}{k} k^{n-1} (-1)^{n-k} \exp\left\{ \frac{-\left[\frac{n(n+1)}{2} + \sqrt{\frac{n(n+1)(2n+1)}{6}}\, t\right]}{k} \right\}$$

$$\left(-\sqrt{\frac{3n(n+1)}{2(2n+1)}} \leq t < \infty \right),$$

and the distribution function is

$$G_n(t) = 1 - \frac{1}{n!}\ \sum_{k=1}^{n} \binom{n}{k} k^{n}\ (-1)^{n-k} \exp\left\{ - \frac{\left[\frac{n(n+1)}{2} + \sqrt{\frac{n(n+1)(2n+1)}{6}}\, t\right]}{k} \right\}$$

$$\left(-\sqrt{\frac{3n(n+1)}{2(2n+1)}} \leq t < \infty \right),$$

From equation (1) and the fact that $T_n = b_1(n)T_n' + b_2(n)$,

$$E(T_n) = \sqrt{\frac{6}{n(n+1)(2n+1)}}\ \sum_{j=1}^{n} (n+1-j) - \sqrt{\frac{3n(n+1)}{2(2n+1)}} = 0,$$

and

$$\mathrm{Var}(T_n) = \frac{6}{n(n+1)(2n+1)} \sum_{j=1}^{n} (n+1-j)^2 = 1.$$

Thus $b_1(n)$ and $b_2(n)$ were chosen to standardise T_n' in such a way that the mean of T_n is zero and the variance of T_n is unity.

Fig.4(2) shows the p.d.f.'s of T_n for $a(j) \equiv 1$,

$b_1(n) = \sqrt{\frac{6}{n(n+1)(2n+1)}}$, $b_2(n) = -\sqrt{\frac{3n(n+1)}{2(2n+1)}}$, for various values of n. Table 6 shows the values of $C_n(\alpha)$, $S_n(\alpha)$ $(n = 2, \ldots, 22)$, for $\alpha = 0.05$ and 0.025 (i.e. the 5%, 95% 2½% and 97½% probability levels of T_n).

4.4 Practical details

The distribution theory for T_n just described is only relevant to the Poisson forest and a randomly placed sampling origin, P. However the measurements $r_1, r_2, \ldots, r_n$ $(n = 2, \ldots)$, and hence T_n, can be made for any spatial pattern and from any point P within the spatial pattern. The distribution of T_n for a random point P within a Poisson forest was used in order to produce suitable values for C_n and S_n, the critical values for clumped and sparse areas of size n. Once produced, these can be used as yardsticks for clumpedness and sparseness in any set of points in the plane.

Within the spatial pattern under consideration a set of grid points, formed by the vertices of a square lattice, are used as sampling origins. From each of these grid points, the distances to the nearest N trees are measured, and then the N-1 values $T_2, \ldots, T_N$ are calculated.

Table 6. The values of $C_n(\alpha)$, $S_n(\alpha)$ for $\alpha = 0.05$ and 0.025, $n = 2, \ldots, 22$.

n	$C_n(0.05)$	$S_n(0.05)$	$C_n(0.025)$	$S_n(0.025)$
2	-1.125	1.947	-1.188	2.572
3	-1.198	1.921	-1.298	2.503
4	-1.256	1.901	-1.371	2.454
5	-1.290	1.885	-1.425	2.415
6	-1.320	1.872	-1.466	2.385
7	-1.343	1.860	-1.499	2.360
8	-1.363	1.851	-1.526	2.345
9	-1.379	1.842	-1.550	2.322
10	-1.392	1.835	-1.570	2.306
11	-1.404	1.828	-1.587	2.293
12	-1.415	1.822	-1.602	2.280
13	-1.424	1.816	-1.616	2.270
14	-1.432	1.812	-1.628	2.260
15	-1.440	1.807	-1.639	2.251
16	-1.446	1.803	-1.649	2.243
17	-1.452	1.799	-1.658	2.235
18	-1.458	1.795	-1.666	2.228
19	-1.463	1.792	-1.674	2.222
20	-1.468	1.789	-1.681	2.216
21	-1.472	1.786	-1.688	2.210
22	-1.477	1.783	-1.692	2.205

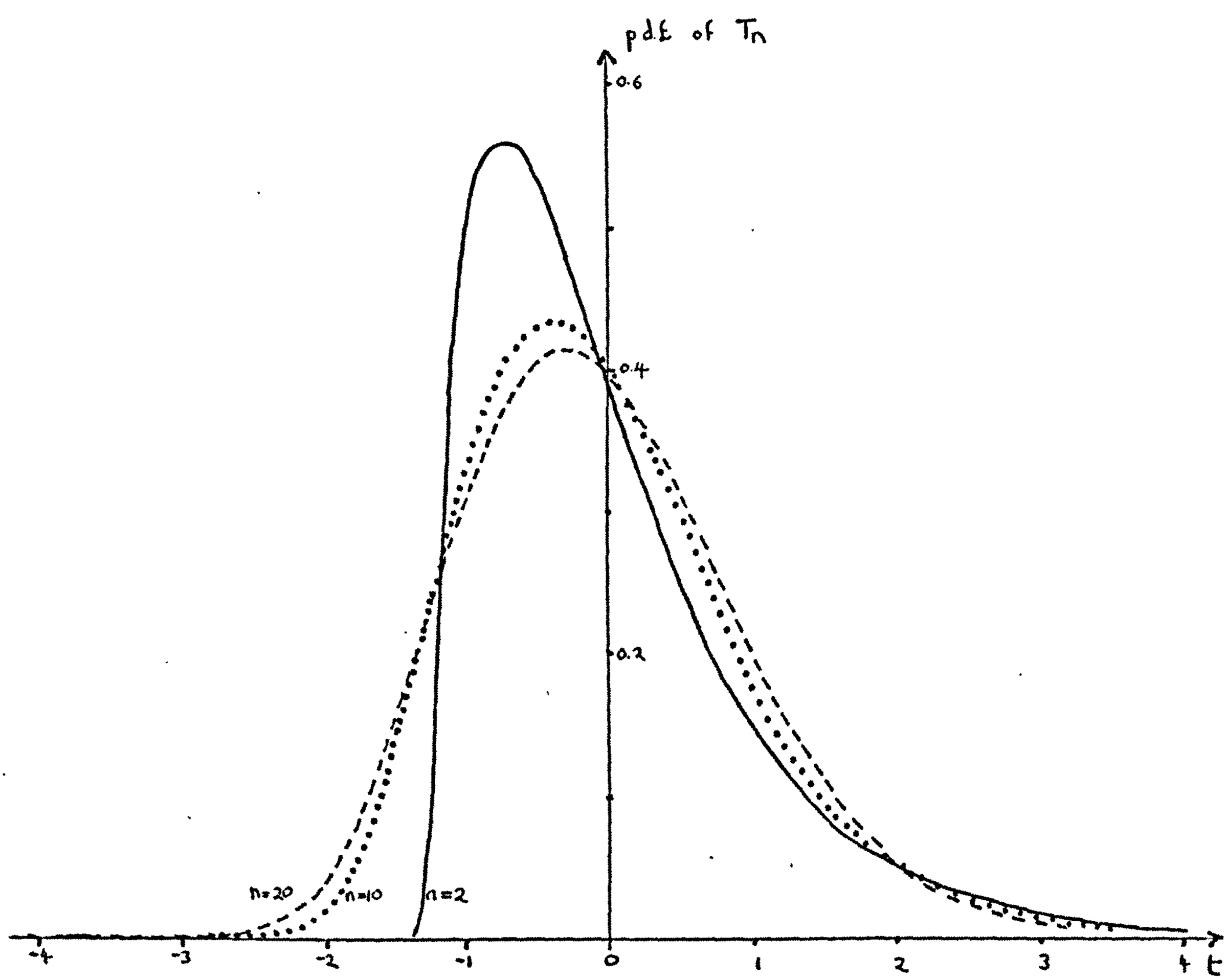

Fig. 4(2) The p.d.f. of T_n for various values of n.

With these values of T_n $(2 \leq n \leq N)$ for each grid point, it is possible to draw a contour map showing clumped and sparse areas of size n, with the aid of a computer package designed for drawing contour maps from values at each of a set of points in the plane. The package used here is SYMAP, which was originally developed at the Laboratory for Computer Graphics and Spatial Analysis, Graduate School of Design, Harvard University, Cambridge, Massachusetts 02138, U.S.A. Examples including the results of mapping Lansing Woods are shown in section 4.6.

4.5 The 'most likely' clumps and sparse areas

It was noted in section 4.1 that a point P may be within clumped and/or sparse areas of several sizes. It may be more informative to give a "most likely" clump or sparse area size which P is in. The following methods for achieving this are just two of several conceivable methods.

(i) Firstly, a particular grid point could be considered to be within a clump of "most likely" size l if

$$\alpha_l = \min_n \left\{ \alpha_n : F_n(T_n) = \alpha_n, (2 \leq n \leq N) \right\} \text{, and } T_l < C_l,$$

and could be considered to be within a sparse area of "most likely" size m if

$$\alpha_m = \max_n \left\{ \beta_n : F_n(T_n) = \beta_n, (2 \leq n \leq N) \right\} \text{, and } T_m > S_m.$$

i.e. for a grid point to be in a clump of size l, α_l must be the smallest probability value for the Poisson forest distribution of T_n,

and to be within a sparse area of size m , β_m must be the largest value.

In practice the number of grid points needed to obtain reasonable results must be very large compared with the total number of trees. The following method which defines clump sizes only will be used in the sequel.

(ii) Within a Poisson forest, the distribution theory for T_n still holds if the distances to the n nearest trees from a random point are measured from a random tree instead. Thus instead of using grid points, the distances to the N nearest trees from each of the trees within the spatial pattern could be recorded.

$$\text{Let } T_n(i) = b_1(n) \sum_{j=1}^{n} \lambda\pi r_{ij}^2 + b_2(n)$$

where r_{ij} is the distance from tree i to its jth nearest neighbour, $b_1(n) = \sqrt{\frac{6}{n(n+1)(2n+1)}}$ and $b_2(n) = -\sqrt{\frac{3n(n+1)}{2(2n+1)}}$.

Define tree i as having "most likely" clump number g+1, if

$$\alpha_g(i) = \min_n \left\{ \alpha_n(i) : F_n(T_n(i)) = \alpha_n(i),\ (1 \leq n \leq N) \right\}, \text{ and}$$

$$T_g(i) < C_g,$$

and zero otherwise.

Thus an integer 0, 2, 3, ..., N is assigned to every tree within the spatial pattern, there being no trees with "most likely" clump size one (i.e. single trees do not constitute a clump).

Then define tree i as being within a clump of "most likely" size ℓ defined by a set, S_ℓ, of ℓ trees, if tree $i \in S_\ell$ and there exists a tree $k \in S_\ell$ which has "most likely" clump number $\ell - 1$ and the

rest of the members of S_l are the $l - 1$ nearest neighbours to tree k, such that $S_l \not\subset S_m$ where S_m forms a "most likely" clump of m trees. The idea behind this definition is made clear by the example discussed below.

From this definition a tree may be within several clumps which overlap, but a clump cannot be a subset of the trees contained in another clump. Fig.4(3) shows the positions of twelve trees labelled from A to L, together with their "most likely" clump numbers, such that two clumps are formed. Trees A, B, C, D, E and F form a clump of size six, trees F, G, H, and I form a clump of size 4, and trees J, K and L are not in any clumps. Note that tree B is within the clump of size six although it has "most likely" clump number four, and that trees C and D do not form a clump of size two as they are both contained in the clump of size six. Tree E is contained in the clump of size six although it has "most likely" clump number zero, because it is one of the 5 nearest neighbours to tree A. Tree F is in the two clumps because it is the one of the nearest neighbours to both tree A and tree G.

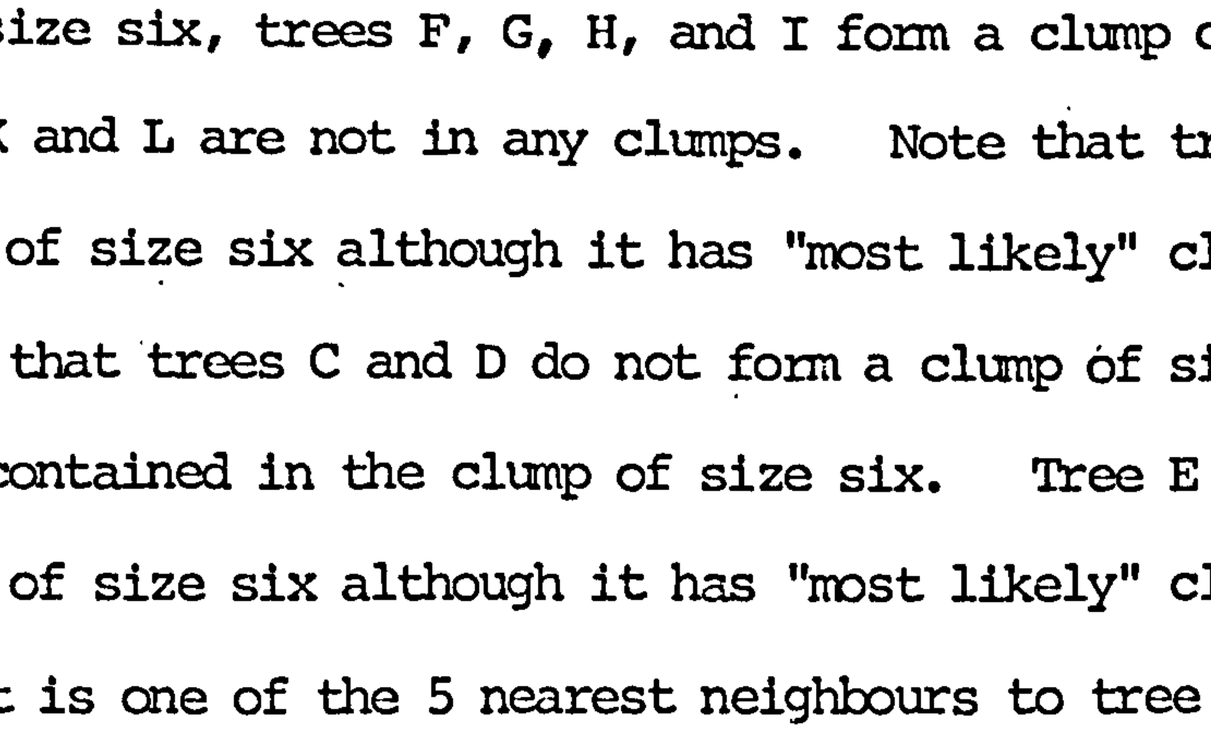

Fig. 4(3) Examples of "most likely" clumps

The contours in Fig.4(3) are drawn by hand to illustrate which trees are in each clump. It will be seen that when there are many trees within the pattern forming many clumps, it is easier to omit the hand drawn contours, just leaving the "most likely" clump numbers for the trees, ~~and where~~ the absence of a number implying that the number is zero.

The tree-based technique just described cannot be applied successfully to sparse areas due to the lack of trees from which to measure the appropriate distances. Trees could be shown to be within some sparse areas, where there exist a few scattered trees, but sparse areas void of trees would not be shown up.

4.6 Results

The grid point method of mapping the clumped and sparse areas of a spatial pattern was used in (i) a Poisson forest generated by a pseudo-random number generator; (ii) a modified Thomas process (see Chapter 2 page 33) with mean number of offspring 5, and radial dispersion 0.2; (iii) a population of trees placed at the vertices of a square lattice of side 1.0, and then displaced randomly, the radial coordinates of the displacement having p.d.f.

$$\frac{1}{2\pi d^2} \quad r \exp(-\tfrac{1}{2}r^2/d^2), \qquad 0 \leqslant \theta \leqslant 2\pi, \quad 0 \leqslant r < \infty,$$

(here d was taken as 1.0); (iv) the trees in Lansing Woods, as described in Chapters 1, 2 and 3.

The value of N was chosen as 22 for two reasons. Firstly, to enable edge effects to be kept small. Secondly, because for $N \geqslant 23$ the rounding errors badly distorted the distribution function of T_n when calculated by computer, and thus preventing C_n and S_n from being found. The sampling area for each data set was chosen as a 10.4 in. by 10.4 in. square placed symmetrically within the 15 in. by 15in. area containing the trees. (Note that 1 in. represents 61.6ft.)

Within the sampling area, a square grid of 23 by 23 points was placed to cover the area entirely, and then for each set of data, and for each grid point, the values of T_n (n = 2, ..., 22) were found. The computer package SYMAP was then used on each set of data to map the clumped and sparse areas for several levels (sizes) between 2 and 22. Typical output from SYMAP is shown overleaf. For each tree within each data set, the "most likely" clump size was found as indicated in section 4.5. Results obtained are found in Figs.4(4), 4(5), 4(6), 4(7), 4(8), 4(9), 4(10), 4(11) and 4(12).

For each set of data there corresponds one Figure, consisting of four diagrams. Each Figure has its key on the relevant preceding page. Note that for some of the data sets, the subsets of trees forming clumps as defined by the "most likely" clump size numbers are enclosed in a heavy black line. However when there are many trees close together this is not very practical and it is probably just as informative to show the "most likely" clump size numbers for each tree, the absence of a number indicating it to be zero. For each data set, the clumped and sparse areas at different levels as drawn by SYMAP, are shown, different coloured contours indicating

CONFORMATIONAL AND PROBABILITY PROPERTIES AND SPATIAL ANALYSIS
Research Group on Models
Harvard University
Cambridge, Massachusetts 02138
UNITED STATES OF AMERICA

TIME = 000.00

P.MAP

C LEVEL ID 0.00

ELECTIVE

0 NUMBER OF LEVELS IS 3
1 MAP SIZE IS 10.00 INCHES LONG BY 10.00 INCHES WIDE
4 LOWER DATA LIMIT IS -00.00
5 UPPER DATA LIMIT IS 00.00
10 DATA POINTS WILL NOT BE LISTED
11 NO HISTOGRAM HAS BEEN REQUESTED FOR APPEAR
4 LEVEL SIZES AND PROPORTIONS IN 1) 00.00 2) 0.00 3) 00.00
7 NEW SYMBOLS ARE F R

0 SUPPRESS DATA POINT SYMBOLS ON CONFORMANT MAP

0.00 MINUTES END INPUT

TIME = 000.10

MAP 1

C LEVEL ID 0.00

MAP SCALE = 1.0000 INCHES ON OUTPUT MAP/UNITS ON SOURCE MAP

MAP SHOULD BE PRINTED AT 0.0 ROWS PER INCH AND 10.0 COLUMNS PER INCH

ROW = (ROWS COORDINATE = 0.00) * 0.0000
COLUMN = (COLS COORDINATE = 0.00) * 10.0000

STANDARD SYMBOL DARKNESS IS 0.0100

0.00 MINUTES FOR INITIAL CALCULATIONS

TIME = 000.10

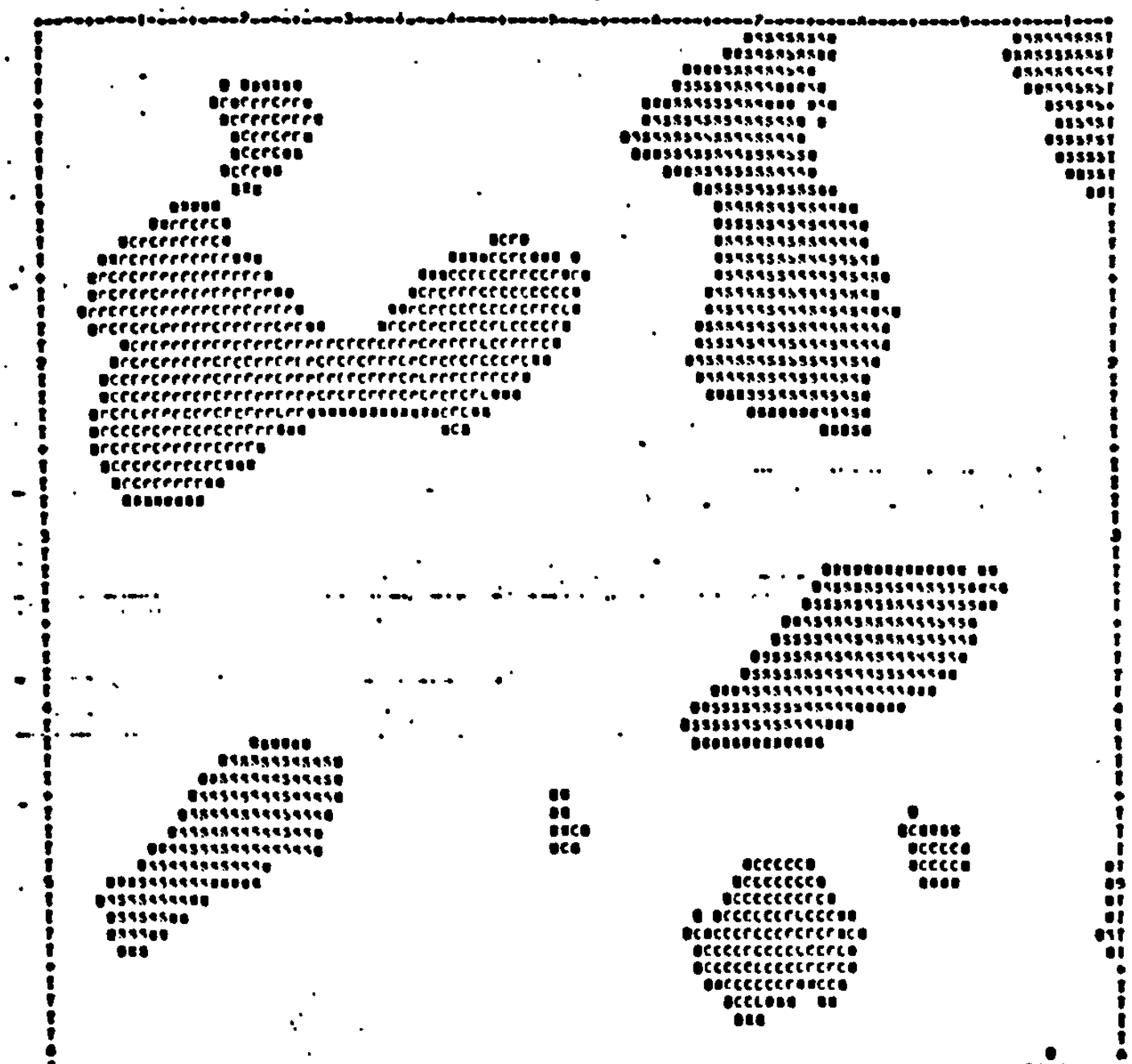

SYMBOLS

0.00 MINUTES END MAP

TIME = 071.00

C LEVEL ID 0.00 RED OAKS

DATA VALUE EXTREMES ARE -0.00 0.00

OBSERVED VALUE RANGES APPLYING TO EACH LEVEL
(PARENTHESES INCLUDED IN HIGHEST LEVEL ONLY)

MINIMUM -00.00 -0.00 0.00
MAXIMUM -0.00 0.00 00.00

PERCENTAGE OF TOTAL OBSERVED VALUE RANGES APPLYING TO EACH LEVEL

00.00 0.00 00.00

different levels. The continuous lines indicate clumped areas, and the broken lines indicate sparse areas. Thus for example a blue broken contour indicates a sparse area of size ten, while a green continuous contour indicates a clumped region of size two. Also given for the data sets, except the first, is a diagram of the position of the trees, to aid the viewing of the clumped and sparse areas in relation to the positions of the trees.

Key to Fig. 4(4) (POISSON FOREST)

4(4) (i) "Most likely" clump sizes for the simulated Poisson forest for $C_n(\alpha)$ defined by the 2½% probability level of T_n. (i.e. $\alpha = 2\frac{1}{2}$).

4(4) (ii) "Most likely" clump sizes for the simulated Poisson forest for $C_n(\alpha)$ defined by the 5% probability level of T_n, (i.e. $\alpha = 5$).

4(4) (iii) Contours of the clumped and sparse areas of the simulated Poisson forest with $C_n(\alpha)$ and $S_n(\alpha)$ defined by the 2½% probability level of T_n.

4(4) (iv) Contours of the clumped and sparse areas of the simulated Poisson forest with $C_n(\alpha)$ and $S_n(\alpha)$ defined by the 2½% probability level of T_n.

Colour code

Colour	level		
—	2	continuous line	- clumped area
—	5	broken line	- sparse area
—	10		
—	22		

(i)

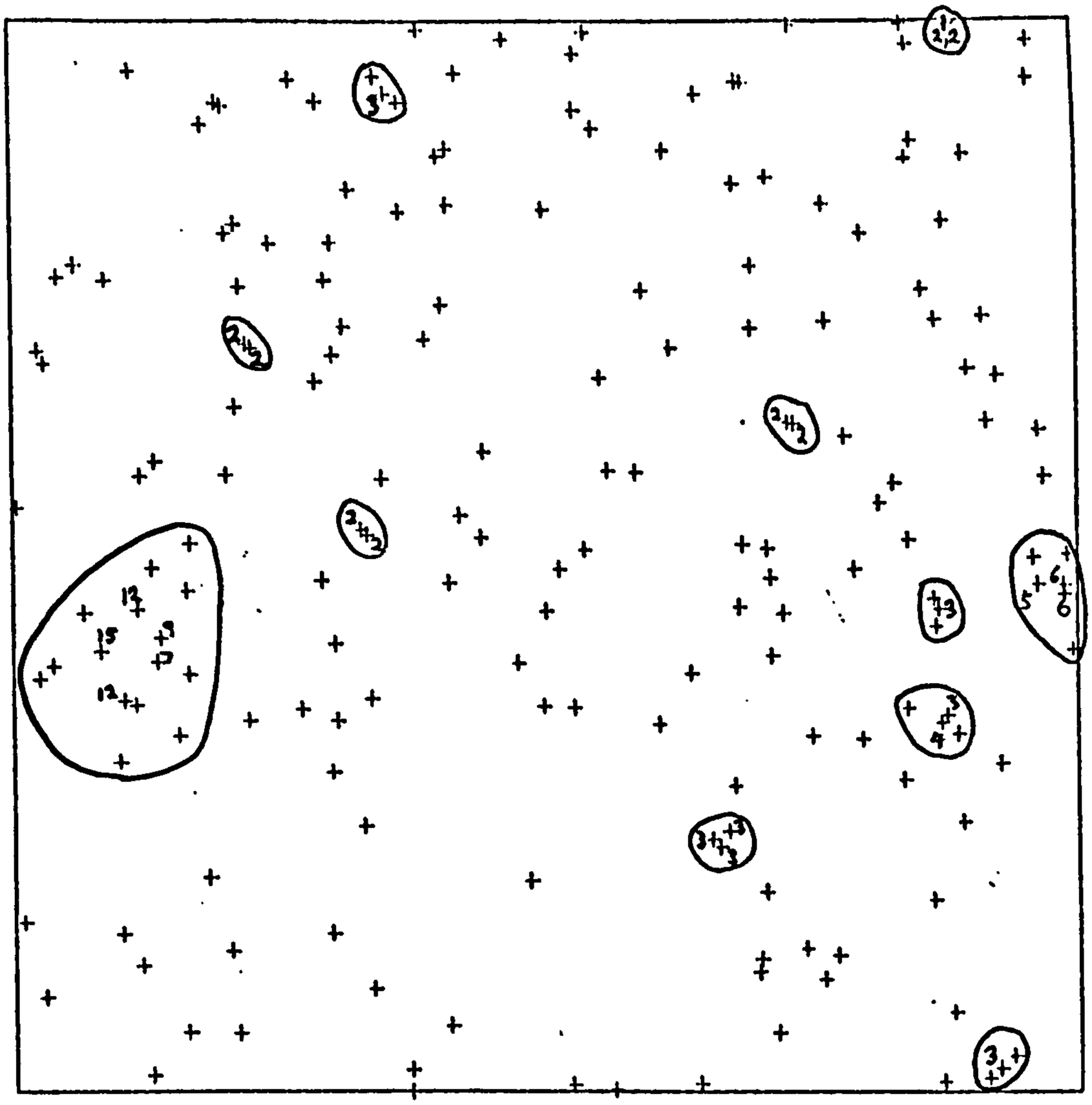

(ii)

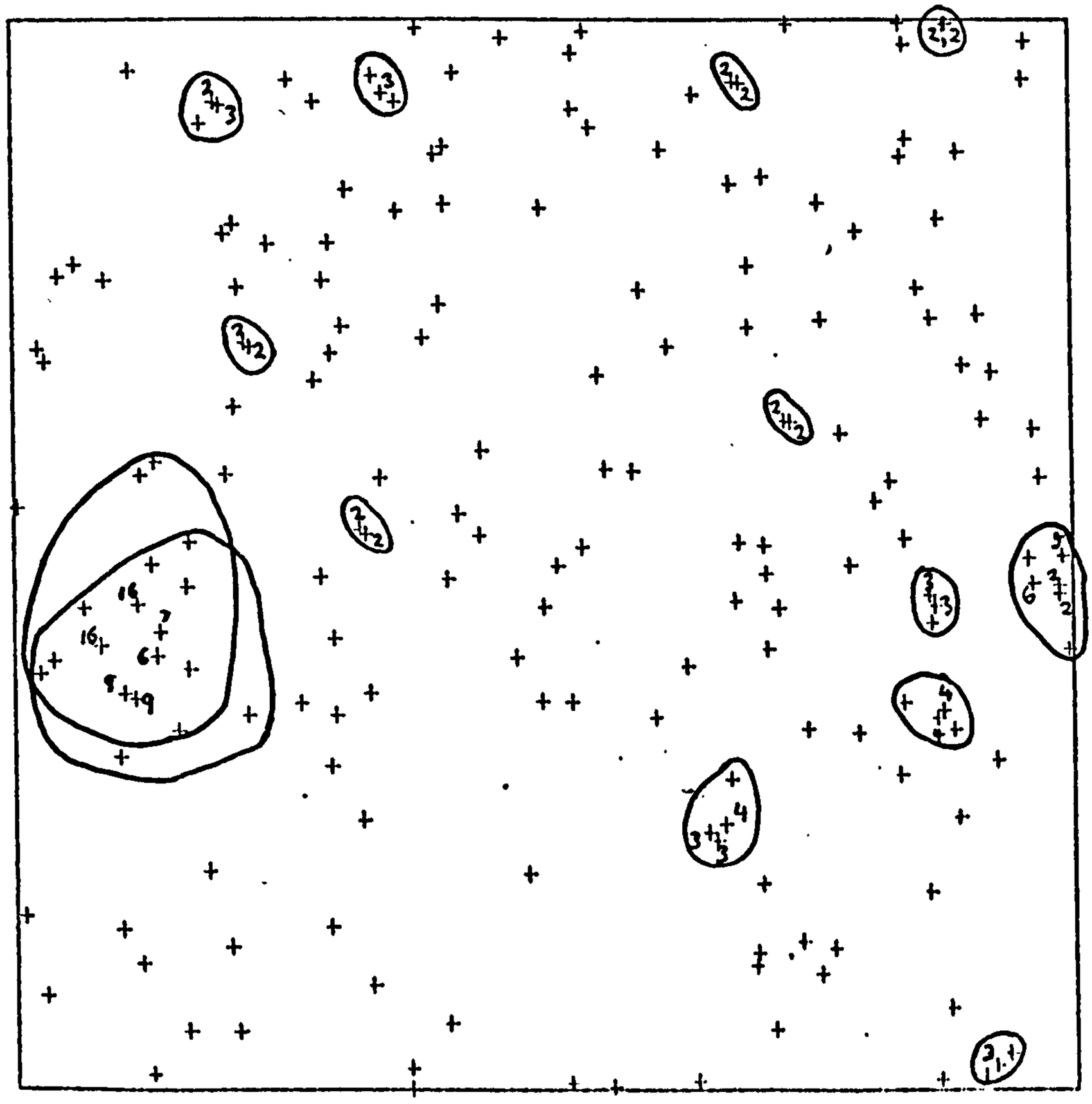

(iii)

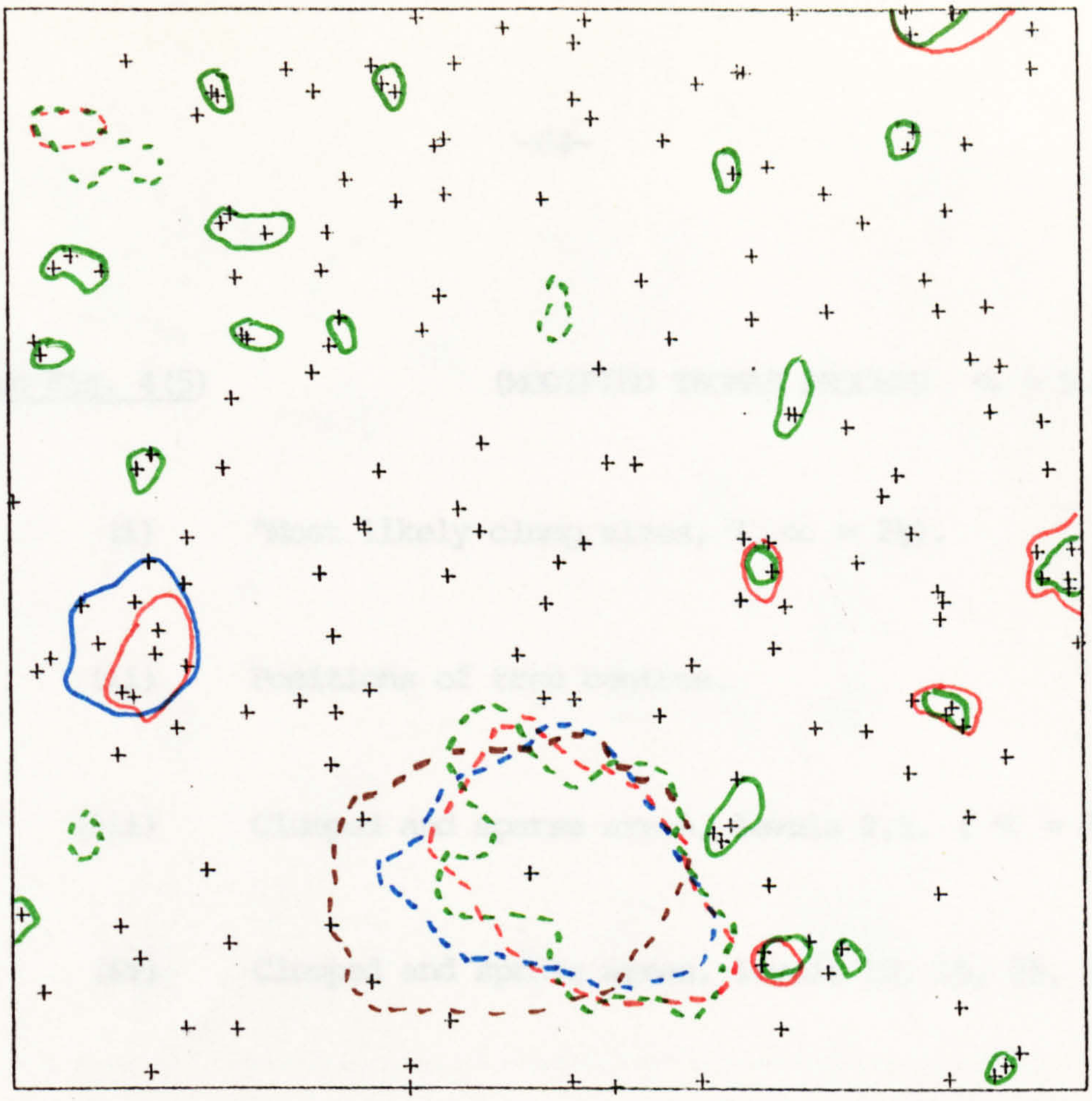

(iv)

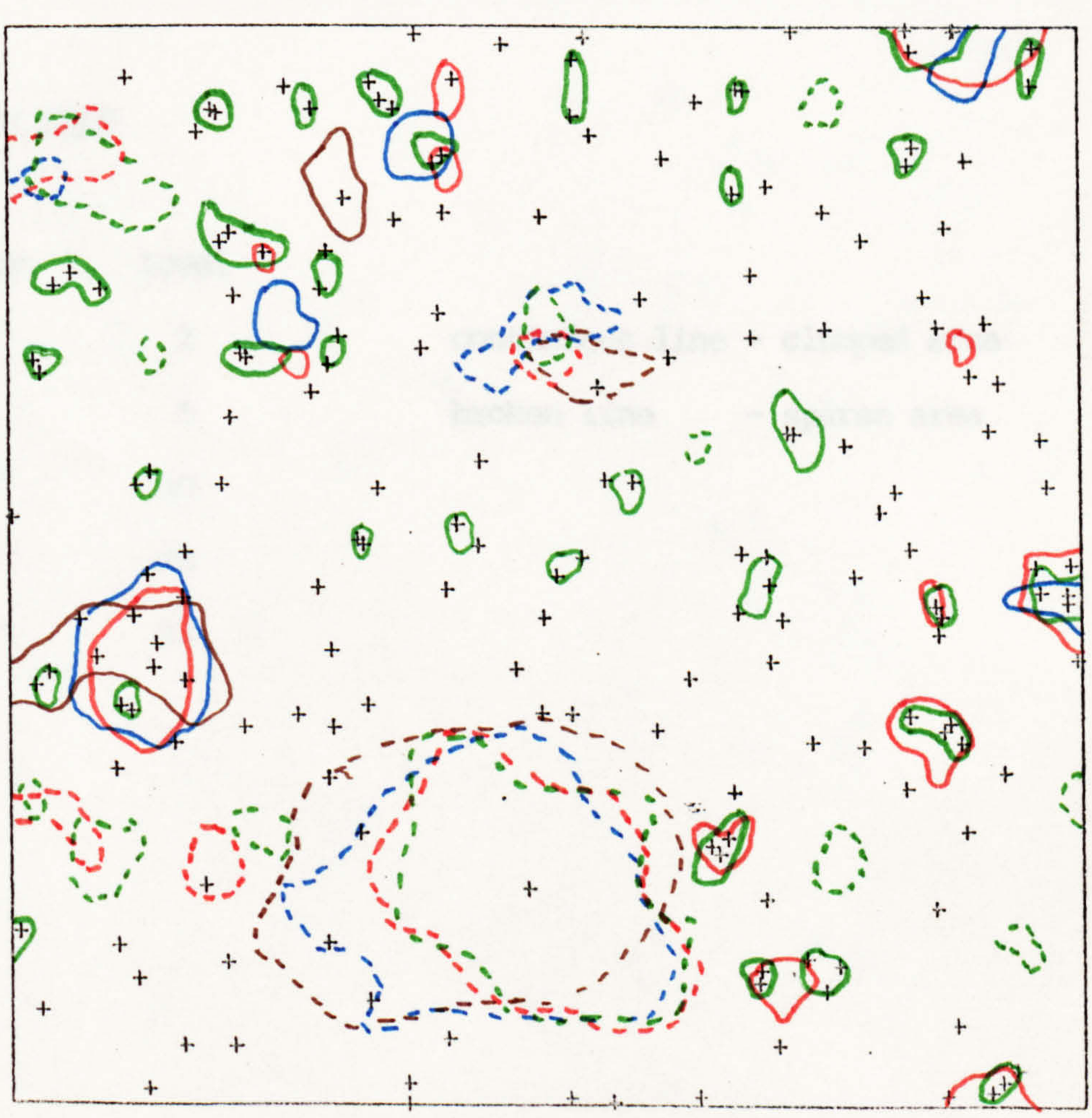

Key to Fig. 4(5) (MODIFIED THOMAS PROCESS $\alpha = 5.0, \sigma = 0.2$)

4(5) (i) "Most likely clump sizes, ($\alpha = 2\frac{1}{2}$).

4(5) (ii) Positions of tree centres.

4(5) (iii) Clumped and sparse areas, levels 2,5, ($\alpha = 2\frac{1}{2}$).

4(5) (iv) Clumped and sprase areas, levels 10, 15, 22, ($\alpha = 2\frac{1}{2}$).

Colour code

colour	level	
—	2	continuous line - clumped area
—	5	broken line - sparse area
—	10	
—	15	
—	22	

(i)

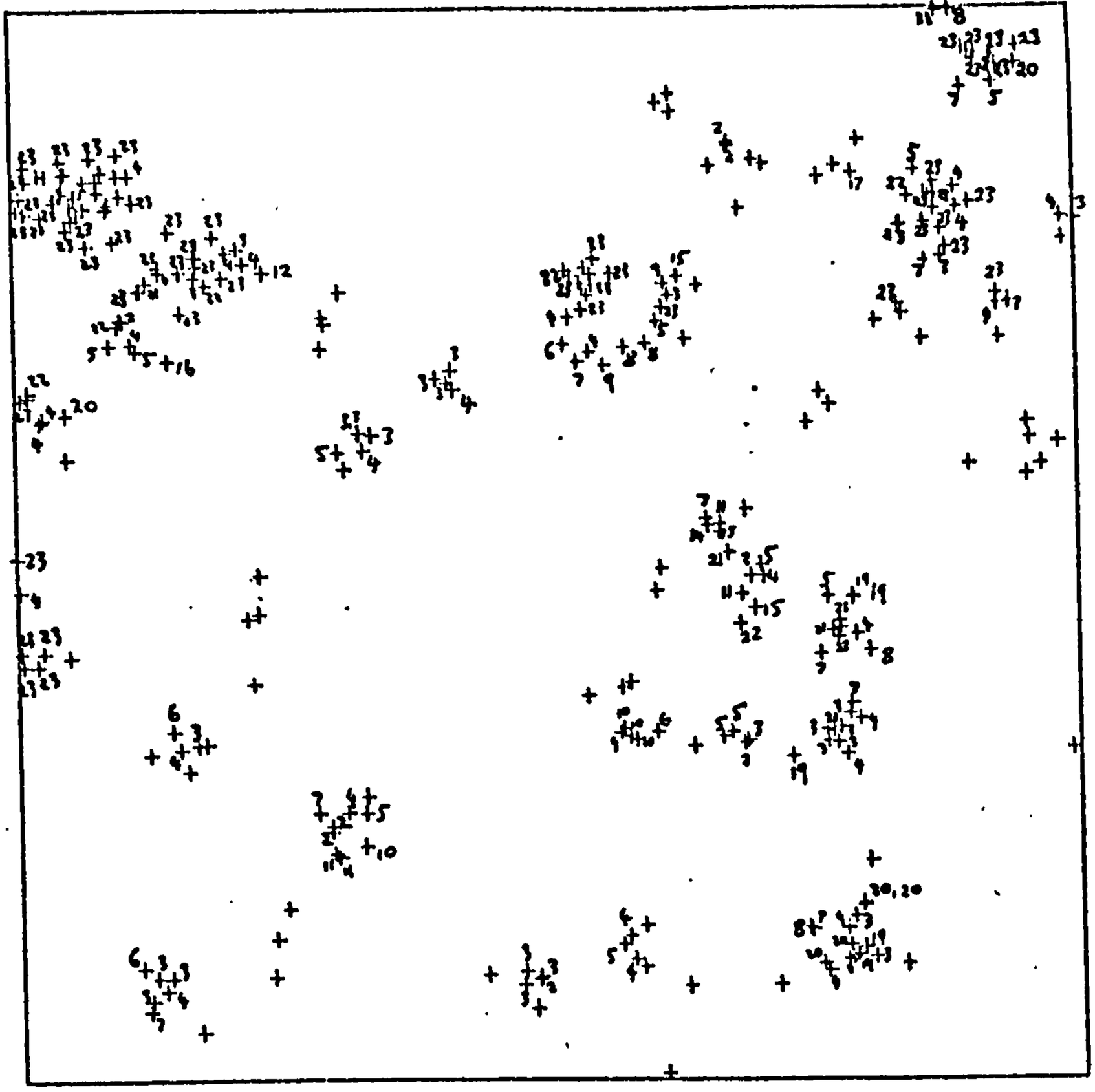

(ii)

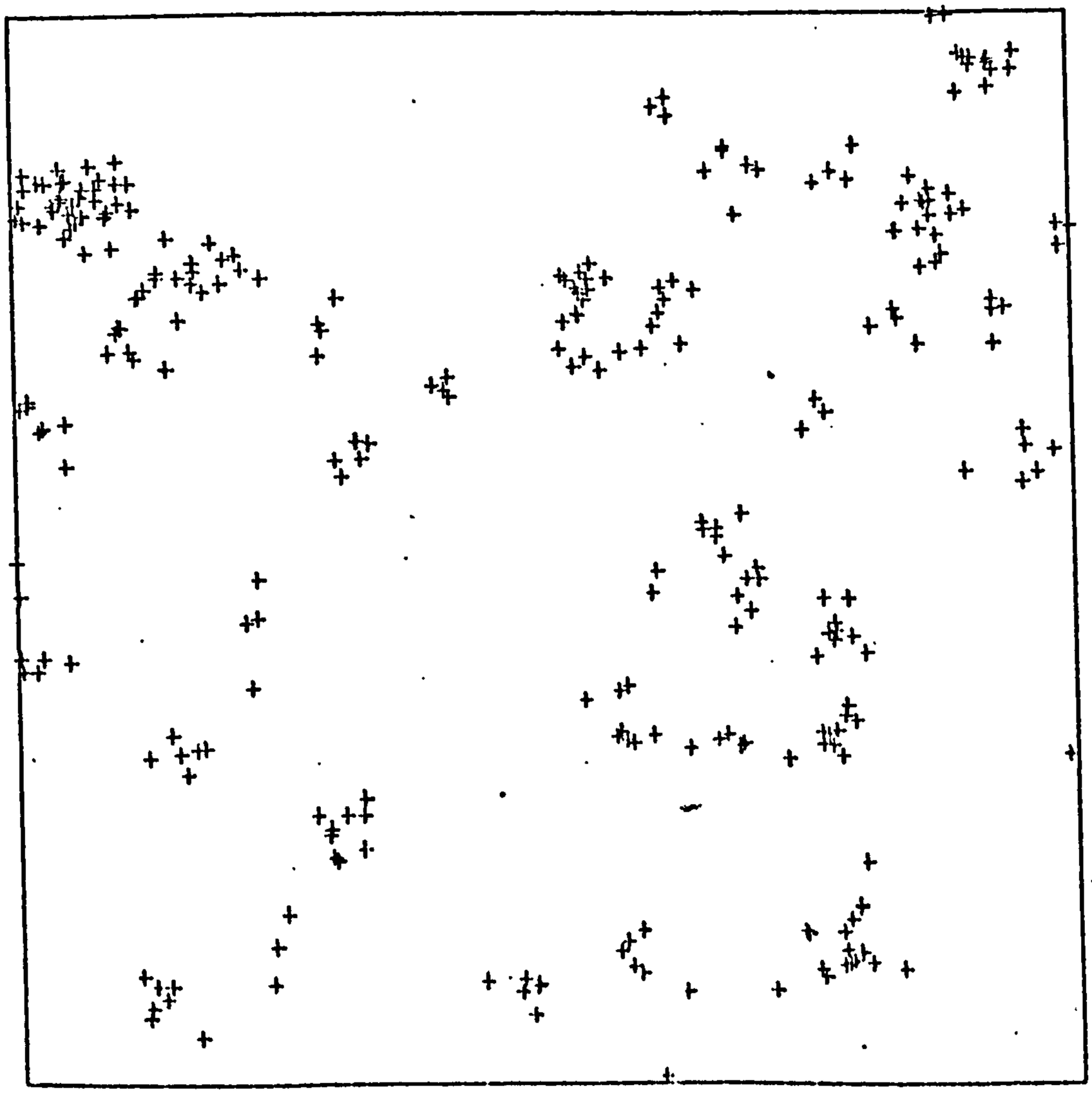

(ii)

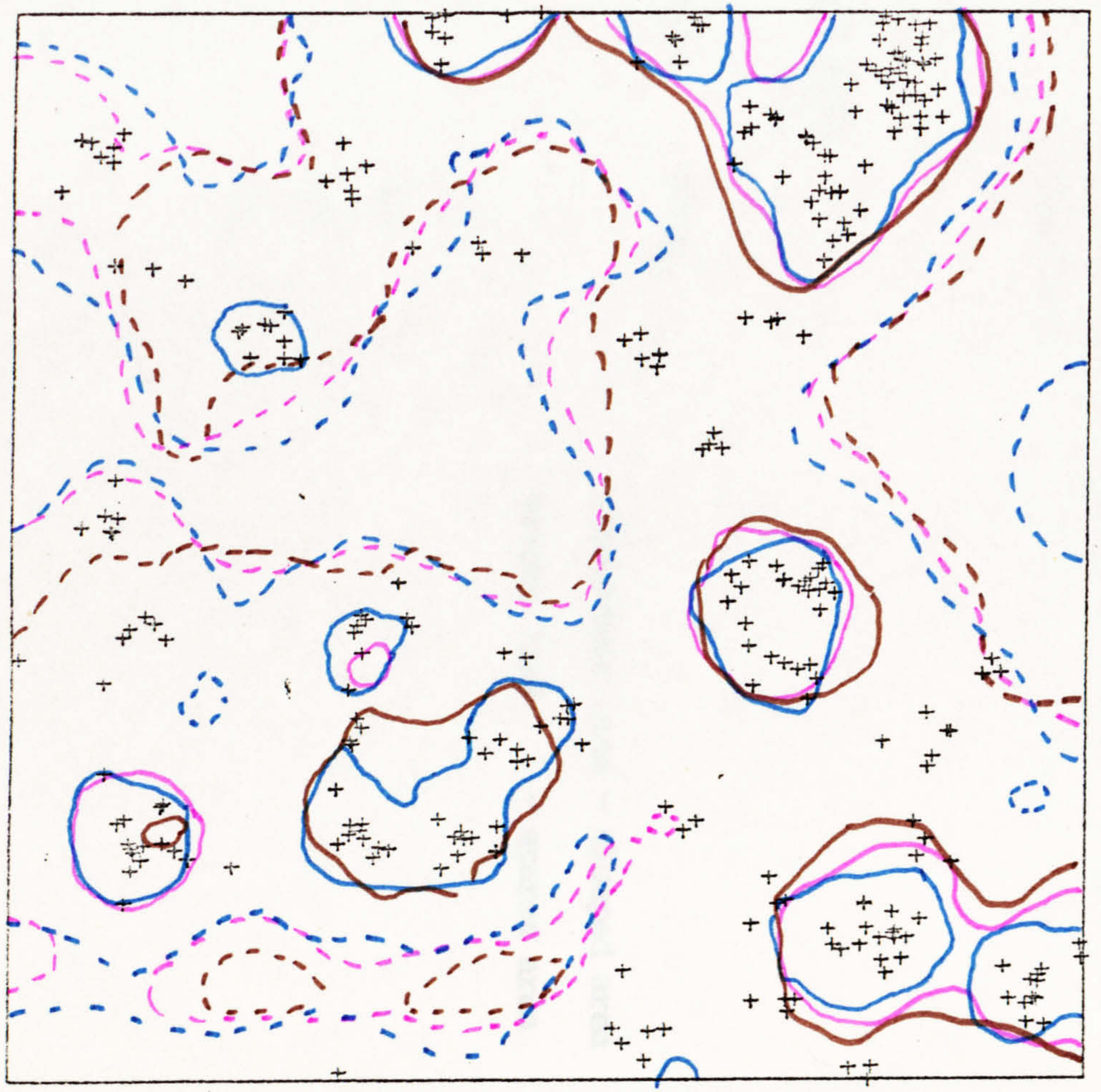

(iii)

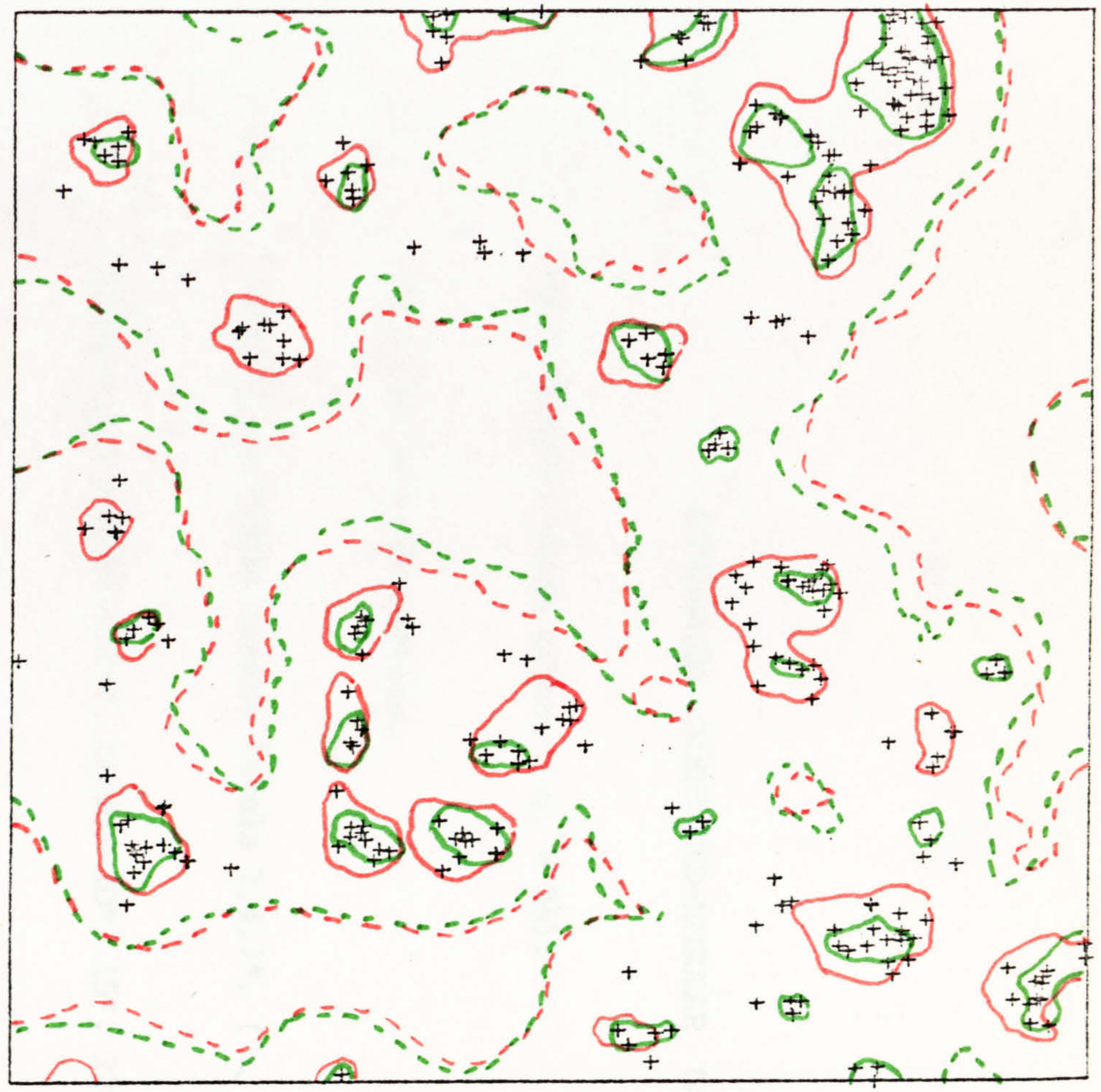

Key to Fig.4(6) (SIMULATED DISPLACED-REGULAR DATA)

4(6) (i) "Most likely" clump sizes, (α = 2½).

4(6) (ii) Positions of tree centres.

4(6) (iii) Clumped and sparse areas, levels 2,4,7*, (α = 2½).

4(6) (iv) Clumped and sparse areas, levels 10*, 15*, 22*, (α = 2½).

*Note that there are no areas, clumped or sparse at this level.

Colour code

colour	level	
—	2	continuous line - clumped area
—	4	broken line - sparse area
—	7	
—	10	
—	15	
—	22	

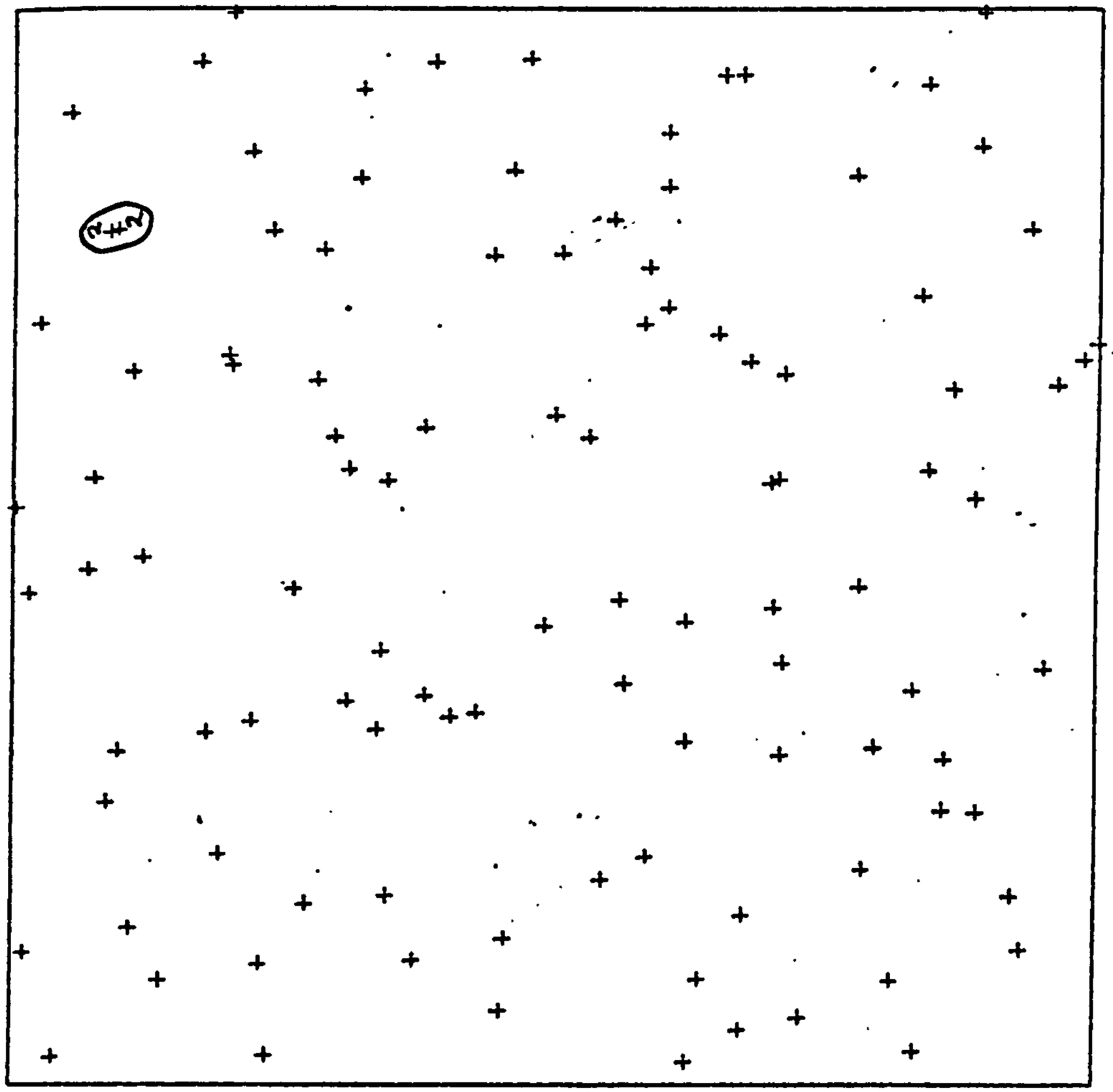

(a)

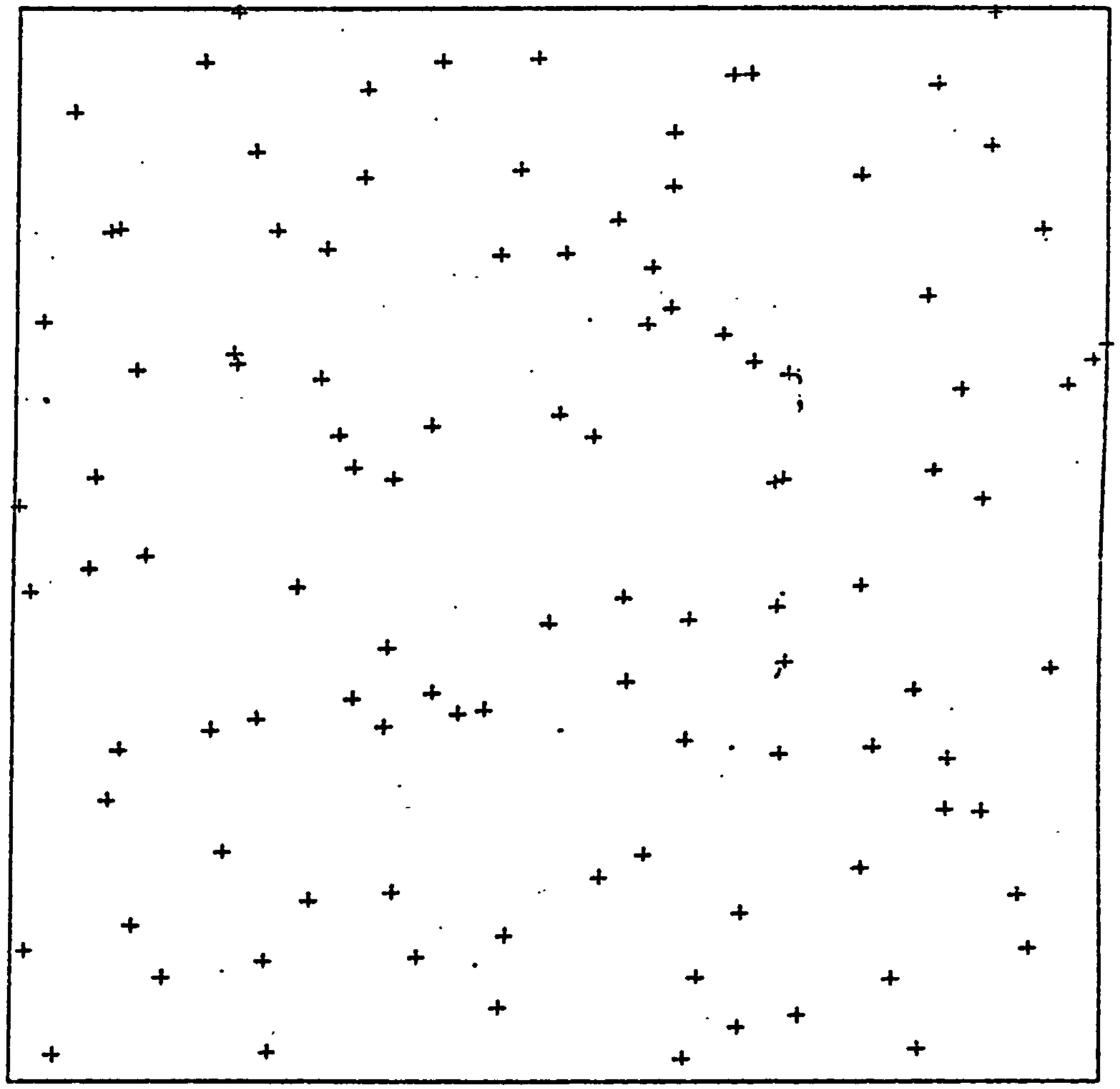

(b)

(iii)

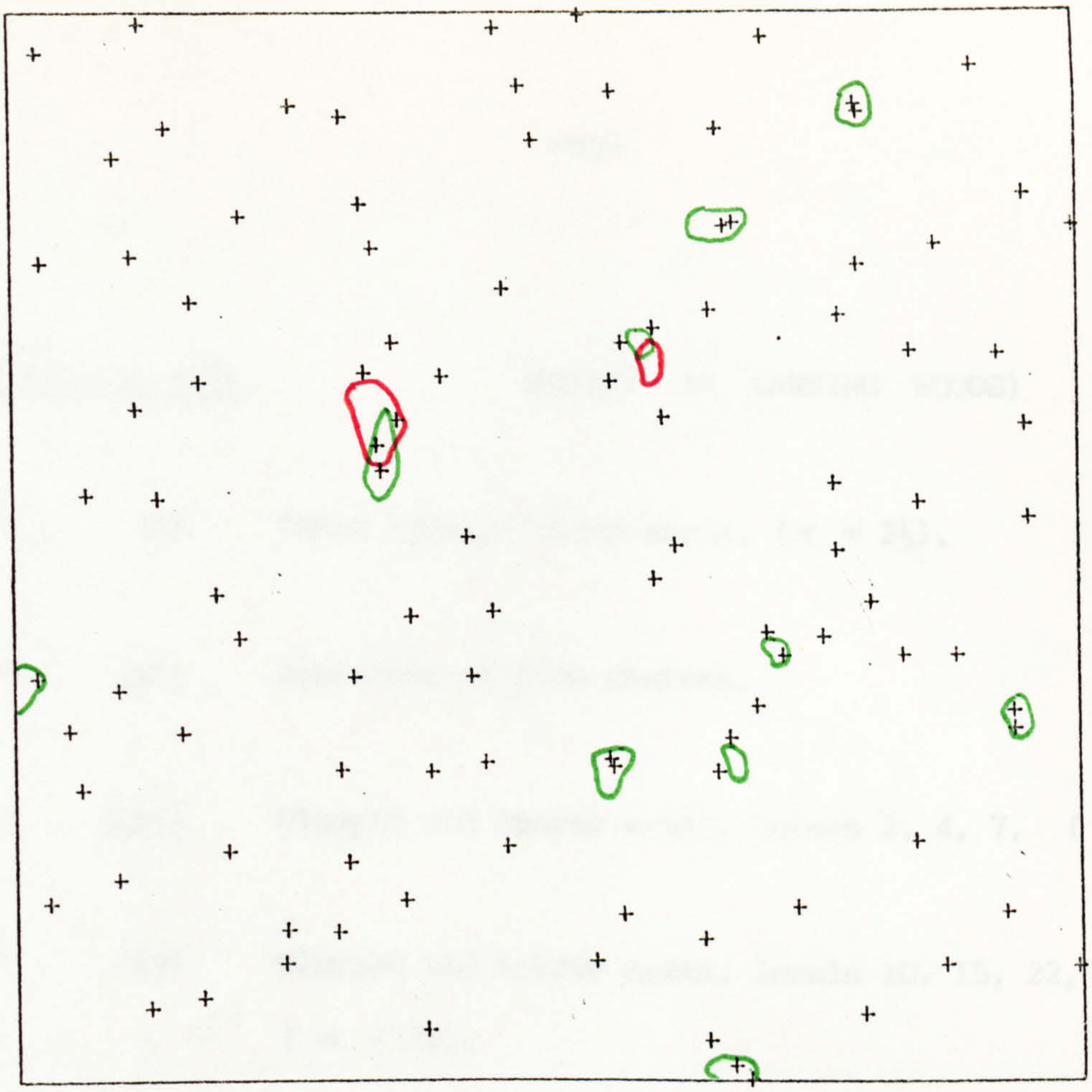

(iv)

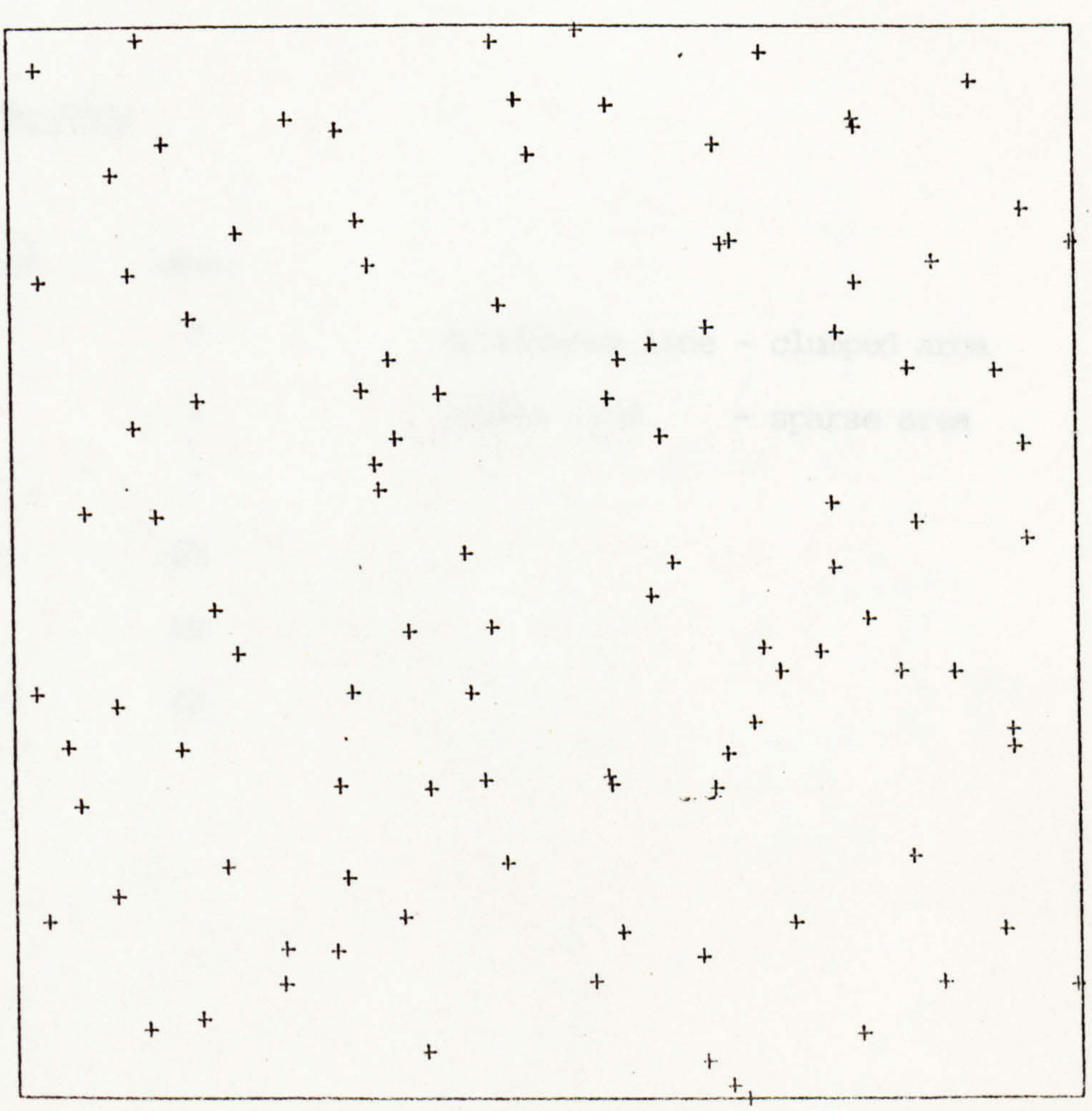

Key to Fig. 4(7) (MAPLES IN LANSING WOODS)

4(7) (i) "Most likely" clump sizes, ($\alpha = 2\frac{1}{2}$).

4(7) (ii) Positions of tree centres.

4(7) (iii) Clumped and sparse areas, levels 2, 4, 7, ($\alpha = 2\frac{1}{2}$).

4(7) (iv) Clumped and sparse areas, levels 10, 15, 22, ($\alpha = 2\frac{1}{2}$).

Colour code

Colour	level	
—	2	continuous line - clumped area
—	4	broken line - sparse area
—	7	
—	10	
—	15	
—	22	

(i)

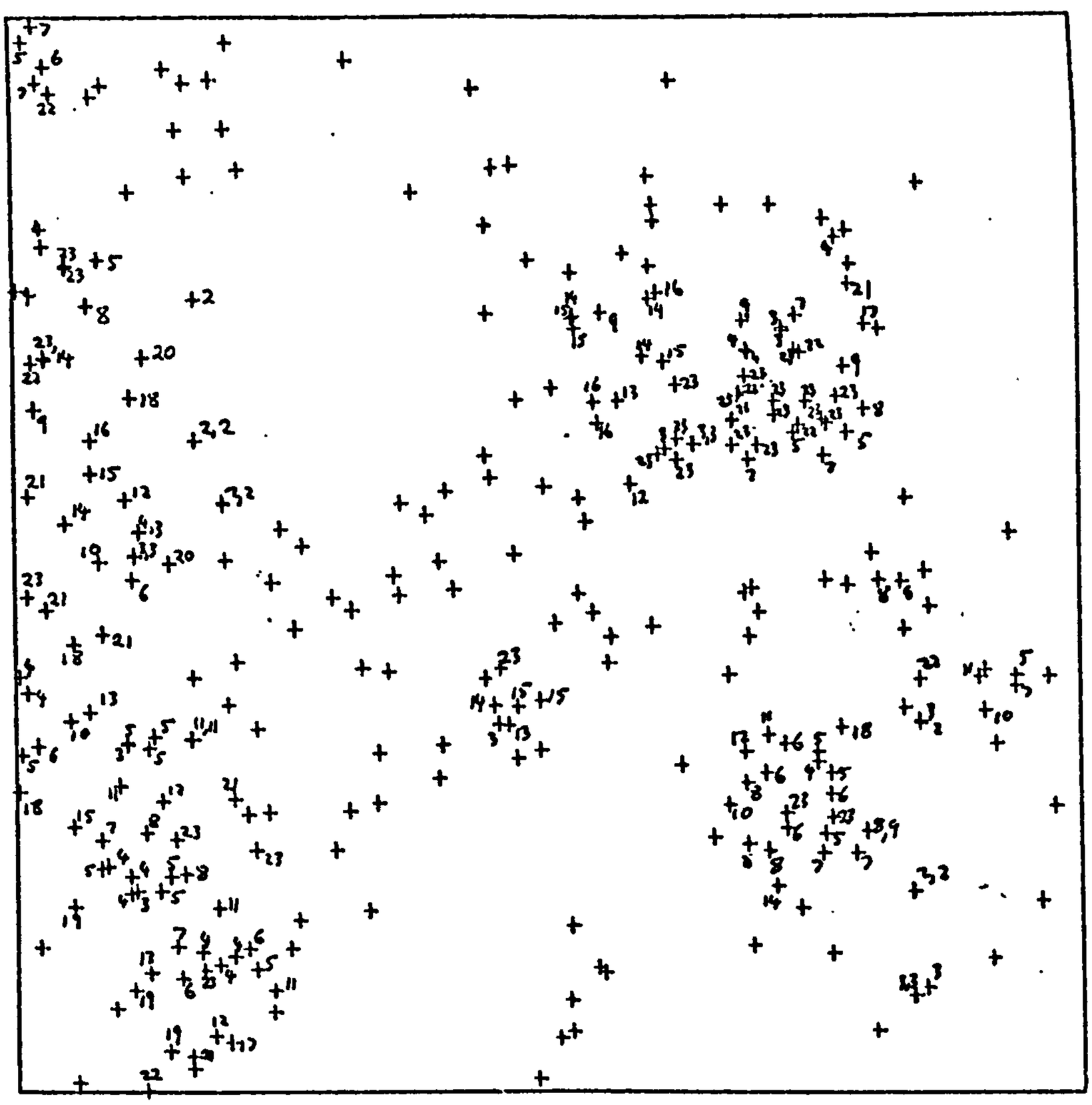

(ii)

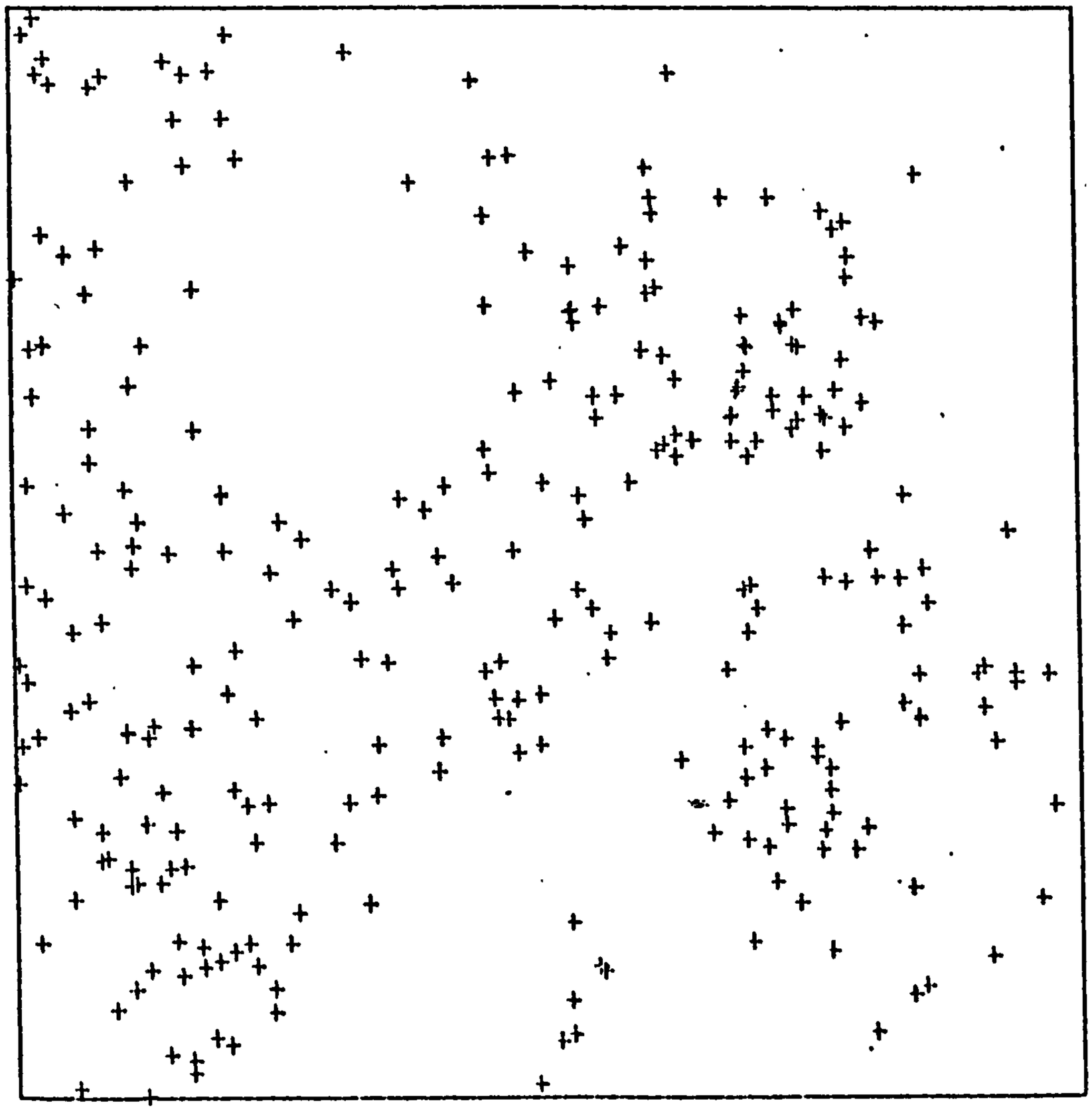

(iii)

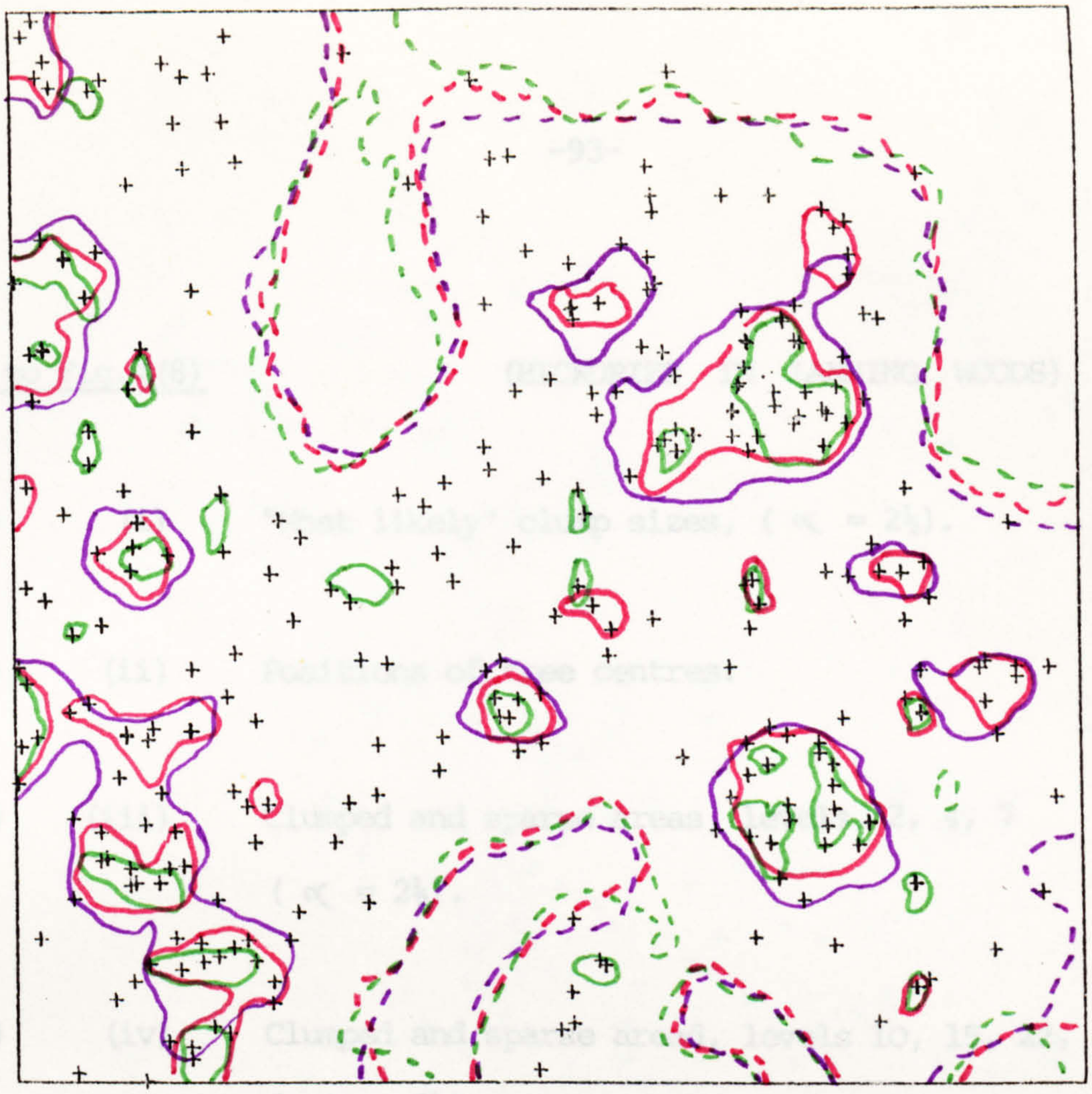

(iv)

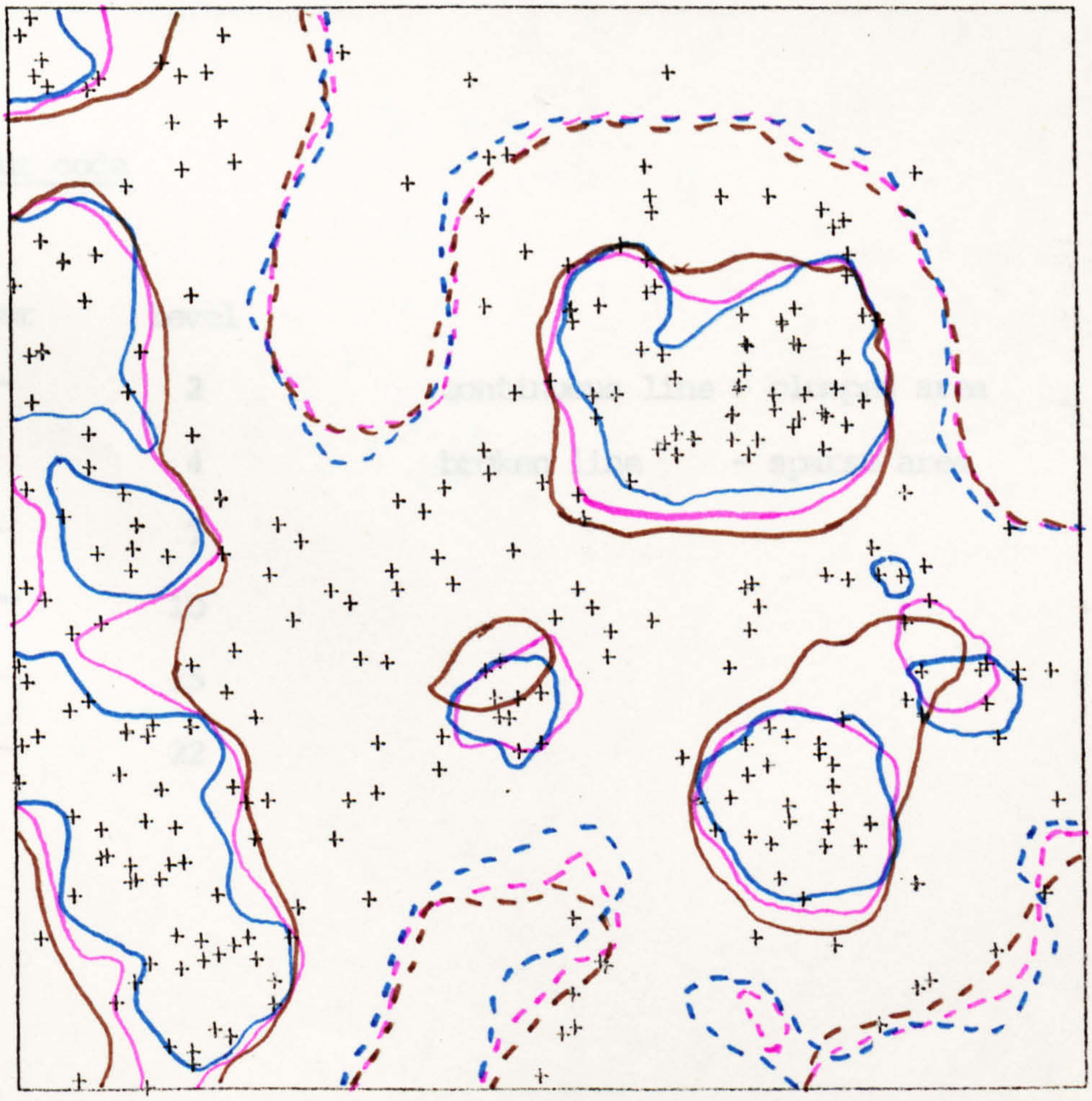

Key to Fig.4(8) (HICKORIES IN LANSING WOODS)

4(8) (i) "Most likely" clump sizes, ($\propto = 2\frac{1}{2}$).

4(8) (ii) Positions of tree centres.

4(8) (iii) Clumped and sparse areas, levels, 2, 4, 7 ($\propto = 2\frac{1}{2}$).

4(8) (iv) Clumped and sparse aread, levels 10, 15, 22, ($\propto = 2\frac{1}{2}$).

Colour code

Colour	level	
—	2	continuous line - clumped area
—	4	broken line - sparse area
—	7	
—	10	
—	15	
—	22	

(i)

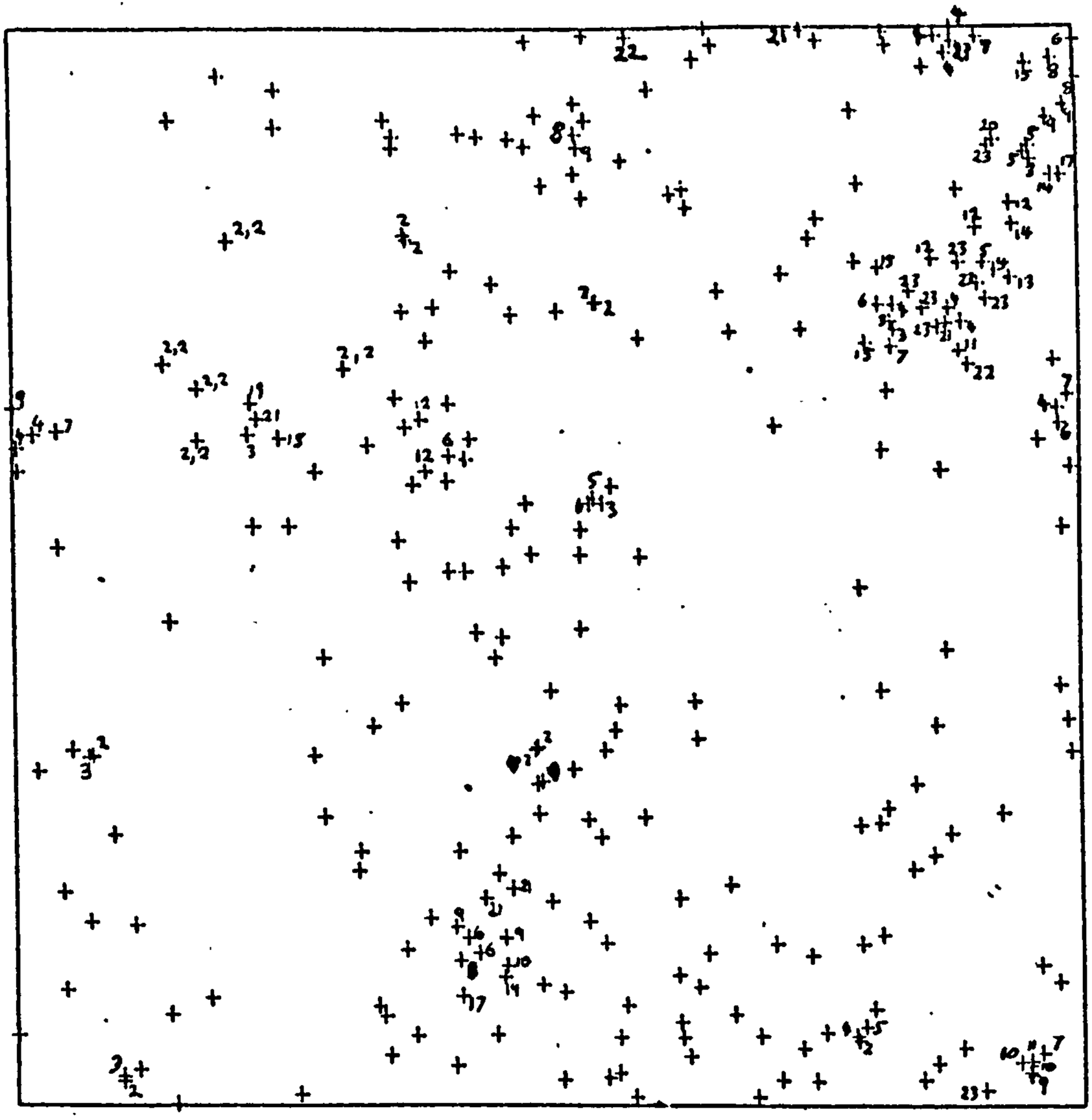

(ii)

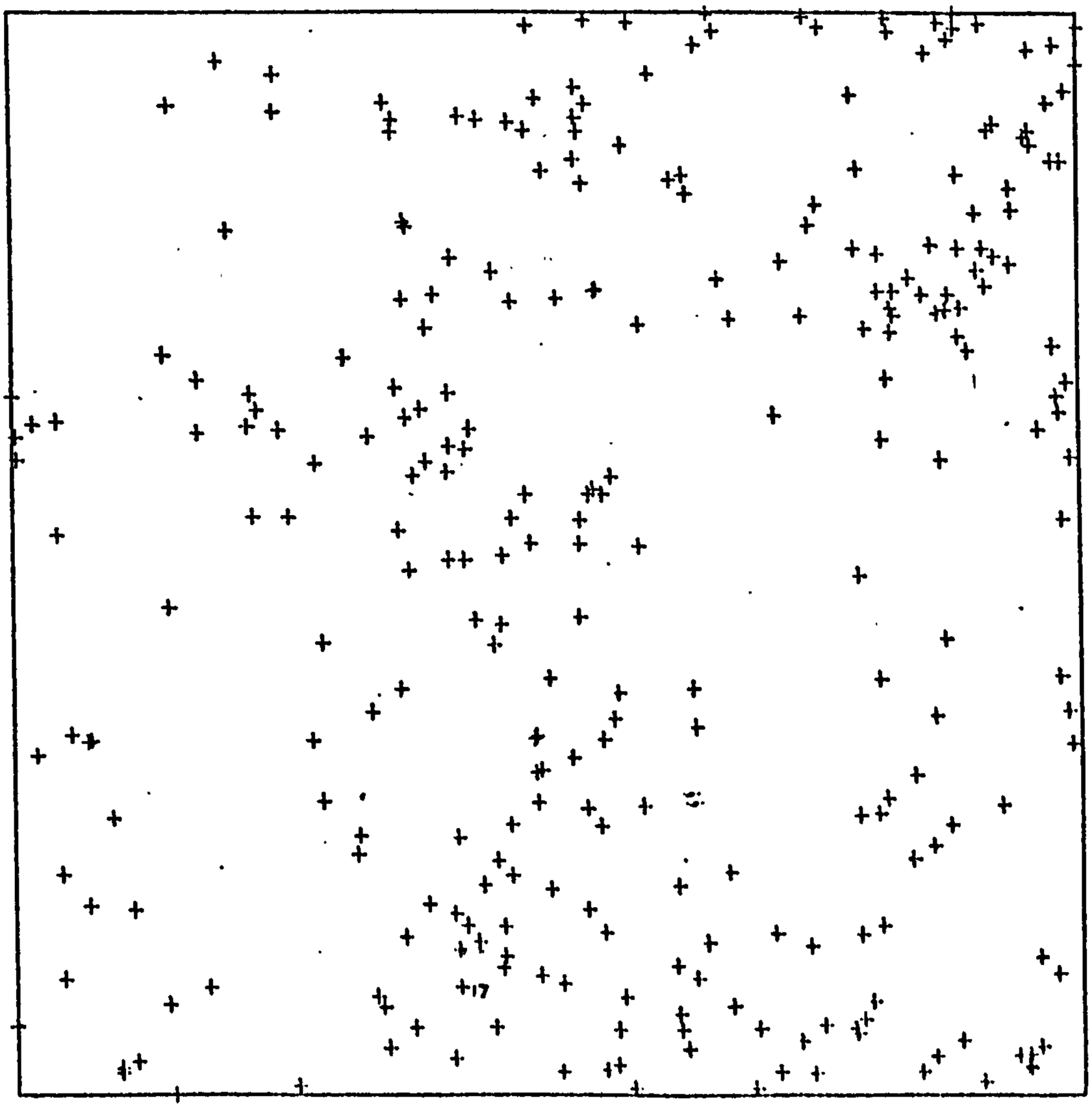

(iii)

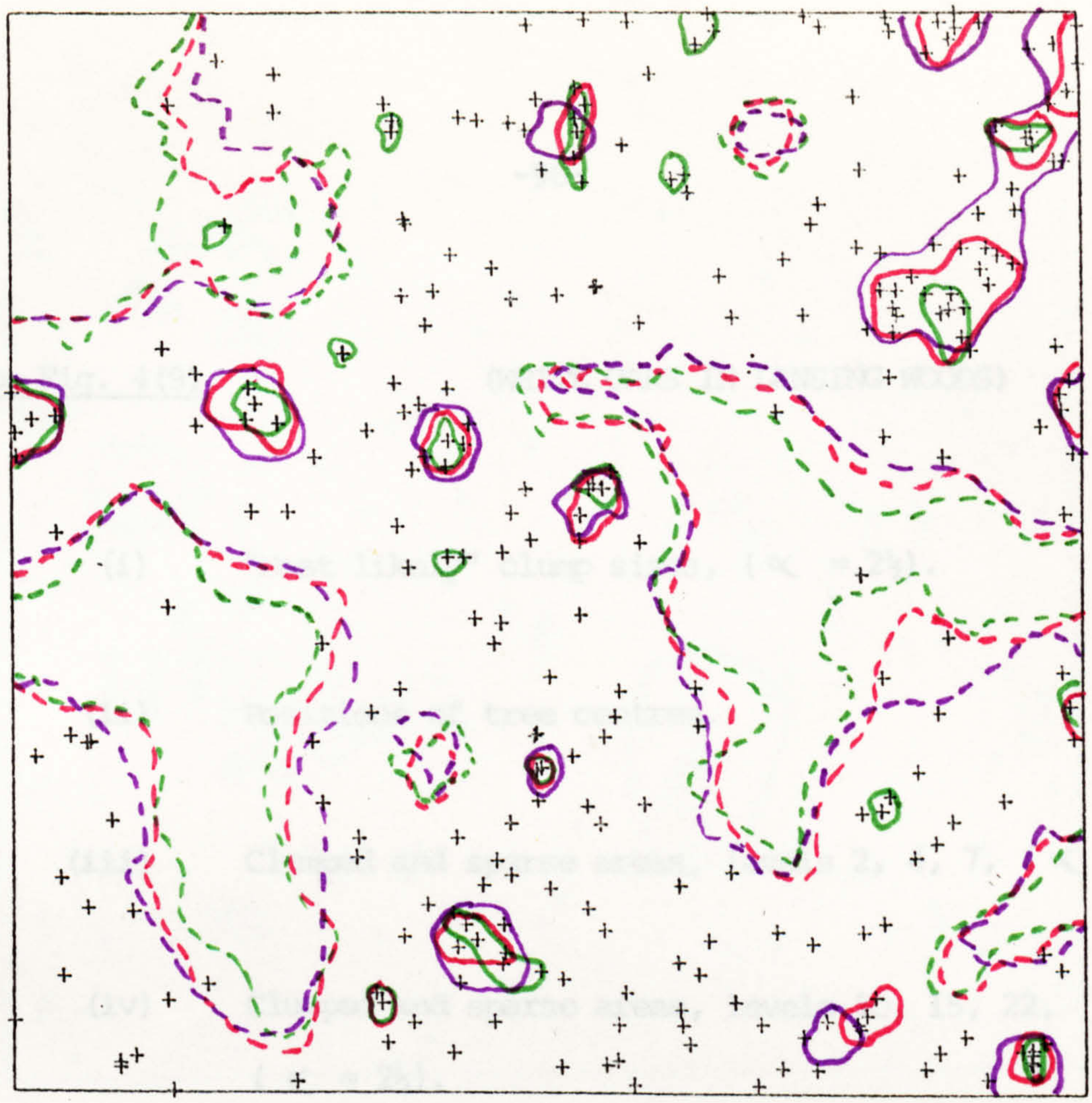

(iv)

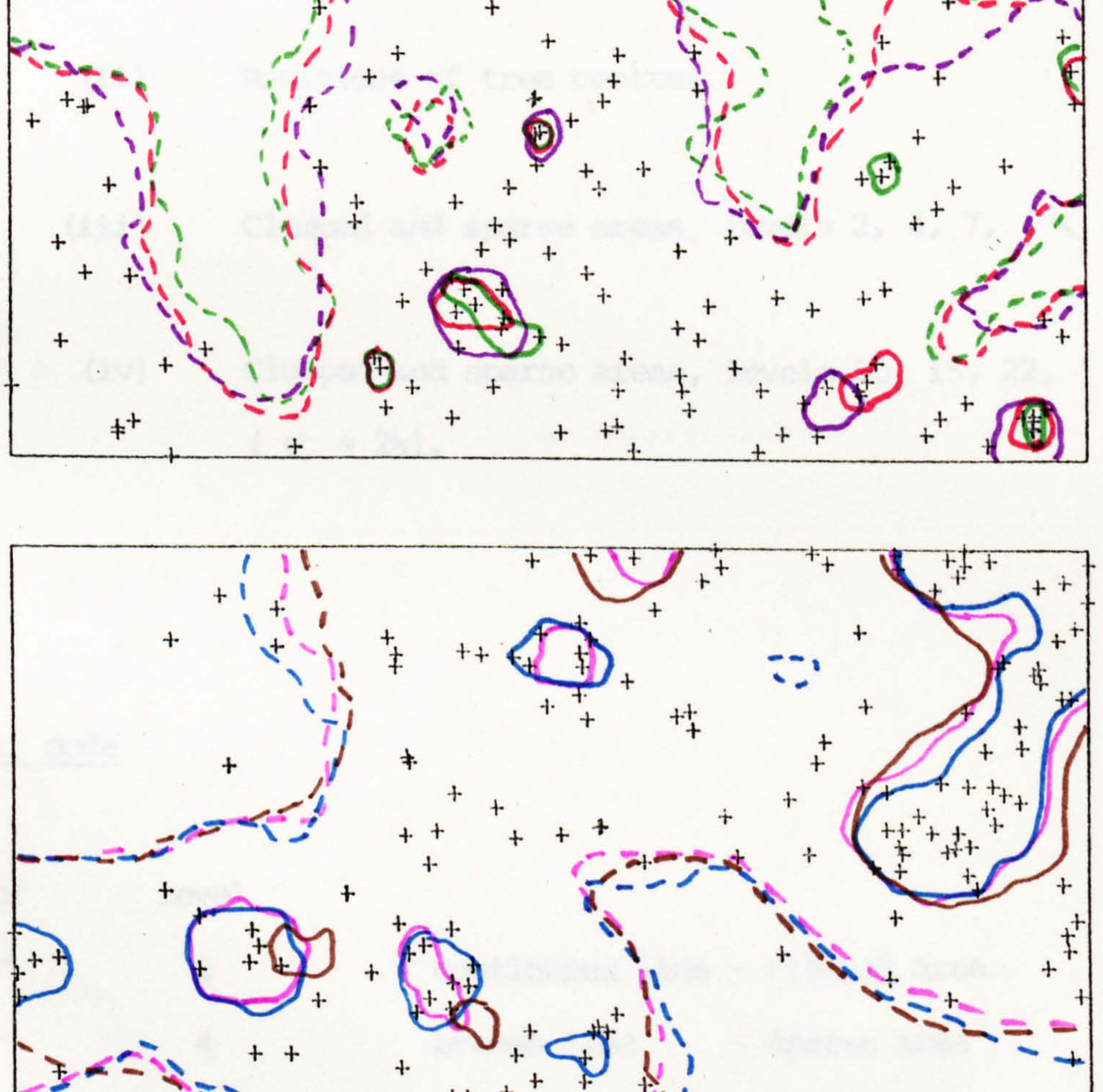

Key to Fig. 4(9) (WHITE OAKS IN LANSING WOODS)

4(9) (i) "Most likely" clump sizes, (α = 2½).

4(9) (ii) Positions of tree centres.

4(9) (iii) Clumped and sparse areas, levels 2, 4, 7, (α = 2½).

4(9) (iv) Clumped and sparse areas, levels 10, 15, 22, (α = 2½).

Colour code

Colour	level	
——	2	continuous line - clumped area
——	4	broken line - sparse area
——	7	
——	10	
——	15	
——	22	

(i)

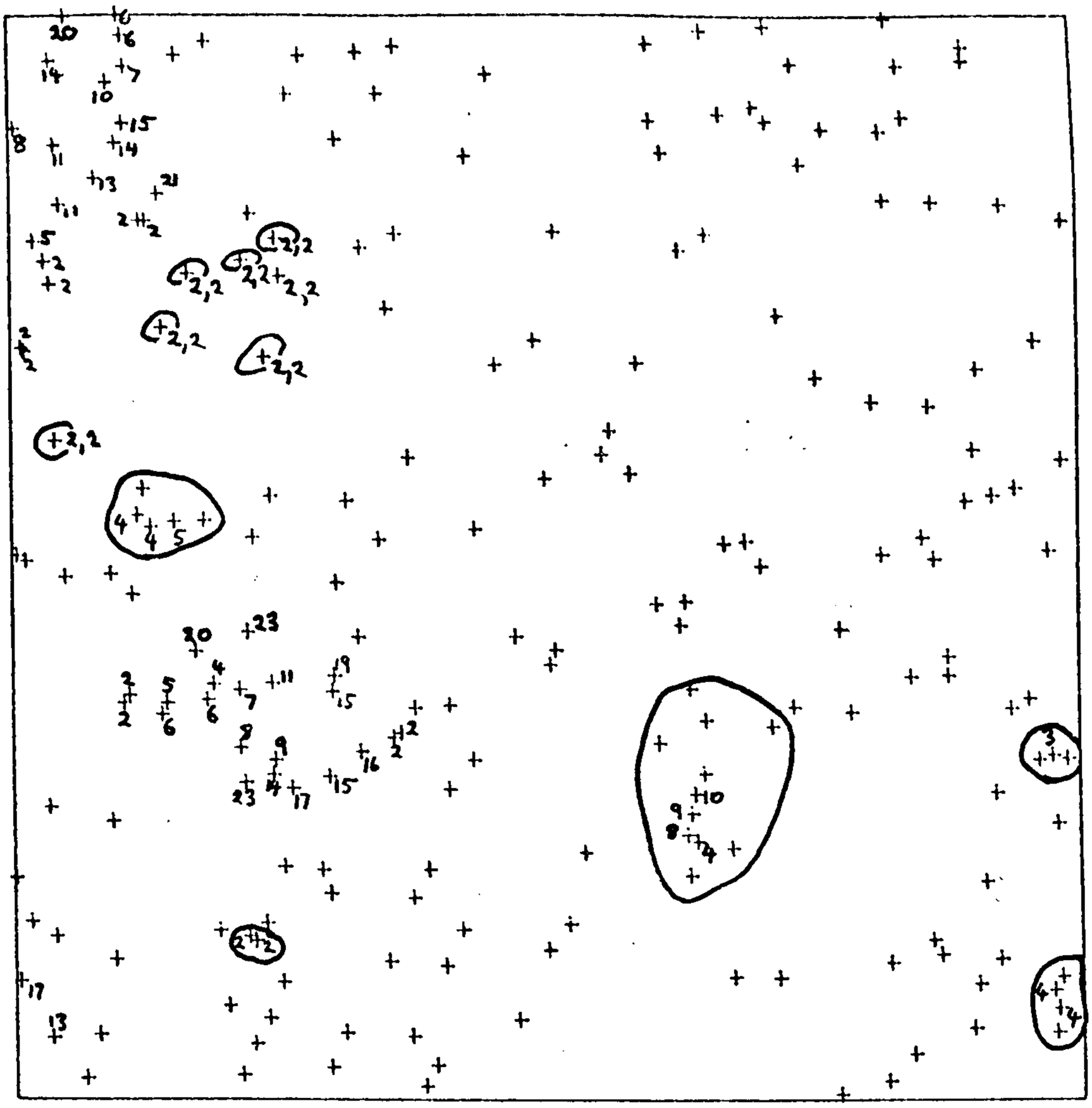

(ii)

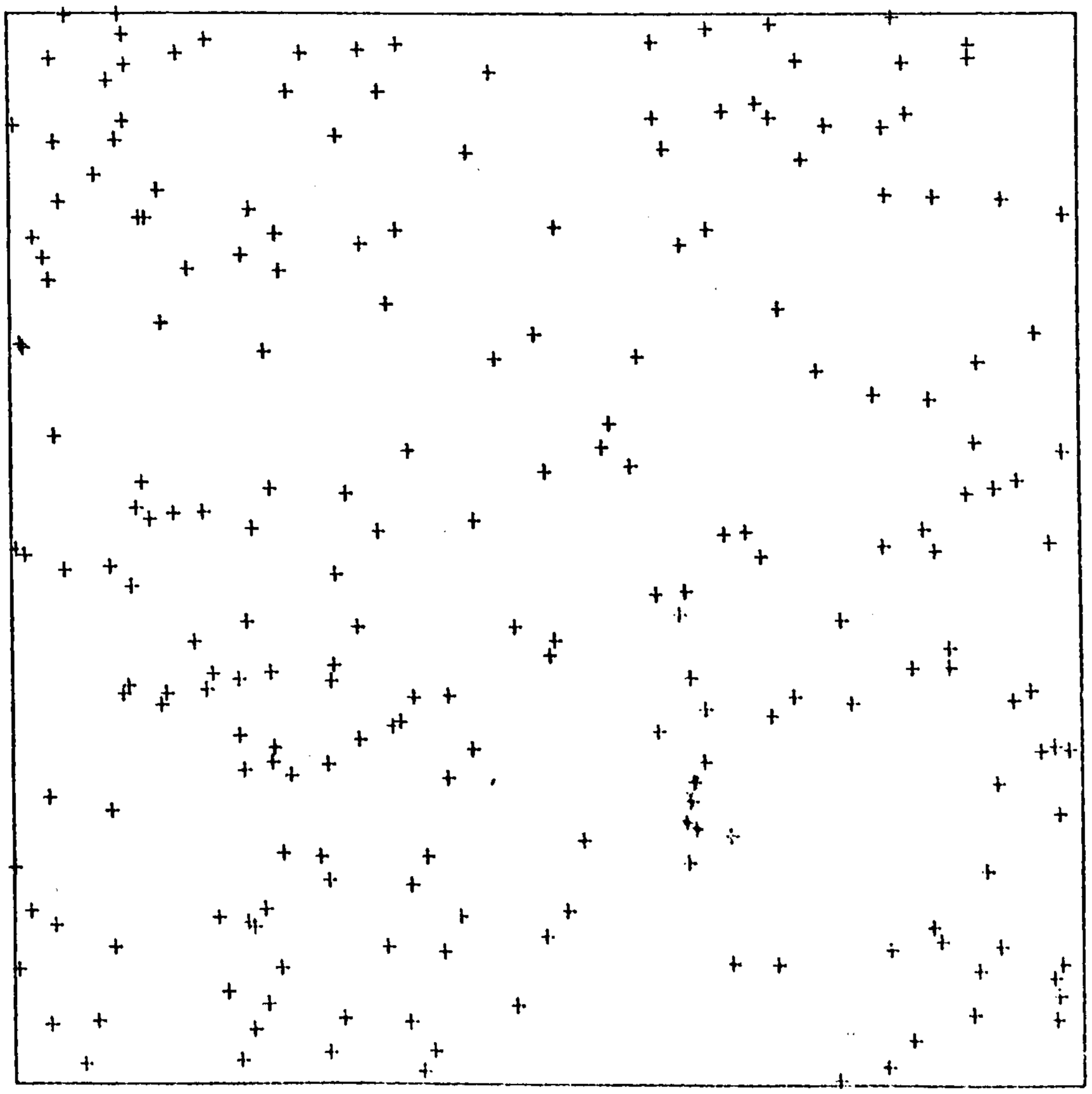

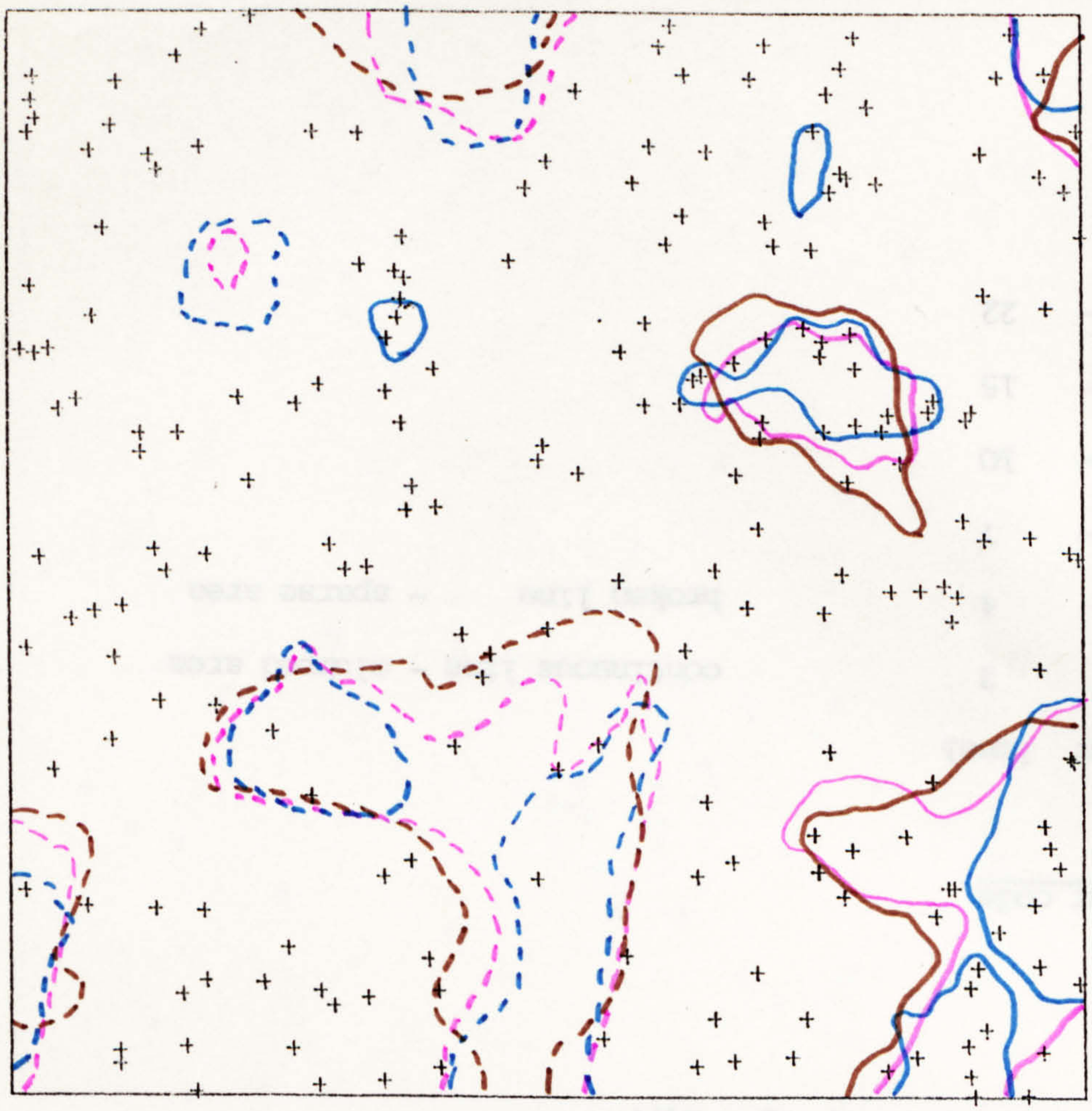

(iv)

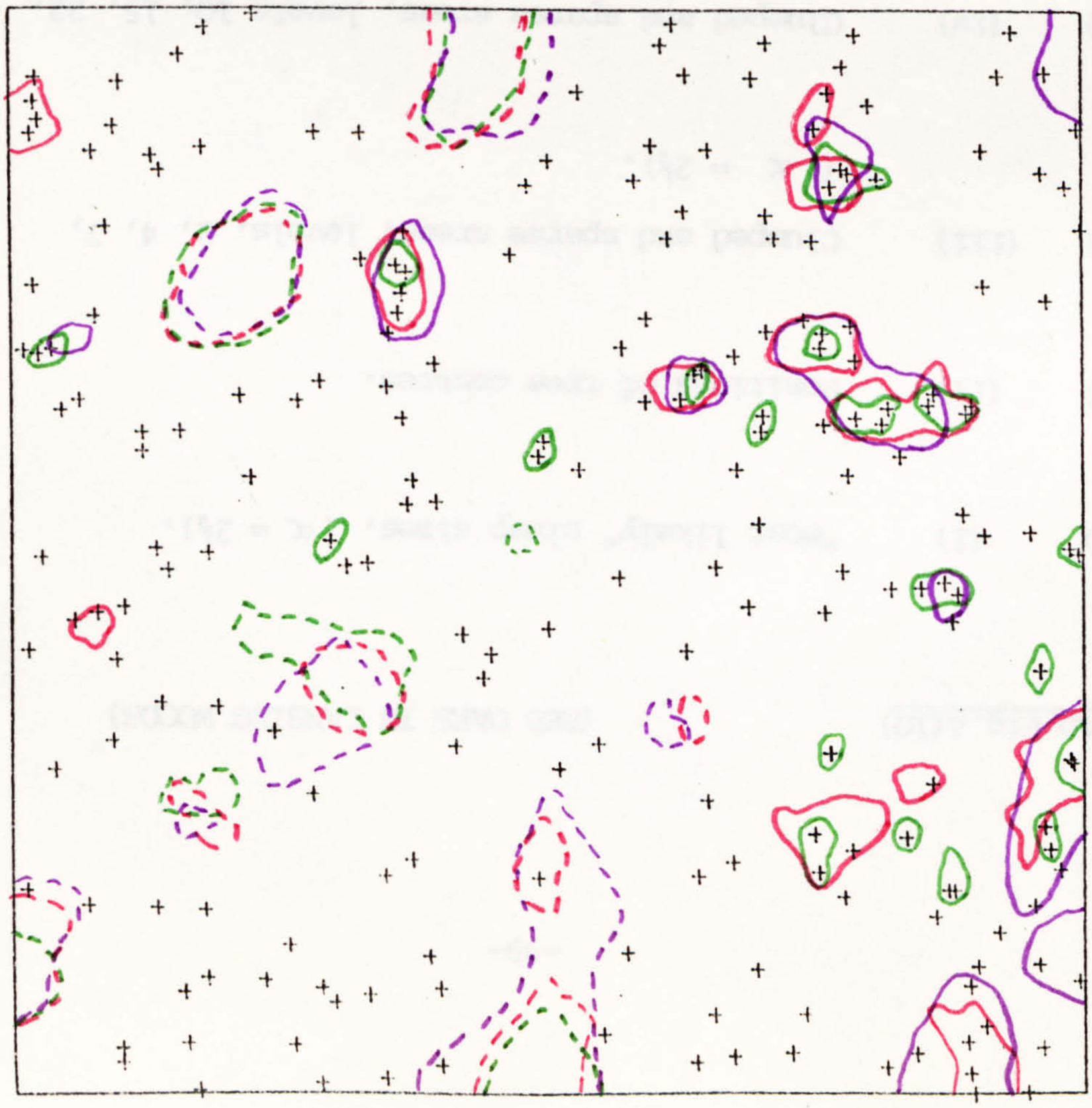

(v)

Key to Fig.4(10) (RED OAKS IN LANSING WOODS)

4(10) (i) "Most likely" clump sizes, ($\alpha = 2\frac{1}{2}$).

4(10) (ii) Positions of tree centres.

4(10) (iii) Clumped and sparse areas, levels, 2, 4, 7, ($\alpha = 2\frac{1}{2}$).

4(10) (iv) Clumped and sparse areas, levels 10, 15, 22, ($\alpha = 2\frac{1}{2}$).

Colour code

Colour	level	
——	2	continuous line - clumped area
——	4	broken line - sparse area
——	7	
——	10	
——	15	
——	22	

(i)

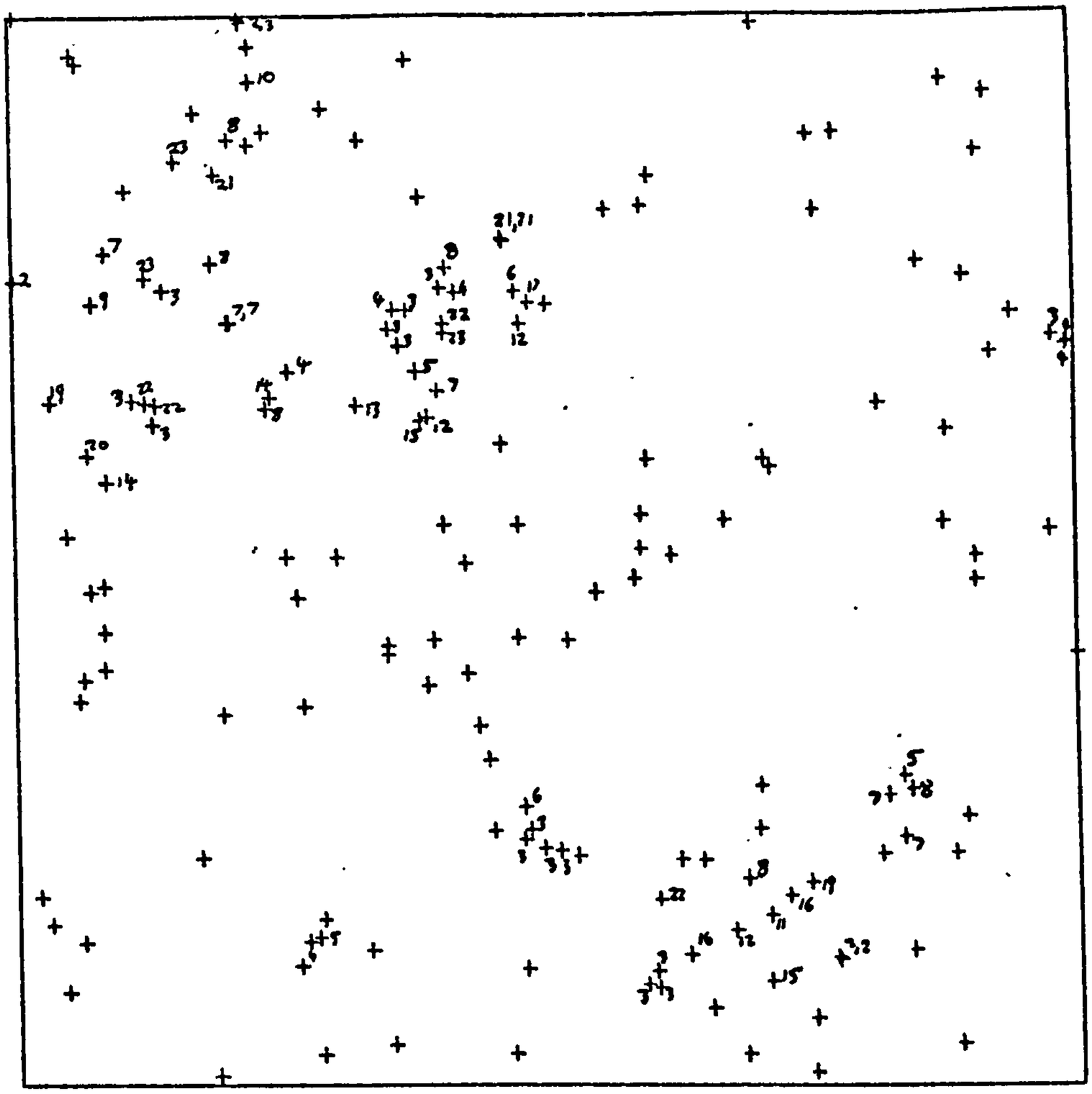

(ii)

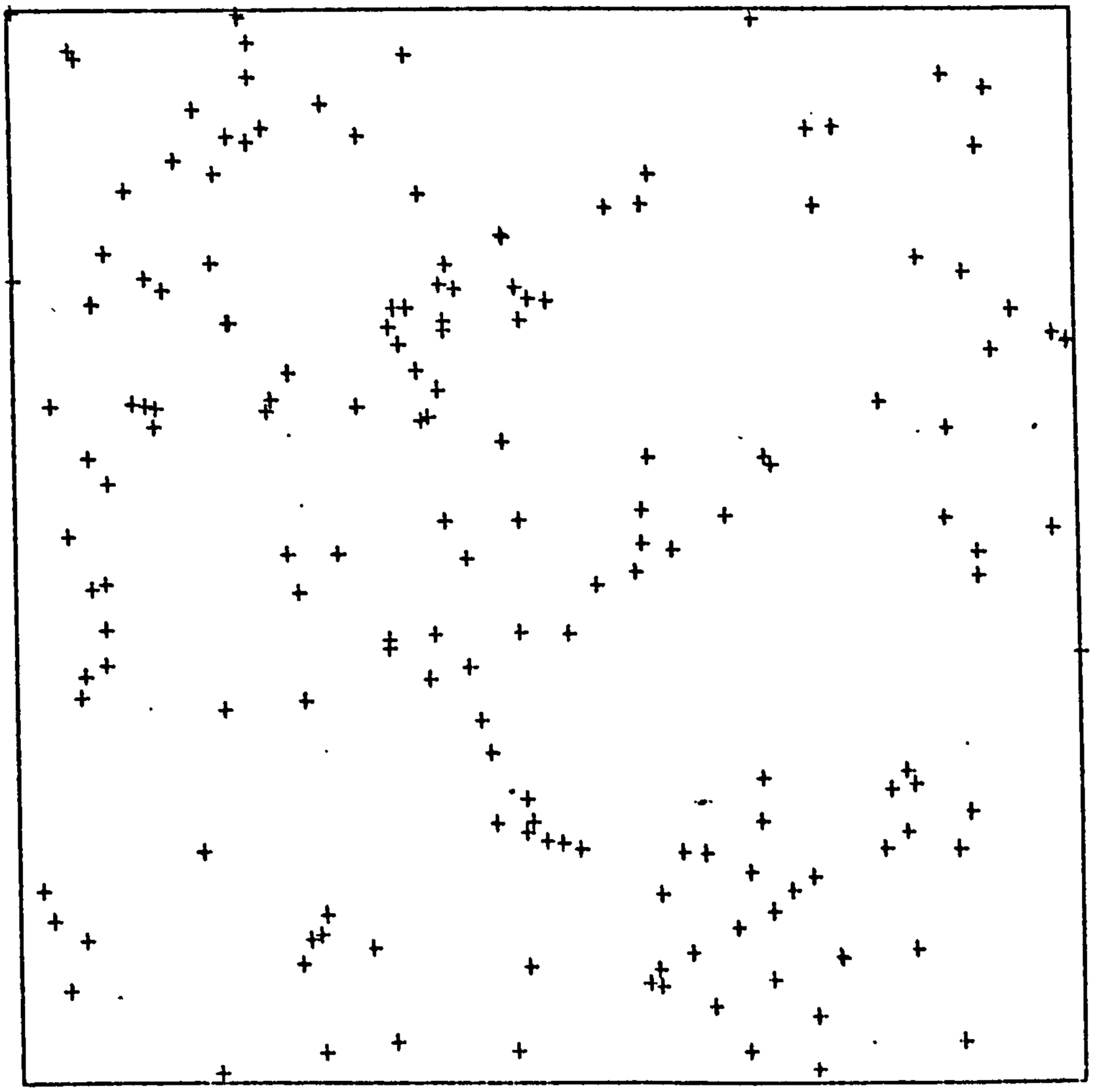

(iii)

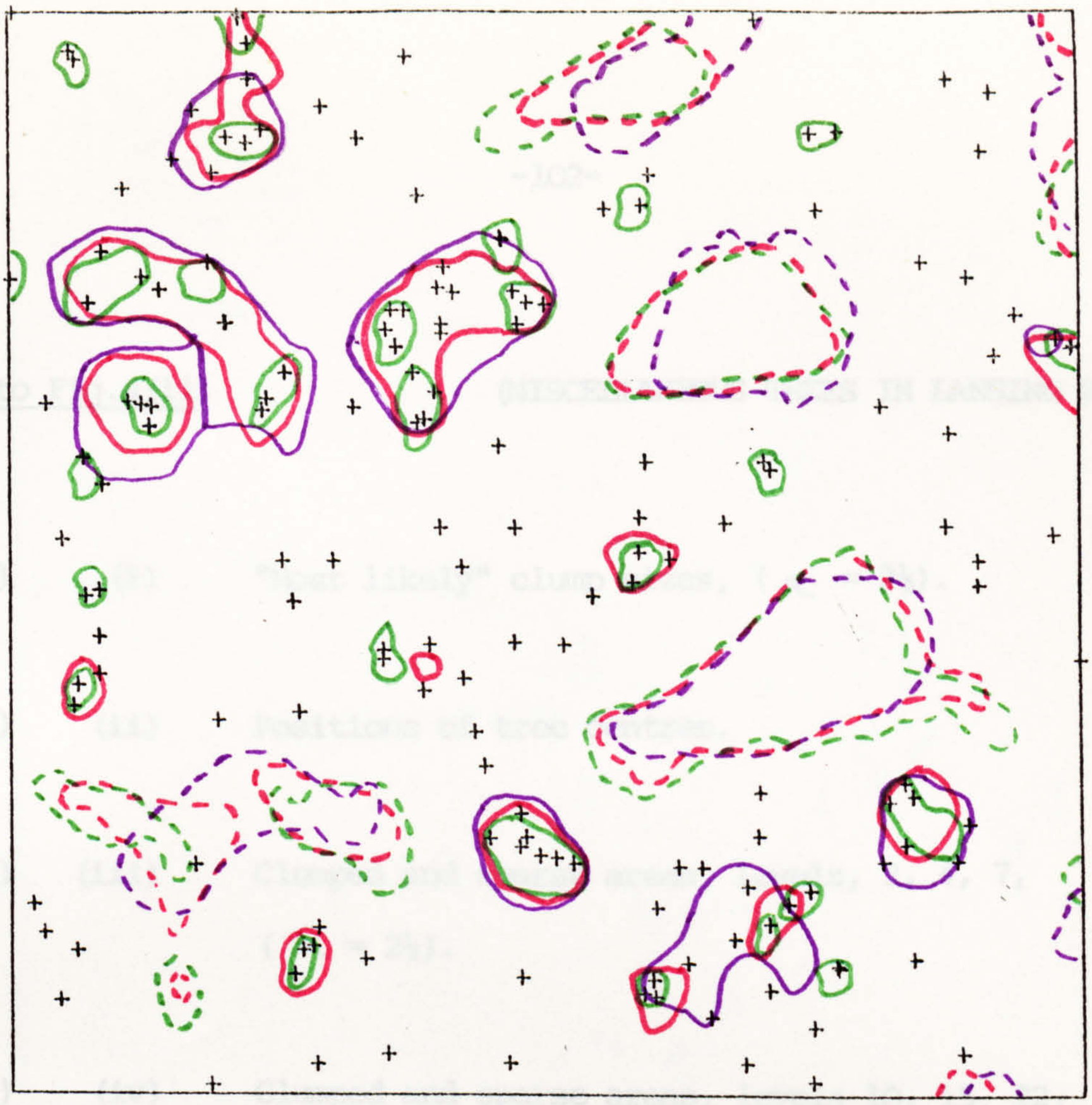

(iv)

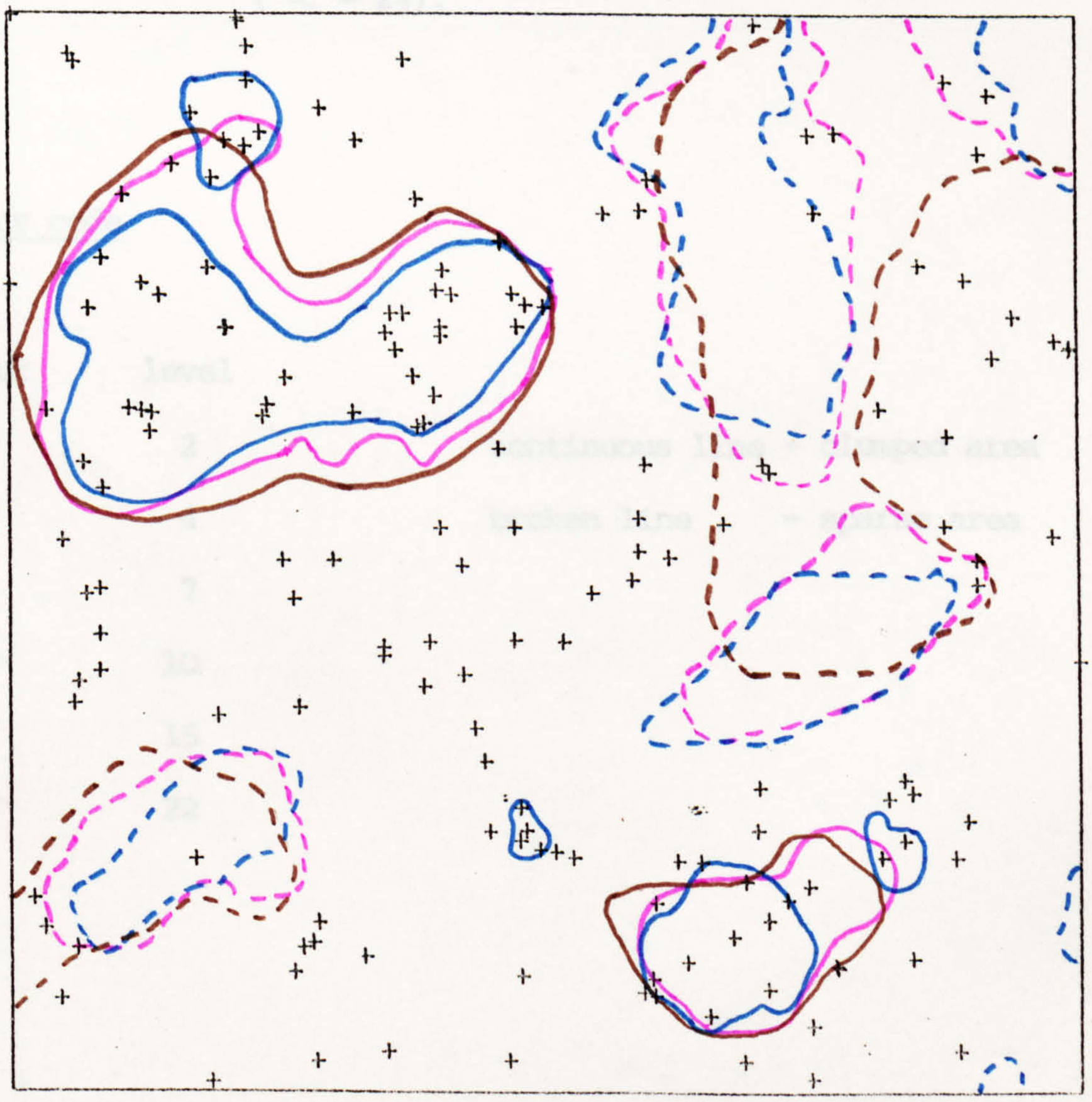

Key to Fig.4(11) (MISCELLANEOUS TREES IN LANSING WOODS)

4(11) (i) "Most likely" clump sizes, ($\propto = 2\frac{1}{2}$).

4(11) (ii) Positions of tree centres.

4(11) (iii) Clumped and sparse areas, levels, 2, 4, 7, ($\propto = 2\frac{1}{2}$).

4(11) (iv) Clumped and sparse areas, levels 10, 15, 22, ($\propto = 2\frac{1}{2}$).

Colour code

Colour	level	
—	2	continuous line - clumped area
—	4	broken line - sparse area
—	7	
—	10	
—	15	
—	22	

(i)

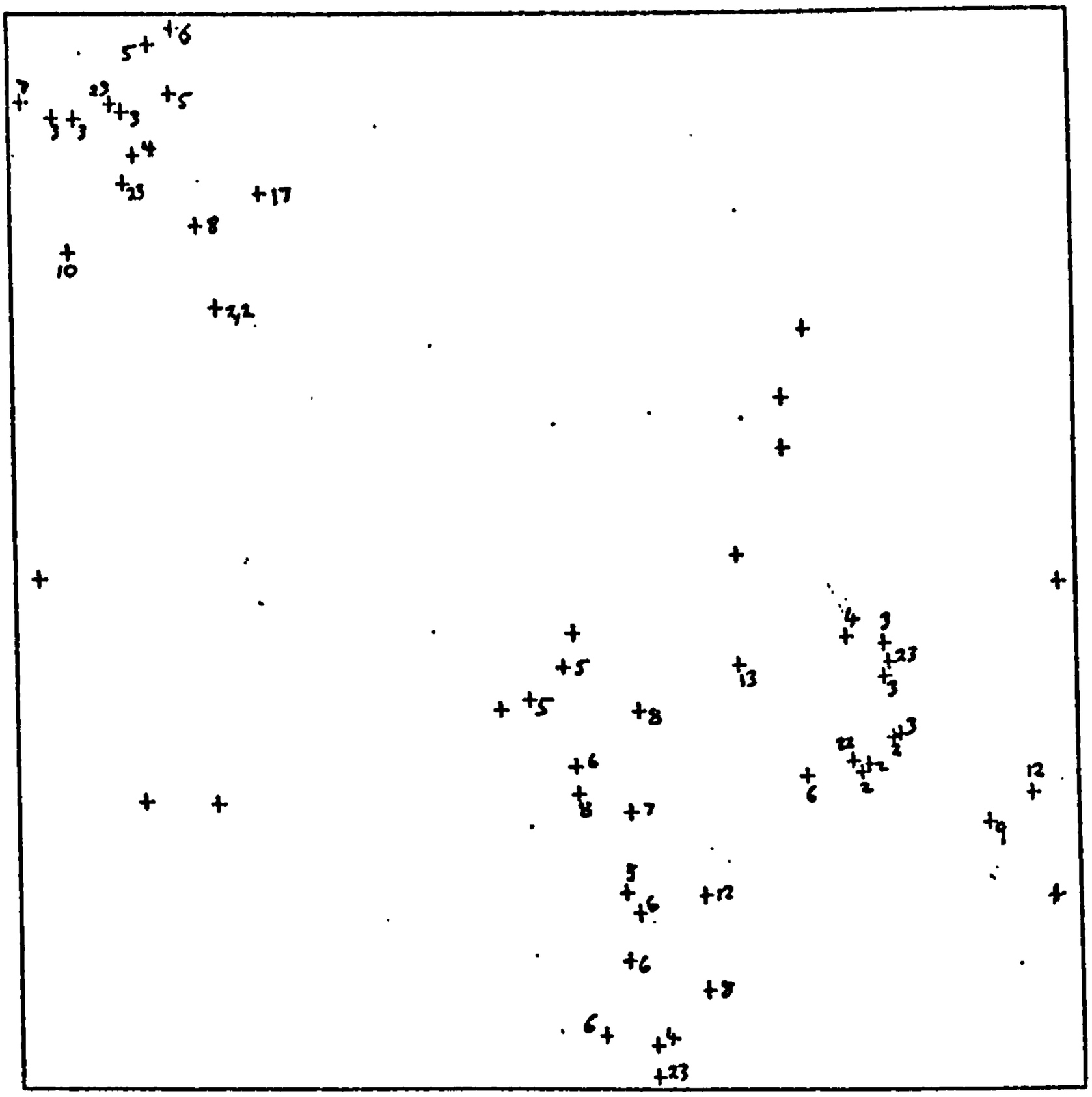

(ii)

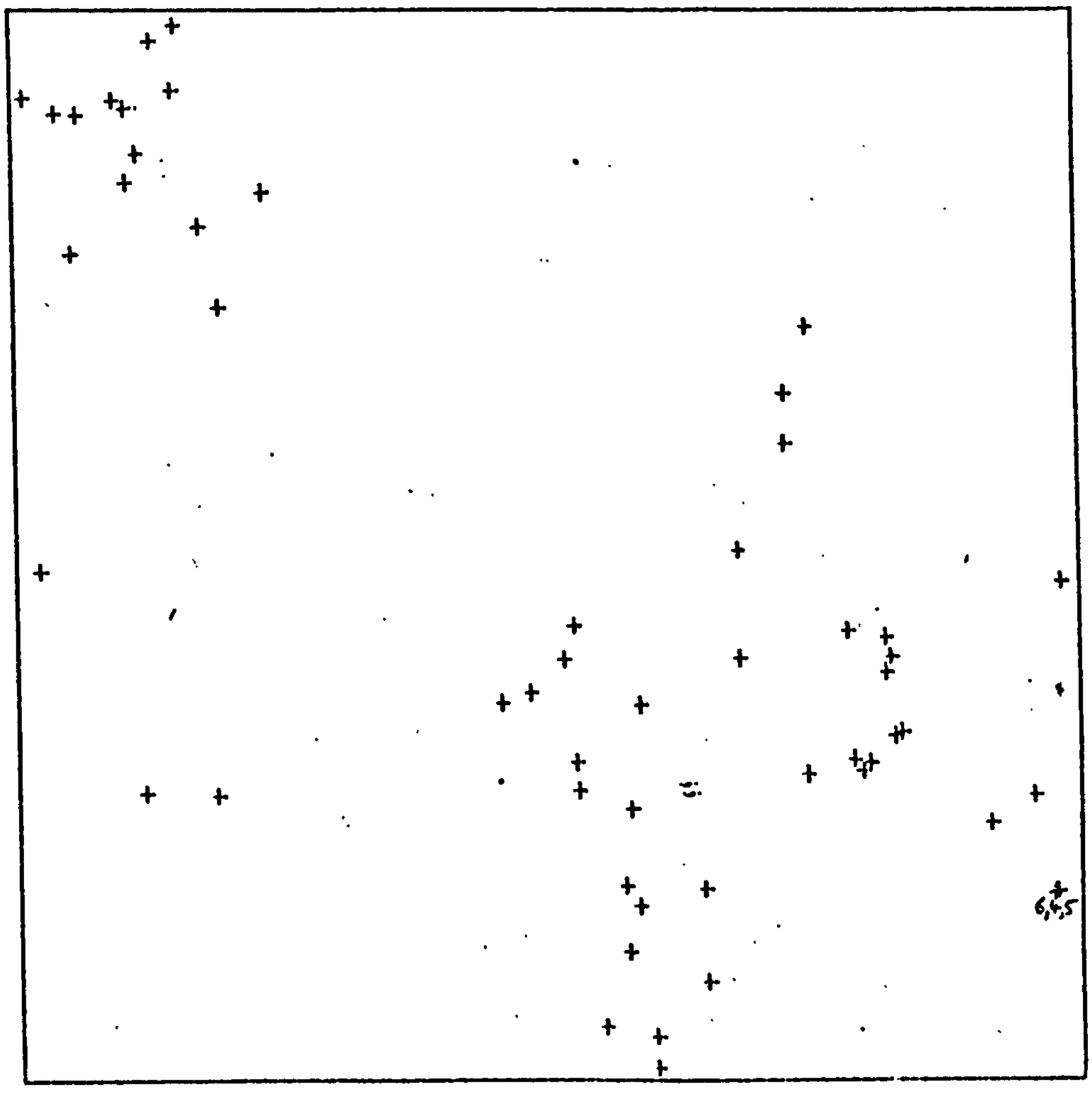

(iii)

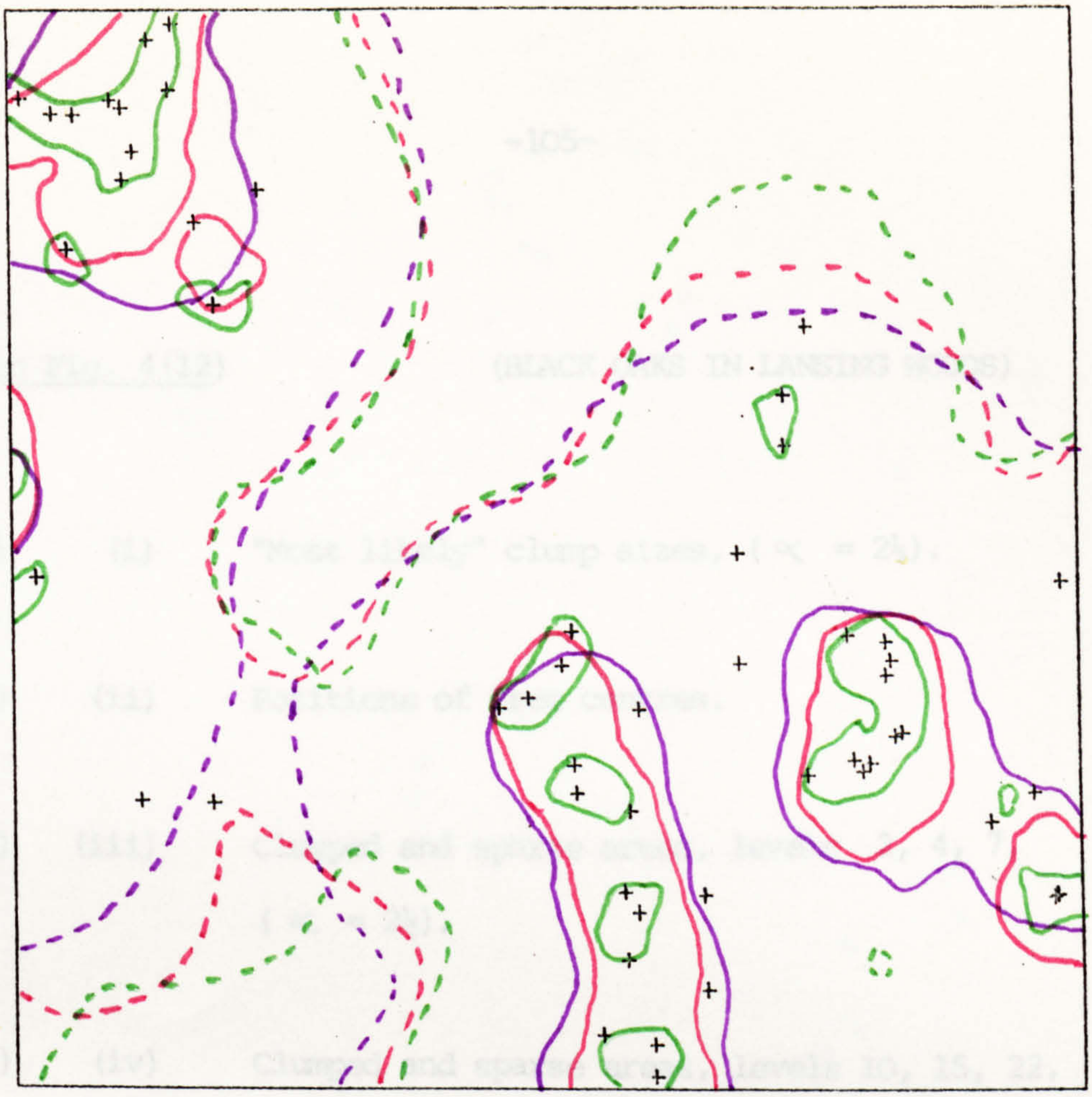

(iv)

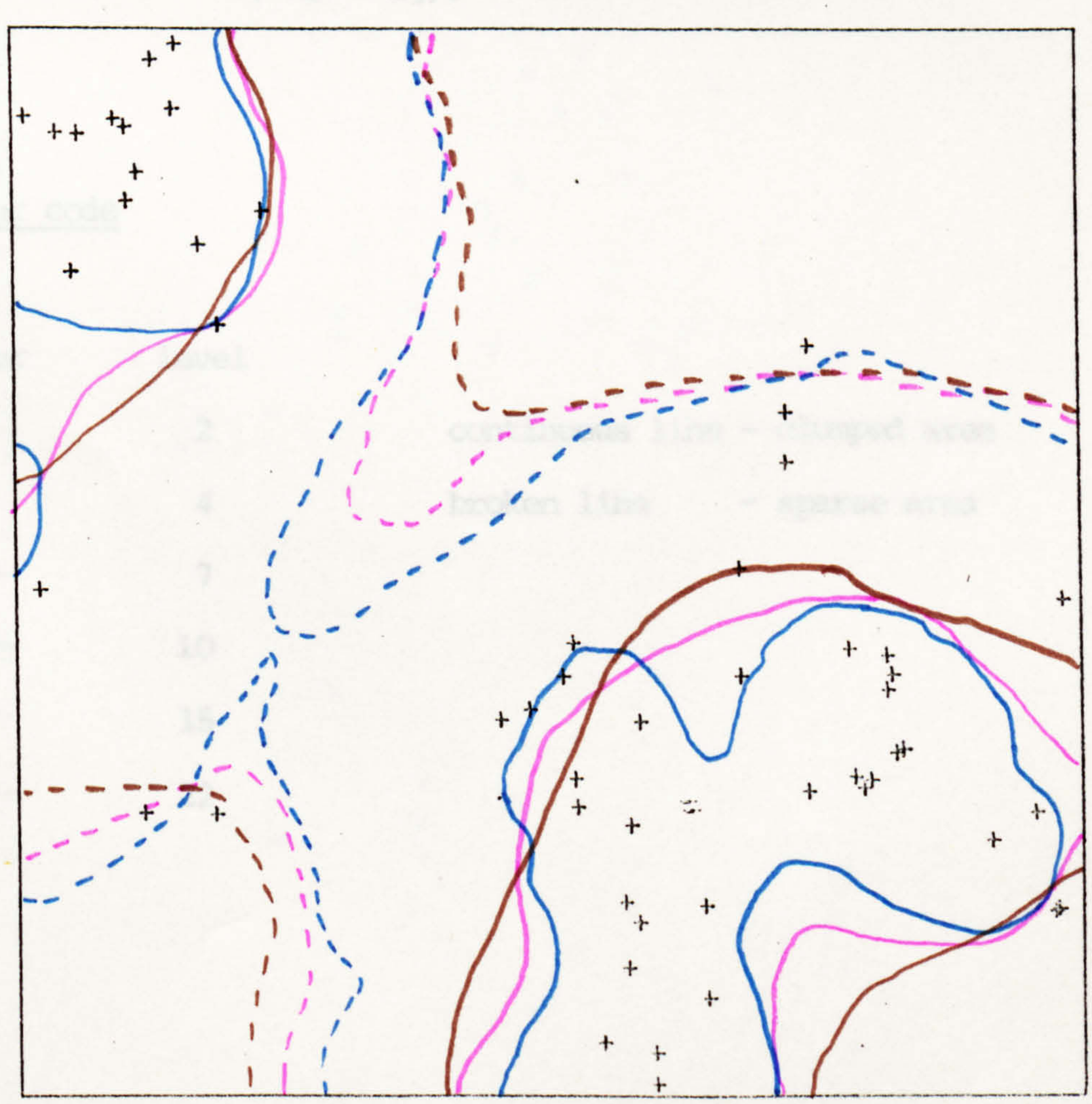

Key to Fig. 4(12) (BLACK OAKS IN LANSING WOODS)

4(12) (i) "Most likely" clump sizes, ($\propto$ = 2½).

4(12) (ii) Positions of tree centres.

4(12) (iii) Clumped and sparse areas, levels 2, 4, 7, ($\propto$ = 2½).

4(12) (iv) Clumped and sparse areas, levels 10, 15, 22, ($\propto$ = 2½).

Colour code

Colour	level	
—	2	continuous line - clumped area
—	4	broken line - sparse area
—	7	
—	10	
—	15	
—	22	

(i)

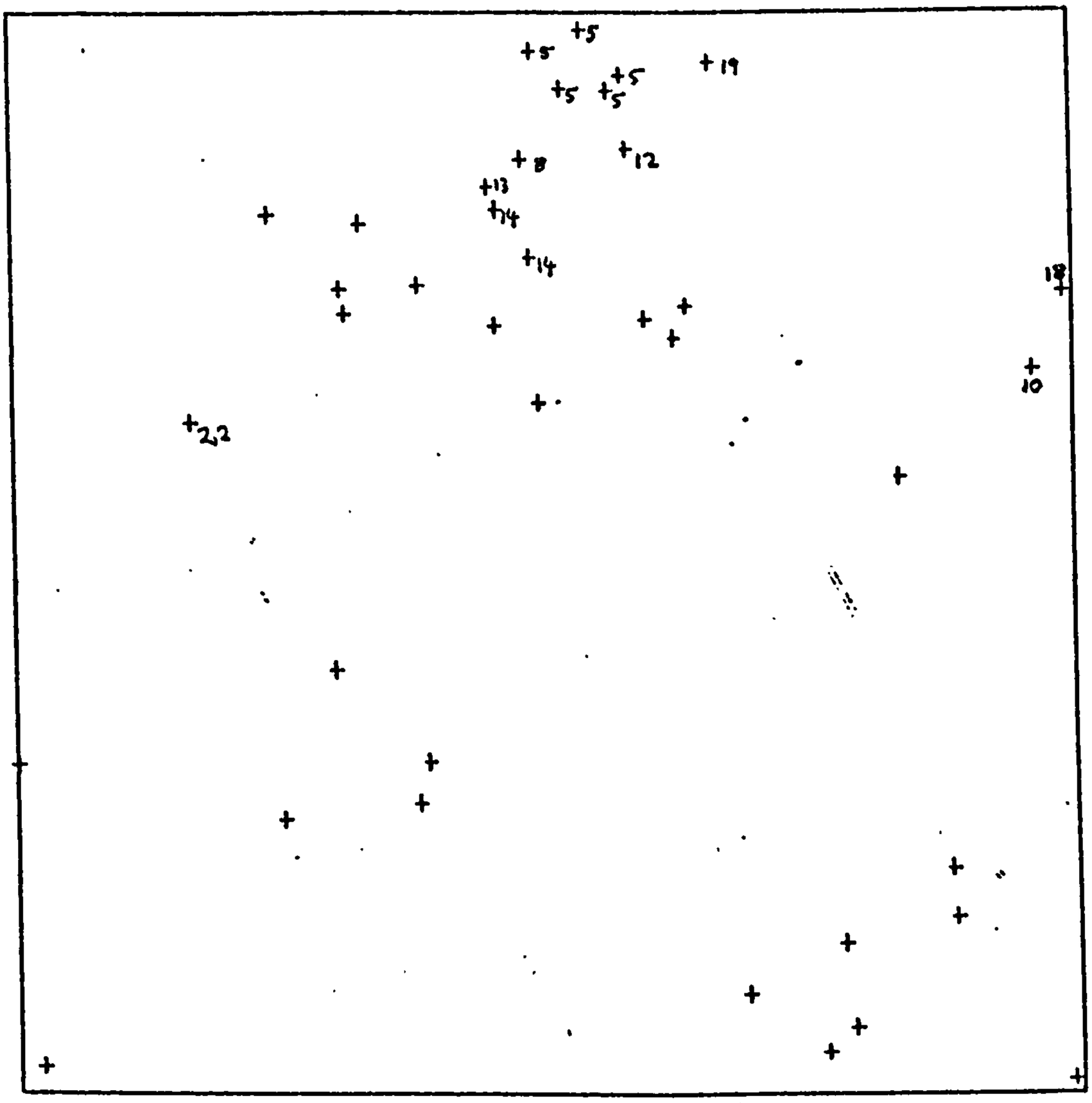

(ii)

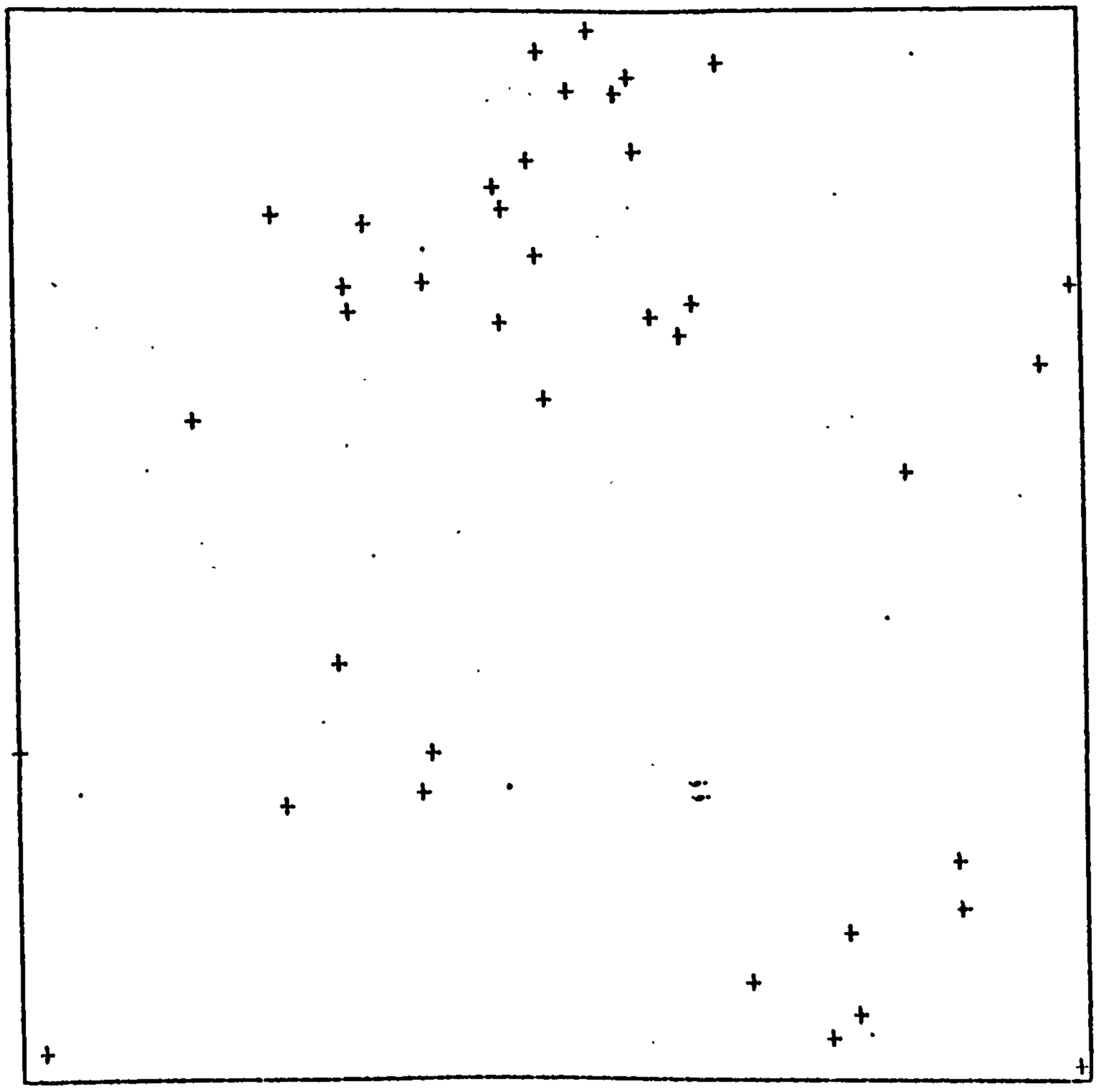

(iii)

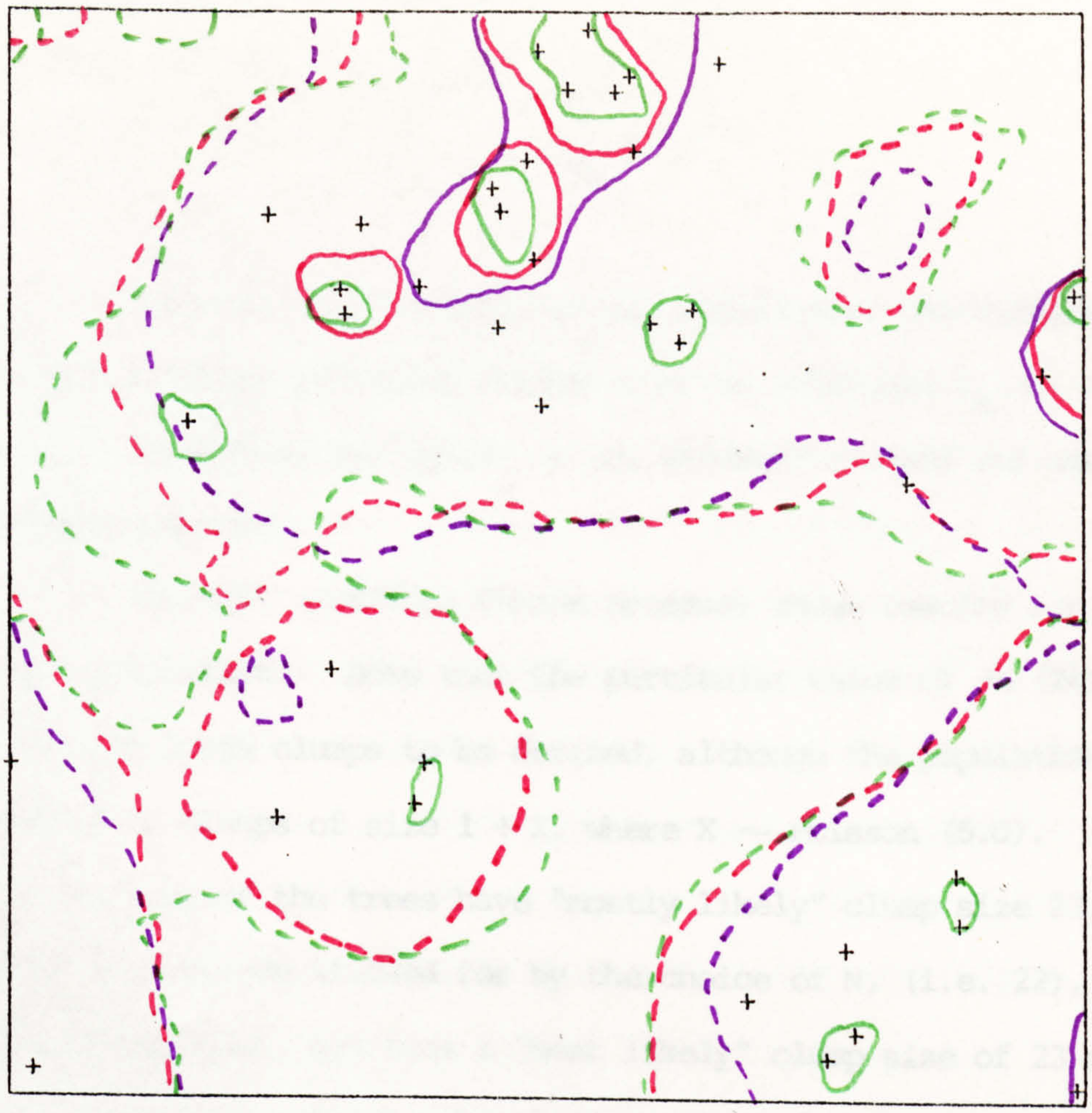

(iv)

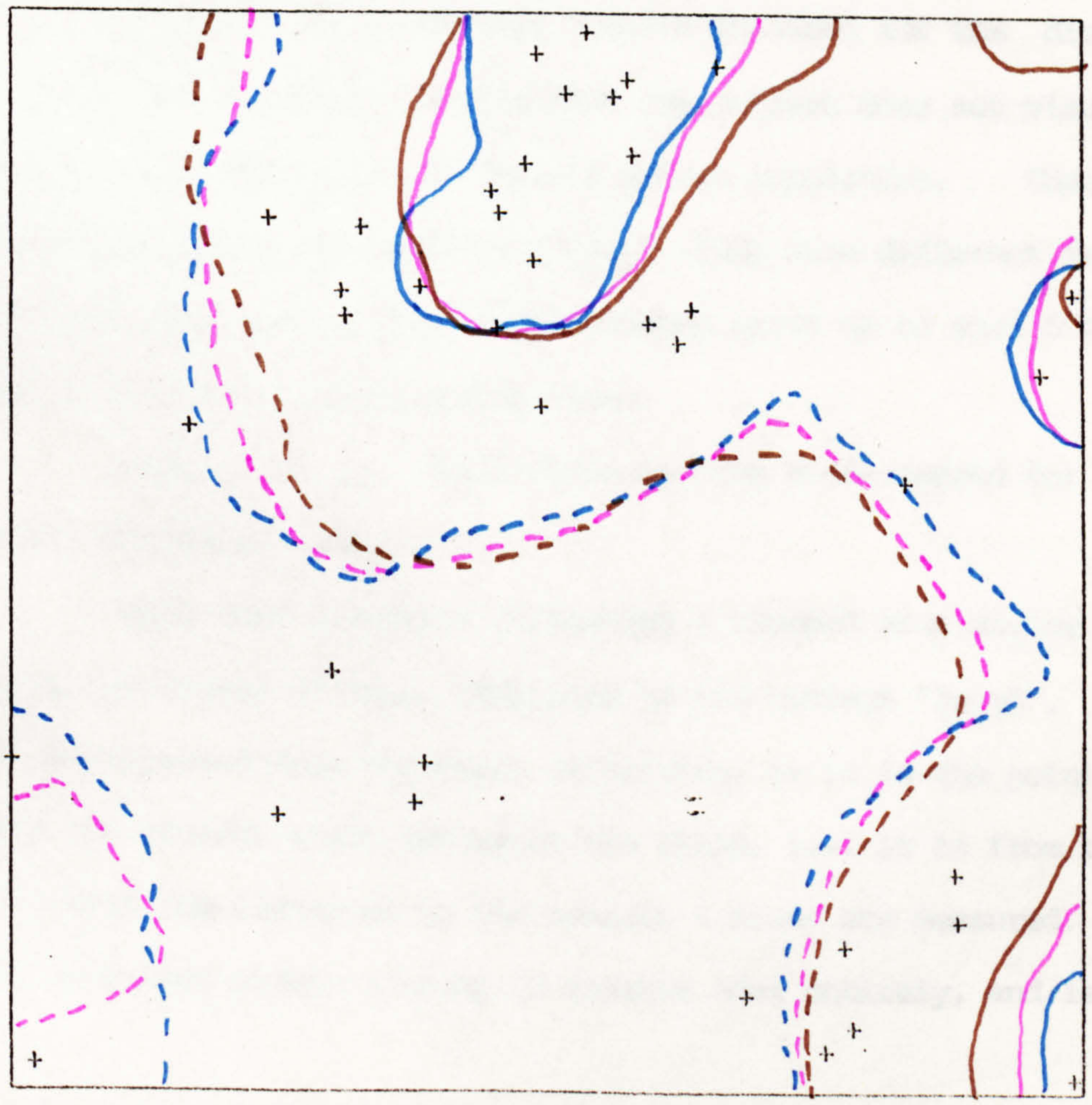

Fig.4(4) (the Poisson forest) illustrates the differences obtained by taking different values of α to calculate $C_n(\alpha)$ and $S_n(\alpha)$. Obviously the larger α is, the more clumped and sparse areas are obtained.

Fig.4(5) (Modified Thomas process) shows results for a very clumped population. Note that the particular value of α (2½%) allows very large clumps to be defined, although the population was generated by clumps of size 1 + X, where X ~ Poisson (5.0). Note also that many of the trees have "mostly likely" clump size 23. This is the maximum allowed for by the choice of N, (i.e. 22), due to practical purposes, and thus a "most likely" clump size of 23 must be interpreted as a "most likely" clump size of at least 23.

Fig.4(6) shows pleasing results obtained for the displaced-lattice population model, noting that the pattern does not visually differ a great deal from the Poisson forest population. There are only two trees with a "most likely" clump size different from zero (i.e. both are 2), only small clumped areas up to size 5 are defined, and there are no sparse areas.

Figs. 4(7),..., 4(12) shows Lansing Woods mapped for clumped and sparse areas.

Note that a contour containing a clumped area may or may not contain the number of trees indicated by the contour "level". This is to be expected from the basic definition, as it is the points contained within the contour which determine the clump, i.e. it is from these points that the distances to the nearest n trees are measured. The trees contained within a clump is another idea entirely, and is taken

into account by the method of "most likely" clumps in section 4.5. Some sparse areas are seen to contain trees. However by definition a sparse area is an area where the local density is somewhat less than the overall density and thus some trees are allowed within sparse areas.

The contour maps of different species in Lansing Woods can be compared in order to give some information on the relationship between the species, e.g. whether they tend to occur together or repel each other. Accordingly we are brought to the theory of bivariate processes in the plane which is discussed in the next chapter.

CHAPTER 5

THE SPECTRAL ANALYSIS OF TWO-DIMENSIONAL, BIVARIATE POINT PROCESSES FOR USE IN FORESTRY

5.1 The spectra

In this chapter, an outline is made of the spectral theory for a bivariate point process in the plane, taking the form of a synthesis, not explicitly given before, so far as one is aware, of existing spectral methods as applied in, (1) the two dimensional univariate case (Bartlett (1964)), and in (ii) the one-dimensional bivariate case (D. R. Cox and P. A. W. Lewis (1972)). Only the counting process will be considered, the "intervals" being more awkward to deal with, i.e. we deal with counts of events in rectangular regions (or intervals) in the plane, rather than "distances" between events which are more natural in one dimension anyway. The theory will be given in the spirit of a paper by Bartlett (1964), and will then be applied to some tree position data.

Suppose there are two types of events, A and B, such that they form a stationary (2nd order), bivariate point process in the plane.

Let $\underline{N}(\underline{r}) = (N^A(\underline{r}), N^B(\underline{r}))$ be the number of type A and type B events in the rectangle, (0,0), (0,y), (x,y), (x,0), where $\underline{r} = (x,y)$.

It is assumed that the process is regular (i.e. no multiple events). Now

$$E\left\{dN(\underline{r})\right\} = \underline{\lambda}\, dr, \qquad \text{where } dr = dxdy,$$

$$d\underline{N}(\underline{r}) = \underline{N}(\underline{r} + d\underline{r}) - \underline{N}(\underline{r}), \quad \text{and} \quad \underline{\lambda} = (\lambda^A, \lambda^B),$$

λ^A, λ^B constants.

This is a result of the stationarity of the process. Let

$$E\left\{d\underline{N}^T(\underline{r})\ d\underline{N}(\underline{r}')\right\} = \left\{\underline{\lambda}^T\underline{\lambda} + \underline{\gamma}(\underline{r} - \underline{r}')\right\} d\underline{r}\, d\underline{r}', \quad (\underline{r} \neq \underline{r}')$$

where T denotes the transpose.

The complete covariance density function for $\underline{N}(\underline{r})$ is then defined by

$$\underline{\gamma}(\underline{r} - \underline{r}') + \begin{pmatrix} \lambda^A & 0 \\ 0 & \lambda^B \end{pmatrix} \delta(\underline{r} - \underline{r}') \quad ,$$

where $\delta(\underline{r} - \underline{r}')$ is the two dimensional Dirac delta function.

Denote $\underline{\gamma}(\underline{r} - \underline{r}')$ by $\begin{pmatrix} \gamma^A(\underline{r} - \underline{r}') & \gamma^{AB}(\underline{r} - \underline{r}') \\ \gamma^{AB}(\underline{r} - \underline{r}') & \gamma^B(\underline{r} - \underline{r}') \end{pmatrix}$, and thus $\gamma^A(\underline{r} - \underline{r}')$ is the complete autocovariance of $N^A(\underline{r})$, $\gamma^B(\underline{r} - \underline{r}')$ is the complete autocovariance of $N^B(r)$, and $\gamma^{AB}(\underline{r} - \underline{r}')$ is the cross-covariance of $N^A(\underline{r})$ and $N^B(\underline{r})$.

The complete spectral function for $N^A(\underline{r})$ is then

$$\phi^A(\underline{w}) = \frac{1}{4\pi^2}\left\{\int e^{-i\underline{w}.\underline{r}}\ \gamma^A(\underline{r})d\underline{r} + \lambda^A\right\},$$

where $\underline{w}.\underline{r} = w_x x + w_y y$. Denote $4\pi^2\phi^A(\underline{w})$ by $g^A(\underline{w})$ for convenience.

Similarly the complete spectral function for $N^B(\underline{r})$ is

$$\phi^B(\underline{w}) = \frac{1}{4\pi^2}\left\{\int e^{-i\underline{w}.\underline{r}}\ \gamma^B(\underline{r})d\underline{r} + \lambda^B\right\}.$$

The cross spectral function for $N^A(\underline{r})$ and $N^B(\underline{r})$ is

$$\phi^{AB}(\underline{w}) = \frac{1}{4\pi^2}\left\{\int e^{-i\underline{w}.\underline{r}}\ \gamma^{AB}(\underline{r})\ d\underline{r}\right\},$$

and once again denote $4\pi^2 \phi^{AB}(\underline{w})$ by $g^{AB}(\underline{w})$, which has a real part $c^{AB}(\underline{w})$ and an imaginary part $q^{AB}(\underline{w})$.

5.2 Estimation of the spectra

Suppose the A and B events are contained within a square area of side L for convenience, and that their coordinates are (x_i^A, y_i^A), $i = 1, \ldots, n^A$, (x_j^B, y_j^B), $j = 1, \ldots, n^B$. An estimate of the spectrum for $N^A(\underline{r})$ is then

$$I^A_{p,q} = J^A_{p,q} \; J^{A\,*}_{p,q} \; ,$$

where

$$J^A_{p,q} = \sqrt{\frac{2}{L}} \sum_{s=1}^{n^A} \exp\left\{ i(x_s^A w_p + y_s^A w_q) \right\},$$

and * denotes the complex conjugate, and $(w_p, w_q) = \underline{w}$.

Thus

$$I^A_{p,q} = \frac{2}{L^2} \sum_{s=1}^{n^A} \sum_{r=1}^{n^A} \exp\left\{ i \left[(x_s^A - x_r^A) w_p + (x_s^A - x_r^A) w_q \right] \right\}.$$

It can be shown (e.g. see D. R. Cox and P. A. W. Lewis (1966)) that in order to make the bias of $I^A_{p,q}$ zero for the Poisson process, $w_p L$ and $w_q L$ must each be a multiple of 2π. Thus take

$$w_p = 2\pi p/L, \quad w_q = 2\pi q/L, \quad p,q = \ldots -1, 0, 1, \ldots .$$

In effect $I^A_{p,q}$ is a "power spectrum" and estimates "$\sigma^2 g^A(\underline{w})$". To estimate the normalized spectrum, $g^A(\underline{w})/\lambda^A$, the "distance" scale is normalized by the estimate n^A/L^2 of λ^A. Thus an estimate of the normalized spectrum of $N^A(\underline{r})$ with a normalized frequency scale is

$$\tilde{I}^A_{p,q} = \frac{2}{n^A} \sum_{s=1}^{n^A} \sum_{r=1}^{n^A} \exp\left\{ i\left[\frac{n^A}{L} (x^A_s - x^A_r)\left(w_p \frac{L}{n^A}\right) + \frac{n^A}{L}(y^A_s - y^A_r)\left(w_q \frac{L}{n^A}\right)\right]\right\},$$

$$= \frac{2}{n^A} \sum_{s=1}^{n^A} \sum_{r=1}^{n^A} \exp\left\{ i\left[(x^{A\prime}_s - x^{A\prime}_r)w'_p + (y^{A\prime}_s - y^{A\prime}_r)w'_q\right]\right\},$$

where $\underline{w}' = (w'_p, w'_q) = (2\pi p/n^A, 2\pi q/n^A)$, $x^{A\prime}_s = x^A_s n^A/L$, $y^{A\prime}_s = y^A_s n^A/L$, and noting that $w_p L$, $w_q L$ is still a multiple of 2π as required.

Similarly,

$$\tilde{I}^B_{p,q} = \frac{2}{n^B} \sum_{s=1}^{n^B} \sum_{r=1}^{n^B} \exp\left\{ i\left[(x^{B\prime}_s - x^{B\prime}_r)w'_p + (y^{B\prime}_s - y^{B\prime}_r)w'_q\right]\right\},$$

where $\underline{w}' = (w'_p, w'_q) = (2\pi p/n^B, 2\pi q/n^B)$, $x^{B\prime}_s = x^B_s n^B/L$, $y^{B\prime}_s = y^B_s n^B/L$.

In a similar manner the estimate of the normalized cross spectrum is

$$\tilde{I}^{AB}_{p,q} = \frac{2}{\sqrt{n^A n^B}} \sum_{s=1}^{n^A} \sum_{r=1}^{n^B} \exp\left\{ i\left[(x^{A\prime}_s - x^{B\prime}_r)w'_p + (y^{A\prime}_s - y^{B\prime}_r)w'_q\right]\right\},$$

where $\underline{w}' = (w'_p, w'_q) = (2\pi p/\sqrt{n^A n^B}, 2\pi q/\sqrt{n^A n^B})$, $x^{A\prime}_s = x^A_s\sqrt{n^A n^B}/L$, $y^{A\prime}_s = y^A_s\sqrt{n^A n^B}/L$, $x^{B\prime}_r = x^B_r\sqrt{n^A n^B}/L$, $y^{B\prime}_r = y^B_r\sqrt{n^A n^B}/L$

Table 7(i) The periodogram for Maples in a square area of side 5 in. (1 in. representing 61.67 ft.) in Lansing Woods.

p ⟶ positive

q ↓ positive

3.59	2.64	2.21	2.28	1.79	2.61	2.01	1.50
2.48	1.86	2.06	1.76	1.39	3.61	1.75	2.19
2.09	2.32	1.89	2.22	1.47	2.15	2.56	2.50
2.39	2.75	2.02	3.81	2.43	1.51	3.19	2.78
1.79	1.37	3.42	2.33	2.06	2.27	2.42	2.39
1.90	1.79	1.70	2.30	2.32	1.90	2.64	2.37
2.89	3.24	2.75	2.87	2.20	1.60	1.29	2.04
2.08	2.40	2.78	2.06	0.98	1.65	1.86	2.18

negative ⟵ p

1.93	3.26	1.73	1.82	2.58	2.15	1.79	3.25	
2.11	1.46	2.29	1.49	3.17	1.55	2.13	2.68	q ↓
1.40	2.75	1.44	2.22	1.76	1.48	2.11	1.85	positive
1.28	1.73	2.49	1.99	2.62	2.13	1.86	3.31	
2.06	2.65	1.88	1.35	2.45	2.38	2.33	1.66	
1.64	2.38	2.80	2.42	2.20	1.57	1.95	2.13	
2.00	2.66	2.36	1.32	1.57	2.16	1.99	2.53	
2.68	2.25	1.40	1.38	2.71	2.92	2.41	2.20	

Table 7(ii) The periodogram for Hickories in the same area.

p ⟶ positive

q ↓ positive

3.39	3.04	2.37	2.45	1.93	2.81	2.17	1.62
3.16	3.15	2.86	1.72	2.62	1.58	0.72	2.12
2.93	3.10	2.86	3.09	1.73	1.28	2.05	2.51
2.82	2.23	1.43	2.86	2.37	2.78	2.15	2.11
1.43	1.70	2.11	1.86	2.73	1.29	1.40	1.91
2.24	2.70	2.27	2.47	1.45	1.05	2.24	2.28
1.85	1.74	2.52	2.73	2.21	2.71	1.73	0.89
2.34	1.99	1.84	2.87	2.33	1.82	1.79	1.72

negative ⟵ p

1.81	2.17	1.82	1.23	2.12	1.73	3.22	2.91	
2.67	2.77	2.03	2.03	2.20	2.42	2.71	1.78	
1.10	1.21	1.57	1.32	2.34	1.62	1.92	2.78	q ↓
1.54	2.68	1.34	2.84	2.01	2.08	1.88	1.75	
1.38	2.35	2.54	2.46	2.19	2.54	2.17	1.60	positive
2.01	2.48	1.15	2.20	1.61	1.43	2.50	1.47	
2.39	2.10	1.94	2.60	2.19	2.74	1.43	2.05	
1.71	1.35	1.40	1.16	1.90	2.11	2.15	2.56	

Table 7(iii) The real part of the two-dimensional cross periodogram for the Maples and Hickories

p ⟶ positive

q ↓ positive

-1.19	0.46	-.046	0.75	0.70	-0.54	0.08	0.27
-0.69	0.24	-0.20	0.29	-0.10	-0.42	0.12	0.64
0.22	-0.51	0.79	-0.44	-0.02	0.11	0.25	0.14
-0.08	-0.51	0.17	0.69	0.05	0.16	-0.06	0.44
-0.46	-0.13	-0.33	-0.62	0.02	-0.31	0.34	0.41
0.26	-0.54	0.09	0.19	0.06	0.17	-0.13	-0.65
-0.34	-0.03	-0.50	0.44	0.51	0.17	-0.17	-0.11
-0.01	-0.06	-0.37	0.17	0.10	-0.54	-0.11	-0.46

negative ⟵ p

q ↓ positive

0.11	0.52	-0.05	0.01	0.13	0.02	-0.41	-1.00
1.10	-0.74	-0.26	0.14	-0.70	-0.30	-0.44	-0.74
0.24	0.09	0.08	0.18	-0.31	0.21	-0.01	0.45
-0.42	-0.09	-0.15	-0.62	0.26	-0.00	-0.28	-0.19
-0.12	-0.34	0.40	-0.55	0.00	-0.41	-0.15	-0.39
-0.24	0.45	-0.17	0.23	0.39	0.01	-0.04	-0.19
-0.60	-0.11	-0.09	0.15	-0.02	0.18	0.26	0.01
0.43	0.47	-0.05	-0.15	0.22	0.08	-0.16	-0.55

Table 7(iv) The imaginary part of the two dimensional cross periodogram for the Maples and Hickories.

p ⟶ positive

q ↓ positive

1.21	-0.10	-0.50	-0.25	-0.50	0.46	0.12	-0.11
0.00	0.08	-0.47	0.46	0.10	0.23	-0.34	0.29
0.07	0.39	-0.81	0.52	-0.26	-0.39	0.10	0.58
0.39	0.13	-0.50	0.36	-0.51	0.12	-0.54	0.10
-0.21	-0.31	-0.79	-0.54	0.37	0.03	0.49	0.65
0.15	0.18	0.26	-0.78	-0.29	0.12	-0.54	0.18
-0.07	-0.20	-0.44	-0.44	0.02	0.14	-0.02	-0.23
0.67	0.09	-0.82	-0.46	0.38	-0.36	0.25	0.68

negative ⟵ p

q ↓ positive

-0.41	-0.18	-0.68	-0.28	0.41	-0.30	-0.31	0.03
-0.86	0.10	-0.11	0.22	0.77	-0.32	0.28	-0.07
-0.23	0.03	0.21	0.17	0.19	-0.21	-0.03	-0.28
-0.29	-0.13	-0.27	0.43	0.60	-0.24	0.04	0.37
-0.20	-0.37	-0.33	0.21	-0.21	-0.32	0.19	-0.63
0.21	0.16	-0.39	0.22	-0.44	-0.00	1.05	0.54
-0.35	-0.29	-0.08	0.72	0.04	0.36	0.34	-0.32
-0.27	-0.41	-0.15	0.15	0.39	-0.03	-0.20	0.52

The periodograms, $\tilde{I}^{A}_{p,q}$, $\tilde{I}^{B}_{p,q}$ and the cross periodogram $\tilde{I}^{AB}_{p,q}$ for the counting process of the Maples and Hickories in a small section of Lansing Woods (see Chapters 1, 2, 3 and 4) were calculated and are presented in a similar manner to results obtained by Bartlett (1964) for other data. The spectra are smoothed by averaging the values over separate 4 x 4 grids. Table 7 shows the results obtained.

Note that the spectra in Table 7 are not evaluated at $p = q = 0$ as the bias is greatest near $\underline{w} = \underline{0}$. The individual values for the auto-spectra can be tested, with null hypothesis of a Poisson process, as χ^2_2 values, and the sum of the values in each 4 x 4 grid as χ^2_{32} values. Given that the null hypothesis is not rejected for both the A and B events, zero correlation between the two types of events can be tested for (see e.g. Cox and Lewis (1966), Jenkins and Watts (1969)). However when the A and B events do not form Poisson processes testing hypotheses becomes more difficult, and the matter is not entered upon here.

5.3 The Isotropic case

Inspecting two dimensional spectra as in Table 7 is a hard task. It can be made easier if not only stationarity is assumed, but also isotropy, which implies that the processes are independent of direction. Then the spectra can be averaged over the angle Θ between $\underline{w}' = (w'_p, w'_q)$ and each $\underline{r} - \underline{r}'$, so that they depend only on w.

The periodogram for the A type events was seen to be

$$\tilde{I}^{A}_{p,q} = \frac{2}{n^A} \sum_{s=1}^{n^A} \sum_{r=1}^{n^A} \exp\left\{ i \left[w'_p (x_s^{A'} - x_r^{A'}) + w'_q (y_s^{A'} - y_r^{A'}) \right] \right\} .$$

$$= \frac{2}{n^A} \sum_{s=1}^{n^A} \sum_{r=1}^{n^A} \exp\left\{ i \left[w \cos(\theta) (x_s^{A'} - x_r^{A'}) + w \sin(\theta) (y_s^{A'} - y_r^{A'}) \right] \right\},$$

and hence

$$E_\theta (\tilde{I}^{A}_{p,q}) = \frac{2}{n^A} \sum_{s=1}^{n^A} \sum_{r=1}^{n^A} \frac{1}{2\pi} \int_0^{2\pi} \exp\left\{ i \left[w \cos(\theta) (x_s^{A'} - x_r^{A'}) + w \sin(\theta) (y_s^{A'} - y_r^{A'}) \right] \right\} d\theta ,$$

$$= \frac{2}{n^A} \sum_{s=1}^{n^A} \sum_{r=1}^{n^A} J_o(w d^A_{rs}),$$

where $d^A_{rs} = \left\{ (x_s^{A'} - x_r^{A'})^2 + (y_s^{A'} - y_r^{A'})^2 \right\}^{\frac{1}{2}}$, $J_o(.)$ is the Bessel function of order zero. [Note

$$\frac{1}{2\pi} \int_0^{2\pi} \exp\left[i(a \cos\theta + b \sin\theta) \right] d\theta = J_o(\sqrt{a^2+b^2}) \;]$$ (see Bartlett(1955)).

Thus the isotropic spectrum of the A type events is estimated at $w = 2\pi p/n^A$, $p = 0, 1, \ldots$ by

$$\frac{2}{n^A} \sum_{s=1}^{n^A} \sum_{r=1}^{n^A} J_o (w d^A_{rs}),$$

and similarly the isotropic spectrum of the B's is estimated at $w = 2\pi p/n^B$, $p = 0, 1, \ldots$ by

$$\frac{2}{n^B} \sum_{s=1}^{n^B} \sum_{r=1}^{n^B} J_o(w\, d_{rs}^B) .$$

The cross periodogram for the A and B events was seen to be

$$\tilde{I}_{p,q}^{AB} = \frac{2}{\sqrt{n^A n^B}} \sum_{s=1}^{n^A} \sum_{r=1}^{n^B} \exp\left\{ i\left[w'_p(x_s^{A'} - x_r^{B'}) + w'_q\ (y_s^{A'} - y_r^{B'})\right]\right\},$$

and thus the isotropic cross spectrum is estimated at

$w = 2\pi p/\sqrt{n^A n^B}$, $p = 0, 1, \ldots$ by

$$\frac{2}{\sqrt{n^A n^B}} \sum_{s=1}^{n^A} \sum_{r=1}^{n^B} J_o(w\, d_{rs}^{AB}),$$

where $d_{rs}^{AB} = \left\{(x_s^{A'} - x_r^{B'})^2 + (y_s^{A'} - y_r^{B'})^2\right\}^{\frac{1}{2}}$. Note that the imaginary part of the isotropic cross spectrum is zero. This is because

$$E_\Theta(\tilde{I}_{p,q}^{AB}) = \frac{2}{\sqrt{n^A n^B}} \sum_{s=1}^{n^A} \sum_{r=1}^{n^B} \frac{1}{2\pi} \int_0^{2\pi} \exp\left\{ i\left[w(x_s^{A'} - x_s^{B'}) \cos\Theta + w(y_s^{A'} - y_r^{B'}) \sin\Theta\right]\right\} d\Theta ,$$

and thus the imaginary part is

$$\text{constant} \times \sum_{s=1}^{n^A} \sum_{r=1}^{n^B} \int_0^{2\pi} \sin\left[w(x_s^{A'} - x_r^{B'}) \cos\Theta + w(y_s^{A'} - y_r^{B'}) \sin\Theta\right] d\Theta ,$$

which is

$$\text{constant} \times \sum_{s=1}^{n^A} \sum_{r=1}^{n^B} \left\{ \int_0^{\pi} \sin(a\cos\Theta + b\sin\Theta)\, d\Theta + \int_{\pi}^{2\pi} \sin(a\cos\Theta + b\sin\Theta)\, d\Theta \right\}$$

$$= 0 \qquad (a = w(x_s^{A'} - x_r^{B'}),\ b = w(y_r^{A'} - y_r^{B'})).$$

Note that as $w \to \infty$, $E_\Theta(\tilde{I}_{p,q}^{A}) \to 2$ and $E_\Theta(\tilde{I}_{p,q}^{AB}) \to 0$.

5.4 Spectral theory in relation to forestry

It is of interest when dealing with two or more species of plants or trees in the plane to know the relationship between them. As mentioned in chapter one, any statistical or probabilistic results connected with the different species do not prove anything about causal factors but may give some "measurement" of the relationship between the species. To this end Pielou (1969, 1974) discusses two measures of the relationship between two species, namely association and segregation.

Two species are positively associated if they tend both to be present or both to be absent in the same areas. The definition can be made precise for species in discrete habitable units (e.g. leaves on a tree) when one can count the number of units that contain both species, the number that contain one species and not the other and vice versa, and lastly the number of units that contain neither one nor the other. However when the species are in a "continuum" (here the plane), problems arise when trying to sample the populations due to the placing and size of the sampling quadrats. This is discussed at length by Pielou (1969, 1974). As yet there are no distance methods for measuring association between species, and so we propose here to use the isotropic cross spectrum for the counting process instead.

Two species of A and B types are unsegregated if they are randomly mingled. That is, given the positions of all the individuals, are the A's and B's allocated to the positions at random? If not they are segregated either positively or negatively. Positive segregation occurs when A's tend to be near A's and B's near B's, and negative

segregation occurs in the reverse situation. This is discussed more fully by Pielou (1969, 1974).

A method of testing and measuring the segregation between two species is discussed by Pielou (1961, 1969, 1974). It is as follows. For each individual in the two populations the type of its nearest neighbour is recorded and the results set out in a 2 x 2 contingency table thus,

		Species of nearest neighbour A	Species of nearest neighbour B	
Species of base plant	A	a	b	m
	B	c	d	n
		r	s	N

The usual χ^2 test is then carried out to test whether the observed cell frequencies depart from expectation. Note that the test is not strictly valid as under the null hypothesis the events of certain nearest neighbours to each tree are clearly not independent for all the trees.

Pielou then goes on to define a coefficient of segregation,

$$S = 1 - \frac{\text{observed number of mixed pairs}}{\text{expected number of mixed pairs}},$$

$$= 1 - \frac{N(b + c)}{ms + nr}.$$

For an unsegregated population $E(S) = 0$, for a fully segregated population, $S = 1$, and for isolated A - B pairs, $S = -1$. Thus S ranges from -1 to +1.

In section 5.5 the isotropic periodogram, the isotropic cross periodogram and Pielou's coefficient of segregation will be found for various sets of data including the six species in Lansing Woods. The periodograms give insight to the pattern formed by the individual species, while the cross periodogram and Pielou's coefficient give information about the relationship between two species.

5.5 Results

Firstly some remarks are made on the interpretation of the spectra. The isotropic periodogram, $I(w)$ $(= E_\Theta[\hat{I}^A_{p,q}(w)])$, has value $2n^A$ at $w = 0$ and tends to 2 as w tends to infinity. For the Poisson forest, the isotropic spectrum has constant value 2, except for $w = 0$, where the value is $2n^A$. Hence for any particular spatial pattern, $I(w)$ will have value $2n^A$ at $w = 0$, then will decrease and probably oscillate about the value 2 in an erratic way, levelling out to the value 2 as w increases. The value of $I(w)$ for small w, (but not too close to zero, as then bias is appreciable), indicates a great deal about the pattern. If the pattern is clumped, then $I(w)$ will be large for small w, but if the pattern is regular, then $I(w)$ is less than 2 for small w. If $I(w)$ is practically two for all $w > 0$, then the spatial pattern is probably a Poisson forest.

The cross periodogram for two species indicates the nature of the correlation between the counting processes of the two species. The isotropic cross spectrum has imaginary part zero, and if also the real part is zero, then the two species are uncorrelated. The isotropic cross periodogram $I^{AB}(w)$ is biased for w near zero, but for

small w can tell us whether the two species are positively or negatively associated. If the two species are positively associated, then $I^{AB}(w)$ will be large and positive for small w, if they are negatively associated, then $I^{AB}(w)$ will be large and negative for small w.

Note that the measure of segregation is not directly related to the isotropic cross spectrum. This is illustrated by the case of two independently placed Thomas processes. Here the isotropic cross spectrum is identically zero, while the segration coefficient will be appreciably positive implying positive segregation.

Fig.5(2)(i) and Fig.5(2)(ii) show the isotropic periodograms $I^{A}(w)$, $I^{B}(w)$ obtained for two independently simulated Poisson forests within a square of 5 in. x 5 in. (Fig.5(1)). Both the periodograms do not vary significantly from 2. Fig. 5(2)(iii) shows the isotropic cross periodogram, $I^{AB}(w)$ obtained for these two Poisson forests. The bias is appreciable for w less than 0.5, but for $w > 0.5$, $I^{AB}(w)$ does not vary appreciably from zero. Bartlett (1964) shows the bias for the periodograms and cross periodograms is appreciable for $p < n^{1/3}$, where $2\pi p/n = w$, $(p = 0, 1, \ldots)$.

The numbers in the lower right hand corners of Figs. 5(2)(i), (ii), (iii), and for all the Figures showing periodograms, are the number of points over which the periodograms are uniformly smoothed (see e.g. Cox and Lewis (1966)). Also given in each of the Figures showing cross periodograms is the value of Pielou's coefficient of segregation, S.

Fig. 5(4)(i) and Fig.5(4)(ii) again show the periodograms for two Poisson forests within a 5 in. x 5 in. square area. Note the

bias for small w. In fact for each of the four Poisson forests $n = 60$, and thus the bias is appreciable for $p < 4$, or $w < 0.42$. Fig. 5(4)(iii) shows the cross periodogram for these two Poisson forest, indicating that they are highly associated. This is pleasing since the population of the A type trees was generated as a Poisson forest in the usual way and then to each A type tree, a B type tree was allocated and then displaced isotropically a random distance between zero and 0.3 in. Thus the populations were constructed to be highly associated, but individually, Poisson forests. They are as shown in Fig.5(3).

Fig.5(5) shows two regular-type populations, generated independently in the following manner. An A type tree was placed at random within the sampling square of 5 in. x 5 in., and then 59 other A type trees were placed sequentially such that if one of them as it was placed randomly in the square, was within a distance of 0.3 in. from another A type tree, it was replaced again and again at random, until the minimum separation was greater than 0.3 in. The population of B type trees was formed in a similar manner with minimum separation of 0.4 in., and independently of the A type trees.
Fig. 5(6)(i) and Fig. 5(6)(ii) show the isotropic periodograms for the A and B type events. For small w, $I^A(w)$ and $I^B(w)$ are much less than 2, thus showing the populations to be more regular than random. The isotropic cross periodogram does not vary appreciably from zero, which is to be expected as the populations were generated independently.

Fig. 5(7) shows two populations generated similarly to the previously described regular model. The A type trees were generated exactly as before, but this time the B type trees not only have a

minimum separation from B type trees of 0.4 in., but also have a minimum separation from A type trees of 0.4 in. Thus the two populations are negatively associated. Fig. 5(8)(i) and Fig.5(8)(ii) show the periodograms, while Fig.5(8)(iii) indicates the strong negative association between the two populations.

Fig. 5(9) shows a Poisson forest of A type trees, and a population of clumped B type trees, having twenty clump centres, considered as trees, placed at a random distance between zero and 0.3 in. from twenty of the A type trees, chosen at random. Then to each clump centre is allocated a uniformly distributed number of offspring type B trees, the domain being $\{0, 1, 2, 3, 4\}$: Fig.5(10)(i) and Fig. 5(10)(ii) show the periodograms for the A and B populations, while Fig.5(10)(iii) shows the cross periodogram. The periodogram for the B-type trees, shows the population to be extremely clumped, $I^{B}(w)$ being much greater than 2 for an appreciable range of w.

The cross periodogram in Fig.5(10)(iii) shows the species to be correlated in some manner, the large value of $I^{AB}(w)$ for small w indicating that some of the A and B type trees tend to be close together.

Having studied the isotropic auto spectra and isotropic cross spectra of various artificial populations, the species in Lansing Woods can now be subjected to the same methods of analysis. The sampling area was taken as a 10 in. x 10 in. square placed symmetrically within the 15 in. x 15 in. square containing the tree position data of

Lansing Woods (1 in. represents 61.6 ft.). The species are shown in chapter four in relation to the mapping of clumped and sparse areas, (see Figs. 4(7) - 4(12)). It is important to remember that for the spectral analysis of this data, it is assumed that the positions of the trees form an isotropic, stationary point processs. This may be dubious for the Miscellaneous trees and the Black oaks, but they are included for completeness. Pielou's test and coefficient of segregation do not rely on isotropy or stationarity.

Figs. 5(11), 5(12), 5(13), 5(14), 5(15), 5(16) show the smoothed isotropic periodograms for the Maples, Hickories, White oaks, Red oaks, Miscellaneous trees, and Black oaks respectively. The species are then taken in pairs and the fifteen smoothed isotropic cross periodograms are shown in Figs. 5(17) to 5(31). Tabel 8 shows the numbers of trees for each of the species.

Table 8. The numbers of trees for each species within the sampling area.

Type	No. of trees
Maples	296
Hickories	261
White oaks	205
Red oaks	173
Miscellaneous trees	52
Black oaks	35

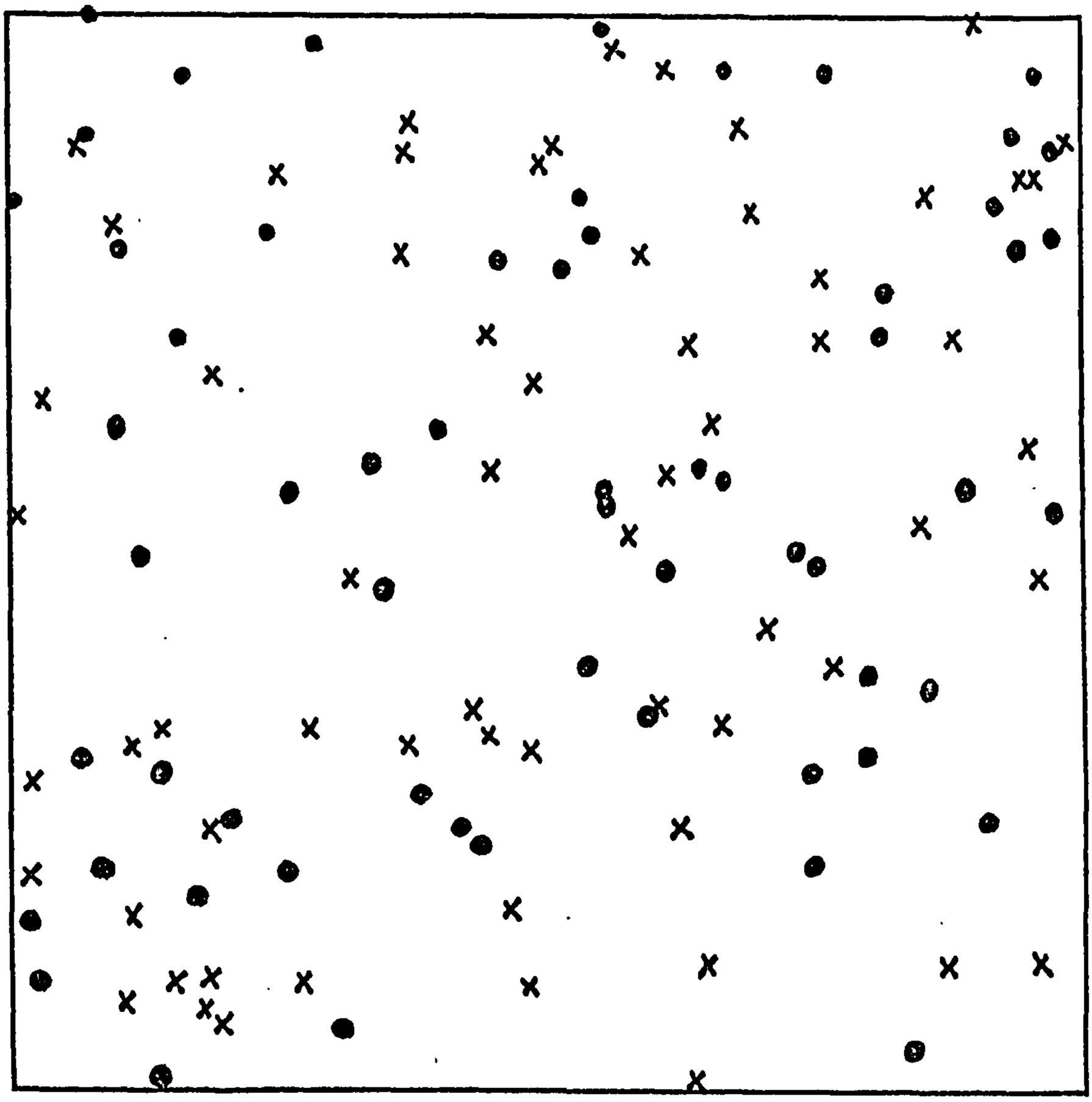

Fig. 5(1) Two Independent Poisson Forests

● - A's Poisson forest
× - B's Poisson forest

Fig. 5(2)(i) $I^A(w)$ for a Poisson forest

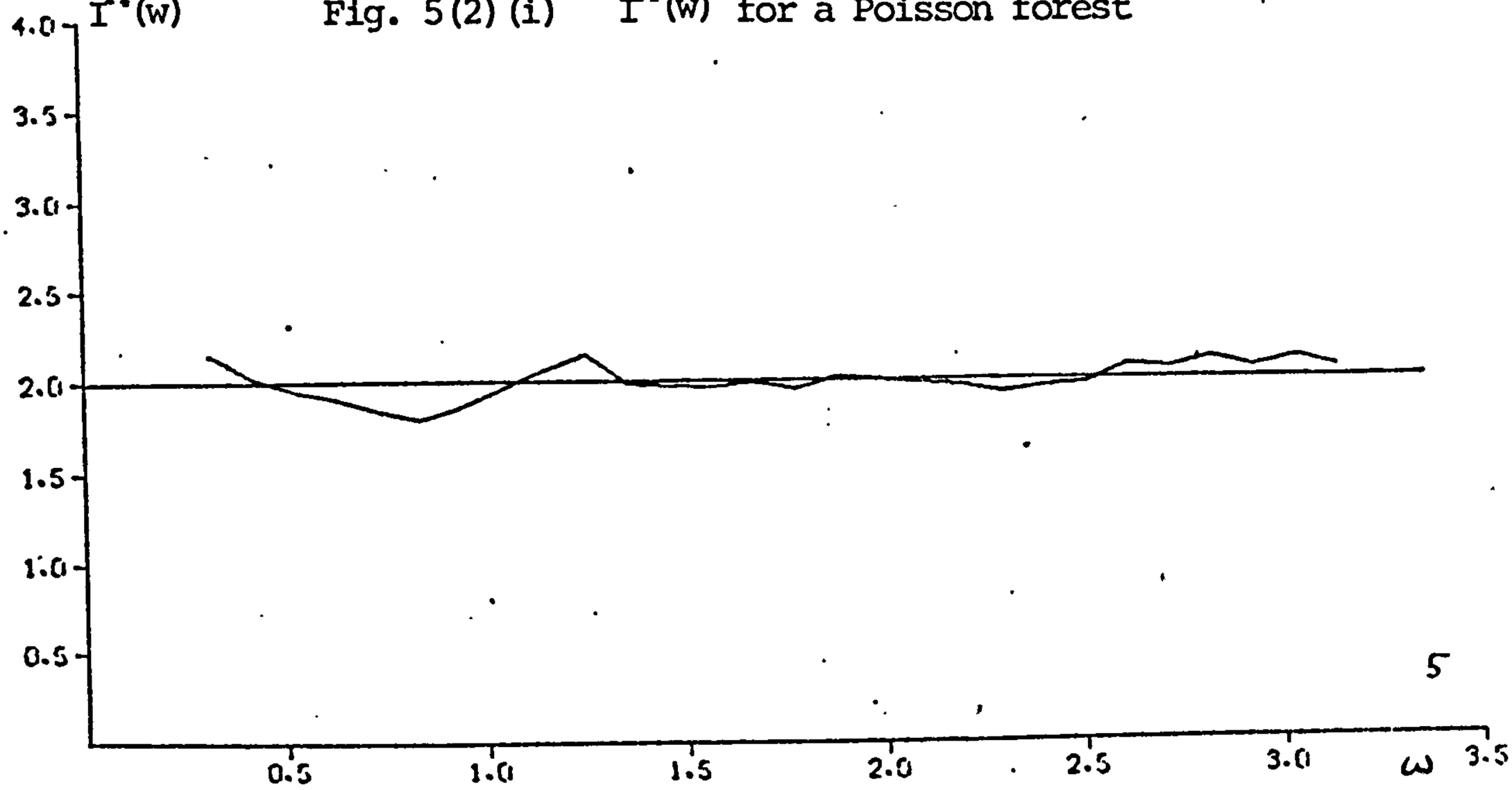

Fig. 5(2)(ii) $I^B(w)$ for a Poisson forest

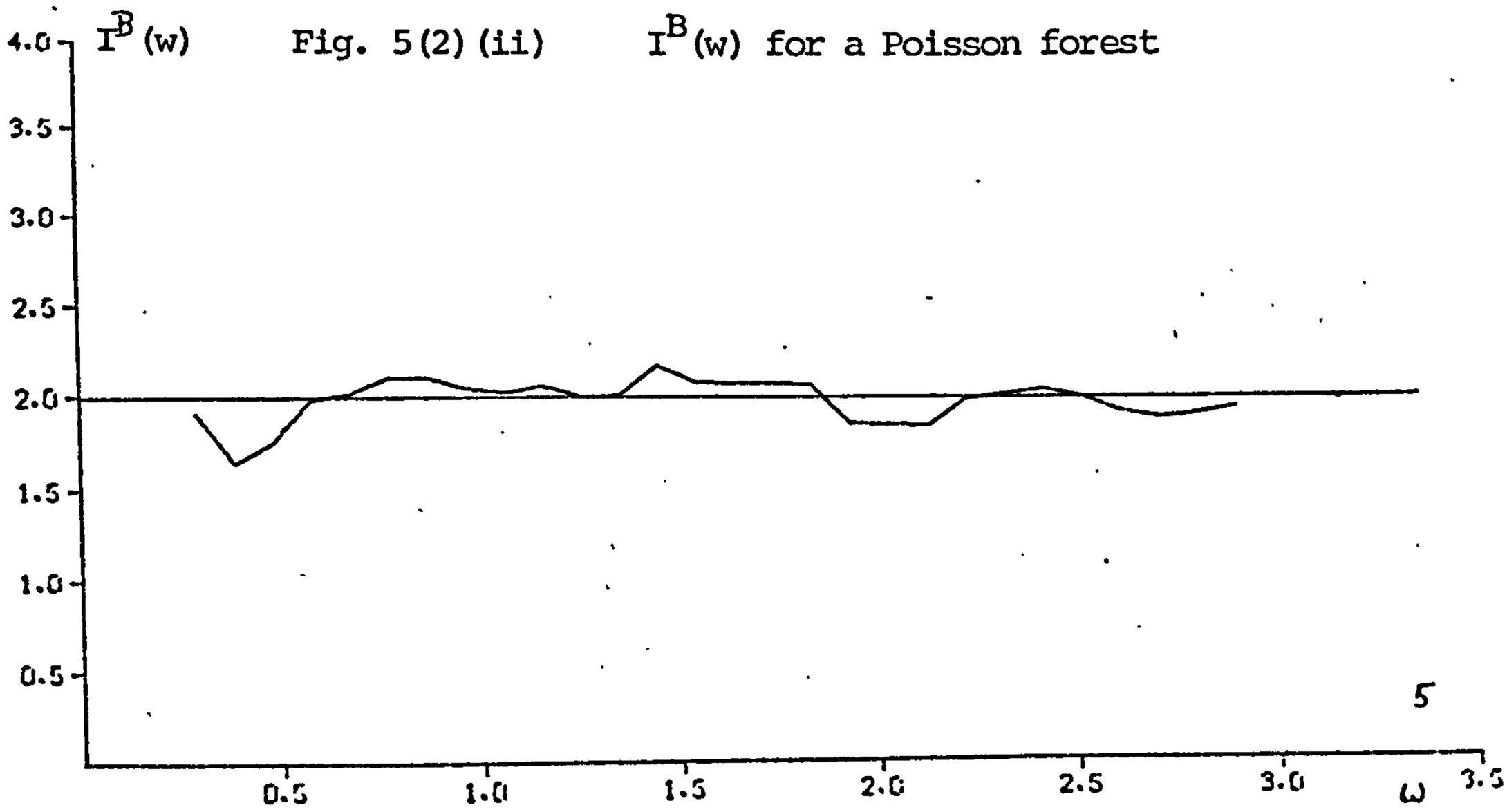

Fig.5(2)(iii) $I^{AB}(w)$ for two independent Poisson forests

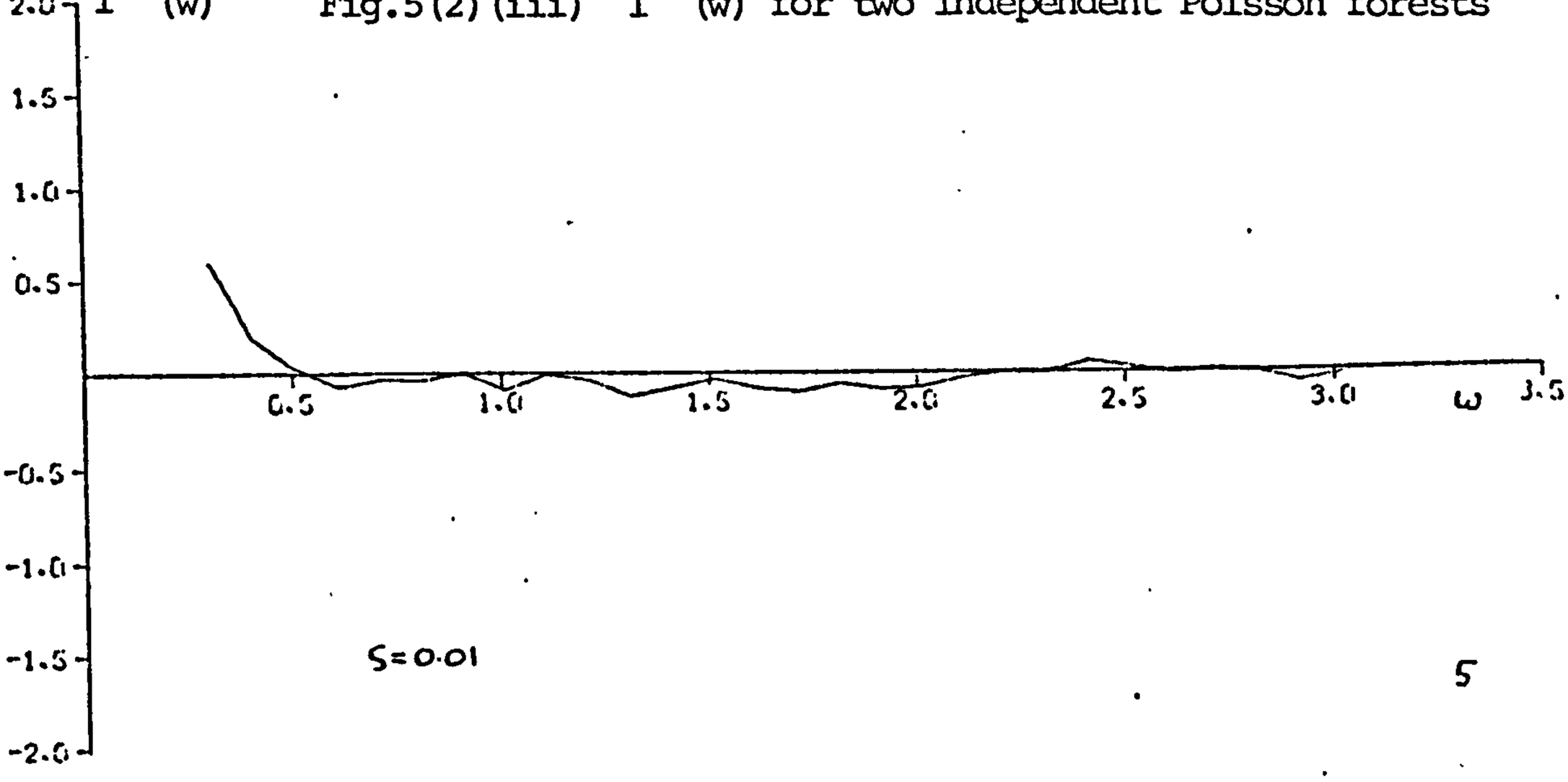

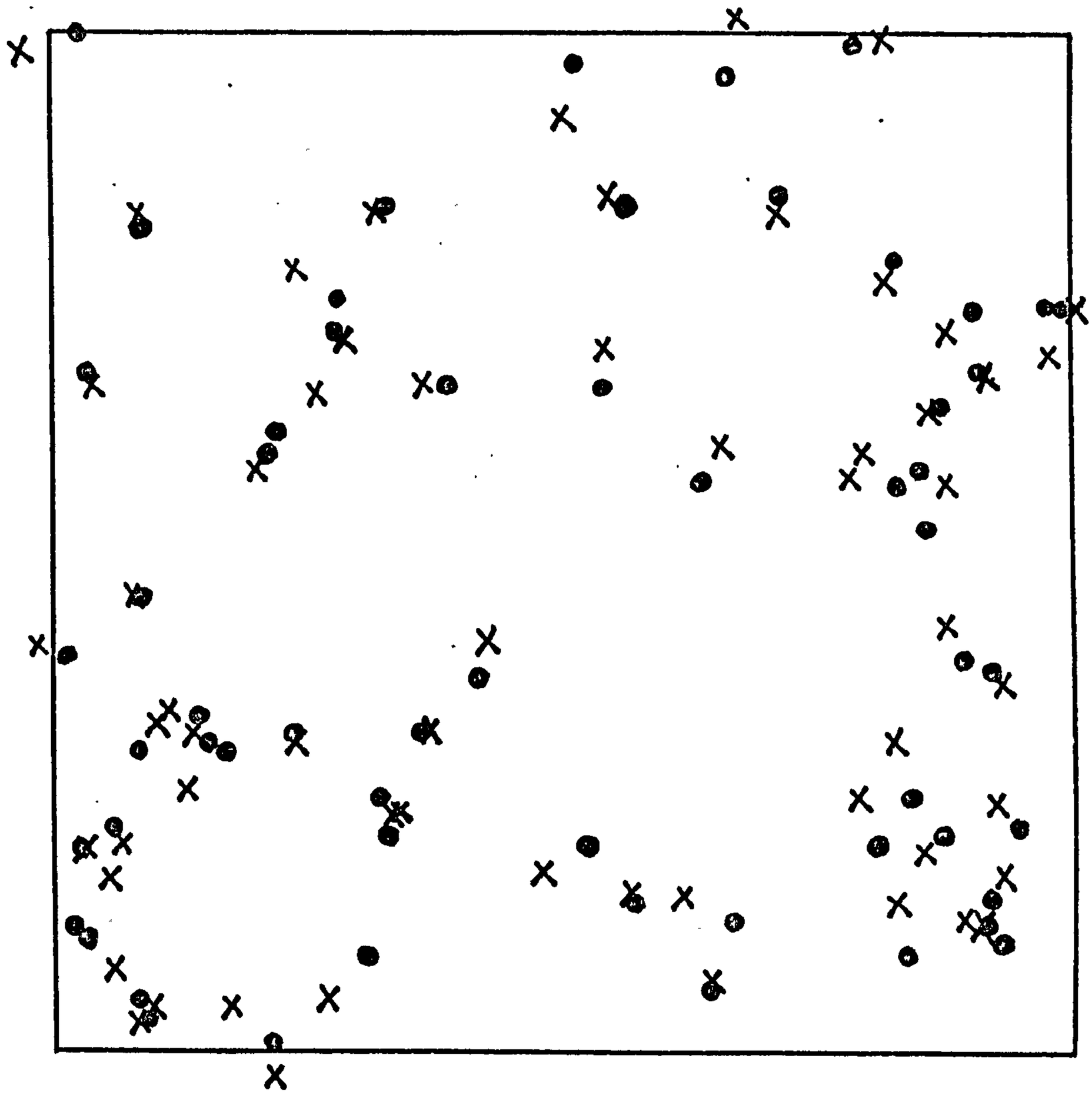

Fig. 5(3) Two associated Poisson forests

● - A's Poisson forest

× - B's Poisson foest

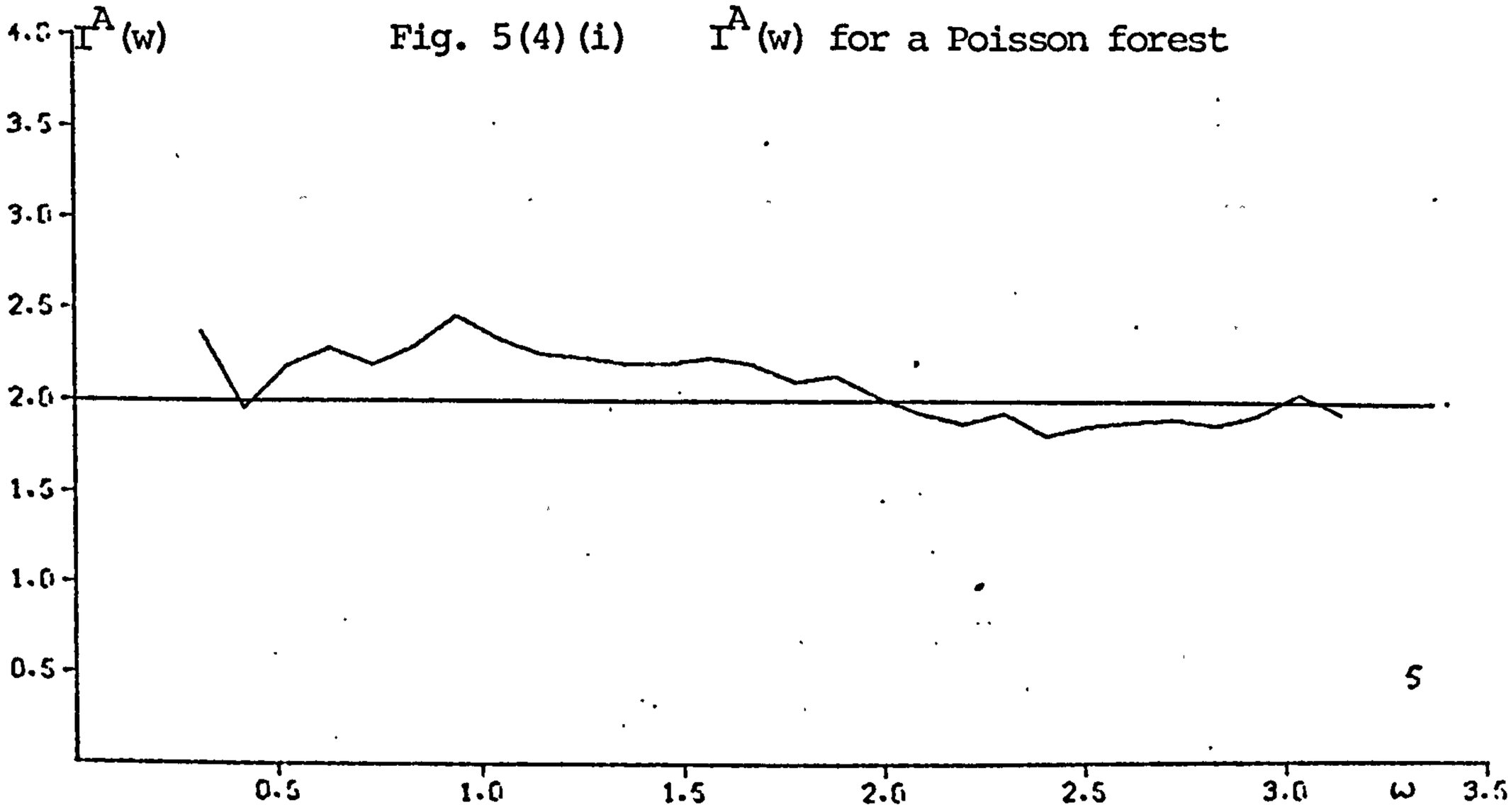

Fig. 5(4)(i) $I^A(w)$ for a Poisson forest

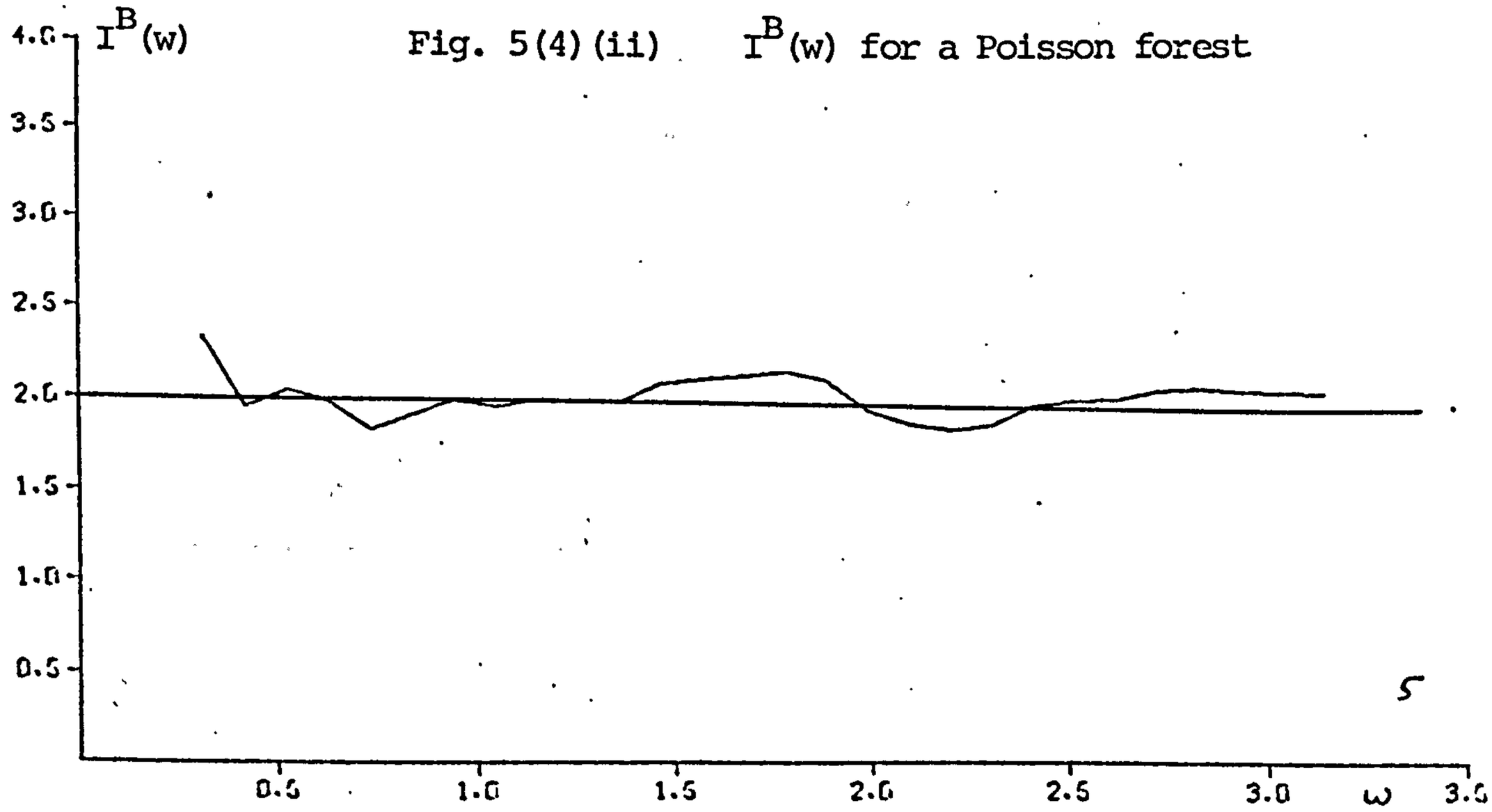

Fig. 5(4)(ii) $I^B(w)$ for a Poisson forest

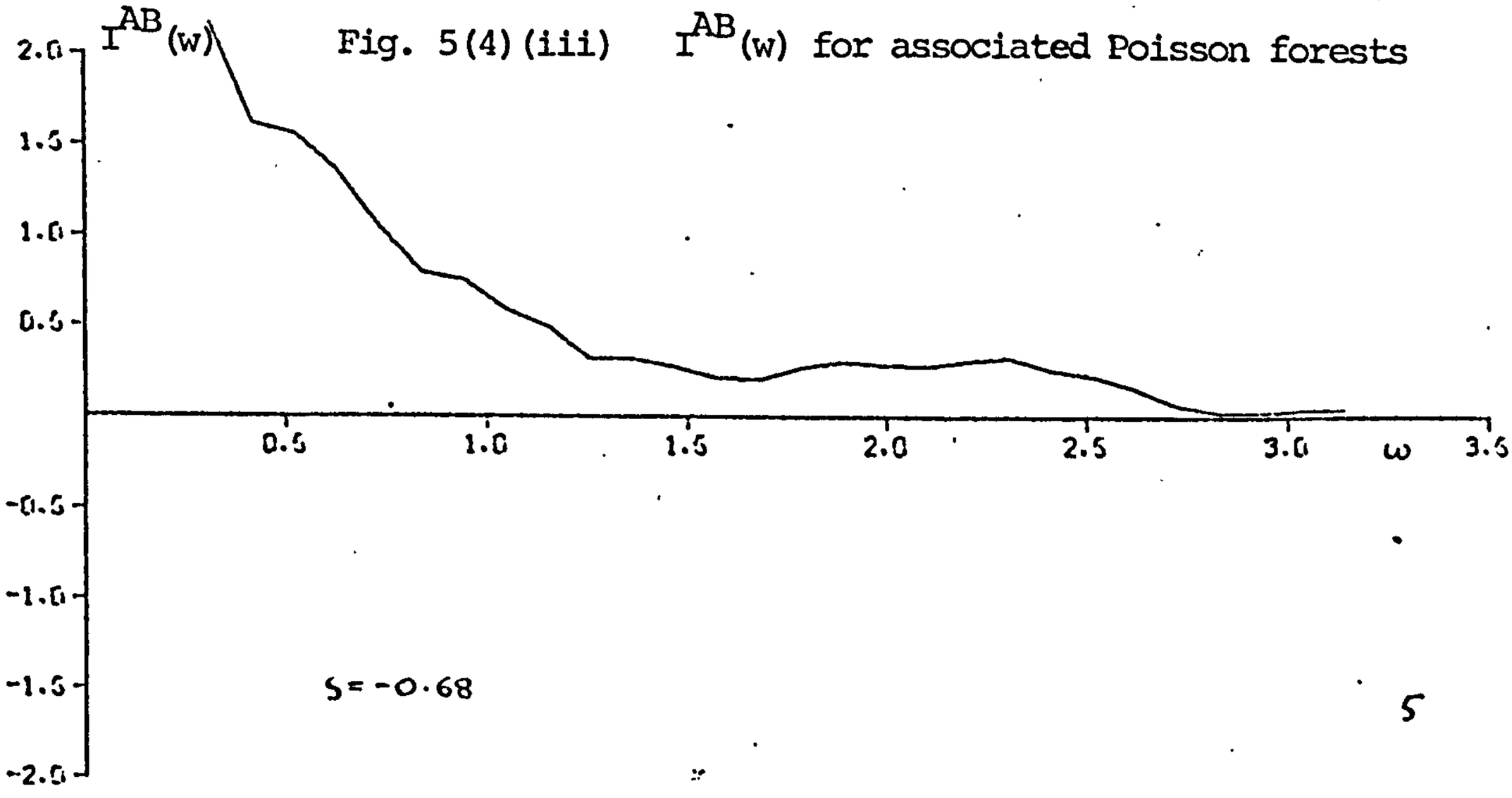

Fig. 5(4)(iii) $I^{AB}(w)$ for associated Poisson forests

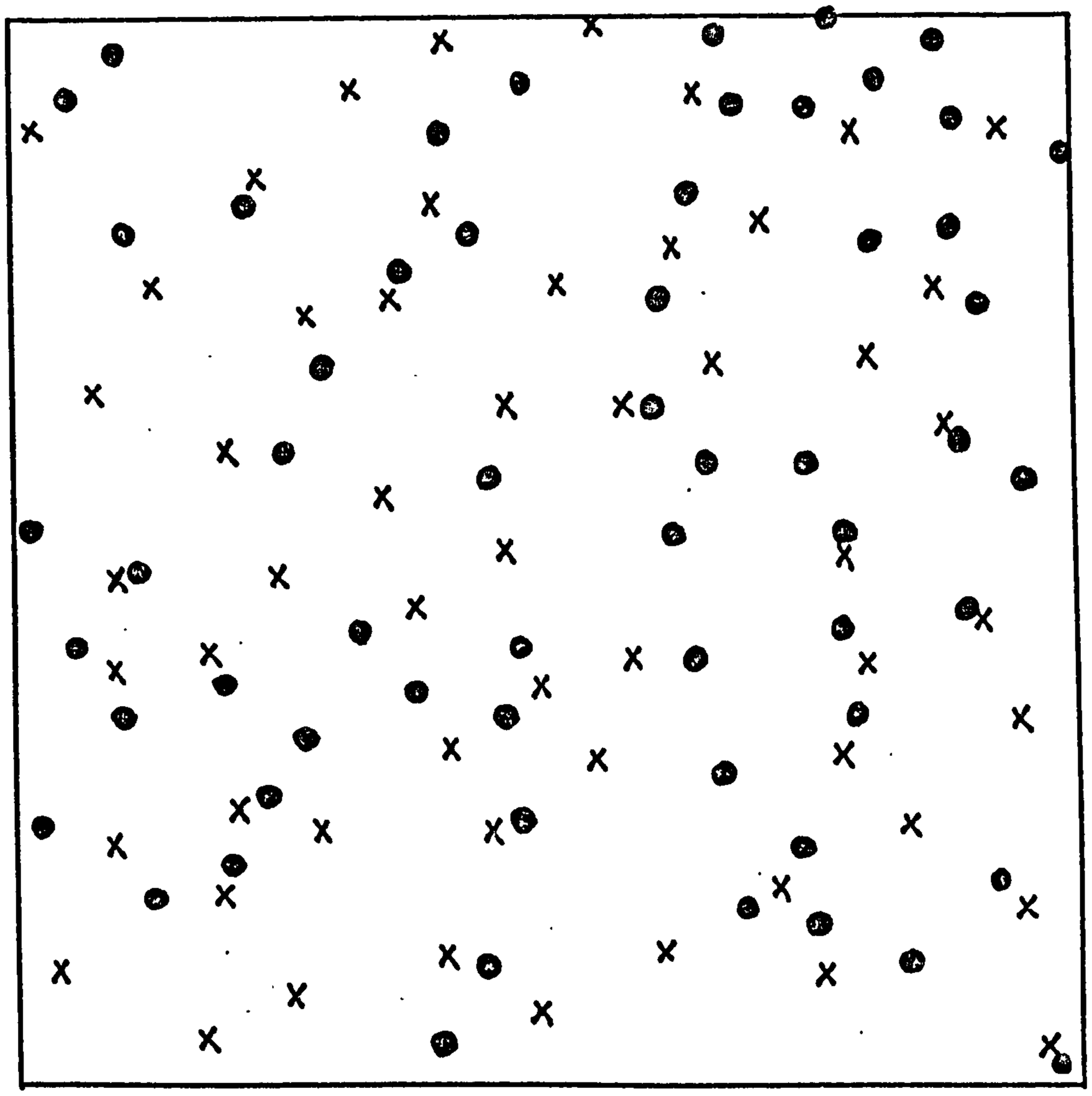

Fig. 5(5) Two independent regular patterns

● - A's regular pattern

X - B's regular pattern

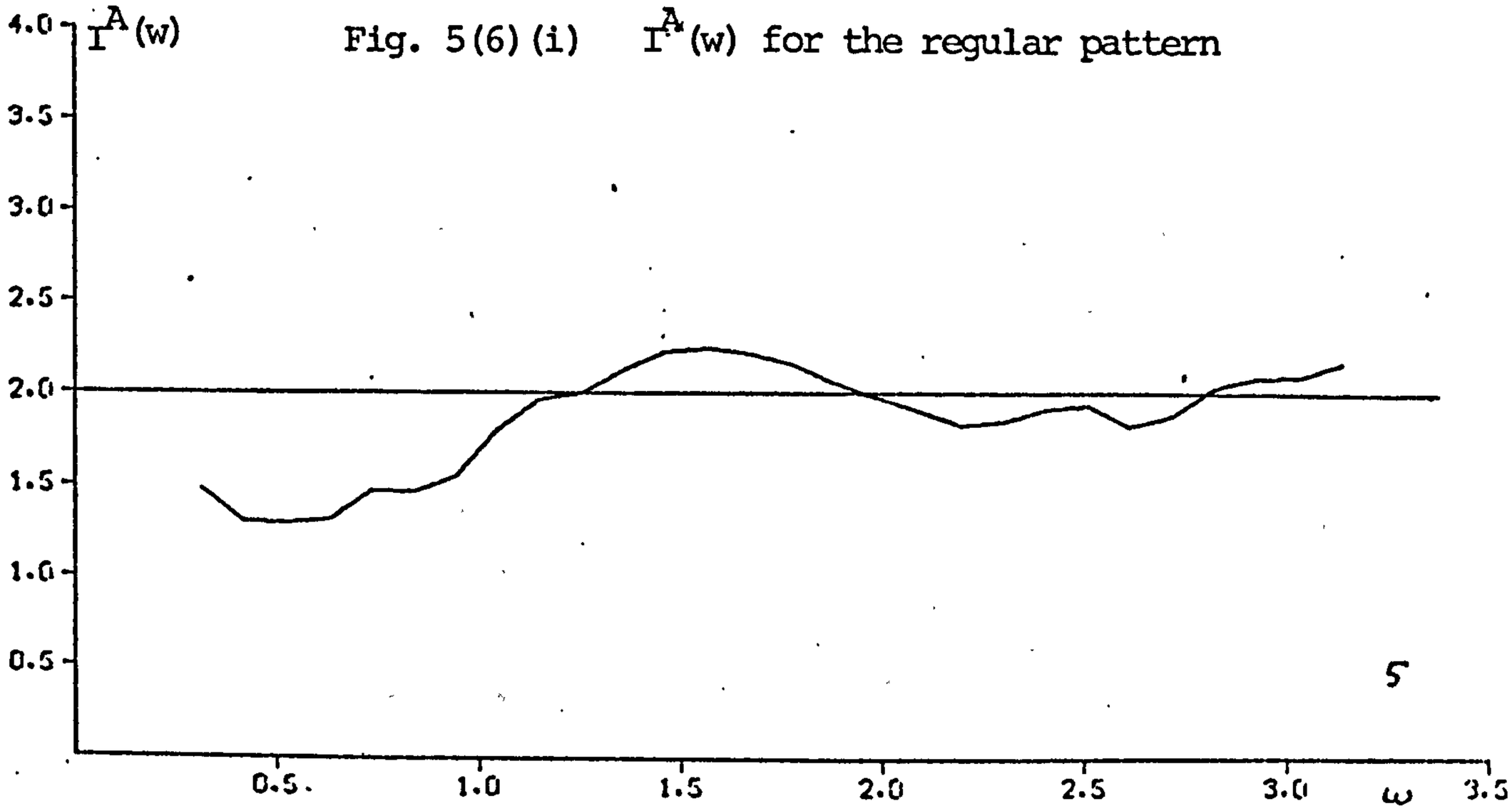

Fig. 5(6)(i) $I^A(w)$ for the regular pattern

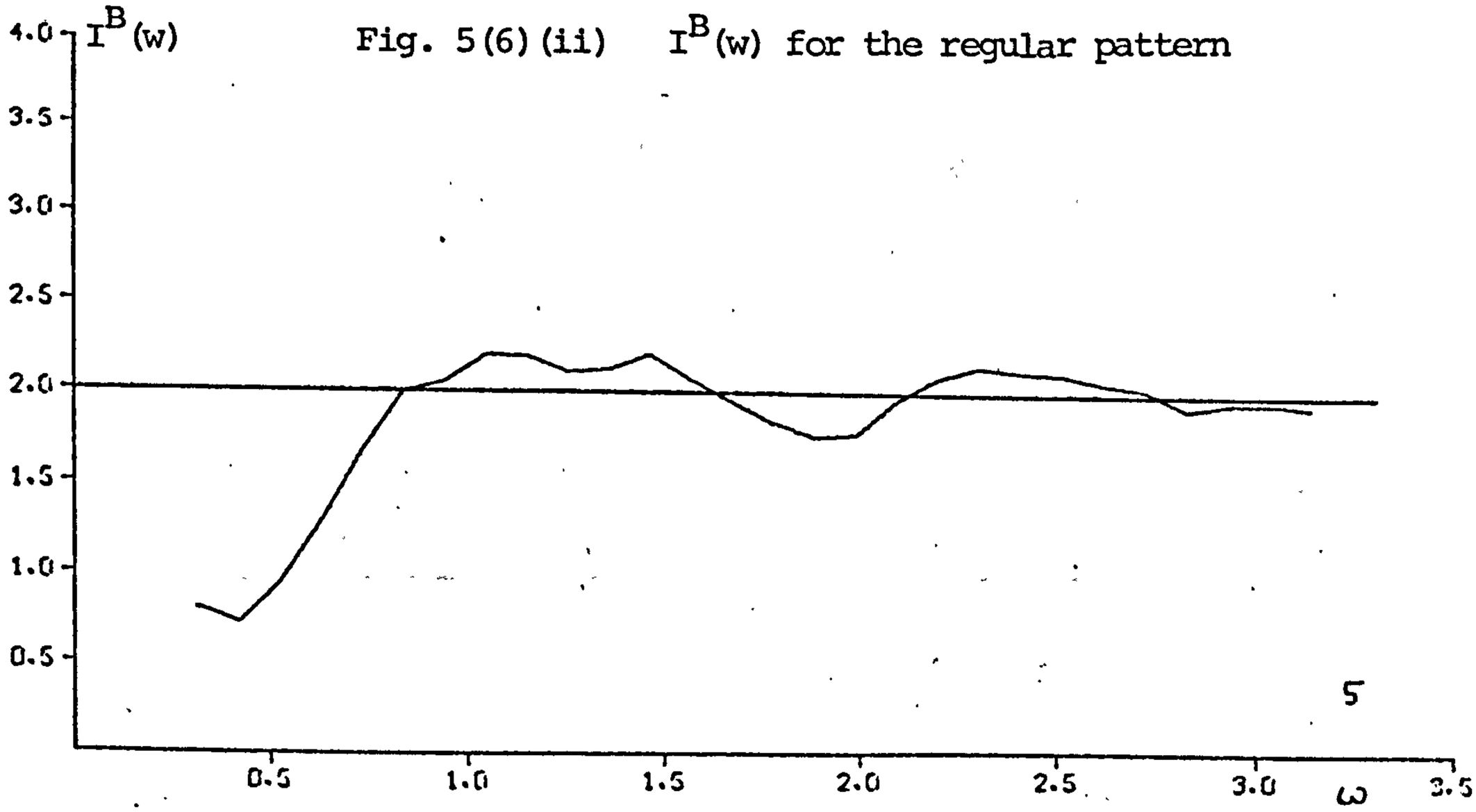

Fig. 5(6)(ii) $I^B(w)$ for the regular pattern

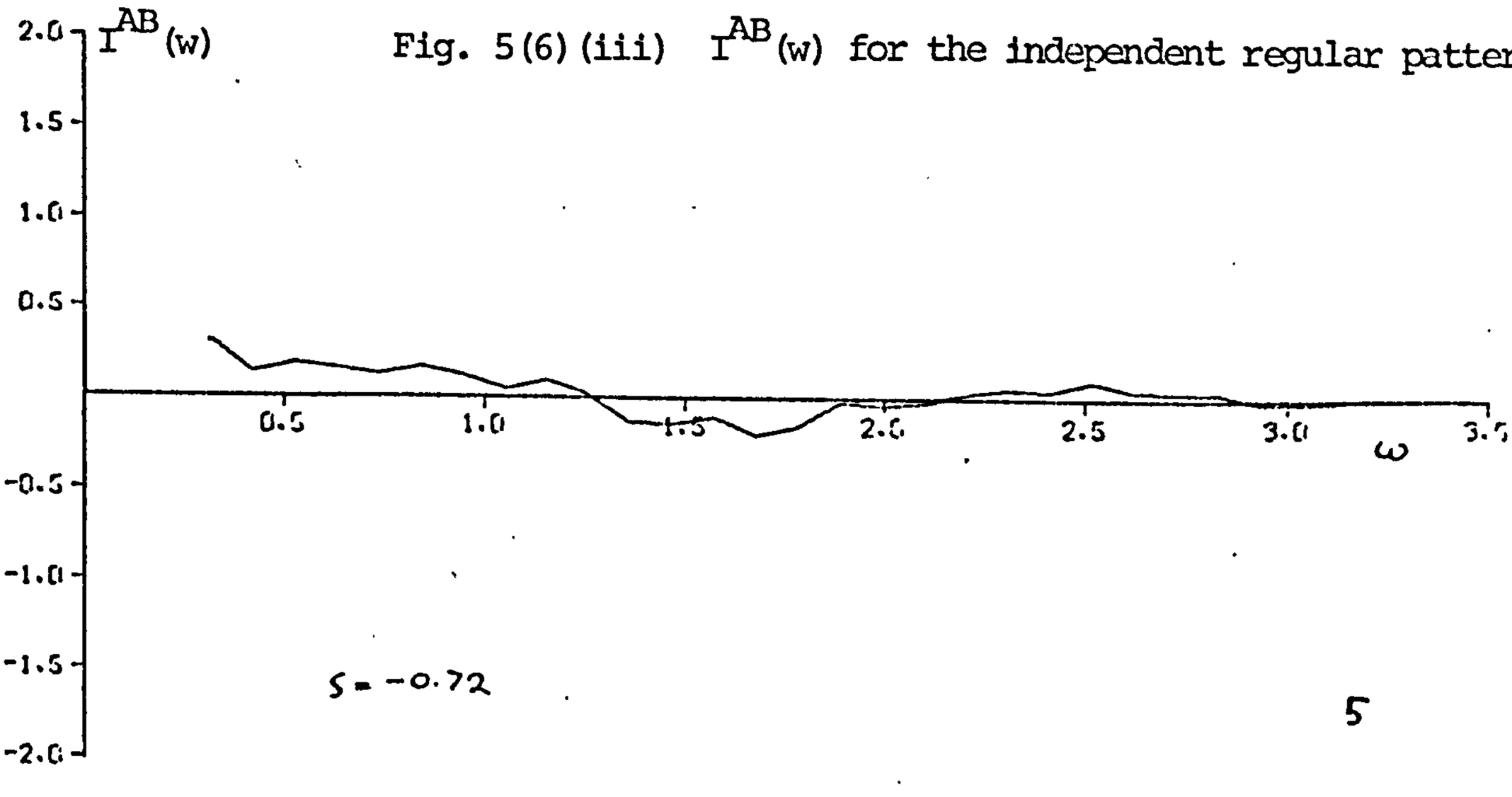

Fig. 5(6)(iii) $I^{AB}(w)$ for the independent regular patterns

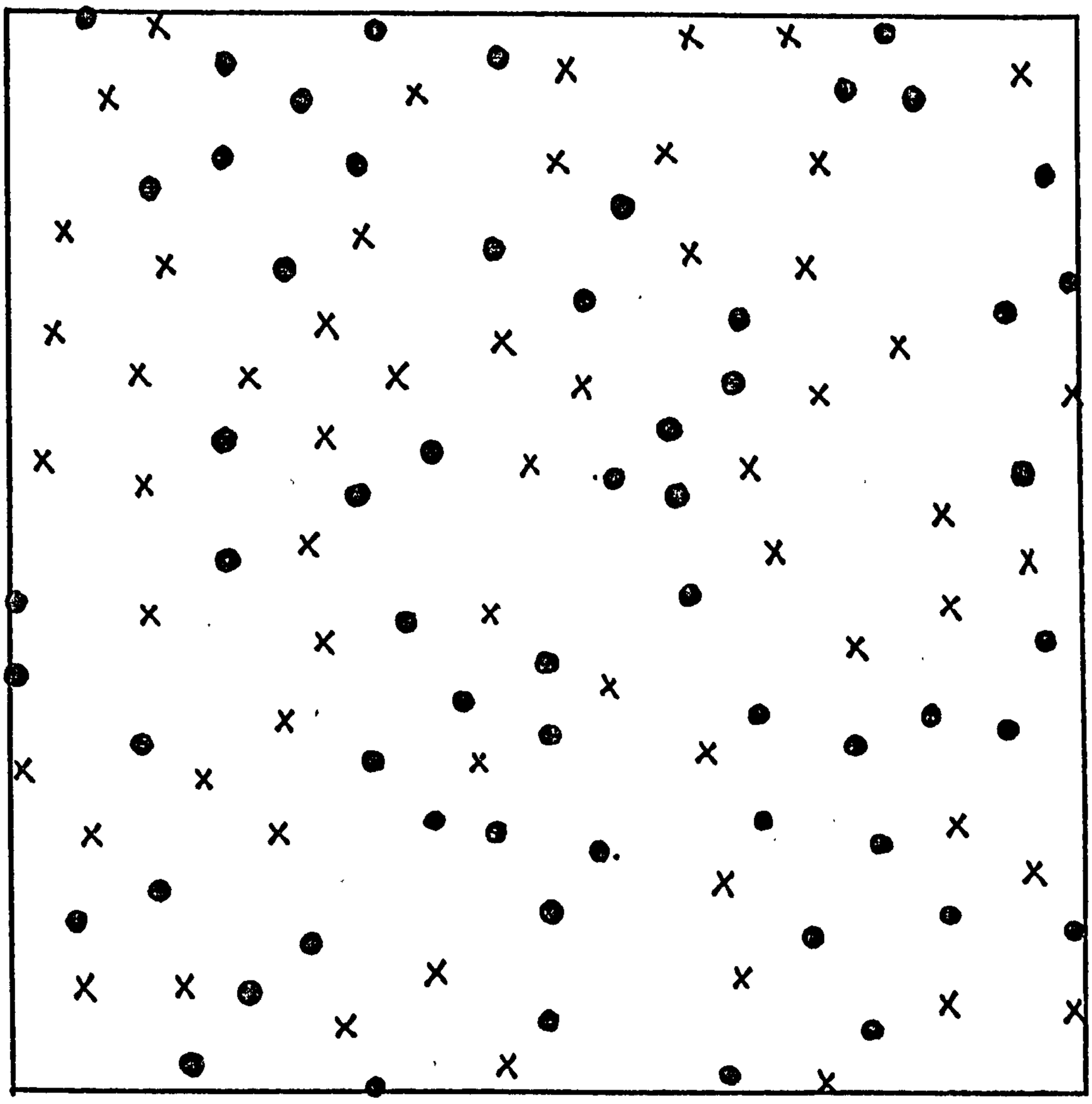

Fig. 5(7) Two inhibitory regular patterns

● - A's regular pattern

× - B's regular pattern

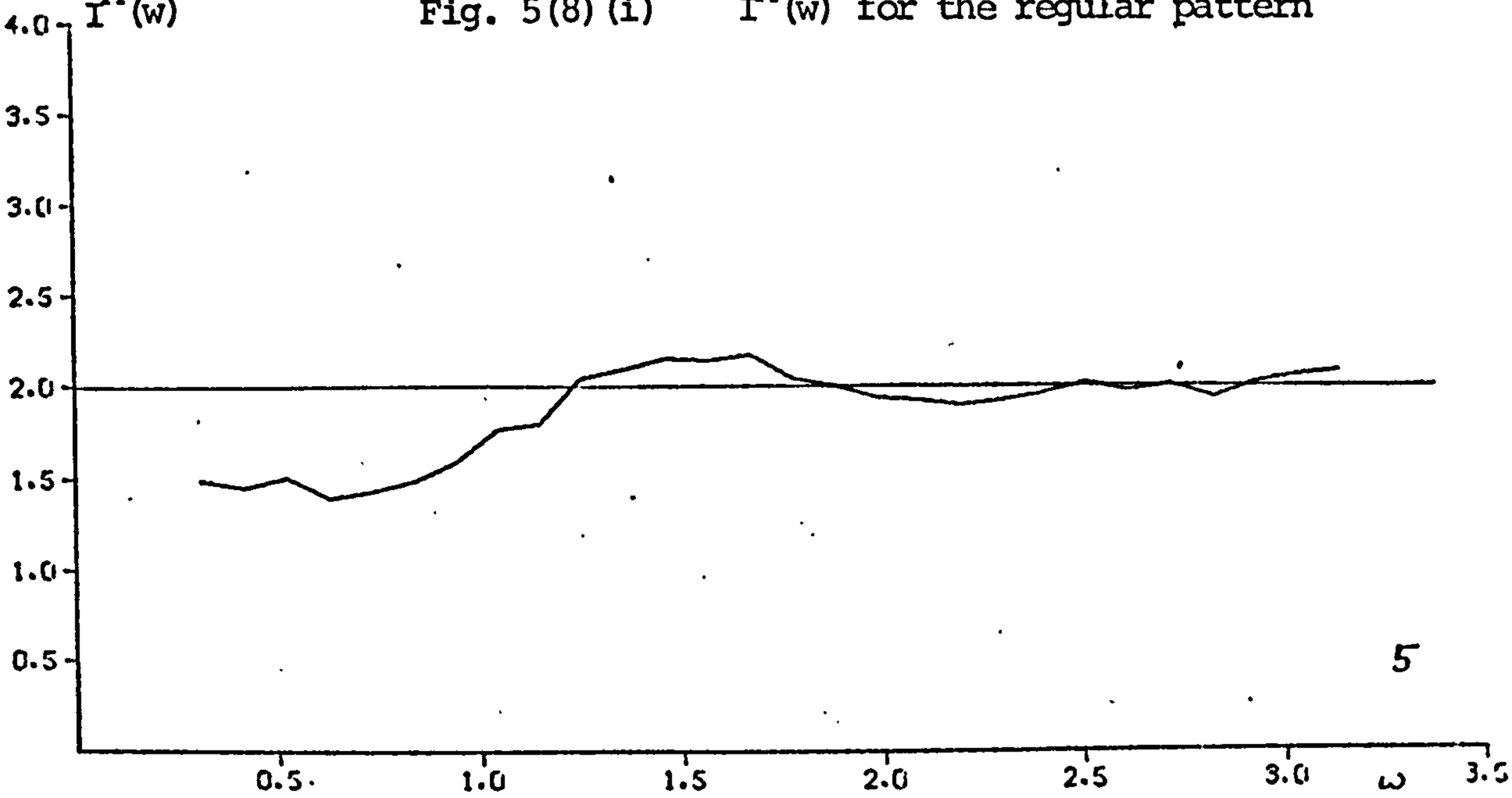

Fig. 5(8)(i) $I^A(w)$ for the regular pattern

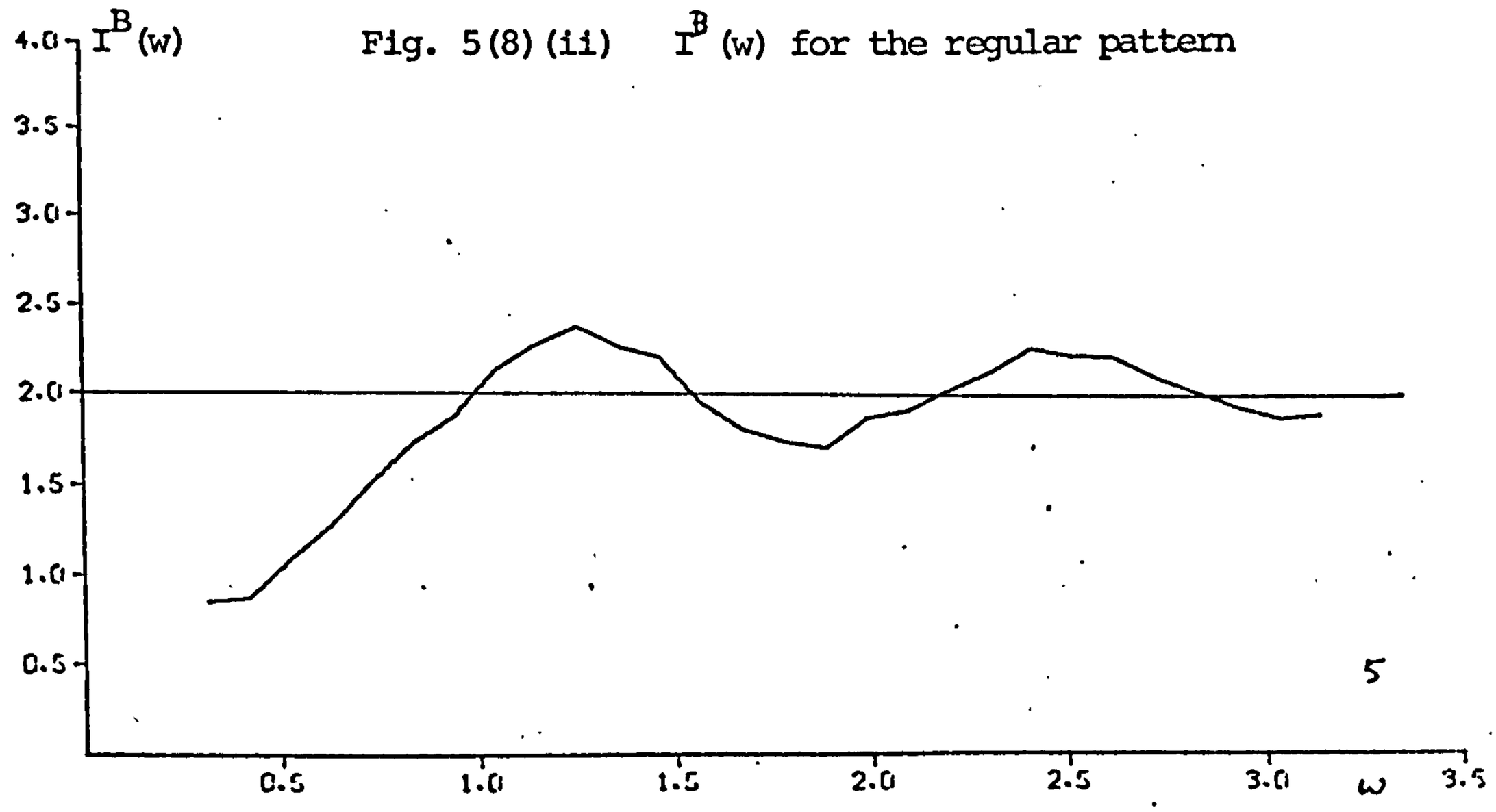

Fig. 5(8)(ii) $I^B(w)$ for the regular pattern

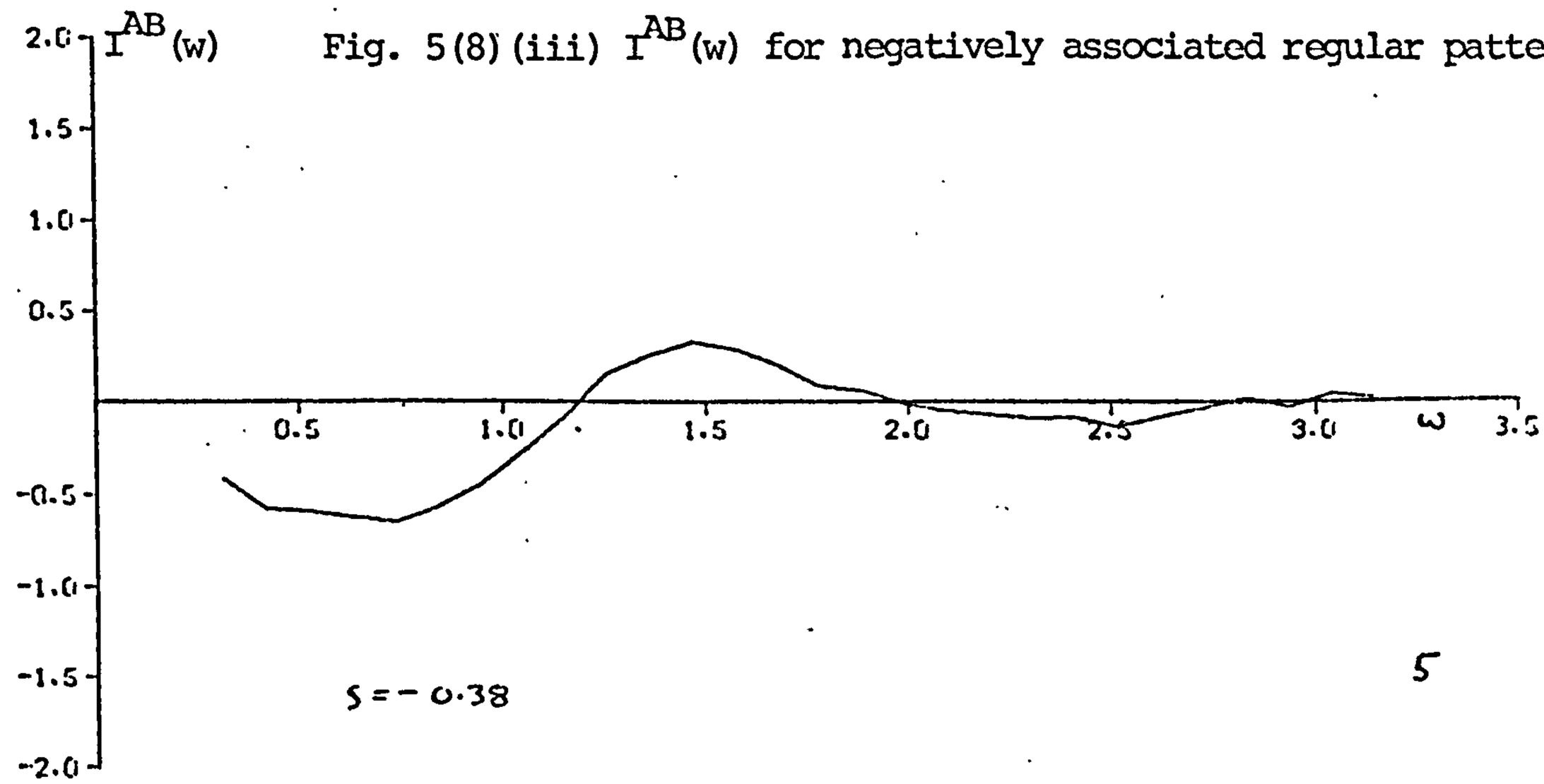

Fig. 5(8)(iii) $I^{AB}(w)$ for negatively associated regular patterns

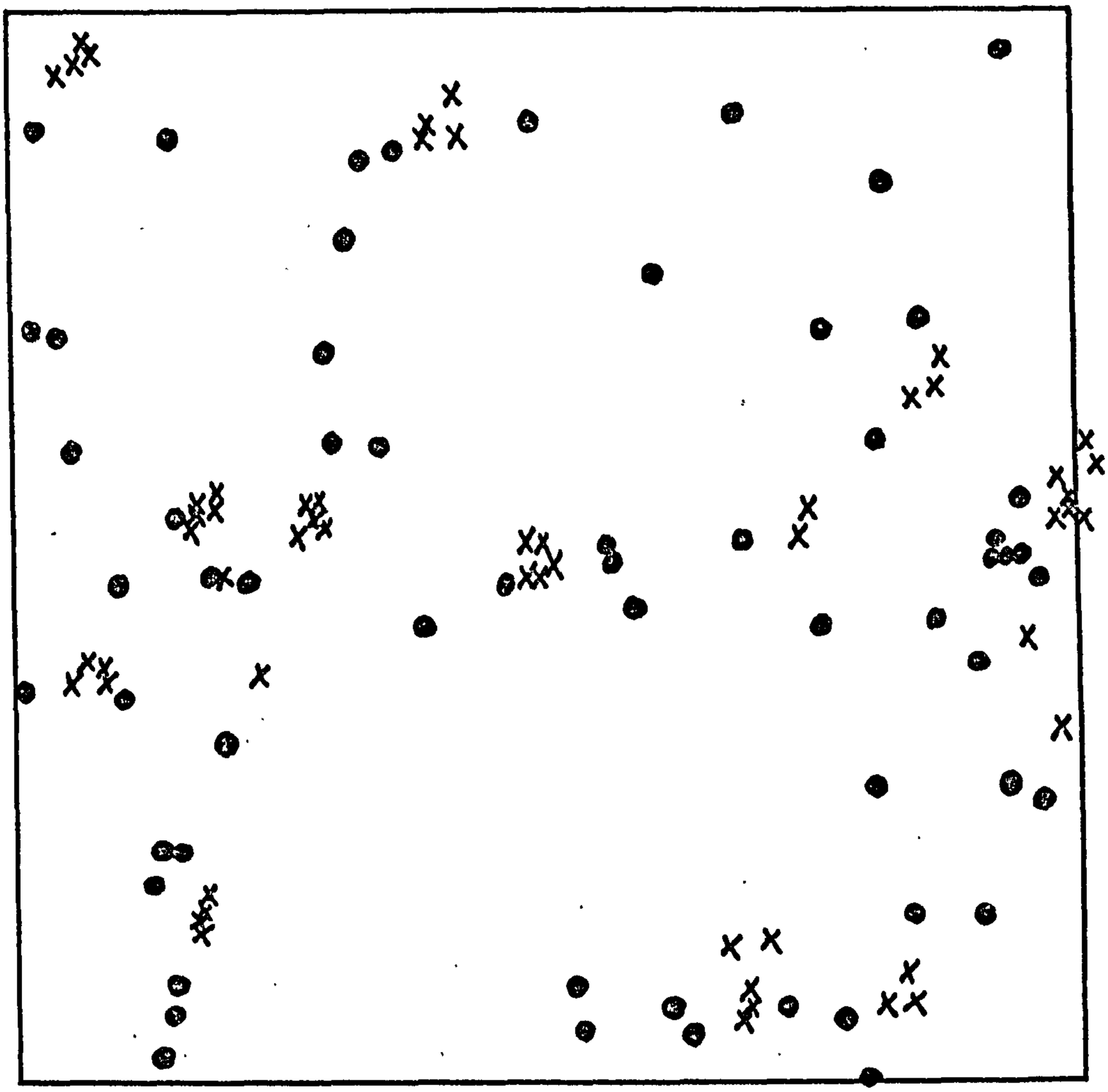

Fig. 5(9) A Poisson forest and a clumped pattern

● - A's Poisson forest

✱ - B's clumped pattern

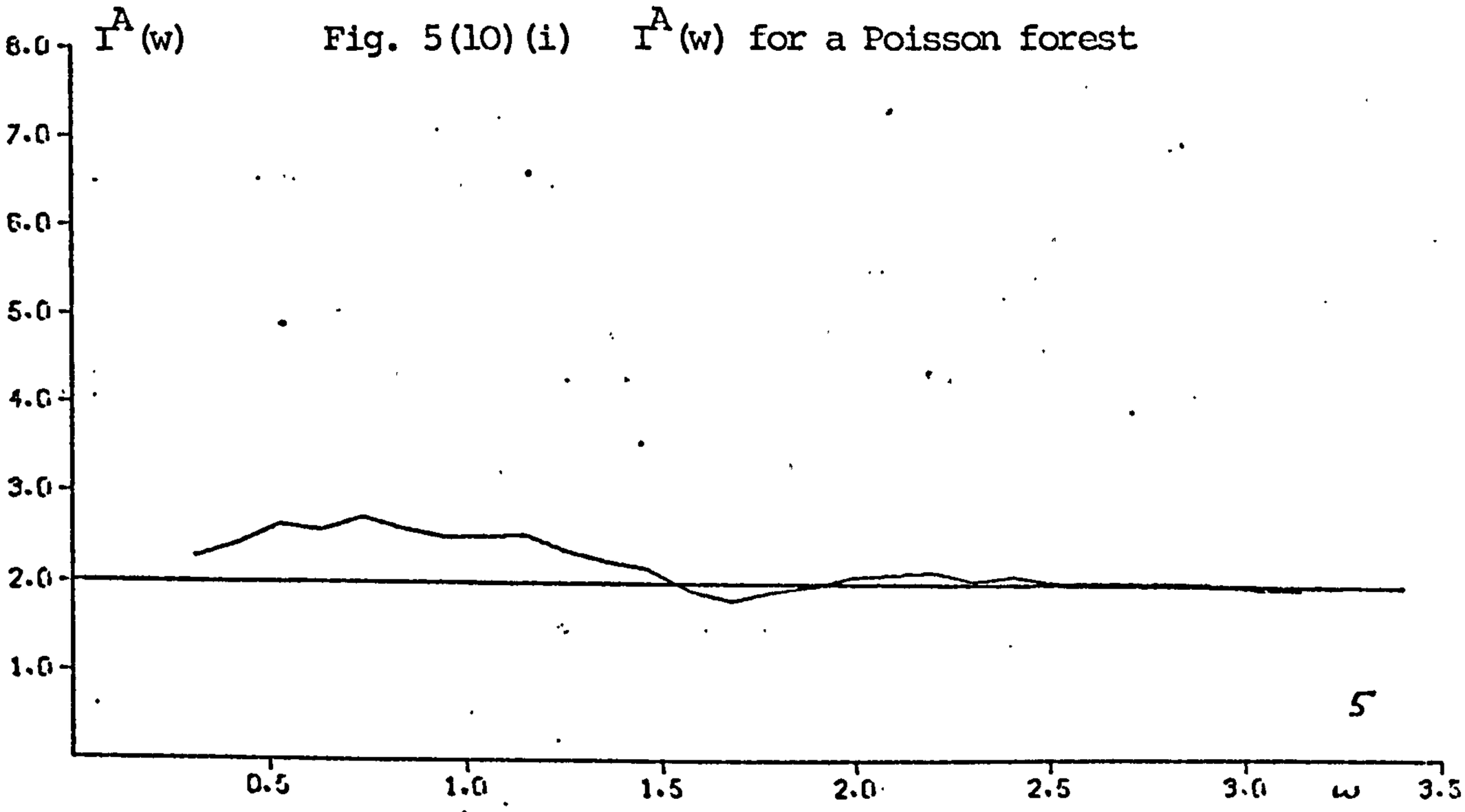

Fig. 5(10)(i) $I^A(w)$ for a Poisson forest

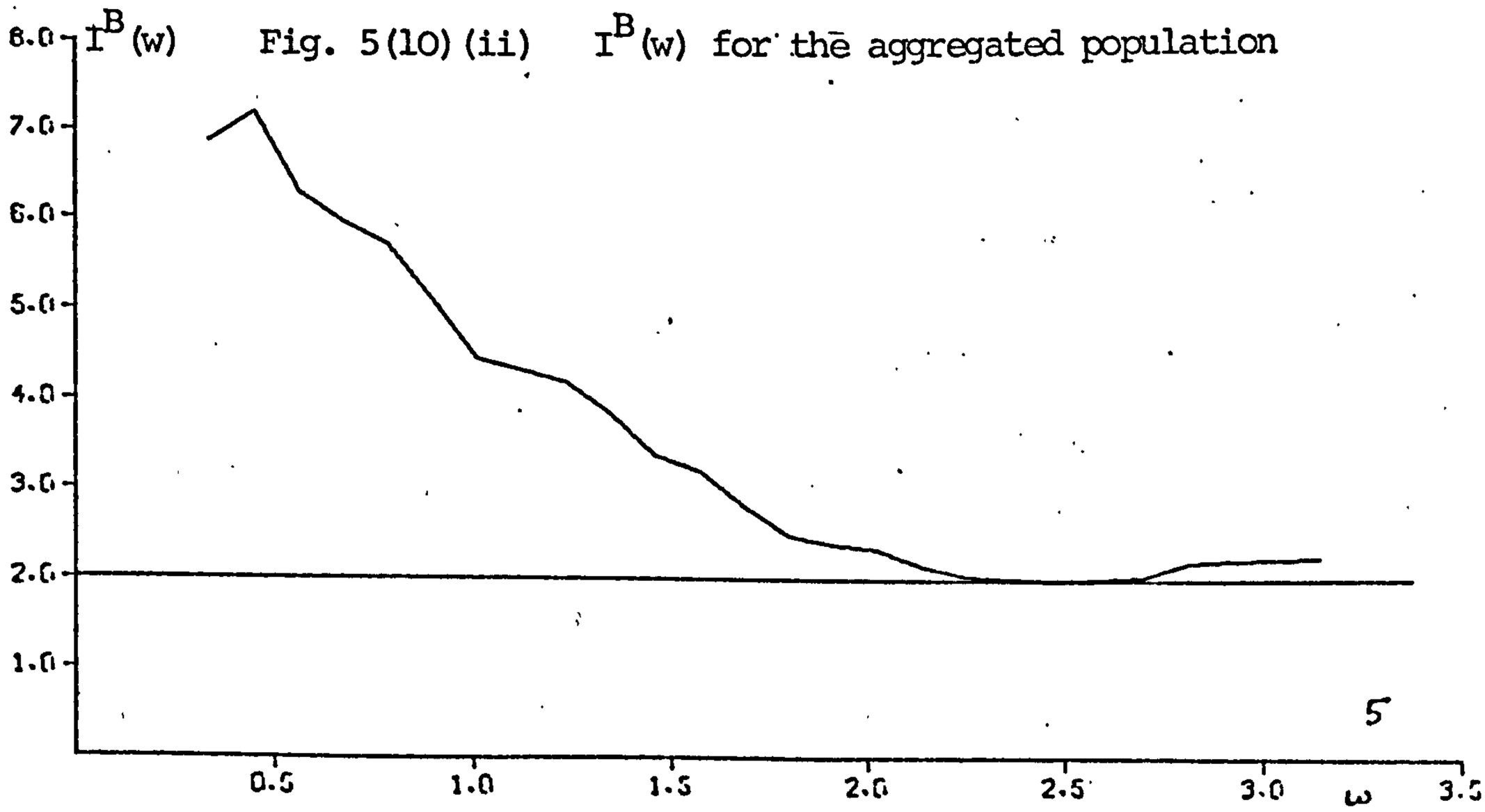

Fig. 5(10)(ii) $I^B(w)$ for the aggregated population

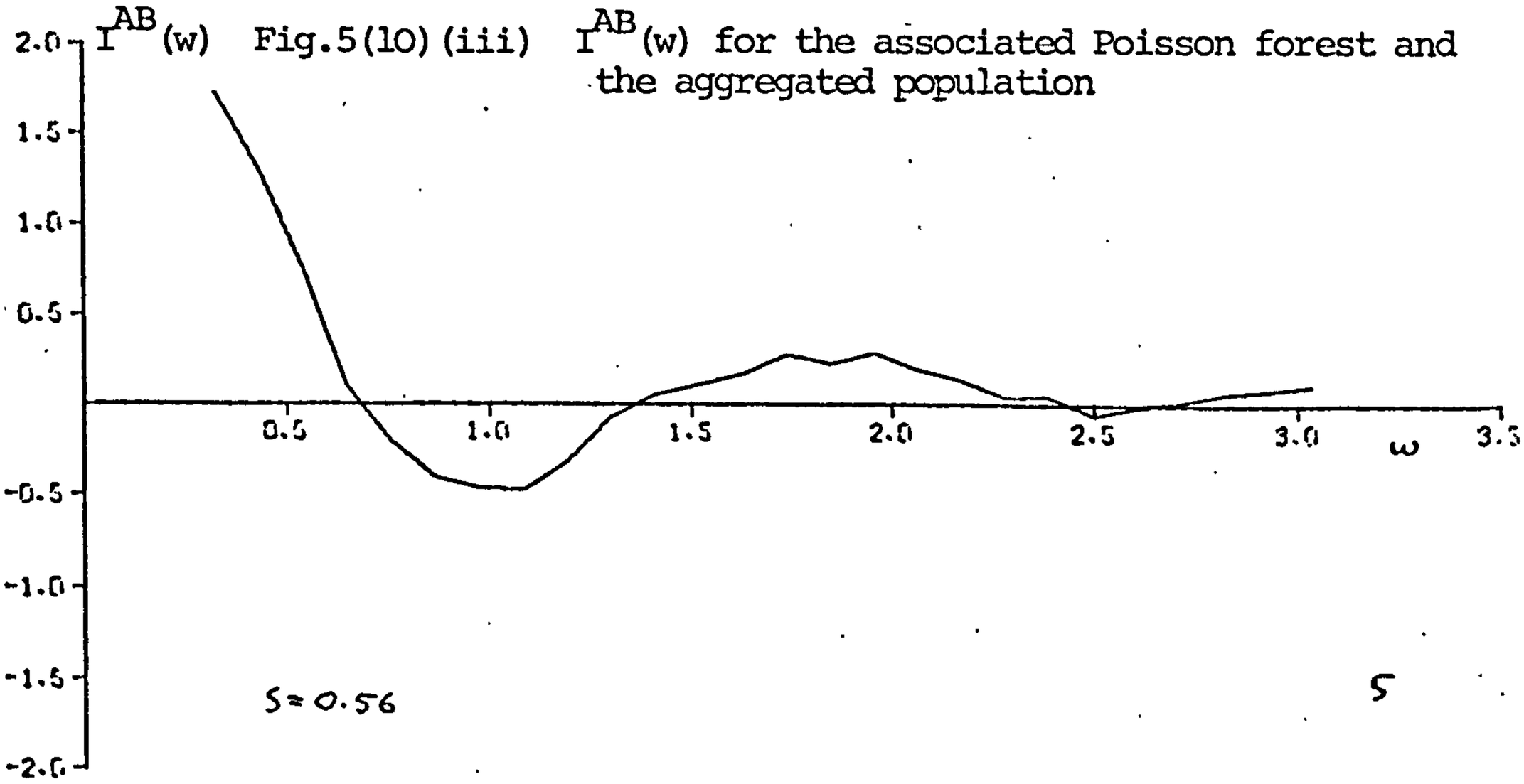

Fig.5(10)(iii) $I^{AB}(w)$ for the associated Poisson forest and the aggregated population

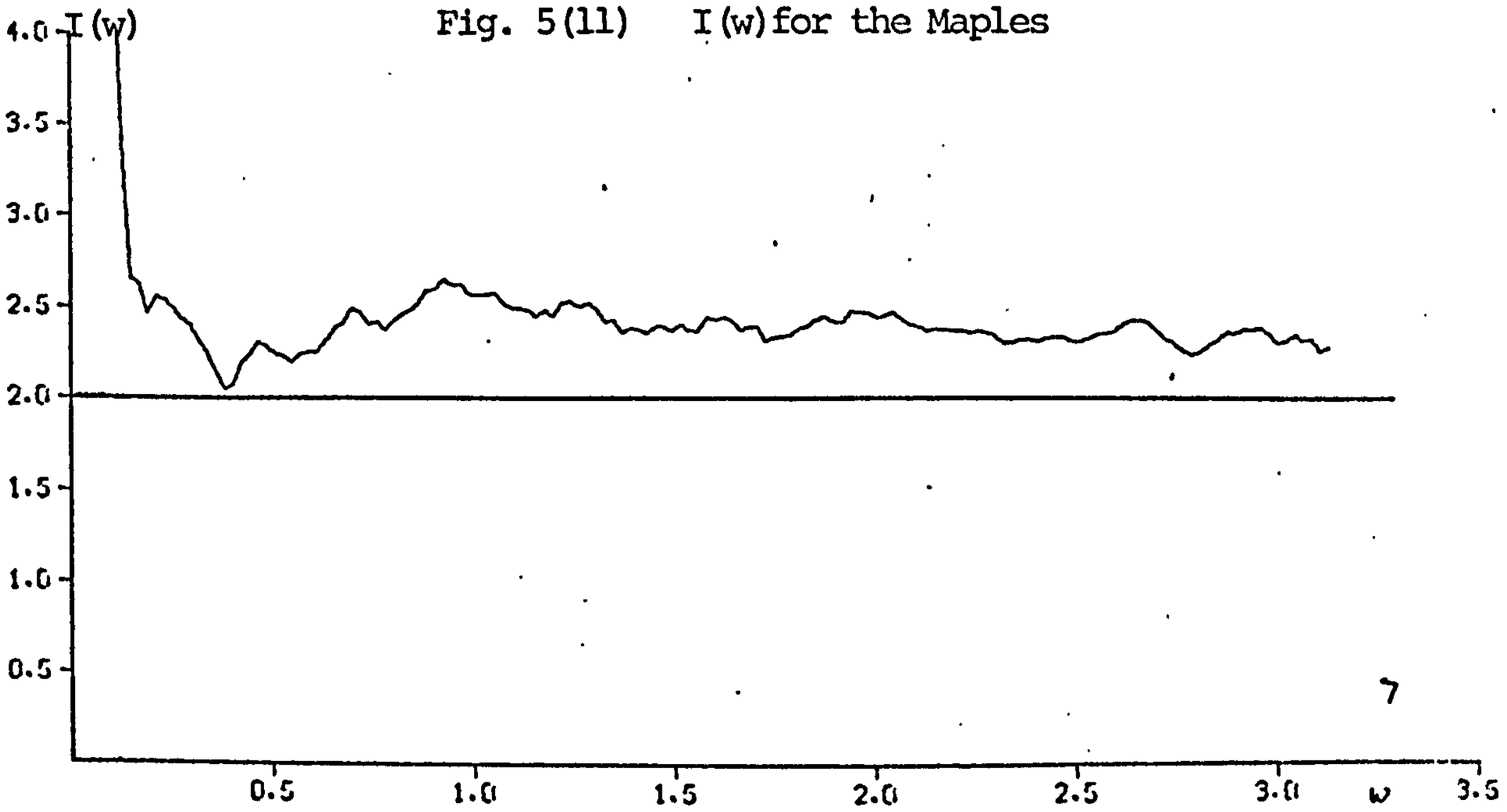

Fig. 5(11) I(w) for the Maples

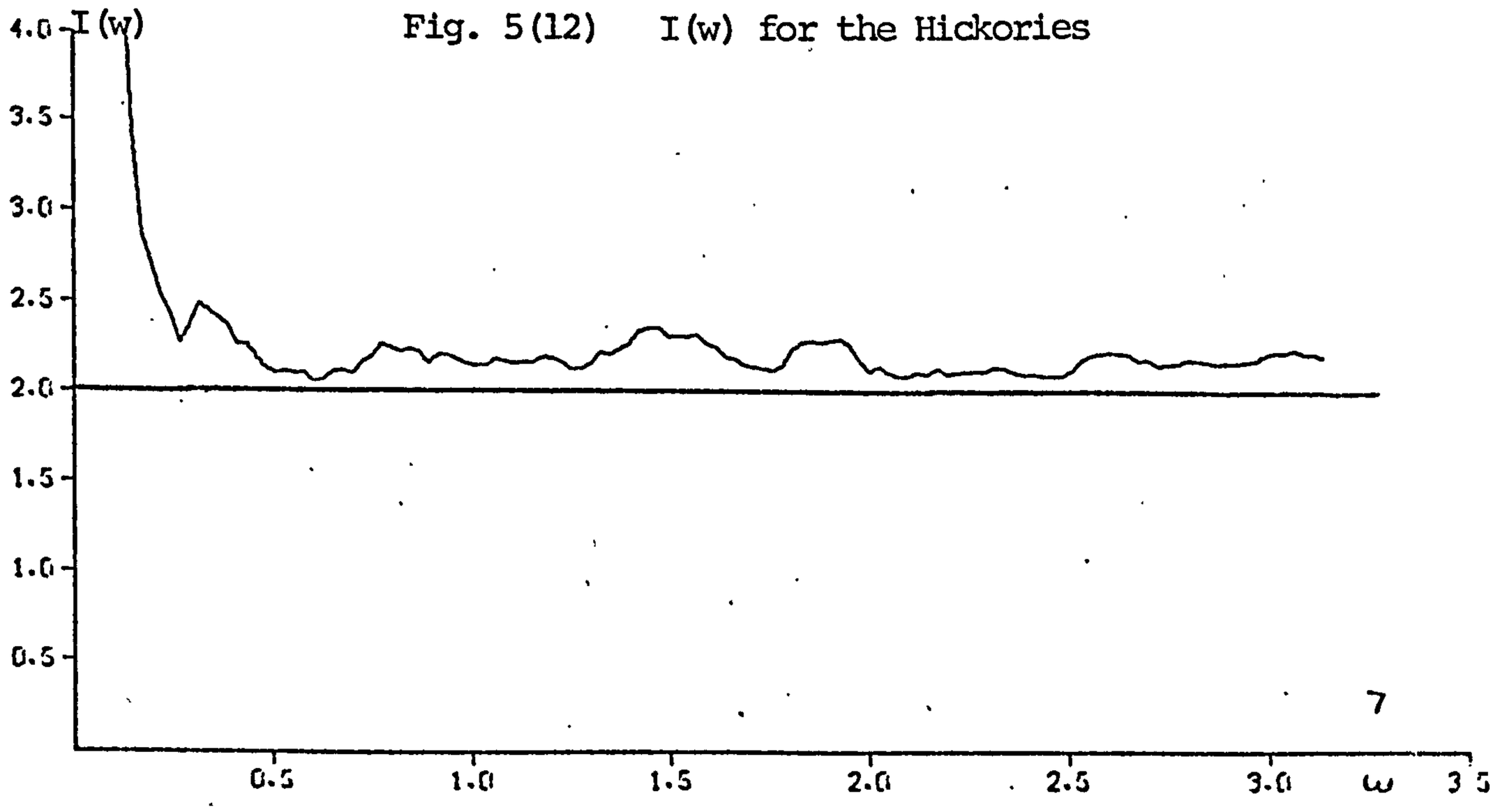

Fig. 5(12) I(w) for the Hickories

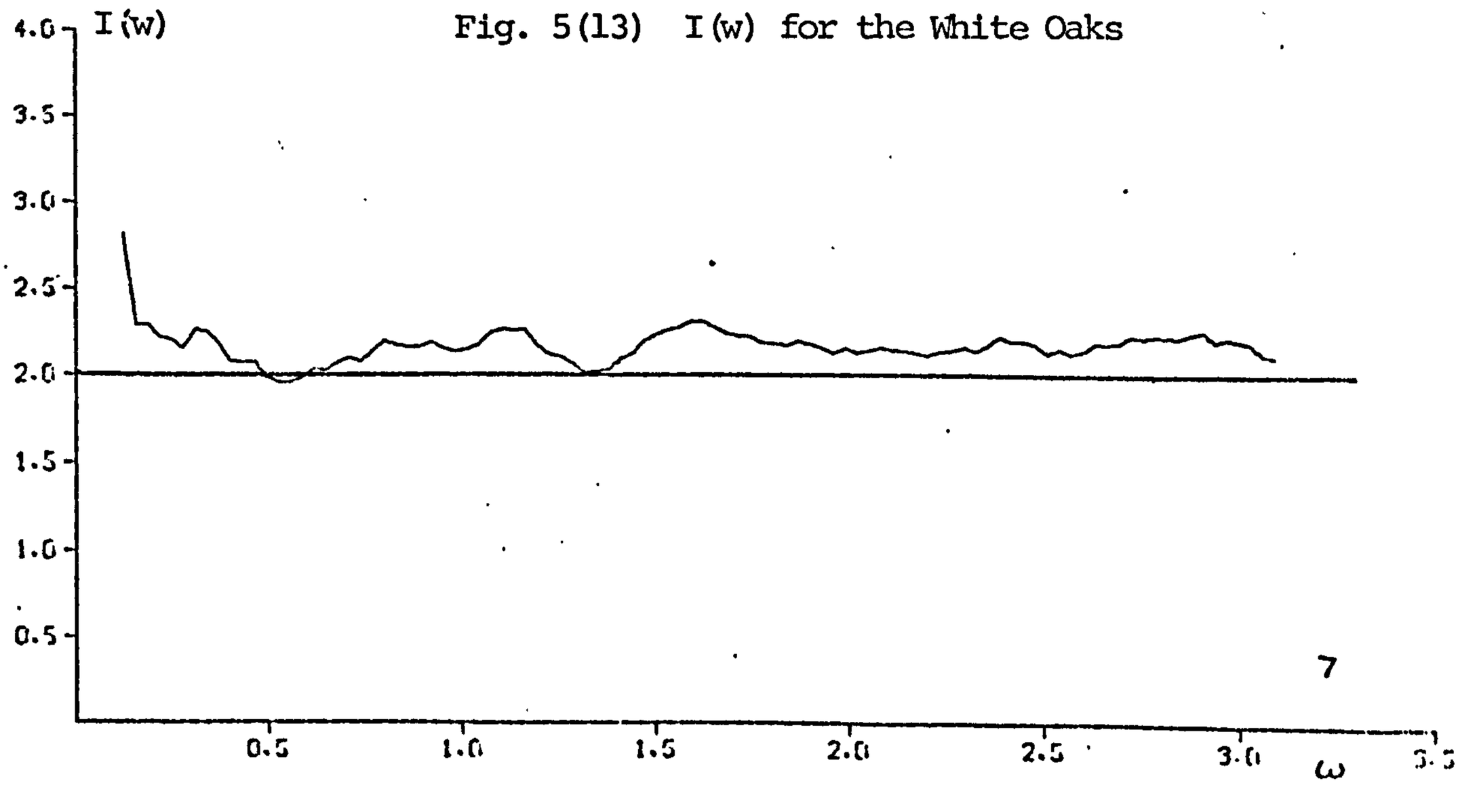

Fig. 5(13) I(w) for the White Oaks

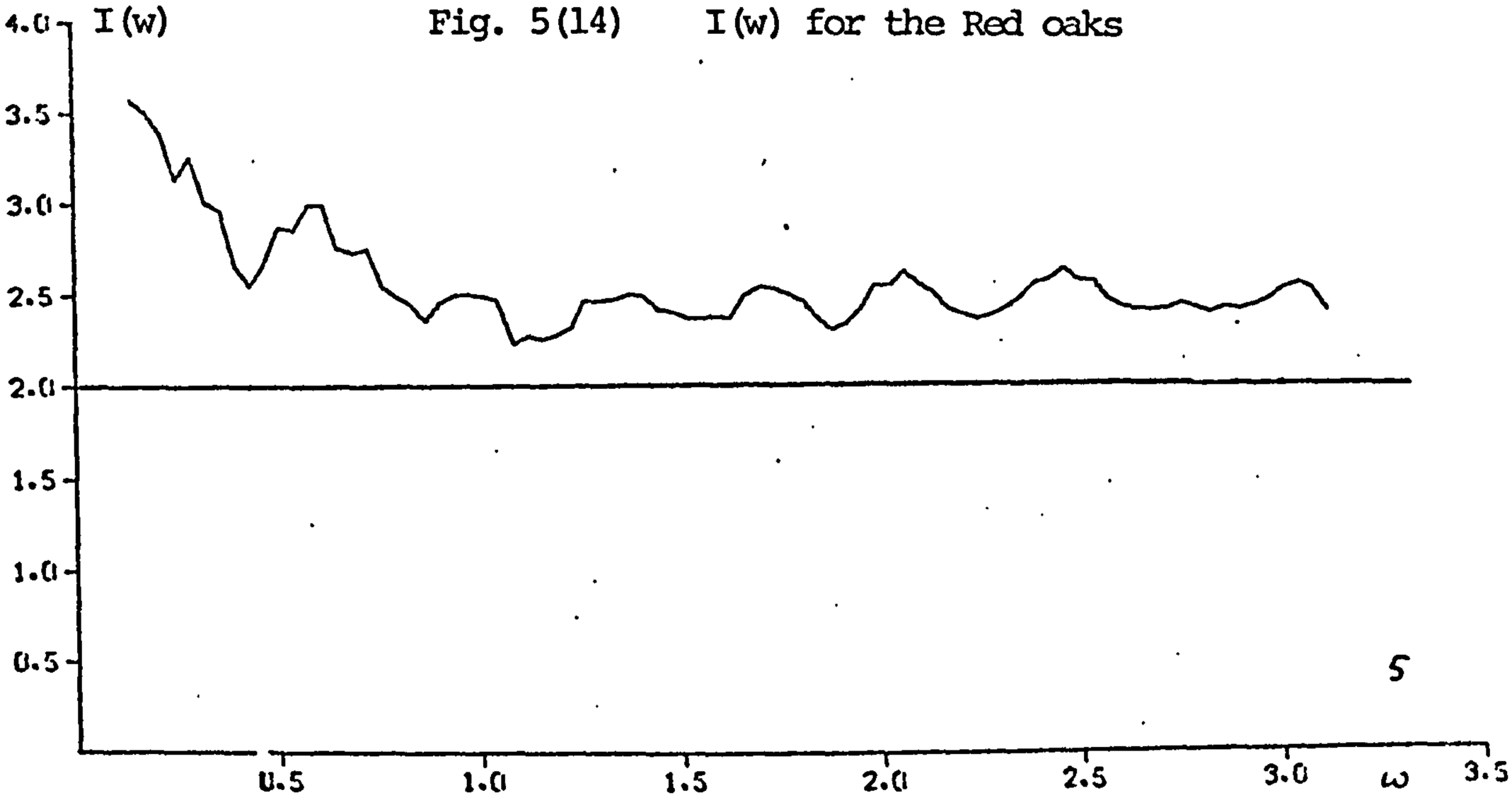

Fig. 5(14) I(w) for the Red oaks

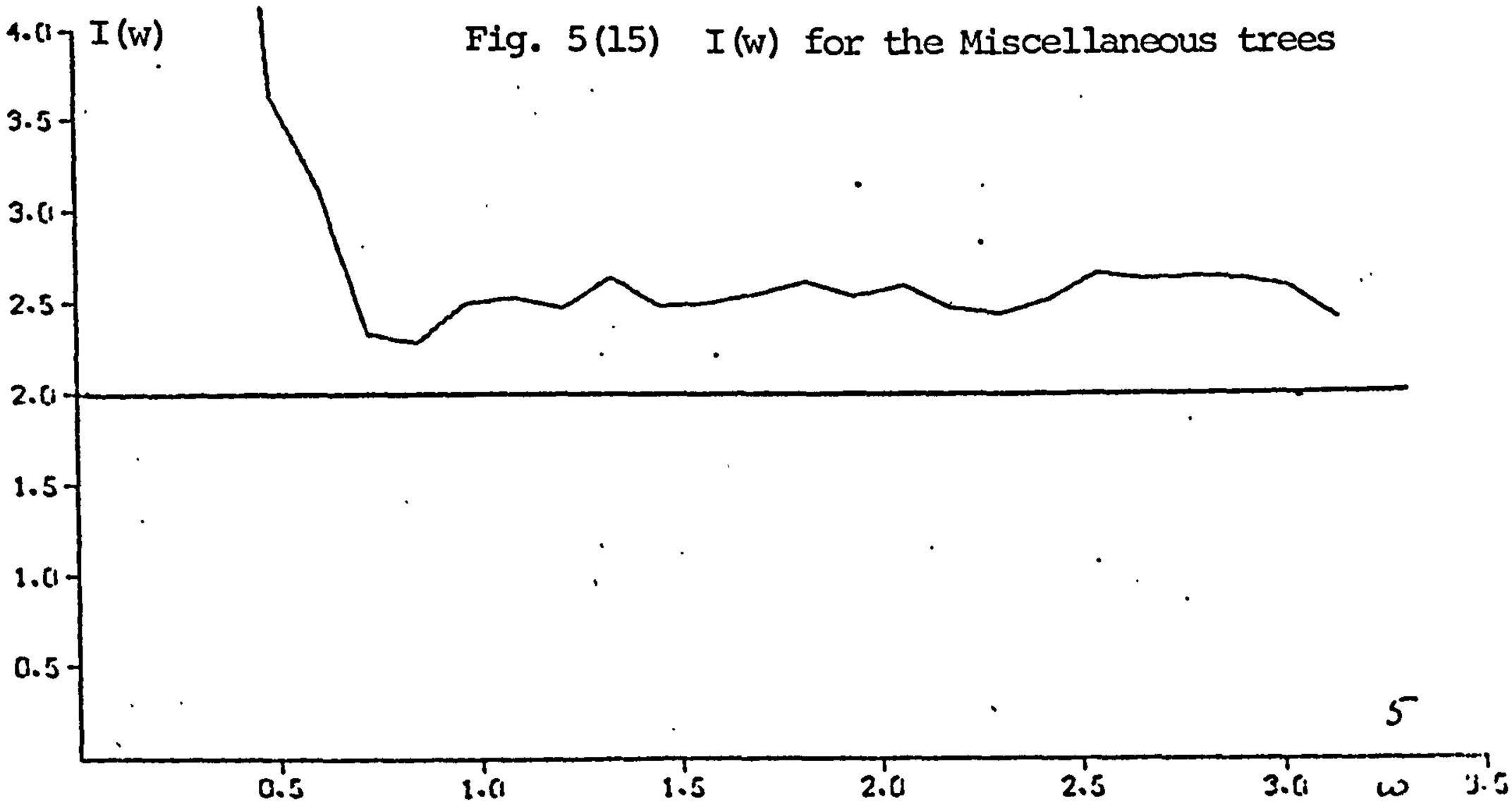

Fig. 5(15) I(w) for the Miscellaneous trees

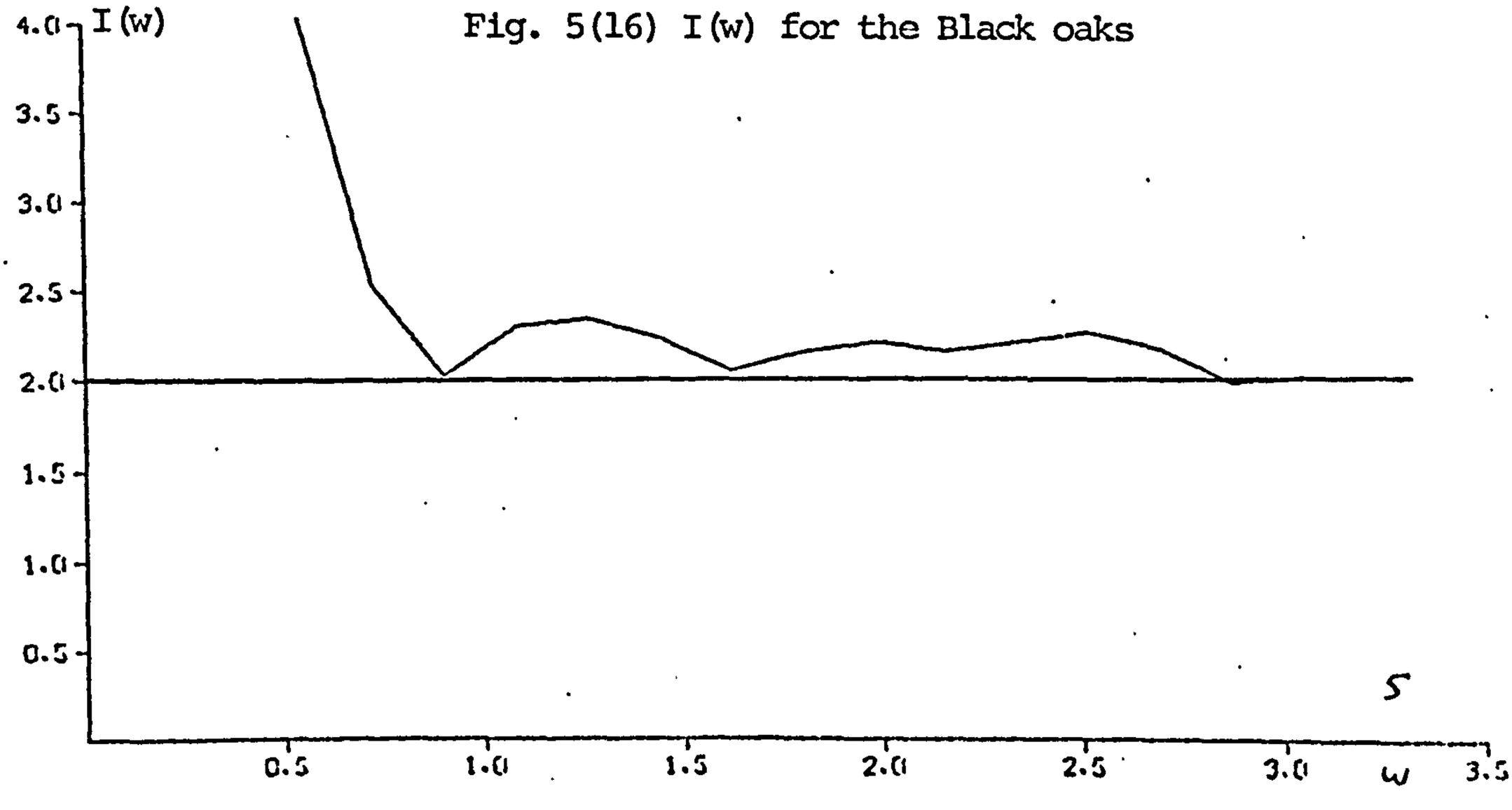

Fig. 5(16) I(w) for the Black oaks

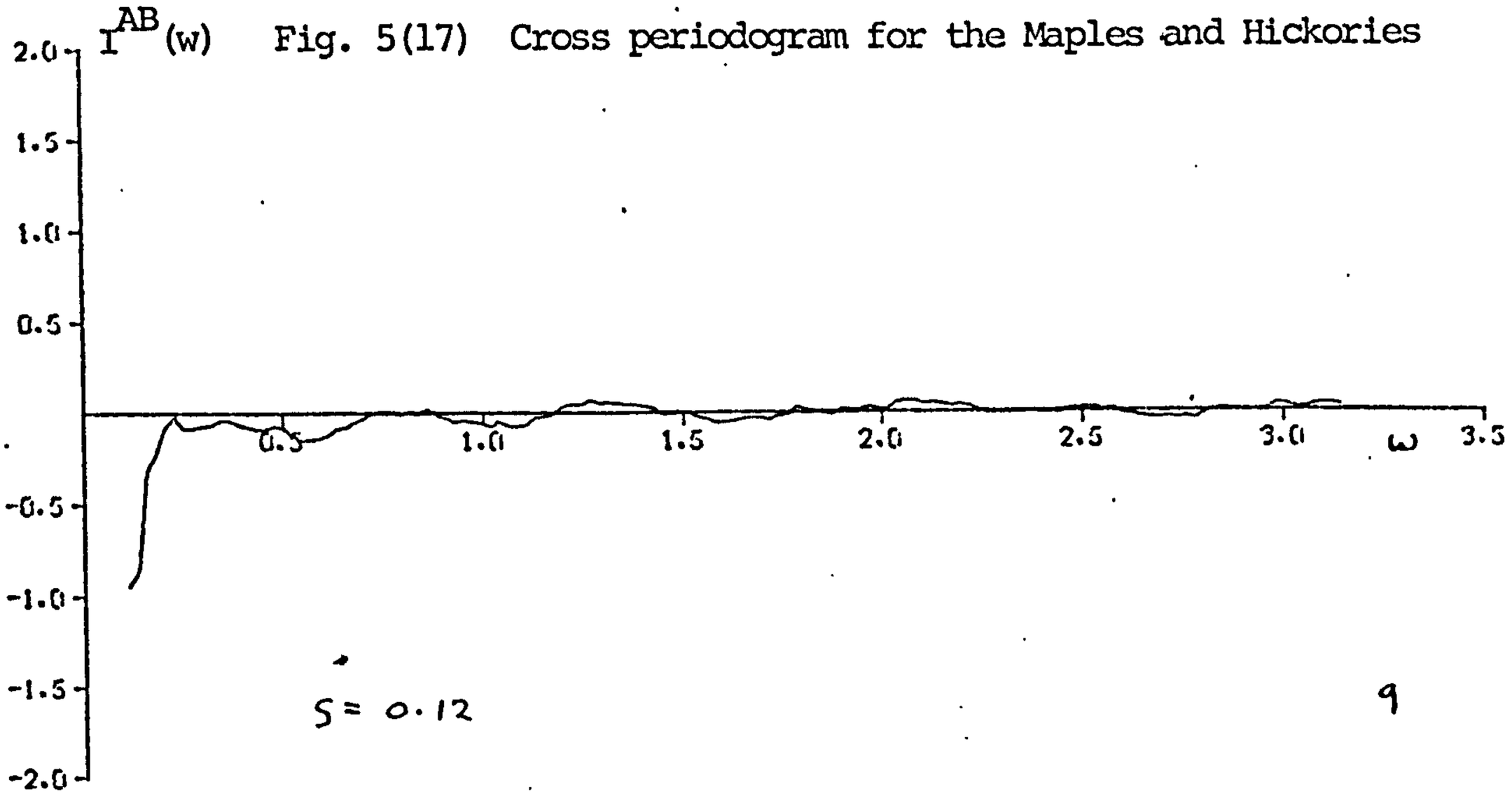

Fig. 5(17) Cross periodogram for the Maples and Hickories

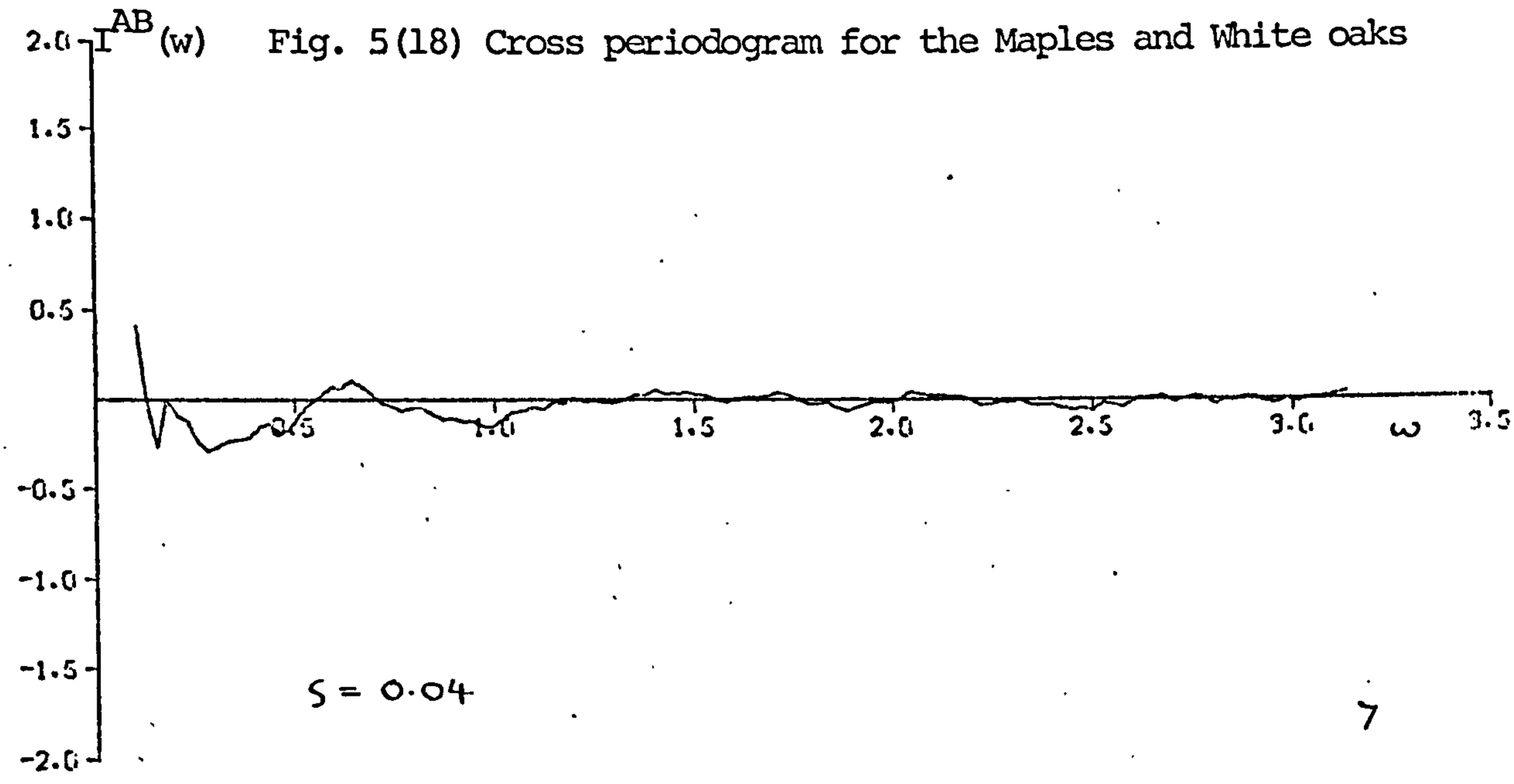

Fig. 5(18) Cross periodogram for the Maples and White oaks

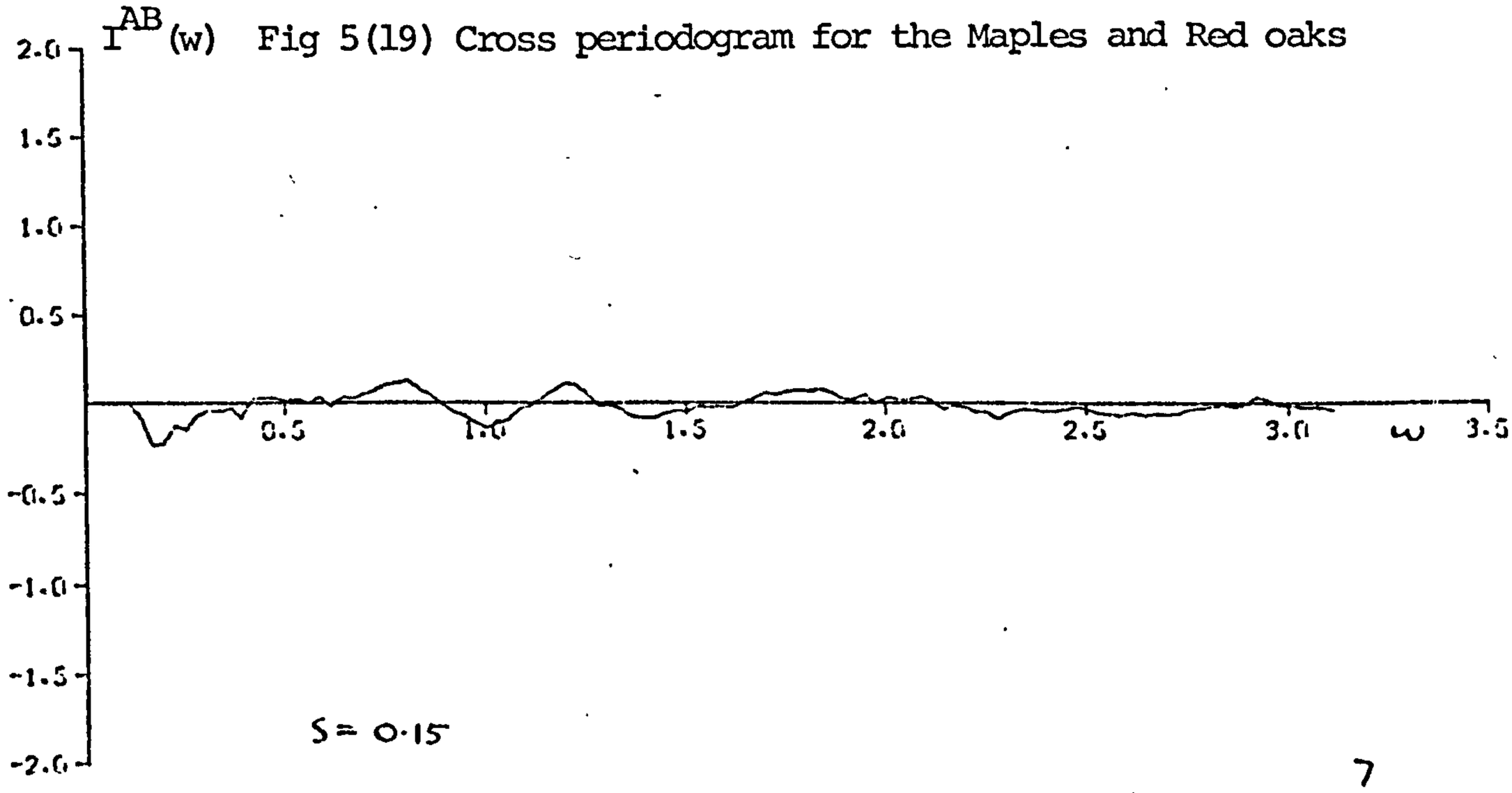

Fig 5(19) Cross periodogram for the Maples and Red oaks

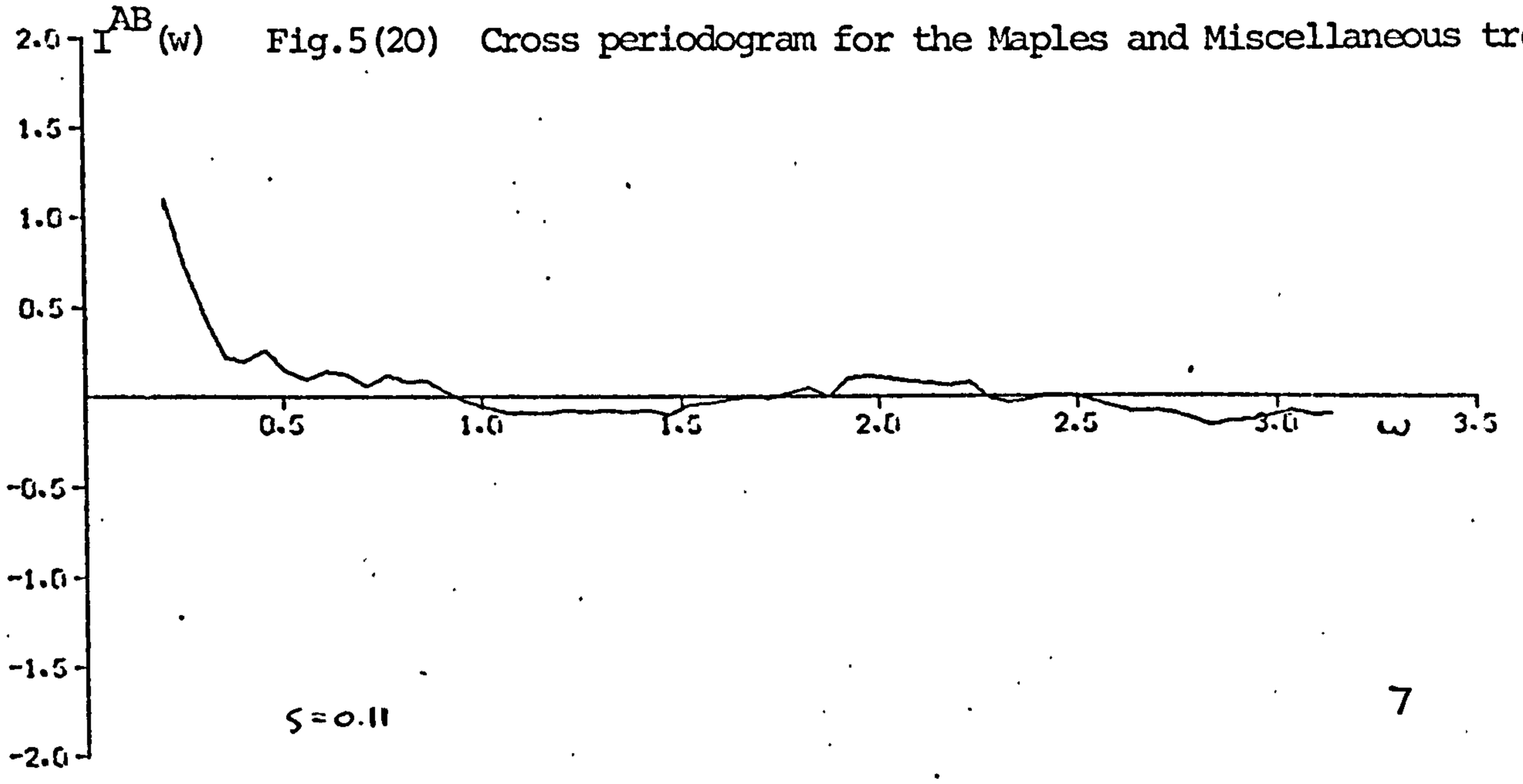

Fig.5(20) Cross periodogram for the Maples and Miscellaneous trees

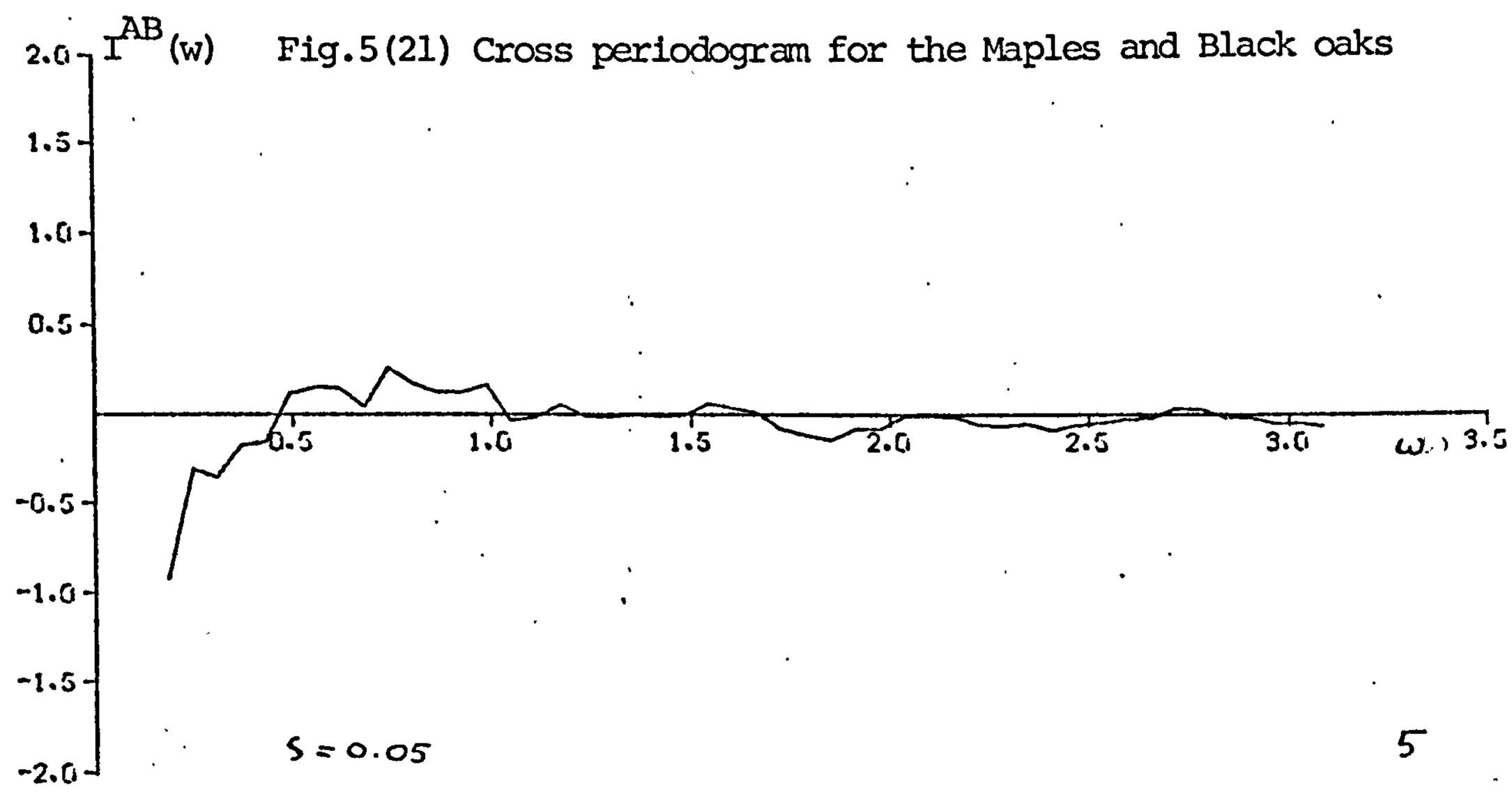

Fig.5(21) Cross periodogram for the Maples and Black oaks

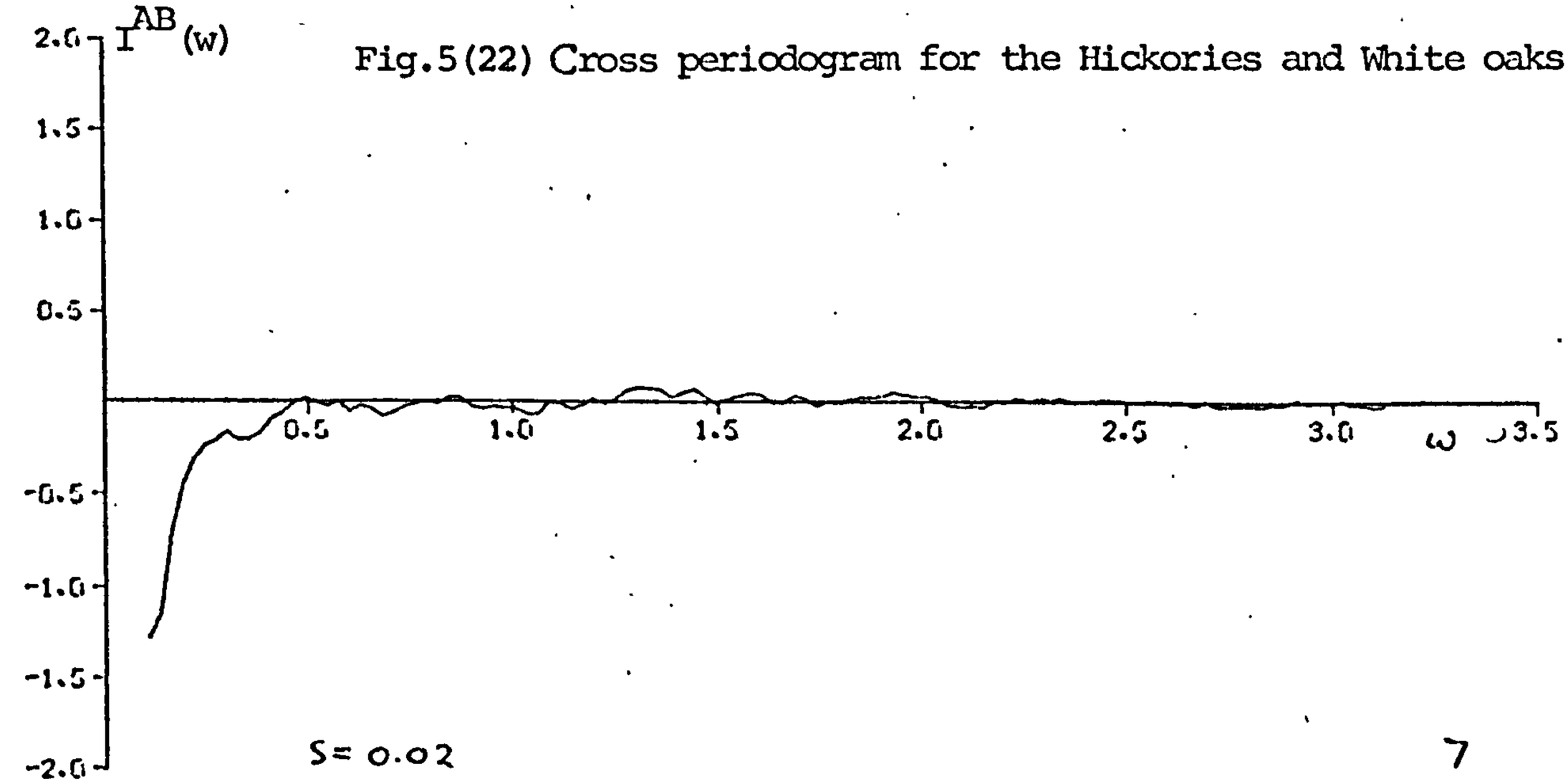

Fig.5(22) Cross periodogram for the Hickories and White oaks.

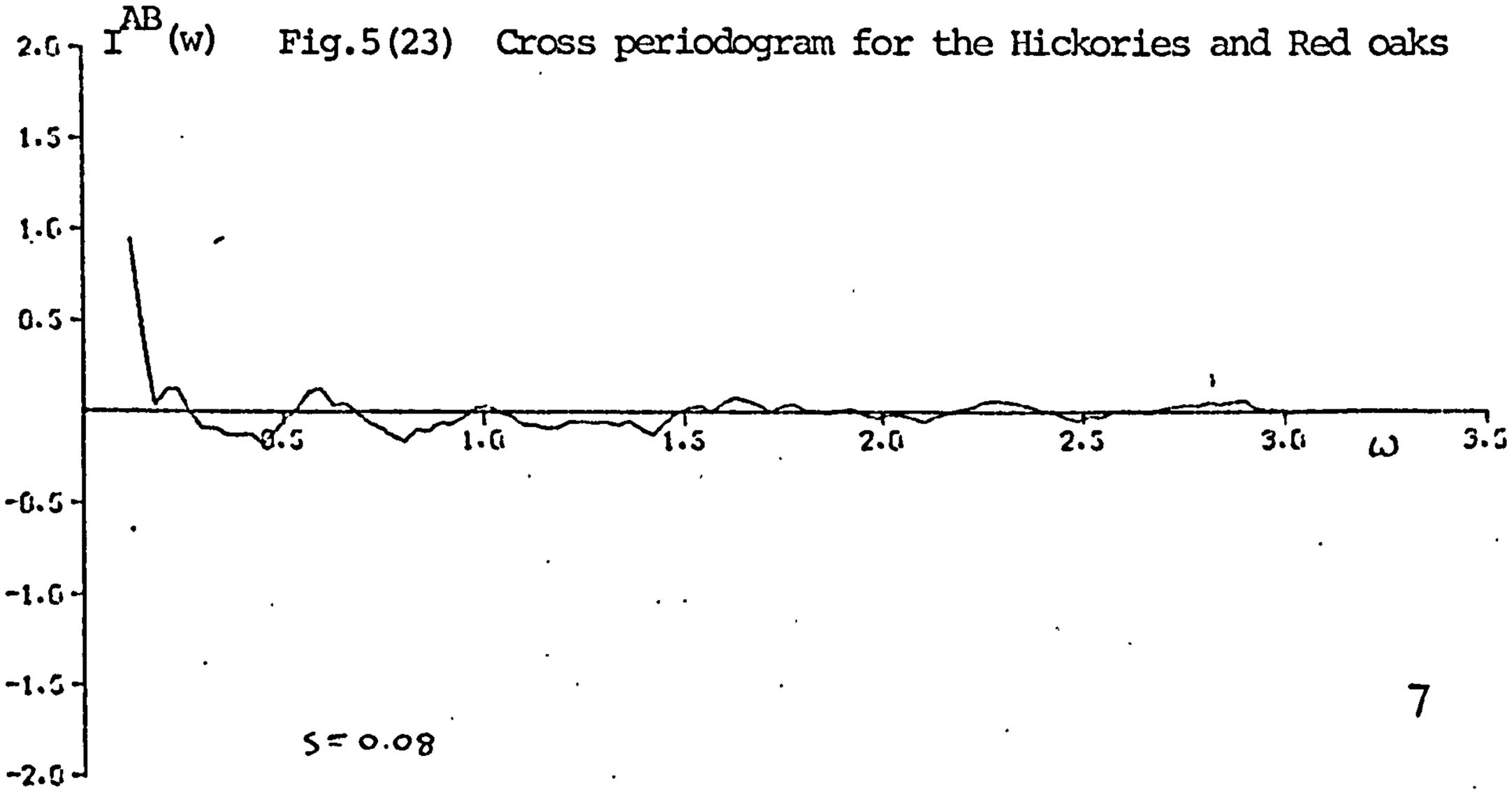

7

Fig.5(23) Cross periodogram for the Hickories and Red oaks

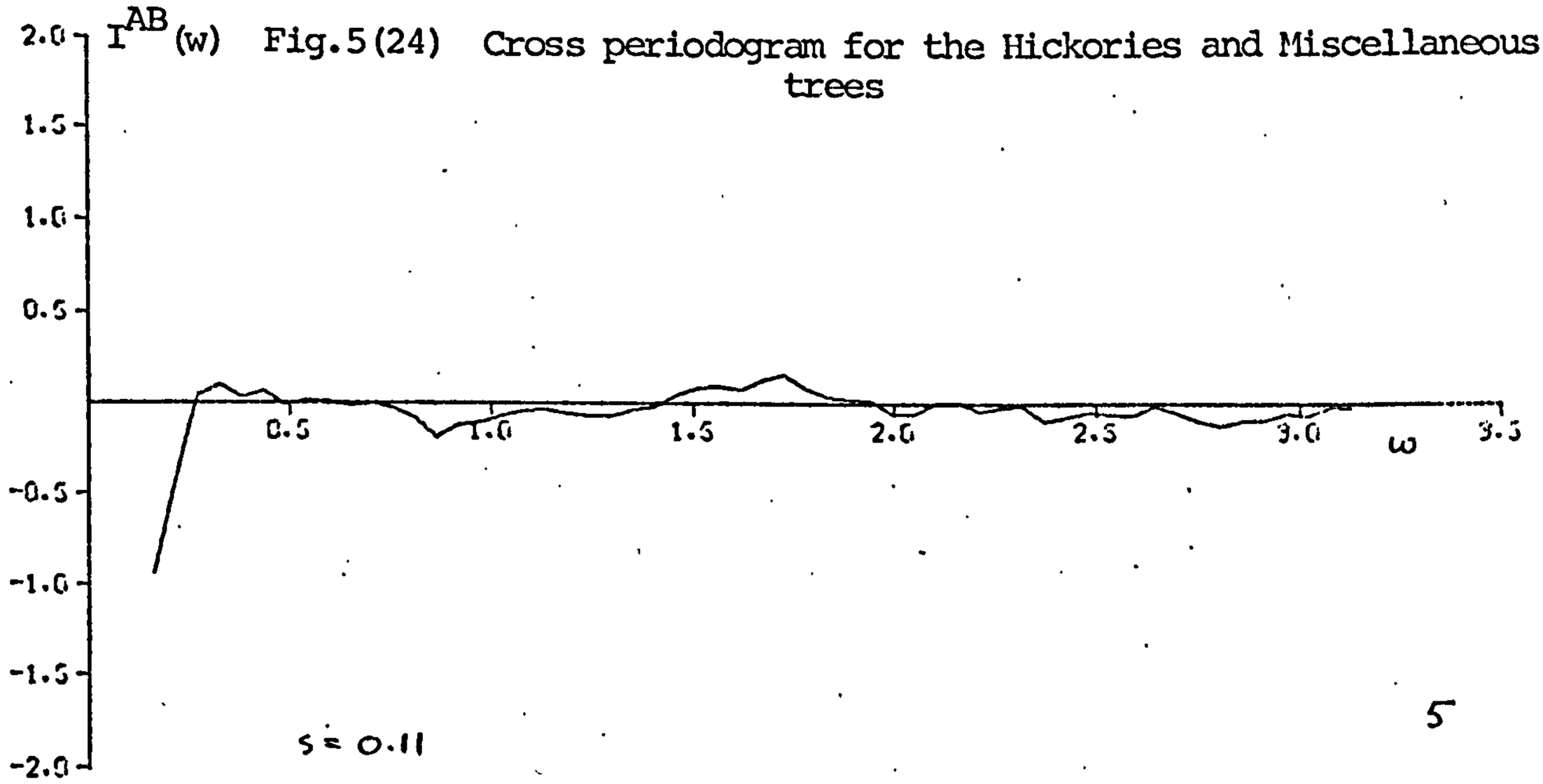

5

Fig.5(24) Cross periodogram for the Hickories and Miscellaneous trees

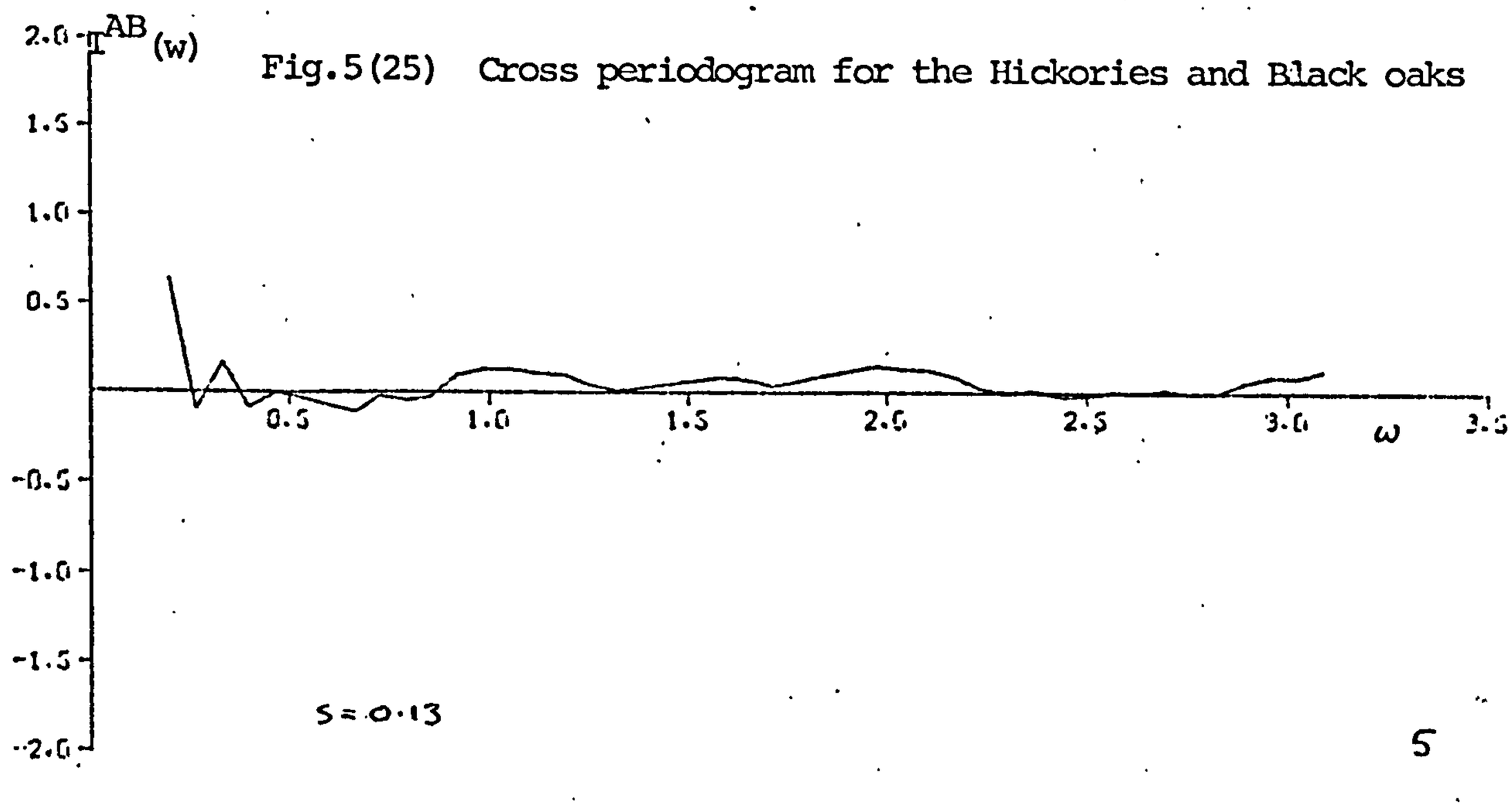

5

Fig.5(25) Cross periodogram for the Hickories and Black oaks

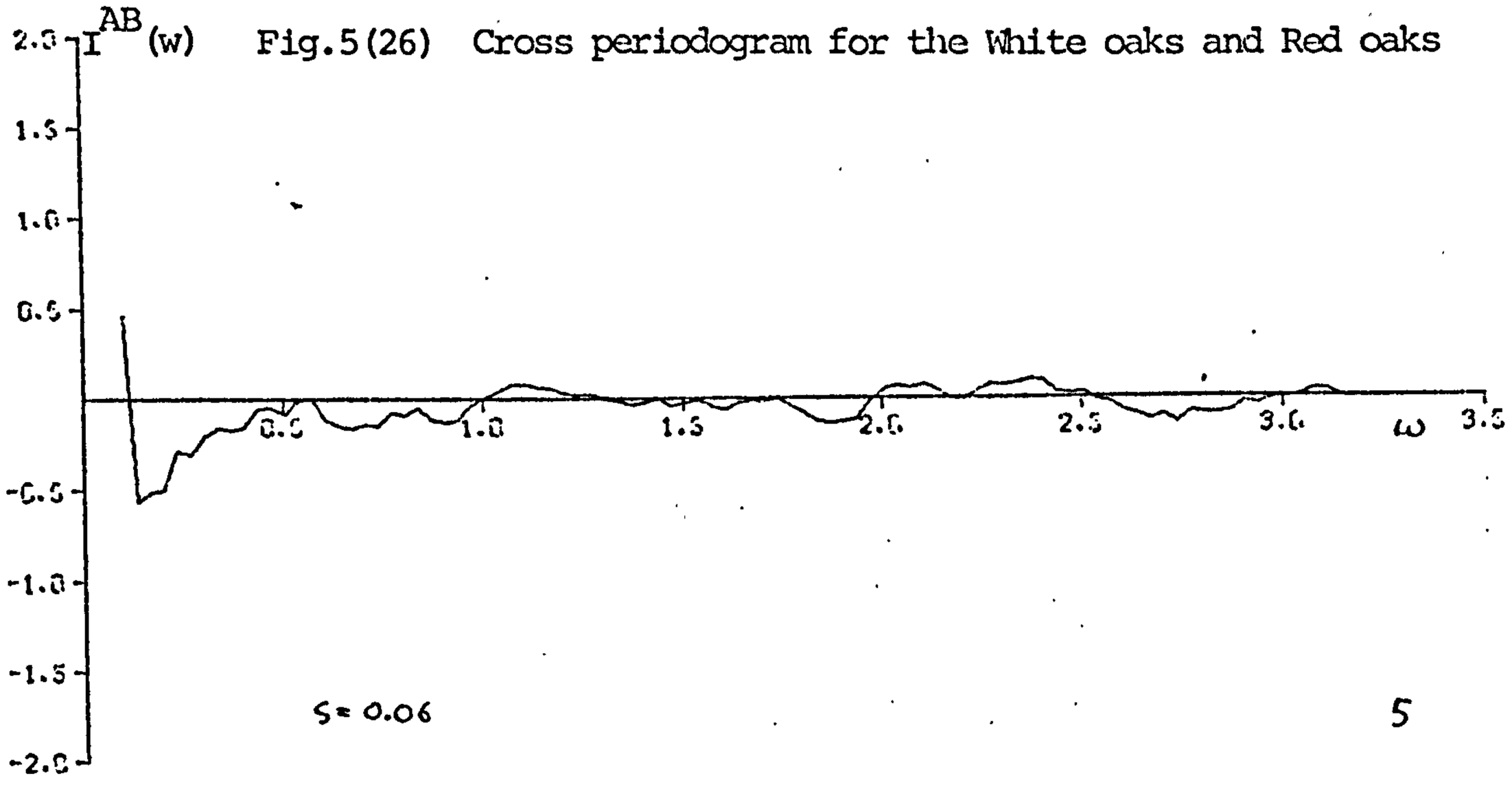

Fig.5(26) Cross periodogram for the White oaks and Red oaks

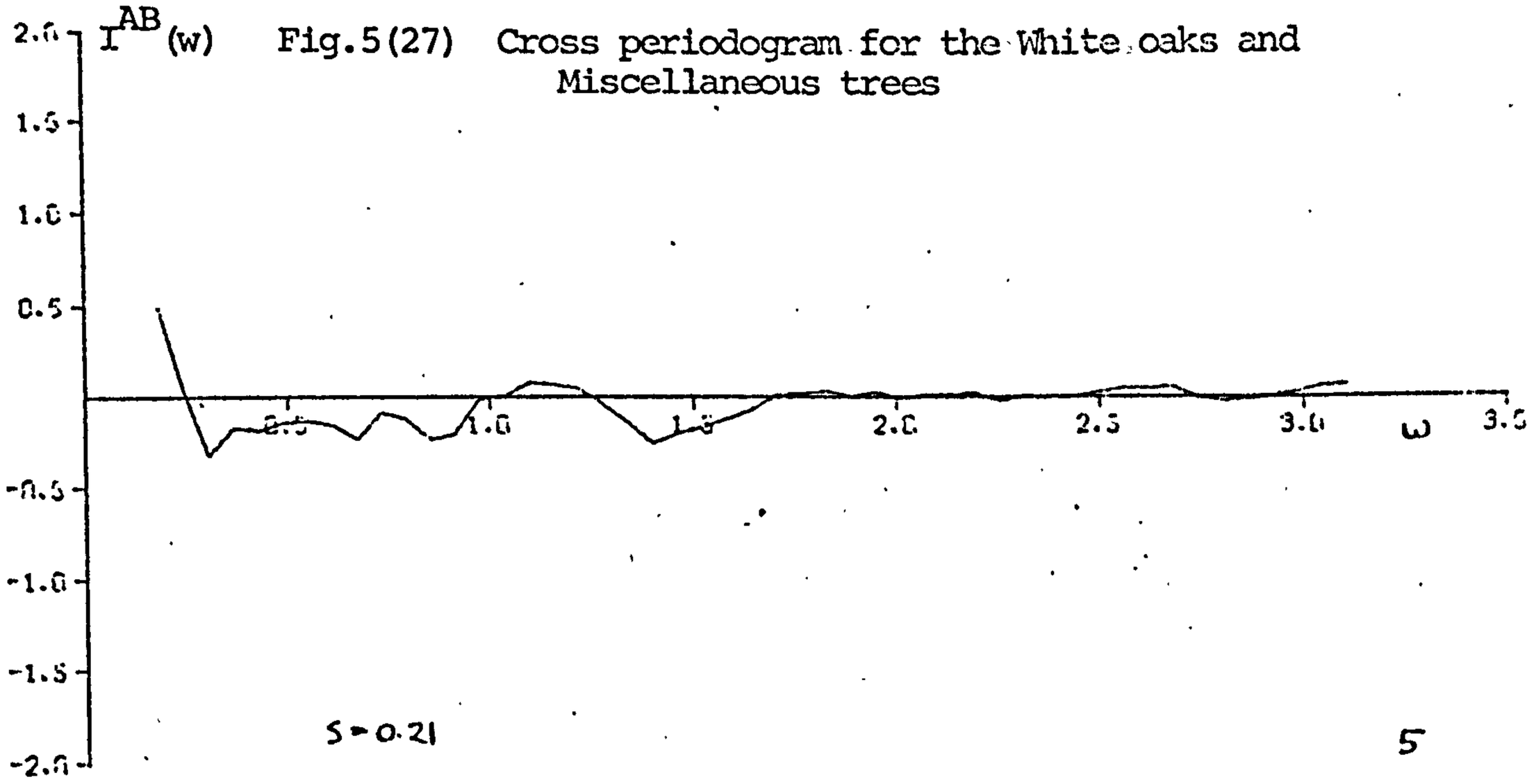

Fig.5(27) Cross periodogram for the White oaks and Miscellaneous trees

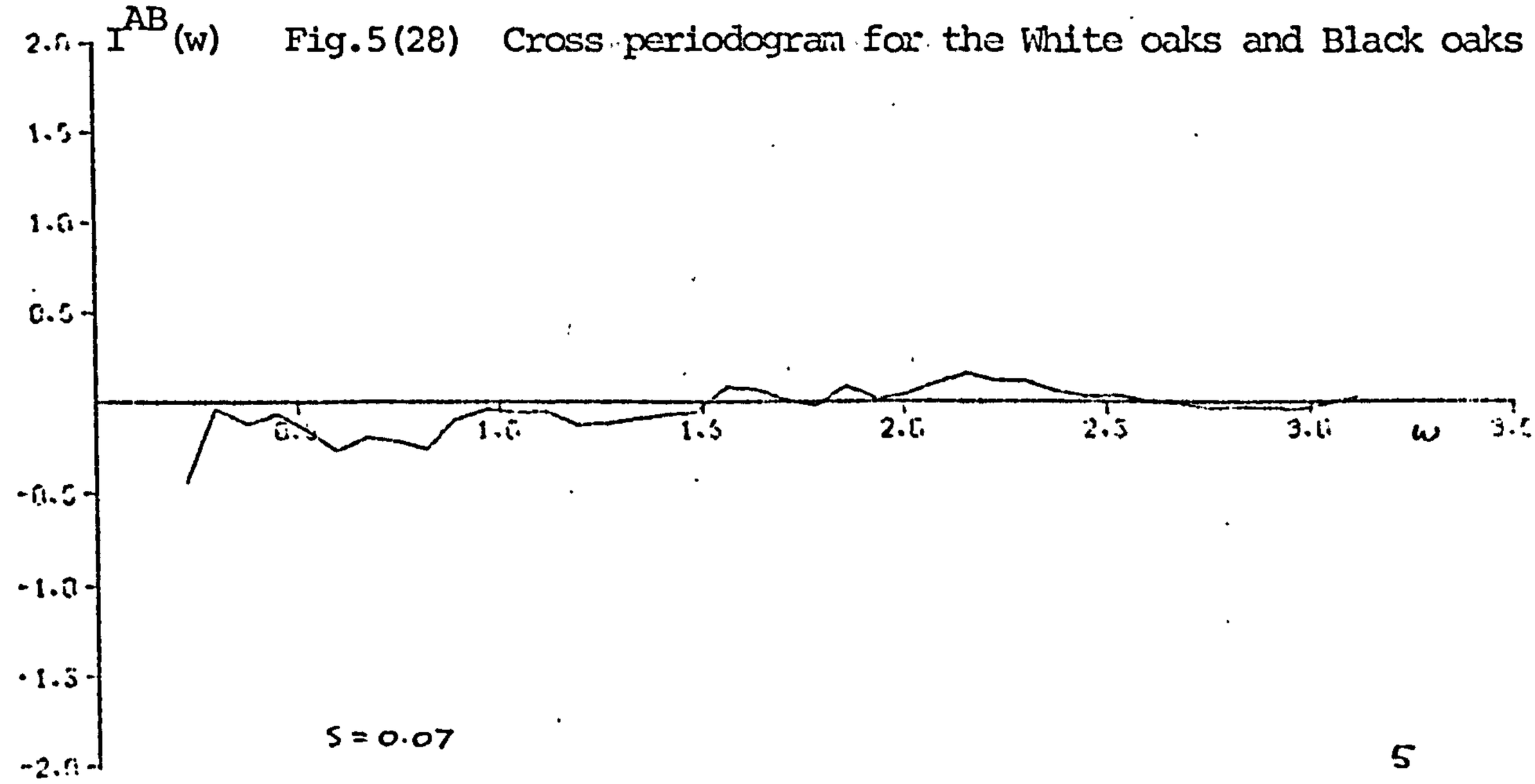

Fig.5(28) Cross periodogram for the White oaks and Black oaks

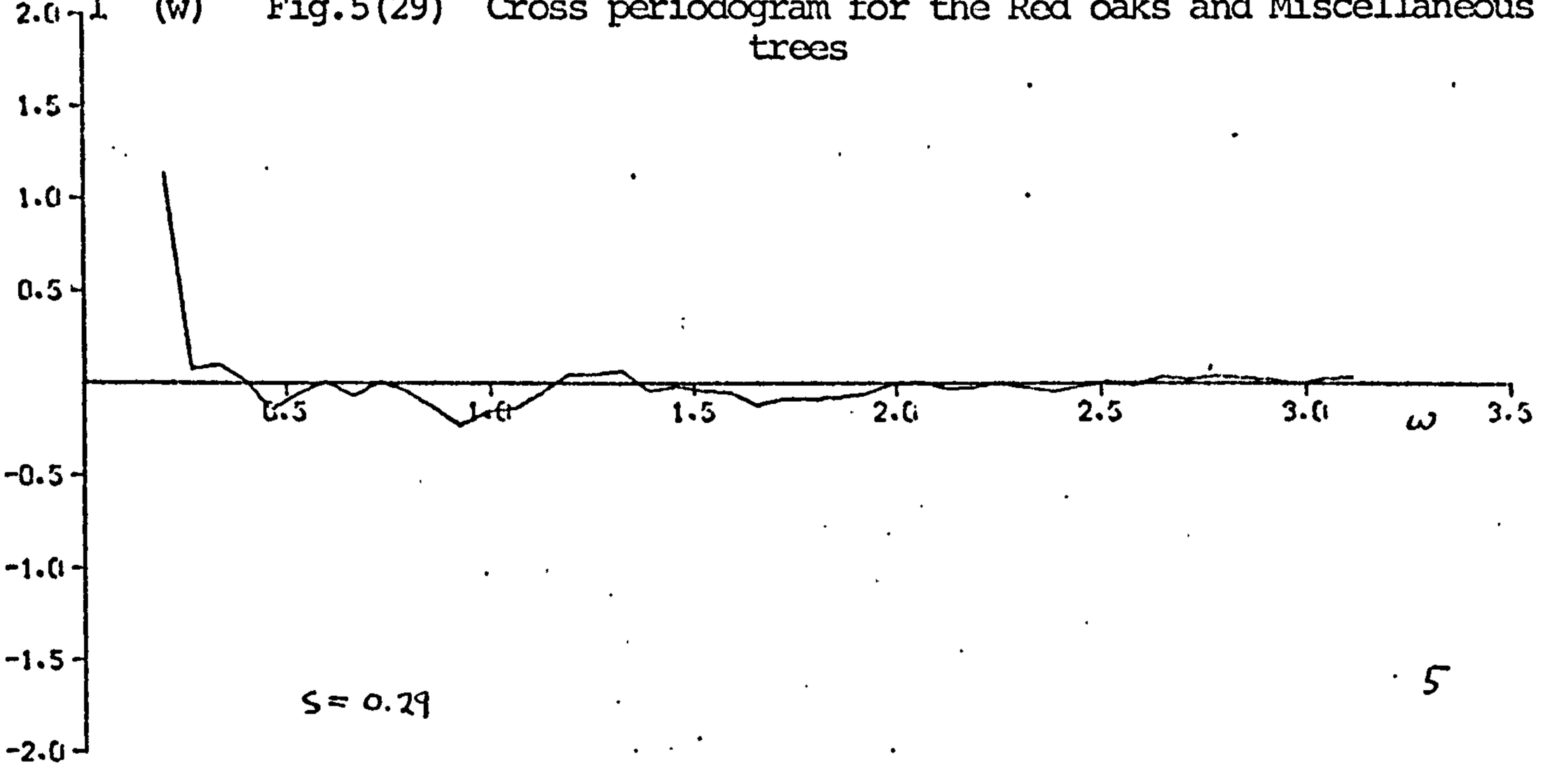

$I^{AB}(w)$ Fig.5(29) Cross periodogram for the Red oaks and Miscellaneous trees

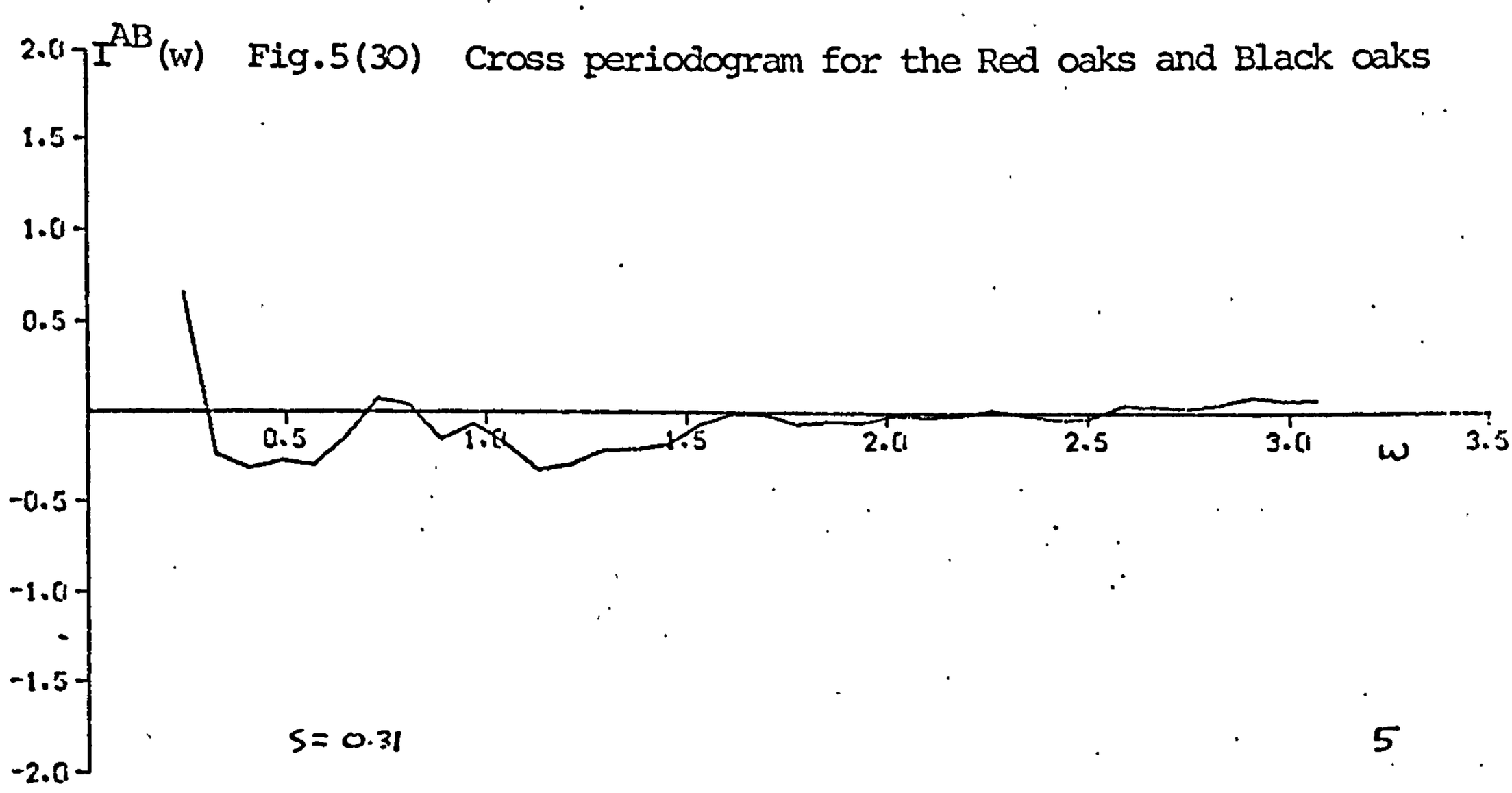

$I^{AB}(w)$ Fig.5(30) Cross periodogram for the Red oaks and Black oaks

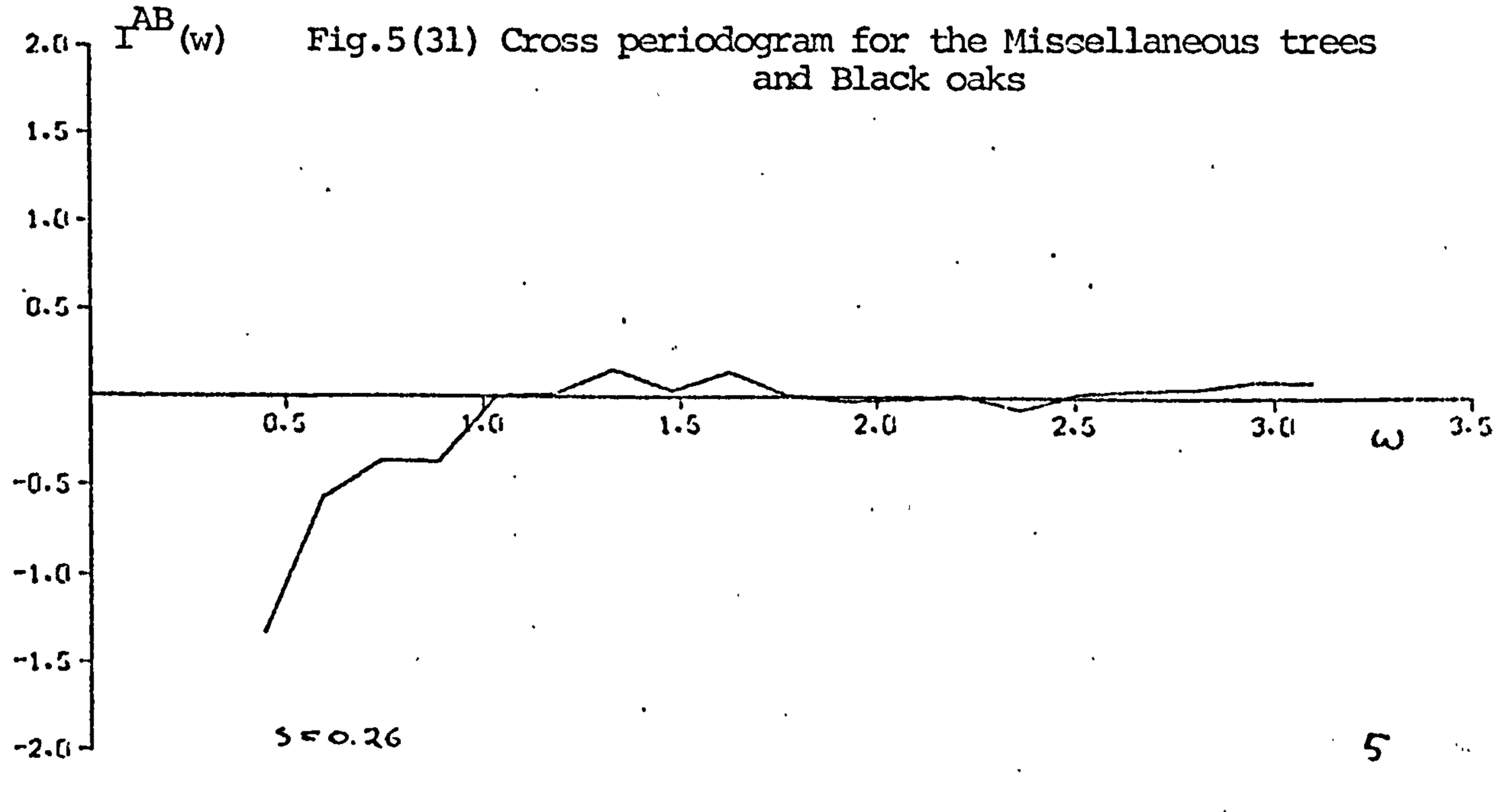

$I^{AB}(w)$ Fig.5(31) Cross periodogram for the Miscellaneous trees and Black oaks

The smoothed isotropic periodograms for the Maples, Hickories and White oaks all tend to oscillate about a limit except for w very small. It appears that for the Maples and Hickories, there is some slight clumping, as I(w) may be large for small w, but this may also be due to the bias. As the limit about which I(w) seems to oscillate is slightly greater than 2 for each of the species, this suggests that they form Poisson forests with a few pairs of trees (or even greater numbers) which are coincident. The periodogram for the Red oaks shows that they are probably slightly clumped, and similarly for the Miscellaneous trees and Black oaks. Again there are probably coincident trees in the Red oak and Miscellaneous tree populations.

The results obtained for the smoothed isotropic cross-periodograms were rather disappointing. It appears that the counts of the species are more or less uncorrelated for all pairs of species except the pair (Miscellaneous trees, Black oaks). However there seems to be some reaction between species at very short distances, the following pairs tending to inhibit each other;

(Maples, Hickories)

(Maples, Black oaks)

(Hickories, White oaks)

(Miscellaneous trees, Black oaks).

As the spectral analysis suggests that the Maples, Hickories and White oaks form practically a Poisson forest, then observation of the cross periodograms of pairs of these species, suggests that only the Maples and White oaks are unsegregated, while the Maples and Hickories, and the Hickories and White oaks are positively segregated. This is

shown to be true by Pielou's test of segregation. Nothing can be said about the segregation of the other species from spectral results because they do not form Poisson forests. However results of Pielou's test made on every set of data discussed are shown in Table 9.

Table 9. Pielou's segregation test, with the coefficient of segregation, S.

Type of trees	χ^2_1 value	S	Type of segregation
Independent Poisson forests	0.00	0.01	unsegregated
Associated Poisson forests	53.47**	-0.68	negative
Regular model (independent species)	58.82**	-0.72	negative
Regular model (associated species)	16.69**	-0.38	negative
Poisson forest and clumped model	36.34**	0.56	positive
(MA, HK)	7.99*	0.12	positive
(MA, WK)	0.48	0.04	unsegregated
(MA, RK)	9.48**	0.15	positive
(MA, MI)	3.26	0.11	unsegregated
(MA, BK)	0.26	0.05	unsegregated
(HK, WK)	0.19	0.02	unsegregated
(HK, RK)	2.53	0.08	unsegregated
(HK, MI)	2.76	0.11	unsegregated
(HK, BK)	3.62	0.13	unsegregated
(WK, RK)	1.29	0.06	unsegregated
(WK, MI)	10.30**	0.21	positive
(WK, BK)	0.65	0.07	unsegregated
(RK, MI)	18.05**	0.29	positive
(RK, BK)	17.89**	0.31	positive
(MI, BK)	5.03**	0.26	positive

** significant at 1%.
* significant at 5%

MA - Maples, HK - Hickories, WK - White oaks, RK - Red oaks,

MI - Miscellaneous trees, BK - Black oaks.

A note on future research

Further methods of describing a spatial pattern other than the regular/random/aggregation scale, are desirable. It may be possible to find a series of indices which characterize patterns more precisely. More tests of randomness will probably join the list of those already in use, even though most spatial patterns in nature are not random.

The area of robust estimation of the density of a spatial point process is a relatively new one. More robust estimators need to be found and compared to those already in use. However for practical reasons all estimators using distance measurements ought to use only distances from points (usually random), and not distances from random trees. Being able to choose a tree at random obviously implies that a list of all the trees is available.

Mapping of the clumped and sparse areas of a spatial pattern, according to chapter four, may or may not have its uses in various fields of study. It may for instance be of interest to the economists or urban geographers, mapping a particular type of shop in a city, needing a rigorous definition of where there are too many shops of this type or too few of them. Advance for the present theory is probably the defining of clump centres, and what might be termed "sparse area centres", and then the testing of hypotheses about the clump centres, etc. For example one could test whether the clump centres form a Poisson forest or not, or whether the trees around a clump centre are at a distance from the clump centre, distributed radial normally, etc.

The spatial analysis of two-type point processes, is a wide open field. There is much scope (and need) for research into the relationships between species cohabiting in the plane. Indeed the general theory of two-dimensional bivariate point processes needs much attention, either through spectral theory or other probabilistic methods. However the theory of one-dimensional bivariate point processes and the theory of two-dimensional univariate point processes, probably need to develop further beforehand.

References

Bartlett, M. S. (1955) An Introduction to Stochastic Processes. C.U.P.

Bartlett, M.S. (1963) The spectral analysis of point processes. J.R.S.S. B, 25, p264-296.

Bartlett, M.S. (1964) The spectral analysis of two-dimensional point processes. Biometrika, 51, p299-311.

Bartlett, M. S. (1974) The statistical analysis of spatial pattern. Adv. Appl. Prob. 6, p336-358.

Bartlett, M. S. (1975) The Statistical Analysis of Spatial Pattern Chapman and Hall.

Besag, J. E., and Gleaves, J. T. (1973) On the detection of spatial pattern in plant communities. Bull. Int. Stat. Inst., 39, p153-158.

Clapham, A. R. (1936) Overdispersion in grassland communities and the use of statistical methods in plant ecology. J.Ecol. p232-251.

Clark, P. J., and Evans, C. (1954) Distance to nearest neighbour as a measure of spatial relationships in populations. Ecology 35, p445-453.

Cox, D. R. (1955) Some statistical methods connected with series of events. J.R.S.S., 17, p129-164.

Cox, D. R., and Lewis, P. A. W. (1966) The Statistical Analysis of Series of Events. Methuen.

Cox, D. R., and Lewis, P. A. W. (1972) Multivariate point processes. In Proc. 6th Berkeley Symposium on Mathematical Statistics and Probability.

David, F. N., and Moore, P. G. (1954) Notes on contagious distributions in plant populations. Ann. Bot. N.S., 18, p.47-53.

Diggle, P. J. (1975) Robust density estimation using distance methods. Biometrika 62, p39-48.

Diggle, P. J., Besag, J.E., and Gleaves, J.T. (1976) On the statistical analysis of spatial point patterns by means of distance methods. Biometrics (submitted).

Eberhart, L. L. (1967) Some developments in distance sampling. Biometrics, 23, p207-216.

Evans, D. A. (1953) Experimental evidence concerning contagious distributions in ecology. Biometrika, 40, p186-211.

Ford, E. D. (1975) Competition and stand structure in some even-aged plant monocultures. J. Ecol., 63, p311-333.

Greig-Smith, P. (1952) The use of random and contagious quadrats in the study of the structures of plant communities. Ann. Bot. N.S., 16, p293-316.

Greig-Smith, P. (1964) Quantitative Plant Ecology, 2nd Edn Butterworths.

Holgate, P. (1965a) Tests of randomness based on distance methods. Biometrika, 52, p345-353.

Holgate, P. (1965b) Some new tests of randomness. J. of Ecol., 53, p261-266.

Holgate, P. (1972) The use of distance methods for the analysis of spatial distribution of points. In Stochastic Point Processes. ed. P. A. W. Lewis, Wiley.

Hopkins, B., and Skellam, J. G. (1954) A new method of determining the type of distribution of plant individuals. Ann. Bot., 18, p213-226.

Jenkins, G. M., and Watts, D. G., (1968) Spectral Analysis and its Applications. Holden-Day.

Lewis, S. M. (1975) Robust estimation of density for a two-dimensional point process. Biometrika, 62, p519-521.

Lloyd, M. (1967) Mean crowding. J. Anim. Ecol., 36, p1-30.

Mountford, M. P., (1961) On E. C. Pielou's index of non-randomness. J. of Ecol., 49, p271-275.

Persson, O., (1971) The robustness of estimating density by distance measurements. In Statistical Ecology, Vol.2, eds. G. P. Patil, E. C. Pielou, and W. E. Waters, Penn. State Uni. Press, p175-190.

Pielou, E. C. (1959) The use of point-to-point distances in the study of the pattern of plant populations. J. of Ecol., 48, p575-584.

Pielou, E. C. (1961) Segregation and symmetry in two-species populations as studied by nearest-neighbour relationships J. of Ecol., 49, p255-269.

Pielou, E. C. (1969) An Introduction to Mathematical Ecology. Wiley.

Pielou, E. C. (1974) Population and Community Ecology. Gordon and Breach Science Publishers.

Pollard, J. H. (1971) On distance estimators of density in randomly distributed forests. Biometrics, 27, p991-1002.

Silvey, S. D. (1970) Statistical Inference. Penguin.

Skellam, J. G. (1952) Studies in statistical ecology. Biometrika, 39, p346-362.

Stiteler, W. M. (1970) Measurement of spatial patterns in ecology. Ph.D. Thesis. Penn. State. Univ.

Stiteler, W. M., and Patil, G. P. (1971) Variance to mean ratio and Morisita's index as measures of spatial patterns in ecological populations. In Statistical Ecology. Vol. 1. eds. G. P. Patil, E. C. Pielou, and W. E. Waters. Penn. State Univ. Press, p423-459.

Thomas, M. (1949) A generalisation of Poisson's binomial limit for use in ecology. Biometrika, 36, p18-25.

Warren, W. G. (1972) Point processes in forestry. In Stochastic Point Processes. ed. P. A. W. Lewis. Wiley.

Whitford, P. B. (1949) Distribution of woodland plants in relation to succession and clonal growth. Ecology, 30, p199-208.